



US Army Corps
of Engineers

MISCELLANEOUS PAPER CERC-89-11

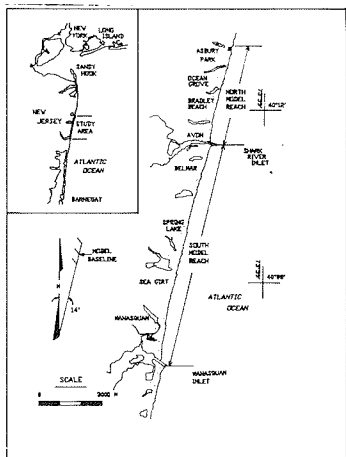
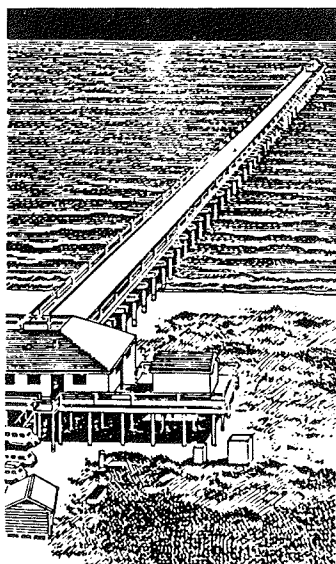
COASTAL PROCESSES FROM ASBURY PARK TO MANASQUAN, NEW JERSEY

by

Mark B. Gravens, Norman W. Scheffner, Jon M. Hubertz

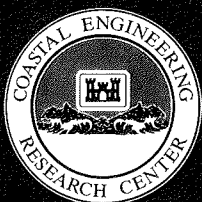
Coastal Engineering Research Center

DEPARTMENT OF THE ARMY
Waterways Experiment Station, Corps of Engineers
3909 Halls Ferry Road
Vicksburg, Mississippi 39180-6199



September 1989
Final Report

Approved For Public Release; Distribution Unlimited



Prepared for US Army Engineer District, New York
New York, New York 10278-0090

Destroy this report when no longer needed. Do not return
it to the originator.

The findings in this report are not to be construed as an official
Department of the Army position unless so designated
by other authorized documents.

The contents of this report are not to be used for
advertising, publication, or promotional purposes.
Citation of trade names does not constitute an
official endorsement or approval of the use of
such commercial products.

Unclassified

SECURITY CLASSIFICATION OF THIS PAGE

REPORT DOCUMENTATION PAGE				Form Approved OMB No. 0704-0188	
1a. REPORT SECURITY CLASSIFICATION Unclassified			1b. RESTRICTIVE MARKINGS		
2a. SECURITY CLASSIFICATION AUTHORITY		3. DISTRIBUTION / AVAILABILITY OF REPORT			
2b. DECLASSIFICATION / DOWNGRADING SCHEDULE		Approved for public release; distribution unlimited			
4. PERFORMING ORGANIZATION REPORT NUMBER(S) Miscellaneous Paper CERC-89-11			5. MONITORING ORGANIZATION REPORT NUMBER(S)		
6a. NAME OF PERFORMING ORGANIZATION USAEWES, Coastal Engineering Research Center		6b. OFFICE SYMBOL (If applicable)	7a. NAME OF MONITORING ORGANIZATION		
6c. ADDRESS (City, State, and ZIP Code) 3909 Halls Ferry Road Vicksburg, MS 39180-6199			7b. ADDRESS (City, State, and ZIP Code)		
8a. NAME OF FUNDING / SPONSORING ORGANIZATION USAED, New York		8b. OFFICE SYMBOL (If applicable)	9. PROCUREMENT INSTRUMENT IDENTIFICATION NUMBER		
8c. ADDRESS (City, State, and ZIP Code) 26 Federal Plaza New York, NY 10278-0090			10. SOURCE OF FUNDING NUMBERS		
			PROGRAM ELEMENT NO.	PROJECT NO.	TASK NO.
			WORK UNIT ACCESSION NO.		
11. TITLE (Include Security Classification) Coastal Processes from Asbury Park to Manasquan, New Jersey					
12. PERSONAL AUTHOR(S) Gravens, Mark B.; Scheffner, Norman W.; Hubertz, Jon M.					
13a. TYPE OF REPORT Final report		13b. TIME COVERED FROM Mar 87 TO Sep 88		14. DATE OF REPORT (Year, Month, Day) September 1989	15. PAGE COUNT 201
16. SUPPLEMENTARY NOTATION Available from National Technical Information Service, 5285 Port Royal Road, Springfield, VA 22161.					
17. COSATI CODES			18. SUBJECT TERMS (Continue on reverse if necessary and identify by block number)		
FIELD	GROUP	SUB-GROUP	See reverse.		
19. ABSTRACT (Continue on reverse if necessary and identify by block number)					
<p>This report describes a study of coastal processes along the Atlantic coast from Asbury Park to Manasquan, New Jersey. Numerical predictive models for storm surge, dune erosion, nearshore wave transformation, and shoreline response were used in conjunction with an intensive analysis of available physical data to assist in the design, evaluation, and implementation of comprehensive shore protection plans for this densely populated and heavily structured coastal region. The study was divided into four independent but interrelated areas: (a) deepwater wave climate analysis and nearshore wave transformation, (b) long-term shoreline response numerical modeling, (c) development of coastal stage-frequency relationships, and (d) numerical modeling of storm-induced dune erosion. The results, interrelations, and recommendations of these tasks are presented in the main body of the report together with guidance for the interpretation of</p> <p style="text-align: right;">(Continued)</p>					
20. DISTRIBUTION / AVAILABILITY OF ABSTRACT <input checked="" type="checkbox"/> UNCLASSIFIED/UNLIMITED <input type="checkbox"/> SAME AS RPT. <input type="checkbox"/> DTIC USERS			21. ABSTRACT SECURITY CLASSIFICATION Unclassified		
22a. NAME OF RESPONSIBLE INDIVIDUAL			22b. TELEPHONE (Include Area Code)	22c. OFFICE SYMBOL	

Unclassified

SECURITY CLASSIFICATION OF THIS PAGE

18. SUBJECT TERMS (Continued).

Asbury Park	New Jersey
Beach erosion	Shark River Inlet
Coastal processes	Shoreline change
Manasquan Inlet	

19. ABSTRACT (Continued).

the numerical model results. The statistics of the wave hindcast data base, along with graphical representations of the model results, are given in the appendices. Six proposed and four revised design alternatives were evaluated using the shoreline response model to predict the planform evolution of the beach. Cross-shore responses of the proposed design alternatives were evaluated in a probabilistic manner using the dune erosion model in conjunction with the stage-frequency relationships.

Unclassified

SECURITY CLASSIFICATION OF THIS PAGE

PREFACE

The coastal processes study reported herein was requested by the US Army Engineer District, New York (NAN), as part of a comprehensive plan of shore protection for Asbury Park to Manasquan, New Jersey. This investigation was conducted by personnel of the US Army Engineer Waterways Experiment Station (WES), Coastal Engineering Research Center (CERC), during the period March 1987 to September 1988. Ms. Lynn Bocamazo was the NAN Technical Monitor for this study.

This report presents the results of four interrelated technical tasks together with a short introduction to the study area with respect to target coastal processes. The four technical tasks include: (a) Nearshore Wave Refraction Study, (b) Numerical Modeling of Long-Term Shoreline Change, (c) Development of Stage Frequency Relationships, and (d) Numerical Modeling of Storm-Induced Dune Erosion. The principal investigator of each of the technical tasks authored that respective section of this report as follows: Parts II and III, Mr. Mark B. Gravens, Coastal Processes Branch (CPB), Research Division (RD), CERC; Part IV, Dr. Jon M. Hubertz, Coastal Oceanography Branch (COB), RD, CERC; and Part V, Dr. Norman W. Scheffner, CPB, RD, CERC. The overall report was edited by Mr. Gravens and Dr. Nicholas C. Kraus, RD, CERC. Dr. Kraus provided technical guidance and review throughout the study.

Work performed in the study was under the general supervision of Dr. James R. Houston and Mr. Charles C. Calhoun, Jr., Chief and Assistant Chief, CERC, respectively; and the direct supervision of Mr. H. Lee Butler, Chief, RD, CERC, and Dr. Steven A. Hughes, Dr. Lyndell Z. Hales, and Mr. Bruce A. Ebersole, former Chief, acting Chief, and Chief, CPB, respectively; and Drs. Edward F. Tompson, Jon M. Hubertz, and Marty C. Miller, former Chief, acting Chief, and Chief, COB, respectively.

Commander and Director of WES during publication of this report was COL Larry B. Fulton, EN. Technical Director was Dr. Robert W. Whalin.

CONTENTS

	<u>Page</u>
PREFACE	1
LIST OF TABLES	3
LIST OF FIGURES	4
CONVERSION FACTORS, NON-SI TO SI (METRIC) UNITS OF MEASUREMENT	7
PART I: INTRODUCTION	8
Scope of Work	8
Organization of this Report	9
Historical and Existing Conditions	10
PART II: WAVE REFRACTION ANALYSIS	14
WIS Data Analysis and Evaluation	14
Wave Hindcast	22
Nearshore Refraction Simulation	27
Wave Refraction Over Beach Fill Borrow Sites	33
PART III: LONG-TERM SHORELINE CHANGE	38
Introduction	38
Description of the Shoreline Change Model GENESIS	39
Model Calibration and Verification	45
Evaluation of Alternative Shore Protection Plans	59
PART IV: STAGE-FREQUENCY RELATIONSHIPS	79
Introduction	79
Methodology	81
Results	84
PART V: NUMERICAL MODELING OF STORM-INDUCED DUNE EROSION	90
Introduction	90
The Dune Erosion Model	90
Existing Conditions	94
Summary Existing Conditions	111
Beach Fill Design Alternatives	111
Summary Design Simulation	119
REFERENCES	126
APPENDIX A: NOTATION	A1
APPENDIX B: STATISTICS OF THE WAVE HINDCAST DATA BASE	B1
WIS Hindcast Summary	B1
Representative Time History of Wave Conditions	B1
APPENDIX C: NEARSHORE WAVE REFRACTION (MODEL RESULTS)	C1
APPENDIX D: PRELIMINARY DESIGN ALTERNATIVES (MODEL RESULTS)	D1

LIST OF TABLES

<u>Table</u>	<u>Page</u>
1 Potential Longshore Sand Transport Rates Using One Wave Condition per Angle Band	17
2 Potential Longshore Sand Transport Rates Using Several Wave Conditions per Angle Band (thousands of cu m per year)	19
3 Potential Longshore Sand Transport Rates Using an Averaged Phase III Wave Time History Derived from Phase II Stations 23 and 27	22
4 Summary of Frequency of Occurrence and Wave Height Characteristics from the WIS Hindcast for Asbury Park (Station 55) and Bay Head (Station 56)	24
5 Summary of Selected Yearly Statistics and Properties of the WIS Hindcast for Asbury Park (Station 55) and Bay Head (Station 56)	25
6 Wave Periods in Offshore Time History by Angle Band for Sea and Swell Wave Conditions	31
7 Increased Water Depths (ft) in Potential Beach Fill Borrow Site 4 .	36
8 Increased Water Depths (ft) in Potential Beach Fill Borrow Site 5 .	37
9 North Model Groin Permeabilities	58
10 South Model Groin Permeabilities	58
11 Existing Profile Characteristics	99
12 Recurrence Period (Years) for Storm-Induced Erosion of the Design Berm (including a 2.0 variability factor)	124
13 Comparison of Recession Simulation for Old and New Design Cross-Section	125
B1 Wave Statistics Categorized by Wave Approach Angle (Station 55) . .	B2
B2 Wave Statistics Categorized by Wave Approach Angle (Station 56) . .	B5
B3 Wave Statistics for the 20-Year Period (1956-1975)	B8
B4 Comparison of Annual Average Wave Height and Wave Events Categorized by Year and Approach Angle for Station 55 (Asbury Park)	B9
B5 Comparison of Annual Average Wave Height and Wave Events Categorized by Year and Approach Angle for Station 56 (Bay Head)	B10
B6 Annual Average Wave Height Analysis	B12
B7 Annual Average Events Analysis	B12
B8 Largest 250 Wave Heights in 20-Year Hindcast, Station 55 (Asbury Park)	B13
B9 Largest 250 Wave Heights in 20-Year Hindcast, Station 56 (Bay Head)	B18
B10 Summary of Storm Events In 250 Largest Waves	B23
B11 Rank of Storm Events By Year	B25

LIST OF FIGURES

<u>Figure</u>	<u>Page</u>
1 Location map for the study area	11
2 WIS Phase III hindcast stations	15
3 Potential longshore sand transport rates	18
4 RCPWAVE grid and angle band definition sketch.	21
5 Nearshore wave refraction grid	29
6 Potential beach fill borrow sites	34
7 Schematic illustration of an idealized equilibrium beach profile.	41
8 Calibration results.	49
9 Final verification, North Model	52
10 Average annual longshore sand transport rate, North Model	53
11 Final verification, South Model.	55
12 Average annual longshore sand transport rate, South Model.	56
13 Variability range, North Model.	60
14 Variability range, South Model.	61
15 North Model, without-project simulation.	64
16 South Model, without-project simulation.	65
17 North Model, revised 100-ft beach fill plan simulation.	66
18 South Model, revised 100-ft beach fill plan simulation.	67
19 North Model, revised 150-ft beach fill plan simulation	70
20 South Model, revised 150-ft beach fill plan simulation	71
21 North Model, revised 100-ft groin and beach fill plan simulation	74
22 South Model, revised 100-ft groin and beach fill plan simulation	75
23 North Model, revised 150-ft groin and beach fill plan simulation	76
24 South Model, revised 150-ft groin and beach fill plan simulation	77
25 Stage frequency curves for Sandy Hook, Monmouth Beach, and Long Beach Island, NJ	85
26 Stage frequency curve for Asbury Park to Manasquan, NJ	87
27 Stage frequency curves for hurricanes: Asbury Park to Manasquan, Monmouth Beach, and Long Beach Island, NJ	88
28 Stage frequency curves for northeasters: Asbury Park to Manasquan, Monmouth Beach, and Long Beach, NJ	89
29 Schematic dune-beach profile (after Kriebel 1984)	93
30 Existing profile locations	95
31 Cross-section of Profile 232	96
32 Cross-section of Profile 244	96
33 Cross-section of Profile 286	97
34 Cross-section of Profile 290	97
35 Shape coefficient A versus sediment diameter (from Moore 1982)	98
36 Hurricane recession-recurrence interval simulations for Profile 232	102
37 Northeaster recession-recurrence interval simulations for Profile 232	102
38 Hurricane recession-recurrence interval simulations for Profile 244	103
39 Northeaster recession-recurrence interval simulations for Profile 244	103
40 Hurricane recession-recurrence interval simulations for Profile 286	104

<u>Figure</u>	<u>Page</u>
41 Northeast recession-recurrence interval simulations for Profile 286	104
42 Hurricane recession-recurrence interval simulations for Profile 290	105
43 Northeast recession-recurrence interval simulations for Profile 290	105
44 Combined hurricane-northeast recession-recurrence interval design curve for Profile 232	106
45 Combined hurricane-northeast recession-recurrence interval design curve for Profile 244	107
46 Combined hurricane-northeast recession-recurrence interval design curve for Profile 286	108
47 Combined hurricane-northeast recession-recurrence interval design curve for Profile 290	109
48 Beach fill design configurations	112
49 Northeast recession-recurrence interval simulations for the 150/100/50 ft wide, 10 ft MSL high design berm	114
50 Northeast recession-recurrence interval simulations for the 150/100 ft wide, 8 ft MSL high design berm	114
51 Northeast recession-recurrence interval simulations for the 50 ft MSL width, 8 ft MSL high design berm	115
52 Hurricane recession-recurrence interval simulations for the 150/100 ft wide, 10 ft MSL high design berm	116
53 Hurricane recession-recurrence interval simulations for the 150/100 ft wide, 8 ft MSL high design berm	116
54 Hurricane recession-recurrence interval simulations for the 50 ft wide, 10 ft MSL high design berm	118
55 Hurricane recession-recurrence interval simulations for the 50 ft wide, 8 ft MSL high design berm	118
56 Combined hurricane-northeast recession-recurrence interval design curve for the 150/100 ft wide, 10 ft MSL high design berm	120
57 Combined hurricane-northeast recession-recurrence interval design curve for the 50 ft wide, 10 ft MSL high design berm . . .	121
58 Combined hurricane-northeast recession-recurrence interval design curve for the 150/100 ft wide, 8 ft MSL high design berm .	122
59 Combined hurricane-northeast recession-recurrence interval design curve for the 50 ft Wide, 8 ft MSL high design curve . . .	123
C1 Sea conditions; wave height, T = 4.0 sec	C2
C2 Sea conditions; wave angles, T = 4.0 sec	C3
C3 Sea conditions; wave height, T = 5.0 sec	C4
C4 Sea conditions; wave angles, T = 5.0 sec	C5
C5 Sea conditions; wave height, T = 6.0 sec	C6
C6 Sea conditions; wave angles, T = 6.0 sec	C7
C7 Sea conditions; wave height, T = 7.0 sec	C8
C8 Sea conditions; wave angles, T = 7.0 sec	C9
C9 Sea conditions; wave height, T = 8.0 sec	C10
C10 Sea conditions; wave angles, T = 8.0 sec	C11
C11 Sea conditions; wave height, T = 9.0 sec	C12
C12 Sea conditions; wave angles, T = 9.0 sec	C13
C13 Swell conditions; wave height, T = 6.0 sec	C14

Figure

Page

C14	Swell conditions; wave angles, T = 6.0 sec	C15
C15	Swell conditions; wave height, T = 7.0 sec	C16
C16	Swell conditions; wave angles, T = 7.0 sec	C17
C17	Swell conditions; wave height, T = 8.0 sec	C18
C18	Swell conditions; wave angles, T = 8.0 sec	C19
C19	Swell conditions; wave height, T = 9.0 sec	C20
C20	Swell conditions; wave angles, T = 9.0 sec	C21
C21	Swell conditions; wave height, T = 10.0 sec	C22
C22	Swell conditions; wave angles, T = 10.0 sec	C23
C23	Swell conditions; wave height, T = 11.0 sec	C24
C24	Swell conditions; wave angles, T = 11.0 sec	C25
C25	Sea conditions; borrow site effect, T= 4.0 sec	C26
C26	Swell conditions; borrow site effect, T = 7.0 sec	C27
D1	North Model, 50-ft beach fill plan simulation	D2
D2	South Model, 50-ft beach fill plan simulation	D3
D3	North Model, 100-ft beach fill plan simulation	D4
D4	South Model, 100-ft beach fill plan simulation	D5
D5	North Model, 150-ft beach fill plan simulation	D6
D6	South Model, 150-ft beach fill plan simulation	D7
D7	North Model, 50-ft groin and beach fill plan simulation	D8
D8	South Model, 50-ft groin and beach fill plan simulation	D9
D9	North Model, 100-ft groin and beach fill plan simulation	D10
D10	South Model, 100-ft groin and beach fill plan simulation	D11
D11	North Model, 150-ft groin and beach fill plan simulation	D12
D12	South Model, 150-ft groin and beach fill plan simulation	D13

CONVERSION FACTORS, NON-SI TO SI (METRIC)
UNITS OF MEASUREMENT

Non-SI units of measurement used in this report can be converted to SI (metric) units as follows:

<u>Multiply</u>	<u>By</u>	<u>To Obtain</u>
cubic yards	0.7646	cubic meters
cubic yards per year	0.7646	cubic meters per year
feet	0.3048	meters
feet per second	0.3048	meters per second
inches	2.54	centimeters
knots (international)	0.5144444	meters per second
miles (US statute)	1.6093	kilometers
miles (nautical)	1.8520	kilometers
yards	0.9144	meters

COASTAL PROCESSES AT ASBURY PARK TO MANASQUAN, NEW JERSEY

PART I: INTRODUCTION

Scope of Work

1. The US Army Engineer Waterways Experiment Station (CEWES), Coastal Engineering Research Center (CERC), was requested to provide technical assistance to the US Army Engineer District, New York (CENAN), in an engineering study of coastal processes along the Atlantic coast from Asbury Park to Manasquan, New Jersey. The study was funded through three DA Form 2544 "Intra-Army Orders for Reimbursable Services" dated 5 March 1987, 16 February 1988 and 18 May 1988.

2. The purpose of the study was to interpret data to assist in the evaluation and implementation of CENAN's comprehensive shore protection plan for this highly utilized stretch of coastline. The long-term performance of various proposed shore protection designs were evaluated through the use of predictive engineering tools. The effect of short-term storm events, including storm surge (stage-frequency) and storm-induced dune erosion, were investigated using a probabilistic approach.

3. Technical portions of the present study were accomplished through four interrelated tasks. The individual tasks are:

- a. Task 1: Nearshore wave refraction study.
- b. Task 2: Numerical modeling of long-term shoreline change.
- c. Task 3: Development of stage-frequency relationships.
- d. Task 4: Numerical modeling of storm-induced beach erosion.

The results of these four tasks are presented in this report.

4. The nearshore wave refraction study (Task 1) encompassed a hindcast of the offshore wave climate and an analysis of the wave hindcasts results with respect to wave shadowing by Long Island and its effect on potential longshore sand transport rates. Wave refraction calculations were made for waves propagating over the existing nearshore bathymetry as well as over a hypothetical bathymetry as modified by possible beach fill borrow dredging.

5. Task 2, numerical modeling of long-term shoreline change, involved the application of a shoreline change numerical model which is driven primarily by the wave information produced in Task 1. The shoreline change model allows the inclusion of groins, jetties, seawalls, and beach fills. The coastal structures implemented in the numerical model may be arbitrarily re-specified both in their physical and spatial characteristics in successive model runs to account for different shore protection designs. Therefore, the design specifications may include the placement of new groins, removal of existing groins, and the arbitrary specification of beach fill locations and placement volumes.

6. Task 3, development of stage-frequency relationships, is the extension of the stage-frequency task in a companion CERC study "Coastal Processes at Sea Bright to Ocean Township, New Jersey" (Kraus et.al. 1988), in which data from another CERC study, the "Fire Island to Mountalk Point Storm Surge Study (FIMP)" (Butler and Prater 1987) were utilized to compute stage-frequency relationships for the Sea Bright to Ocean Township reach. In the present study, results from these previous studies are correlated with those from past studies (which resulted in stage-frequency curves for nearby locations) to infer the stage-frequency relationship for the project area.

7. The beach erosion model utilized in Task 4 estimated storm-induced erosion of beach fill material placed as part of the overall shore protection design. The primary results of this task are dune recession-recurrence curves for both existing and design conditions. These curves are calculated through the use of a numerical cross-shore sand transport model and the storm statistics produced in Task 3.

Organization of this Report

8. This report is divided into five parts. Part I gives an introduction, provides a short review of related literature, and summarizes important previous work. Parts II through V present the results of the four individual study tasks listed in paragraph 3.

9. In conformance with the trend in the United States to employ SI (metric) units of measurement in engineering and science, calculations and

data analyses associated with the numerical models employed in this study were performed and reported in metric units. Most historical engineering work for the New Jersey coast has been done in American customary units, whereas in the related scientific literature dealing with this coast numerical values are given in metric form. For tasks 1, 2, and 4, numerical values have usually been expressed in metric form; however, certain tables and citations contain customary unit conversions. In particular, customary units were employed in discussion of previous engineering results and design specifications in order to provide continuity and ease of cross reference. A table containing conversion factors is given on page 7.

Historical and Existing Conditions

10. This section gives a review of previous work to provide a summary of independent results and data pertinent to the study. Important sources of supplementary information are identified, and an orientation to the study area is given.

11. Orientation to the study area. Detailed and comprehensive background information, as well as the original authorized plan, can be found in the CENAN study report entitled "Atlantic Coast of New Jersey, Sandy Hook to Barnegat Inlet, Beach Erosion Control Report on Cooperative Study (Survey)" (CE 1954). This report should be consulted for the history and original design of the project. The authorized project discussed in this report concerns the approximately 51-mile-long (82 km) stretch of coast from Sea Bright to Barnegat Inlet. In the original improvement plan, the northern portion of this stretch is divided into four regions: Sandy Hook, Sea Bright to Ocean Township, Asbury Park to Manasquan, and Point Pleasant Beach to Seaside Park (CE 1954, p 2 and Table D-1 therein).

12. The present study area is the approximately 8.5-mile-long stretch of coast between Asbury Park and Manasquan, New Jersey (Figure 1). The beaches in the study area are heavily structured, including 81 groins in various states of deterioration, two structurally stabilized tidal inlets, and intermittent sections of sheet pile and wood bulkheads. In general, the beaches within the project area range from approximately 150- to 25-ft wide

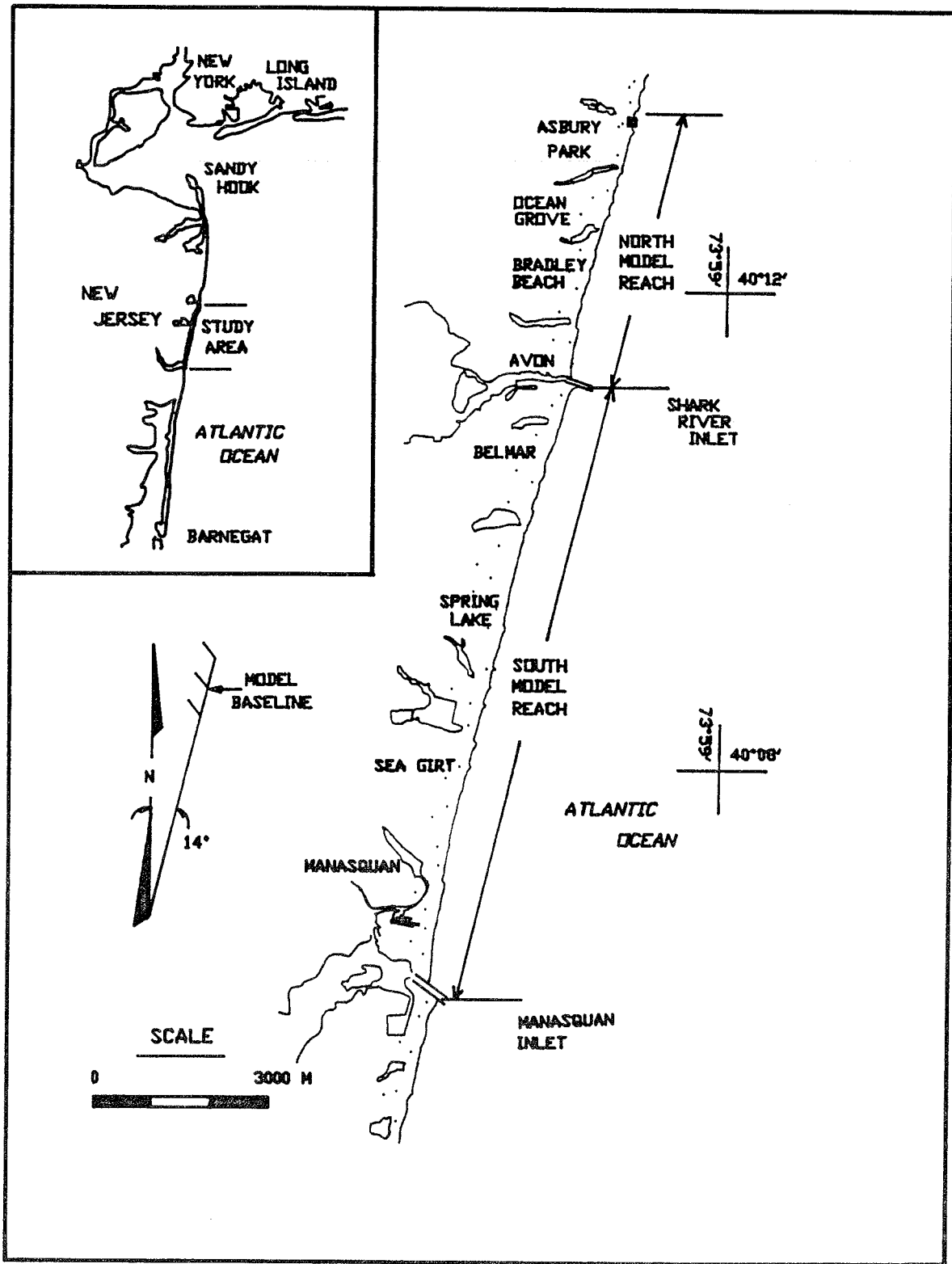


Figure 1. Location map for the study area

and are typically backed by a board walk or bulkhead. There is essentially no coastal dune structure along the project reach. The beaches north of Shark River Inlet range from moderate to narrow in width (typically less than 60 ft), where as the beaches in Belmar (just south of Shark River Inlet) are widest (on the order of 150 ft) observed in the project area. From Belmar south, the beaches tend to become narrower except at Manasquan where a fairly wide beach with comparably high elevation exists adjacent to the north Manasquan Inlet jetty. A detailed field observation report was prepared by Coastal Planning and Engineering / URS Co. (1987) as part of CENAN's comprehensive feasibility study.

13. Previous studies. The Sea Bright to Ocean Township region was the subject of a previous CERC study conducted for NAN between January 1985 and August 1986 (Kraus et al. 1988; Kraus, Gravens, and Mark 1988). This comprehensive study of coastal processes along New Jersey's northern Atlantic shoreline from Sandy Hook to Shark River Inlet provided the basis for the present study. In this study, many procedural guidelines and techniques for the conduct of regional coastal processes modeling studies were established. Although the numerical models utilized in the Sea Bright to Ocean Township study were again used in the present study, the results of the two are not directly comparable because different procedures were used in determining the incident wave climate and in the treatment of the groin boundary condition. These differences are discussed in detail in Parts II and III.

14. An annotated bibliography on coastal literature of the New Jersey coast is given in a CERC report (Gorman 1989) companion to this project. Other pertinent references for general historical and geological information may be found in the work of Kondolf (1978), Gares (1981), Allen (1981), Phillips, Psuty, and McCluskey (1984), and Phillips (1985). Although Sandy Hook is the primary coastal area studied in these papers, the development and continued evolution of Sandy Hook is dependant on coastal processes and sediment supplies within and north of the project area.

15. In contrast to the many geomorphology studies that have been made for Sandy Hook, few published coastal engineering studies can be found for the heavily developed coast to the south, including the present project area. The most well-known coastal engineering study encompassing the project area is the

budget analysis performed by Caldwell (1966) for the New Jersey coast. This study has served as the basis for most subsequent sediment transport work on the New Jersey coast and will be described in detail.

16. Caldwell (1966) made a budget analysis for the New Jersey coast using shoreline survey data available from 1838 to 1953. Most of the shoreline data used by Caldwell appears to be based on work done in the 1954 CE report. Additional data such as impoundment rates at the north jetty of Cold Springs Inlet at Cape May Harbor supplemented the shoreline position data from Barnegat Inlet north to Sandy Hook in the 1954 CE report. Local average yearly longshore sediment transport rates were inferred through shoreline change mapping. The transport rates were based mainly on aerial changes between shoreline surveys. Four shoreline reaches between Barnegat Inlet and Sandy Hook were examined by Caldwell (1966). A nodal point or bifurcation in the longshore transport was found to lie between Barnegat Inlet to the south and Manasquan Inlet to the north, at Dover Township. This result has been reaffirmed and discussed in subsequent studies (Fairchild 1966, Ashley, Halsey, and Buteux 1986) and is the generally accepted conceptual longshore sand transport regime on the New Jersey coast.

17. Net transport rates north of Dover Township were found to be directed to the north, increasing from zero entering the section Mantoloking to Manasquan, and 74,000 yd³/year leaving. The next shoreline reach Caldwell examined coincides with the boundaries of the present project, Manasquan Inlet to Asbury Park. He estimated that 74,000 yd³/year enters the reach at Manasquan Inlet and that 319,000 yd³/year leaves the reach at Asbury Park. Caldwell estimated average annual longshore sand transport rates of 493,000 yd³/year at Sandy Hook.

18. Caldwell (1966) estimated gross longshore sand transport rates on the order of 500,000 yd³/year, to the north all along the New Jersey coast. He went on to state that the gross sand transport rate to the south increased to the south and that a reversal in net littoral drift occurs between Manasquan Inlet and Barnegat Inlet. Potential longshore sand transport rates calculated in the present study, as part of the hindcast wave data analysis (Part II), agree well with Caldwell's (1966) estimates.

PART II: WAVE REFRACTION ANALYSIS

19. This chapter describes procedures and results of the wave refraction task of the study. The wave refraction task consisted of four steps. The first step was an analysis and evaluation of the Wave Information Study (WIS) hindcast data base (Jensen 1983b). Second, the WIS technique was used to generate a Phase III-type 20-year hindcast time history of wave height, direction, and period at two stations along the project coast. One station (WIS Station 55, Figure 2) was located at the northern boundary of the study area off of Deal Lake and the other station (WIS Station 56, Figure 2) at the southern boundary offshore of Bay Head. In the third and fourth steps, a numerical model of wave refraction was employed to obtain a time history of representative wave conditions in shallow water at fixed points alongshore. In the third step, the existing nearshore bathymetry was input to the wave refraction model, and in the fourth step wave refraction was computed over a hypothetical bathymetry which included three excavated beach fill borrow sites.

WIS Data Analysis and Evaluation

20. This sub-task was performed to determine if an adequate accounting of wave energy sheltering or wave shadowing by Long Island is contained in the WIS data for stations located off the northern coast of New Jersey. Wave shadowing by Long Island and the resultant change in wave properties along New Jersey's Atlantic coast is responsible for the overall evolution of the shoreline and the formation of Sandy Hook. As discussed in Part I, the gross longshore sand transport rate to the south increases from Sandy Hook to Barnegat Inlet. This causes a differential net longshore transport rate along the project coast. In fact, the gross transport rate to the south increases to a point where the net transport rate reverses from northerly (north of Manasquan Inlet) to southerly (south of Barnegat Inlet)(Calwell 1966). In order to simulate differential transport rates in the shoreline change model the input wave conditions must contain both a differential in wave height and incident wave angle along the coast. A previous study performed by CERC for

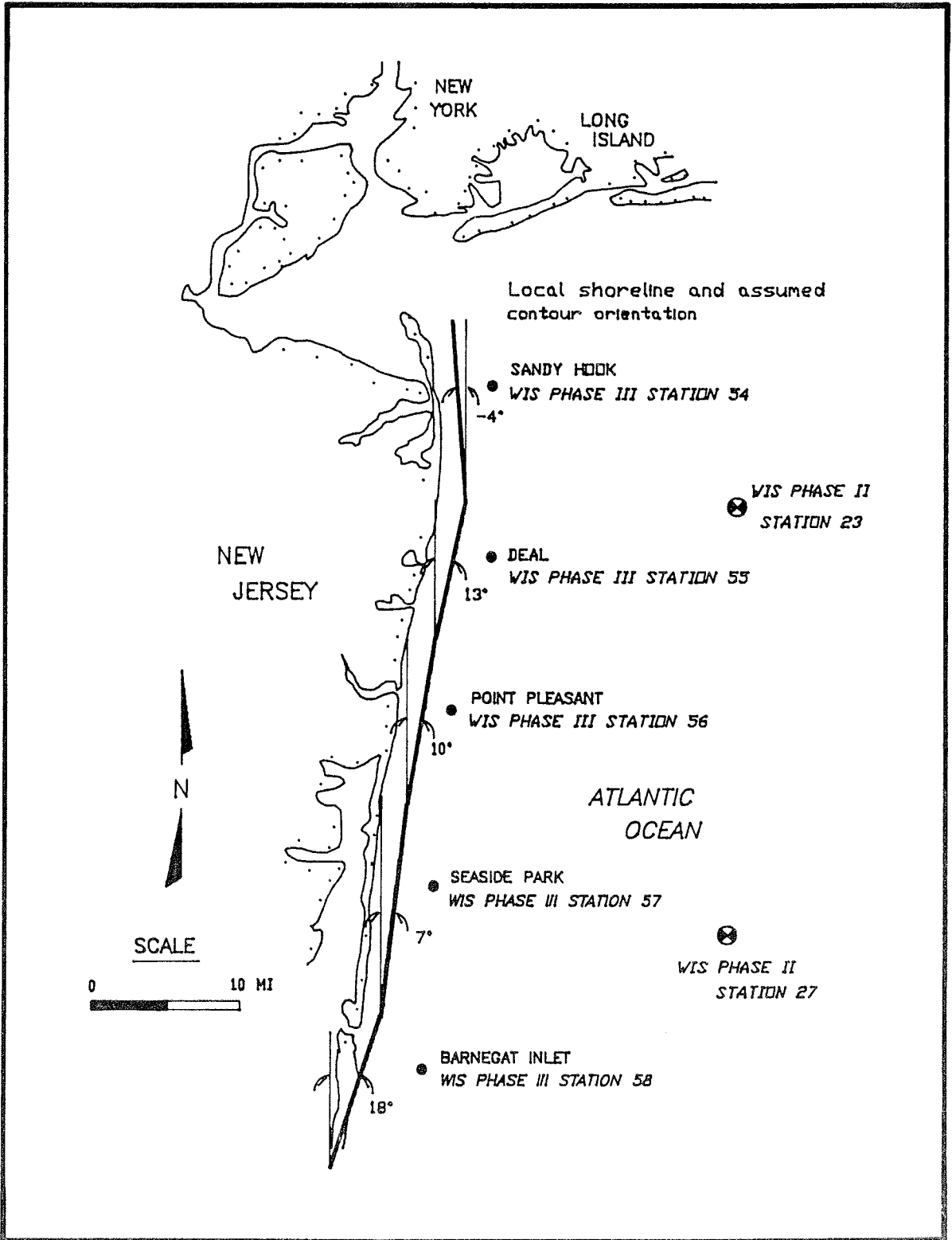


Figure 2. WIS Phase III hindcast stations

the neighboring reach north of the subject study (Kraus et al. 1988) concluded that in order to obtain the correct magnitude and differential in longshore sand transport rates along the coast, wave shadowing by the large land mass of Long Island must be represented in the nearshore wave field.

Desk study

21. Summary wave statistics from the WIS 20-year hindcasts reported in WIS report No. 9 (Jensen 1983a) were used to calculate potential longshore sand transport rates for WIS Phase III Stations 54, 55, 56, 57, and 58. Figure 2 gives the locations of the Phase III stations investigated and illustrates the local shoreline and the assumed contour orientation. The calculated net longshore sand transport rates were directed to the north and increased in magnitude to the north (except for between Stations 57 and 56) from Station 57, south of Seaside Park, to Station 54 at Highland Beach. The net transport rate at Station 58 near Barnegat Inlet was directed to the south. The longshore sand transport rates were calculated using linear wave theory and the energy flux method discussed in the Shore Protection manual Chapter 4 (SPM 1984). A detailed discussion of the calculation procedures used is given by Gravens (1988 and 1989).

22. Potential longshore sand transport rates were calculated using an average wave height and a weighted average wave period for each angle band given in the wave statistics tables. Additionally, the shoreline orientation angle was re-evaluated by plotting the location of the Phase III stations on National Oceanic and Atmospheric Administration (NOAA) nautical chart no. 12123 and measuring the local shoreline orientation. Potential longshore sand transport rates were also calculated for the new shoreline orientations. The calculated net transport rates are given in Table 1, positive values indicate transport directed to the north and negative values to the south.

23. Results of these preliminary calculations were encouraging in that the net transport rates produced were in the proper direction (to the north), and they decreased in magnitude to the south with a reversal at Station 58. The magnitude of the transport rates are, however, small compared to transport rates inferred from historical shoreline change (see Part I).

24. The next step taken in the desk study was the recalculation of potential longshore transport rates using a more refined discretization of the

available wave data. The median wave height for each of the reported wave height bands together with a weighted average wave period for each wave height band were used to calculate the potential longshore sand transport rate. This procedure resulted in an increase in the calculated transport rates. In fact, the transport rates given in Table 2 are well correlated with those inferred from historical shoreline change. The estimated longshore sand transport rates calculated in this study are compared to Caldwell's (1966) estimates in Figure 3.

Table 1
Potential Longshore Sand Transport Rates
Using One Wave Condition per Angle Band

<u>WIS Station</u>	<u>Longshore Transport Rate (cu m per year)</u>	<u>Shoreline Orientation (deg)</u>
54	120,000	356 *
54	73,000	4
55	68,000	13
56	31,000	10 *
56	40,000	9
57	31,000	7 *
57	28,000	12
58	-176,000	18 *
58	-125,000	12

* Shoreline orientation recalculated by locating stations on NOAA nautical chart No. 12123.

25. In summary, longshore sand transport rates with magnitudes on the order of those reported historically can be calculated using statistical summaries from WIS and a standard sand transport rate predictive formula. The wave information in the WIS hindcast data includes the effect of wave energy shadowing by northern land masses (Long Island). Sand transport rates based on WIS hindcast data will result in differential sand transport increasing to the north and a reversal in the net transport direction at some location north of Barnegat Inlet.

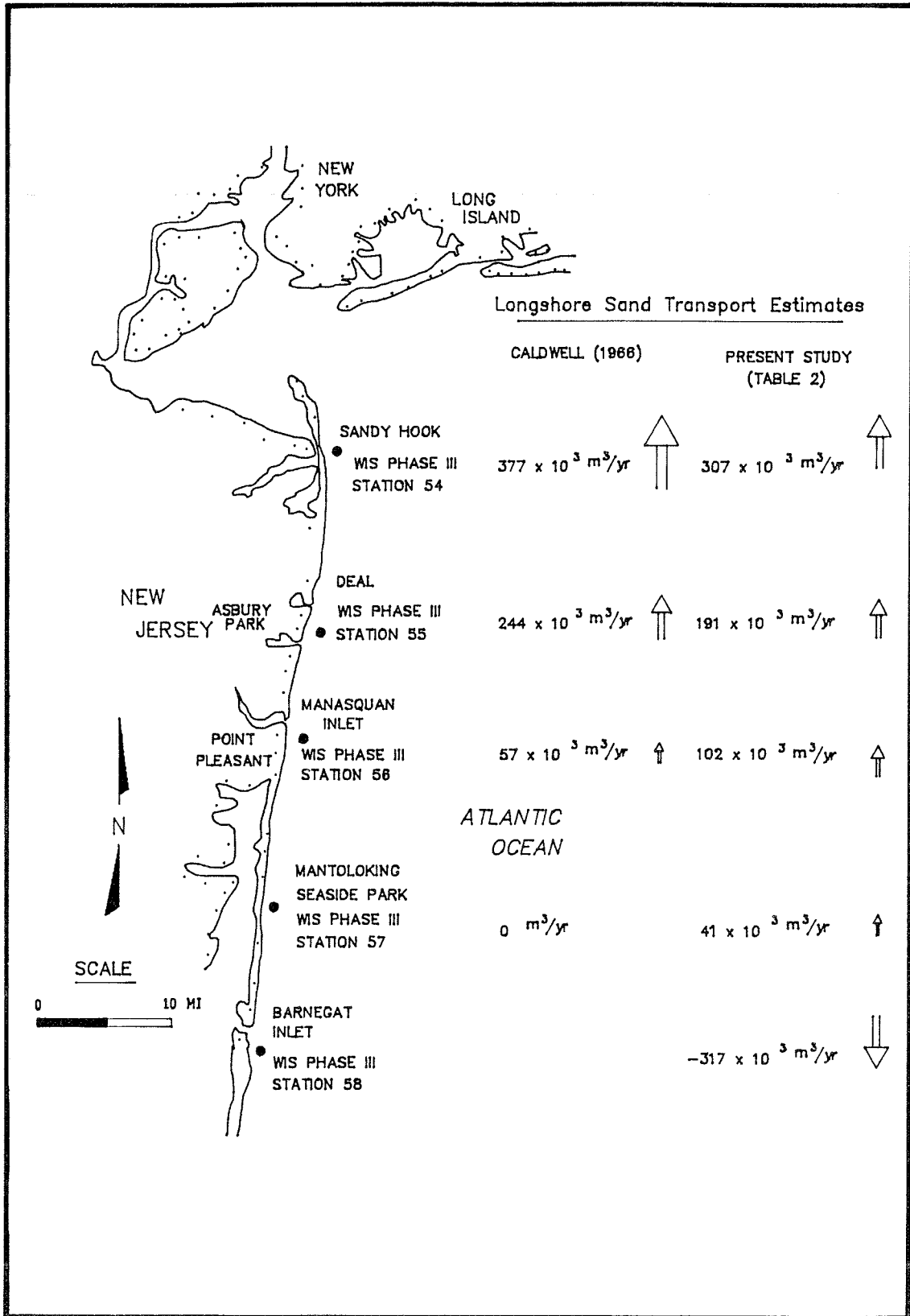


Figure 3. Potential longshore sand transport rates

Table 2
Potential Longshore Sand Transport Rates
Using Several Wave Conditions per Angle Band
(thousands of cu m per year)

Angle Band (central angle)	WIS Phase III Station				
	54	55	56	57	58
-75	0	0	0	0	-7
-45	0	-2	-22	-112	-234
-15	-85	-216	-248	-222	-419
15	196	114	104	115	54
45	188	276	247	246	257
75	8	19	21	14	32
TRANSPORT NORTH	392	409	372	375	343
TRANSPORT SOUTH	85	218	270	334	660
GROSS	477	627	642	709	1003
NET	307	191	102	41	-317

Use of Shadowing Effects Inherent in WIS Data

26. The results of the desk study described above substantiated the fact that the effect of shadowing is included in the WIS hindcast data. The next step was to determine a procedure to take advantage of the data base and represent the shadowing effect in the nearshore wave transformation model and, ultimately, in the shoreline change model. Table 2 shows that the longshore component of wave energy producing sand transport to the north is nearly constant for Phase III Stations 54, 55, 56, and 57. The differences in the calculated net transport rates are the result of the amount of wave energy producing longshore sand transport to the south. The wave parameters which determine longshore sand transport rates are wave height and angle of incidence to the shoreline. Hence, a gradient (or difference in the frequency of occurrence) must exist in the wave height and incident angle of waves approaching from the north between adjacent Phase III stations. The methodology developed for including this effect in the present study is described below.

27. A Phase III-type WIS wave transformation was performed from Phase II Station 23 to a depth equivalent to the offshore boundary of the RCPWAVE bathymetry grid. The transformation assumed one-sided shadowing from 180 to 130 deg (shadowing angles are measured counter-clockwise with respect to the shoreline; see Brooks and Corson (1984)) and a shoreline orientation angle of 13 deg. The resulting 20-year time history of wave conditions was assumed representative of the wave climate at the northern boundary of the project site (off of Asbury Park) in a water depth of 18.6 m (61 ft). In order to obtain a 20-year time history of wave conditions representative of the wave climate at the southern end of the project site, another Phase III WIS wave transformation was performed from Phase II Station 27 to a depth equivalent to the offshore boundary of the RCPWAVE bathymetry grid. This second transformation again used one-sided shadowing from 180 to 130 deg, but the shoreline orientation was specified to be 10 deg consistent with the local trend of the shoreline.

28. The two 20-year time histories were then analyzed, and an average wave height and incident angle gradient was calculated for each angle band. Figure 4 provides an illustration of the interrelationship between the two hindcast stations, the RCPWAVE grid, and the definition of the angle bands. Additionally, the two time histories were independently analyzed, and a 3-year-long time history statistically representative of the 20-year time history at both stations was selected.

29. The 3-year-long time series of wave conditions at the northern and southern stations was then averaged to obtain wave conditions representative of those that could be expected midway between Asbury Park and Manasquan Inlet. In the execution of RCPWAVE, the wave characteristics from the averaged time history were input in the middle of the grid and the calculated wave height, and incident wave angle gradients were utilized to interpolate wave conditions along the offshore boundary of the grid.

30. The above-described procedure was utilized to determine if the time series at two neighboring Phase III stations would be compatible (easily averaged), and if the results of such a procedure would produce reasonable estimates of differential longshore sand transport along the project reach. In order to test the procedure, a one-year-long time history of wave

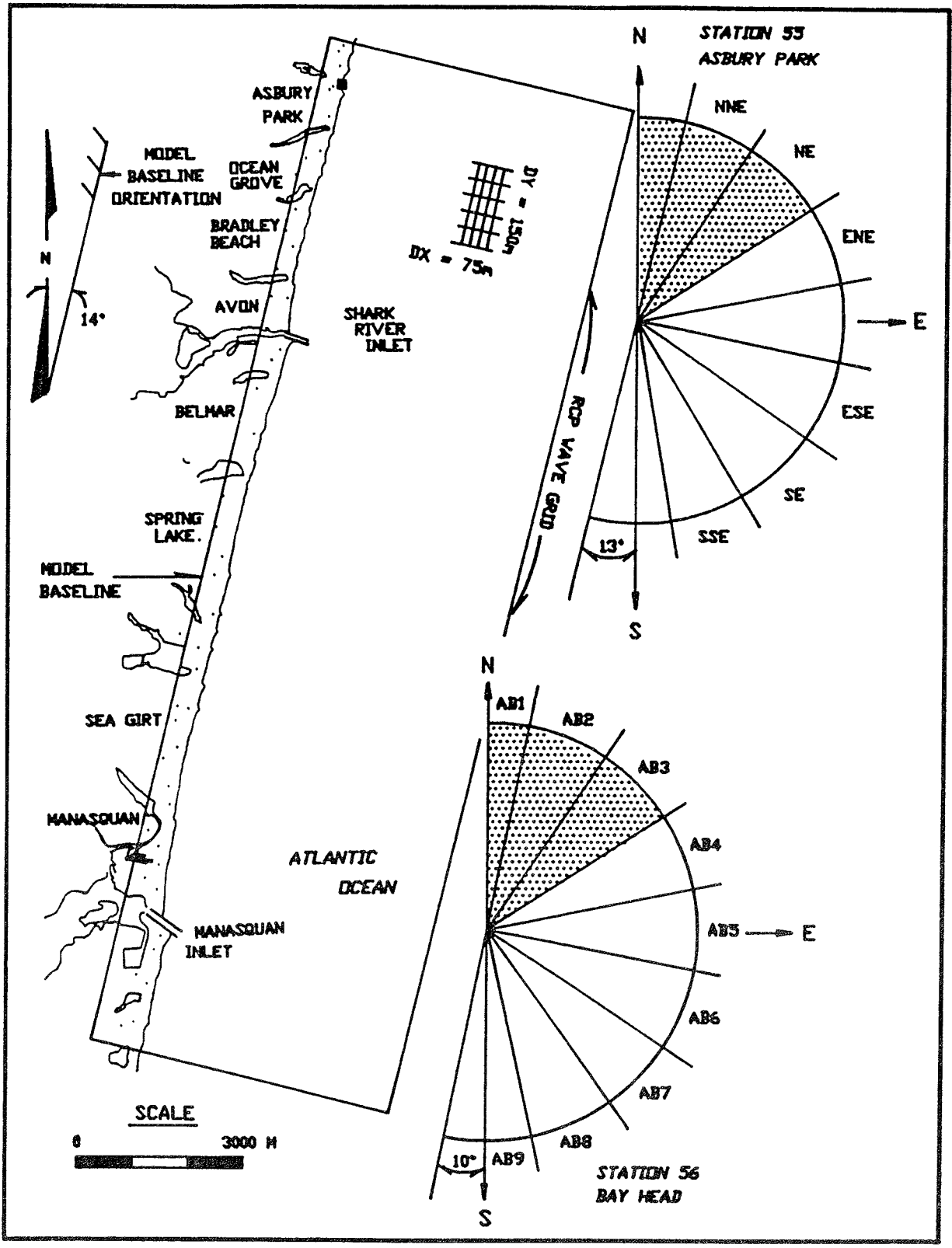


Figure 4. RCPWAVE grid and angle band definition sketch

conditions for WIS Phase III Station 55 was obtained using WIS Phase II Station 23 as input. Another 1-year-long time history of wave conditions for WIS Phase III Station 56 was obtained using WIS Phase II Station 27 as input. Potential longshore sand transport rates were then calculated at both stations using the averaged time series. The input wave heights were increased or decreased by half the calculated wave height and angle gradient. The results of these calculations are given in Table 3.

Table 3

Potential Longshore Sand Transport Rates Using an Averaged Phase III Wave Time History Derived From Phase II Stations 23 and 27

Asbury Park (Phase III Station 55)	
<u>Source</u>	<u>Sand Transport (cu m per year)</u>
Sea	175,000 north
Swell	72,000 north
Combined	247,000 north

Bay Head (Phase III, Station 56)	
<u>Source</u>	<u>Sand Transport (cu m per year)</u>
Sea	135,000 north
Swell	40,000 north
Combined	175,000 north

Differential Sand Transport Rate: 72,000 cu m per year

Wave Hindcast

31. No long-term wave measurements are available for the vicinity of the project. Therefore, the required wave information was generated by means of the WIS hindcast technique. WIS provides a 20-year hindcast for the US Atlantic Ocean coast for the years 1956 through 1975. Phase II of this hindcast includes a 20-year time history of wave height, wave direction, and wave period at 3-hr intervals for both sea and swell components at three points off the New Jersey coast. As stated in the previous section the time history of wave conditions at WIS Phase II Stations 23 and 27 (shown in

Figure 2) were used as input to the Phase III transformation technique. This technique involves transformation of deepwater wave conditions to a specified water depth taking into account the effects of wind-wave interaction, refraction and shoaling over straight and parallel bottom contours, and the sheltering of wave energy by Long Island.

32. Although WIS Phase III information for the area of the project site is available at Stations 55 and 56, which lie approximately at the north and south ends of the project site in water depths of 10 m, special Phase III runs were made to compute the hindcast wave time history at the depth of the seaward boundary of the nearshore wave refraction grid. The WIS transformations were therefore halted at a depth of 18.6 m (61 ft) MLW. Since the Phase III technique does not adequately describe wave propagation and transformation over irregular and greatly varying nearshore bathymetry, a fine-meshed nearshore grid and wave refraction model (Figure 4) were employed to bring the waves into shallower water, with the WIS hindcast providing the input.

Characteristics of the wave hindcast data set

33. Each year of the hindcast contains calculated estimates of the significant wave height, peak spectral period, and peak spectral direction for both locally generated sea and swell conditions at 3-hr intervals. Actually, WIS provides an estimate of an energy-based wave height call H_{mo}^* ; however, for deep water, H_{mo} is effectively equal to the significant wave height H_s which by definition is the average of the highest one-third of the waves in the record or observation. General statistics were compiled for the hindcasts at Asbury Park (Station 55) and Bay Head (Station 56). A complete listing of the statistics for both stations is given in Appendix B and a summary is provided in Tables 4 and 5. Table 4 summarizes characteristics of the hindcasts according to direction of wave approach, and Table 5 gives a comparative summary of the significant wave height and peak spectral period by year. The orientation of the coast, location of the hindcast stations, and the definition of the angle bands is given in Figure 4.

* For convenience, symbols and abbreviations are listed in the Notation, Appendix A.

34. Table 4 shows that between 58 and 67 percent of the hindcast waves originated out of the southern sector (from S through ESE), approximately 15 percent were from the east, and between 7 and 13 percent were out of the east-northeast. Between 11.2 (for Station 55, at Asbury Park) and 14.6 percent (for Station 56, at Bay Head) of the time calm conditions existed indicating that the sea and swell wave conditions were negligible or absent. The zero occurrences given in Table 4 for the northern sector angle bands result from wave shadowing by Long Island, New York.

Table 4

Summary of Frequency of Occurrence and Wave Height Characteristics from the WIS Hindcast for Asbury Park (Station 55) and Bay Head (Station 56)

	<u>Station</u>	<u>N</u>	<u>NNE</u>	<u>NE</u>	<u>ENE</u>	<u>E</u>	<u>ESE</u>	<u>SE</u>	<u>SSE</u>	<u>S</u>
Percent	55	0.0	0.0	0.0	7.0	14.9	6.7	11.7	27.9	20.6
Occur.	56	0.0	0.0	0.0	12.7	14.4	8.6	8.4	23.6	17.7
Average	55	0.00	0.00	0.00	0.39	0.84	0.75	0.56	0.57	0.37
H _s (m)	56	0.00	0.00	0.00	0.54	0.89	0.63	0.67	0.57	0.37
Maximum	55	0.00	0.00	0.00	2.29	6.86	4.09	4.31	3.98	2.49
H _s (m)	56	0.00	0.00	0.00	3.22	6.66	4.32	4.37	3.46	2.21

35. Summarizing the data in Table 5, it is seen that for both stations combined, the average significant wave height for the 20-year hindcast is 0.50 m and the average maximum annual significant wave height is 3.79 m. The average maximum annual significant wave height at Asbury Park (Station 55) is 3.75 m whereas at Bay Head (Station 56) the average maximum annual significant wave height is 3.83 m. The peak spectral wave period varies between 5 and 9 sec annually; however, a peak spectral wave period of 7 sec occurs most frequently in the 20-year hindcast record. The column labeled "Storm Events" in Table 5 gives the ordinal number of the 60 largest storms occurring at both stations in the 20-year hindcast for the associated year.

Wave sheltering

36. The WIS Phase III wave transformation technique allows for wave sheltering by large land masses. In the present case, Long Island restricts

Table 5

Summary of Selected Yearly Statistics and Properties
of the WIS Hindcast for Asbury Park (Station 55) and Bay Head (Station 56)

Year	Station	H_{savg} (m)	T_p (sec)	H_{smax} (m)	Storm Events	Greater than H_{savg}
1956	55	0.56	7	3.33	29,30	yes
	56	0.59	7	3.70		yes
1957	55	0.51	7	3.27	28	yes
	56	0.51	7	3.47		yes
1958	55	0.48	7	3.36	24,46,48,56	no
	56	0.50	7	3.47		-
1959	55	0.43	5,7	3.37	32,60	no
	56	0.42	5	3.33		no
1960	55	0.49	7	3.66	18,26,53	no
	56	0.51	5,9	3.44		yes
1961	55	0.54	9	3.43	11,22,34,52	yes
	56	0.55	9	3.85		yes
1962	55	0.53	5,7	6.86	1,15,38,40, 51,58	yes
	56	0.55	5	6.66		yes
1963	55	0.45	7	2.98	none	no
	56	0.44	7	2.92		no
1964	55	0.53	7	3.67	5,20,39,45,55	yes
	56	0.54	7	4.35		yes
1965	55	0.44	7	3.34	21,41	no
	56	0.42	7	3.49		no
1966	55	0.45	7	3.76	14,17	no
	56	0.44	7	3.35		no
1967	55	0.55	9	3.21	36,47	yes
	56	0.50	9	3.34		-
1968	55	0.45	7	3.28	23,27,49,57	no
	56	0.46	9	3.54		no
1969	55	0.55	7	3.68	12,37	yes
	56	0.54	7	3.52		yes
1970	55	0.48	7	3.59	16,54,59	no
	56	0.50	7	3.48		-
1971	55	0.53	7	3.32	31,33,35,50	yes
	56	0.54	7	3.76		yes
1972	55	0.55	7	4.61	2,8,42,43,44	yes
	56	0.53	7	4.25		yes
1973	55	0.54	7	4.31	4,10,13,19	yes
	56	0.52	7	4.37		yes
1974	55	0.51	7	4.20	3,7,25	yes
	56	0.49	7	4.52		no
1975	55	0.49	7	3.85	6,9	no
	56	0.50	7	3.86		-
AVG		0.50	7	3.79		

Notation: H_{savg} , H_{smax} denote average and maximum significant wave height, respectively; T_p denotes the peak spectral wave period.

the fetch of winds and propagation of waves out of the north directed towards the New Jersey coast. The directional distribution of the potential wave population is modified in two ways if sheltering enters the hindcast. For wind seas, the energy within discrete direction bands is removed (zeroed) if the orientation of the sheltering land body would preclude propagation of wave in the band. For the swell component, all energy in the geometric shadow zone of the land mass is removed. Through the desk study it was determined that the shadowing effect of Long Island is greatest at Sandy Hook and decreases with distance to the south. Because the differential effect of shadowing with distance along the coast is important within the project reach, two hindcast transformations were performed as discussed in paragraphs 27 through 30. Wave height and wave angle gradients between the two hindcast stations were calculated for the individual angle bands shown in Figure 4. The 20-year-long hindcast time histories of sea and swell wave conditions were used in these calculations. These wave height and angle gradients were developed to be used in interpolating input wave conditions along the offshore boundary of the wave transformation model from an averaged input wave condition read from the representative time history of sea and swell wave conditions.

Selection of representative wave conditions

37. The shoreline model (described in Part III) requires input of wave conditions which serve as the primary driving force for the calculation of longshore sand transport and shoreline change. Because the verification period (1977-1987) is not encompassed by the hindcast, and because the model will be used to predict future shoreline changes, a time history of representative wave conditions is required. Since the purpose of the model is to simulate shoreline change occurring over several years, unusually high wave energy and low wave energy years in the hindcast were avoided. The effects of such extremes were simulated, however, in the sensitivity tests performed to investigate the range of variability of shoreline change predictions. The consequences of severe storm events are treated with the beach erosion model, discussed in Part V.

38. Representative wave data were developed for use in both the calibration and verification of the shoreline contour model to historical (surveyed) shoreline change and for the prediction of future shoreline change.

The statistics of average significant wave height and frequency of occurrence by angle band for the entire 20-year hindcast period and annually, were used to select a 3-year-long representative wave climate for the project reach. A more thorough description of the procedure used to select the representative time history of wave conditions is given in Appendix B. The years 1970, 1972, and 1974 were selected (based on the analysis discussed in Appendix B) for composing this representative wave climate. The statistics for these years (for the wave parameters of interest, e.g., H_s and percent occurrence by angle band) are typically within plus or minus one standard deviation of the statistics for the entire hindcast. The average significant wave height for these 3 years is slightly higher than for the 20-year hindcast record at 0.51 m. Eleven of the 60 most severe storm events and 4 of the top 10 are included in the selected representative wave climate. The 3 years of representative wave conditions were purposely chosen to possess slightly higher wave energies than the 20-year hindcast record in order to account for stormier conditions realistically possible and to add conservatism to the shoreline change estimates.

Nearshore Refraction Simulation

Wave transformation model

39. An estimation of wave transformation from the nominal 18.6-m (61 ft) depth to the nominal 4-m (13 ft) depth along the coast was made by application of the Regional Coastal Processes Wave Model, RCPWAVE (Ebersole, Prater, and Cialone 1986). RCPWAVE was specifically designed for use in projects with large spatial extent, such as in the present case. This model is superior to classical wave ray refraction procedures in that energy propagation along wave crests due to irregular bathymetry is accounted for in addition to energy propagation in the direction of ray travel. The model is also more efficient than traditional wave ray models since the governing equations are solved directly on a user-specified depth (bathymetry) grid in the horizontal plane (by an iterative finite difference solution scheme) rather than by ray shooting and interpolation to the grid.

40. Basic assumptions used in RCPWAVE are:

- a. Mild bottom slopes.
- b. Linear, monochromatic, and irrotational waves.
- c. Negligible wave reflection.
- d. Negligible energy losses due to bottom friction or wave breaking outside of the surf zone.

41. These assumptions are common to most numerical models used for engineering applications. Results from the model are expected to be sufficiently accurate to estimate longshore sand transport rates and shoreline changes.

Model grid and boundary conditions

42. The RCPWAVE model bathymetry grid (shown in Figure 4) is rectangular and its alongshore axis is orientated 14 deg east of due north. The grid contains 80 cells across-shore and 151 cells alongshore for a total mesh of 12,080 cells describing the nearshore bathymetry off the project reach. The cell spacing in the alongshore direction is 150 m and is 75 m in the cross-shore direction. The cell size of the RCPWAVE bathymetry grid was selected in order to maximize resolution of any irregularities in the longshore breaking wave field which may be induced by unusual bottom features, and to determine the effect that dredging nearshore borrow sites for beach nourishment will have on the breaking wave pattern.

43. As shown in Figure 4, the grid extends from north of Asbury Park to south of Manasquan Inlet. Across-shore, the grid extends from well inland to about the 20-m contour. The shoreline model will utilize results between alongshore coordinates 45 (Manasquan Inlet) and 141 (Asbury Park). The bathymetry grid was extended beyond the immediate project area to avoid possible inaccuracies from the lateral boundary conditions.

44. The grid was overlaid on NOAA nautical chart no. 12324 (Edition 22, dated January 1984) to assign an average depth to each cell, interpolating as necessary. The data were entered in a computer file for use as input to RCPWAVE. A three-dimensional plot of the bathymetry grid is given in Figure 5

45. RCPWAVE was modified to allow a more detailed specification of wave conditions at the offshore boundary. As written, a single deepwater wave condition is input to RCPWAVE and the numerical model calculates the wave

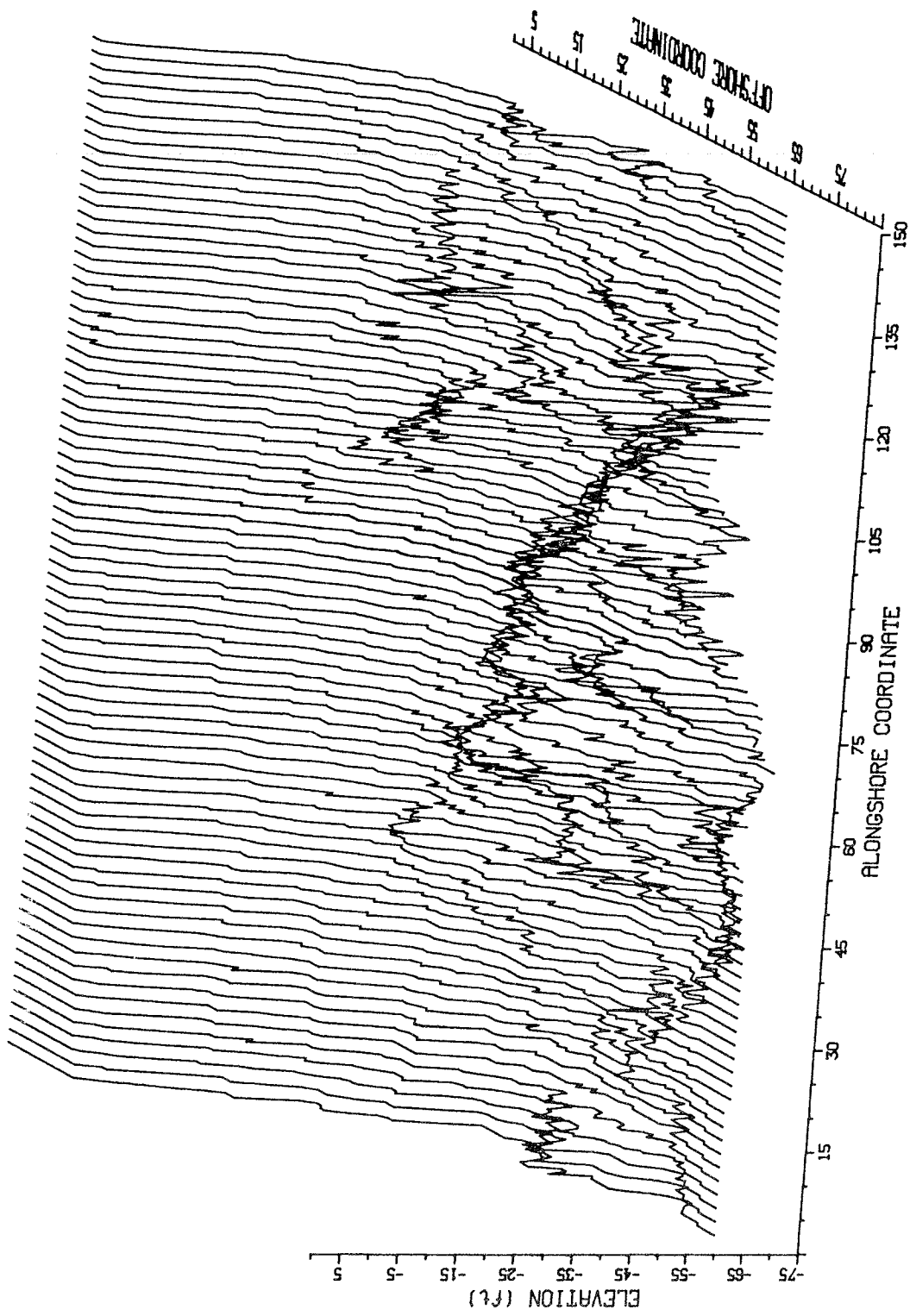


Figure 5. Nearshore wave refraction grid

height and angle at the offshore boundary (dependant on the specified water depth) of the bathymetry grid assuming a plane bathymetry from deep water to the boundary. The modified model allows the explicit specification of the input wave conditions at each coordinate along the offshore boundary of the grid. Wave height, direction, and period as determined by the averaged Phase III WIS hindcast and the calculated wave height and angle gradients provided the offshore boundary condition. The lateral boundary condition is a "no-flow" condition equivalent to specifying a plane beach at the sides. The results of the model runs (a wave height transformation coefficient and wave direction) at specified grid cells along the project area were written to a file for input to the wave refraction and breaking routine employed by the shoreline change model.

Model runs

46. Prior to making production runs, test runs of the model were made to verify the proper operation of the modifications made to the model. Next, the averaged Phase III time history of sea and swell wave conditions was analyzed by angle band to determine the wave periods represented in each of the angle bands for both sea and swell wave conditions. Table 6 provides a listing of the results of this analysis.

47. As shown in Table 6, if an RCPWAVE run were made for each wave event in the representative time history of wave conditions, 7,768 production runs would be required. The expense in both labor and computer charges precluded the execution and storage of so many RCPWAVE runs. Instead, 34 RCPWAVE runs were made for sea conditions (angle bands 4 through 9 for wave periods of 3 - 8 sec, and angle bands 5 through 8 for 9-sec waves). The 2- and 10-sec period waves were assumed to refract similarly to 3- and 9-sec waves, respectively. Hence, if a 2-sec wave is encountered in the offshore time history of sea conditions, the results from the 3-sec wave refraction run in the particular angle band is input to the shoreline change model. Similarly, the RCPWAVE results for a 9-sec wave are used if a 10-sec wave period is encountered in the time history of sea conditions. All of the wave period and angle band combinations shown in Table 6 for swell conditions were run.

Table 6

Wave Periods in Offshore Time History by Angle Band
for Sea and Swell Wave Conditions

Angle Band	Sea conditions						Number of Events	Swell conditions						Number of Events
	4	5	6	7	8	9		4	5	6	7	8	9	
		2	2	2	2	2	161	6	6	6	6	6		214
	3	3	3	3	3	3	883	7	7	7	7	7	7	2346
Wave	4	4	4	4	4	4	1070	8	8	8	8	8		951
	5	5	5	5	5	5	756	9	9	9	9	9		263
Periods	6	6	6	6	6	6	476	10	10	10	10	10		95
	7	7	7	7	7	7	330		11		11	11		157
	8	8	8	8	8	8	66							
		9	9	9	9		19							
		10	10				4							
Totals	641	565	374	376	651	1158	3765	175	926	415	580	1867	63	4026

48. Because RCPWAVE uses linear wave theory and the refraction and shoaling coefficients in linear wave theory are independent of wave height, a unit (1-m) wave height (as modified by the calculated wave height gradient) was used as input for each combination of wave period and angle band investigated. The transformed unit wave height can be interpreted as the product of combined refraction and shoaling coefficients (called a transformation coefficient here). The actual value of the wave height at a particular grid point is the product of the transformation coefficient and the deepwater wave height in the WIS time history. Thus, although only a limited number (63) of combinations of the deepwater wave period and direction were used to describe the transformation of waves from the 20-m contour to the 4-m contour, the wave height of each wave event in the 3 year representative time history was utilized.

49. The output of the production runs consists of the transformation coefficient and wave direction at the nominal 4-m depth at each of the 151 longshore grid cells. The results of all the RCPWAVE runs were compiled into a random access file keyed on input wave period and direction. Knowledge of the deepwater wave height associated with each set of WIS wave conditions

allows the rapid calculation of nearshore wave properties. Plots showing the results of the model runs are contained in Appendix C.

Time series processing

50. A program was developed which linked the 3 year representative time history of wave conditions at the 18.6-m depth to the results of the RCPWAVE runs to create a sequential time history led by the deepwater wave height, period, and direction, followed by the nearshore wave height and direction along the project reach. In linear wave theory, wave period does not vary in the refraction process. The program reads one record of WIS data (height, direction, and period of sea and swell components) and defines a key, based on input period and direction. The keys are then used to enter the random access file and extract the transformed (nearshore) wave conditions. The transformed wave height at each grid cell is obtained as the product of the transformation coefficient and the deepwater wave height in the WIS record.

51. Standard operation of the shoreline change model requires input wave conditions at 6-hr intervals. This interval is considered sufficiently small, both numerically and physically, to accurately represent longshore processes in a shoreline change model with typical grid cell size. Therefore, every other record of the hindcast time history was analyzed. Both sea and swell components were analyzed and used in the shoreline change model (two wave conditions per 6-hr time step).

52. Recent research results stemming from prototype (field) experiments performed by CERC has provided a method of assessing the significance (with respect to longshore sand transport) of a given breaking wave height and direction (Kraus, Gingerich, and Rosati 1988). The capability of a given wave condition to produce significant longshore sand transport is expressed in terms of a parameter related to the longshore discharge of water which, in turn, can be related to the predictive formula for the transport rate used in this study (Equation 3, PART III). A threshold discharge defines the magnitude of the longshore current and/or wave height and direction which must be exceeded for significant longshore transport to occur. A detailed description of this threshold criterion for longshore sand transport and its calculation is given by Kraus, Hanson, and Larson (1988). Each wave condition

in the representative time series was tested against this criterion and if the threshold was not exceeded a calm condition was assumed. Implementation of this condition resulted in significant savings in both required computer storage and computation time in the shoreline change simulations, allowing available resources to be more fully dedicated to model verification and sensitivity testing.

53. The final output from this program is a sequential file that contains a 3-year time history of effective wave heights, periods, and directions at 6-hr intervals at the nominal 4-m depth for each of the longshore grid cells in the project reach. This file constitutes the principal wave input for the shoreline change model.

Wave Refraction Over Beach Fill Borrow Sites

54. For an open-ocean coast, breaking wave height and direction are considered to be the primary factors controlling longshore sand transport and subsequent shoreline change. The pattern of breaking waves is determined by the properties of the incident wave in deep water (wave height, direction, and period) and the bathymetry over which the waves propagate and transform. Alteration of the nearshore bathymetry due to the excavation of nearshore beach fill borrow sites has the potential to change the breaking wave pattern along the coast. The sand transport rate along the beach could be modified to such a degree that the naturally occurring evolution of the beach plan shape would be changed by an amount sufficient to have engineering significance.

55. Three open-ocean borrow sites are actively being considered as borrow sources for the project beach fill. The locations and configurations of the borrow sites are indicated on Figure 6. The borrow areas will be referred to herein as borrow areas 4A, 4B, and 5. A complete description of the borrow sites investigated in the present study as well as several other borrow sites which are outside of the nearshore bathymetry utilized herein, including data on the characteristics of the potential borrow material is given in a report prepared for the US Army Corps of Engineers, New York District, by Alpine Ocean Seismic Survey, Inc. (1985).

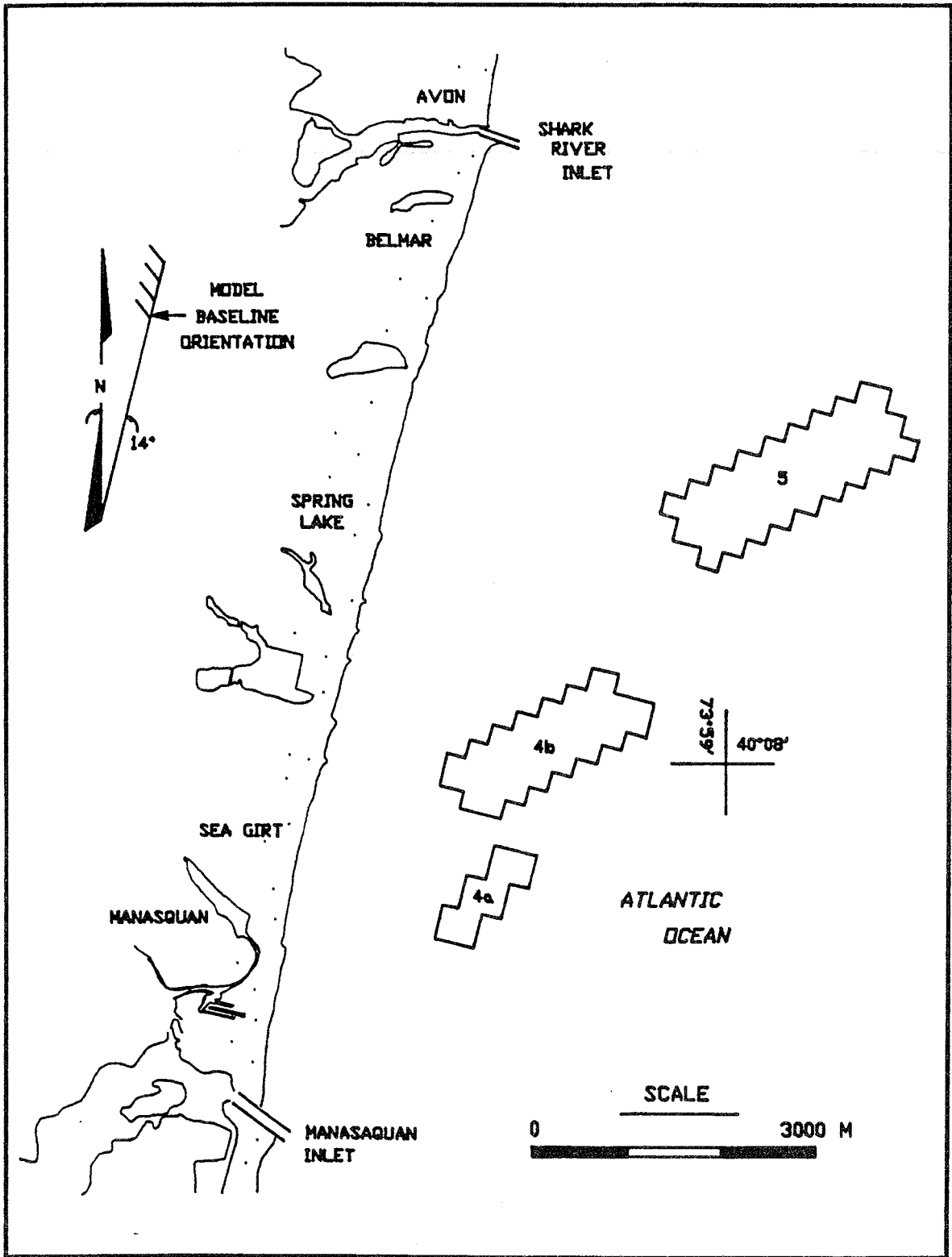


Figure 6. Potential beach fill borrow sites

56. The borrow sites under consideration lie relatively close to shore in water depths ranging from approximately 12 m (40 ft) to 15 m (50 ft) MLW. A 7-sec linear wave traveling in water of this depth has a length of about 65.5 m (215 ft), and the corresponding depth to wavelength ratio is approximately 0.2. This depth to wave length ratio is much less than 0.5, the ratio at which waves are traditionally judged to be influenced by the bottom. Therefore, an investigation into the effect of borrow site excavation on the wave refraction and shoreline change was conducted.

57. The RCPWAVE bathymetry grid was modified to represent sea bottom conditions after dredging of the proposed borrow sites. The modifications to the bathymetry grid in terms of the added water depths (in feet) at specific grid cells are given in Tables 7 and 8. The volume of sediment removed from the borrow areas as assumed by the data presented in Tables 7 and 8 is as follows: (1) borrow area 4A, 843,000 cu m (1.1 million cu yd), (2) borrow area 4B, 2 million cu m (2.6 million cu yd), (3) borrow area 5, 5.3 million cu m (7 million cu yd).

Borrow area model runs

58. The entire suite of RCPWAVE runs (63 model runs) was made to obtain a database of nearshore wave conditions corresponding to the dredged bathymetry. Plots of the results of these model runs and comparisons with the original (existing bathymetry) RCPWAVE runs are contained in Appendix C. For each of the shore protection design alternatives evaluated, two shoreline change model runs were made. One model run used the nearshore waves that were refracted over the existing bathymetry, and the other used waves that were refracted over the dredged bathymetry. An inherent assumption embedded in the data base of nearshore wave conditions refracted over the dredged bathymetry is that the excavated holes will remain empty. Of course natural infilling of the borrow holes is expected. The perturbing effect of the dredging, therefore, will decrease with time.

59. The following general conclusions were reached with respect to the results of the borrow site wave refraction runs.

- a. In general, wave heights directly behind (in the shadow of) the borrow areas are lower and the wave heights adjacent to the borrow areas are greater.

b. At the nominal 4-m depth, wave heights will increase or decrease by as much as 20 percent and wave angles will change by as much as 1.5 deg in the vicinity of the borrow hole.

c. The region of significant change in refracted wave height and direction is approximately 7.5 km (4.5 mi) wide and can move alongshore by as much as 3.0 km (1.9 mi) depending on the deep-water wave direction.

d. Changes in refracted wave height and direction are small for short-period (4 sec) waves and increase with the wave period.

Table 7

Increased Water Depths (ft) in Potential Beach Fill Borrow Site 4

Borrow Area 4A										
Offshore										
Coordinate	Alongshore Bathymetry Grid Coordinate									
	63	62	61	60	59	58				
42	10	10	-	-	-	-				
41	8	10	10	10	-	-				
40	7	9	9	10	10	9				
39	6	8	8	8	10	10				
38	5	7	7	7	9	10				
37	-	-	6	6	7	8				
36	-	-	-	-	6	6				

Borrow Area 4B										
Offshore										
Coordinate	Alongshore Bathymetry Grid Coordinate									
	74	73	72	71	70	69	68	67	66	65
48	-	9	8	-	-	-	-	-	-	-
47	-	10	10	-	-	-	-	-	-	-
46	-	10	10	7	-	-	-	-	-	-
45	9	10	10	9	6	-	-	-	-	-
44	8	10	10	10	7	5	-	-	-	-
43	7	8	10	10	9	6	-	-	-	-
42	-	7	9	10	10	7	5	-	-	-
41	-	6	8	10	10	9	6	-	-	-
40	-	-	7	8	10	10	7	5	-	-
39	-	-	6	7	9	10	8	5	5	-
38	-	-	-	6	7	8	8	5	5	-
37	-	-	-	-	6	7	7	6	5	5
36	-	-	-	-	-	6	6	6	5	5
35	-	-	-	-	-	5	5	5	6	6
34	-	-	-	-	-	-	4	5	5	5
33	-	-	-	-	-	-	-	5	5	-
32	-	-	-	-	-	-	-	4	4	-
31	-	-	-	-	-	-	-	-	4	-

Table 8

Increased Water Depths (ft) in Potential Beach Fill Borrow Site 5

Borrow Area 5 Offshore		<u>Alongshore Bathymetry Grid Coordinate</u>									
<u>Coordinate</u>	<u>95</u>	<u>94</u>	<u>93</u>	<u>92</u>	<u>91</u>	<u>90</u>	<u>89</u>	<u>88</u>	<u>87</u>	<u>86</u>	<u>85</u>
64	-	-	15	-	-	-	-	-	-	-	-
63	-	-	17	-	-	-	-	-	-	-	-
62	-	18	18	16	-	-	-	-	-	-	-
61	-	19	19	17	16	-	-	-	-	-	-
60	20	20	20	18	17	16	-	-	-	-	-
59	19	20	20	19	18	17	-	-	-	-	-
58	18	19	20	20	19	18	16	-	-	-	-
57	17	18	18	20	20	19	18	16	-	-	-
56	-	16	17	19	20	20	19	17	15	-	-
55	-	-	15	18	19	20	20	18	16	-	-
54	-	-	-	17	18	19	20	19	17	13	-
53	-	-	-	16	17	18	19	19	18	15	13
52	-	-	-	-	16	17	18	18	17	15	15
51	-	-	-	-	-	16	17	17	17	15	-
50	-	-	-	-	-	-	17	16	17	15	-
49	-	-	-	-	-	-	16	16	17	15	-
48	-	-	-	-	-	-	-	15	16	-	-
47	-	-	-	-	-	-	-	-	15	-	-

PART III: LONG-TERM SHORELINE CHANGE

Introduction

60. The primary task of the study was to numerically simulate long-term shoreline change along New Jersey's Atlantic coast between Asbury Park and Manasquan, and to evaluate the performance of various shore protection design alternatives. The shoreline contour model GENESIS (Hanson 1987) was utilized for the assessment of the longshore sand transport processes and long-term shoreline change along the project reach.

61. On an open-ocean coast such as the present project study area, shoreline change occurring over several years or decades is believed to be controlled by the transport of sand alongshore. The dominant process producing this alongshore movement of sand is the energy dissipation associated with the breaking of waves at oblique angles to the shoreline. Prior to the development of numerical models of shoreline evolution, the sediment budget analysis technique was applied in studies of this type. The basic budget analysis still commonly used in coastal engineering and geology is an arithmetic balance of beach volume changes with inputs and outflows of sediment at the landward, seaward, and lateral boundaries of the region considered. The shoreline change model GENESIS is a highly sophisticated implementation of the sediment budget analysis method, in which the change in beach volume is calculated at finely spaced intervals (specifically, at 50 m intervals in this study) along the project reach as a function of time-varying wave conditions.

62. The budget study of Caldwell (1966) as well as subsequent studies have concluded that longshore sand transport is the dominant process controlling the long-term shoreline evolution of the New Jersey's Atlantic coast. Hence, the application of a numerical shoreline change model is expected to be a valid extension of previous work, and an efficient tool for quantifying the long-term fate of proposed shore protection designs.

63. The structure of this chapter is presented in three sections. Section 1 is an introduction to the shoreline change model which includes a summary of the basic model assumptions and a discussion of the structures

evaluated in the model. Since numerous groins exist in the project reach and significant infrastructure is in place immediately landward of the beach, an understanding of the seawall and groin boundary conditions implemented in the model is important. The position of the shoreline is, to a significant extent, constrained by these coastal structures both in the model and the prototype. Section 2 contains the calibration and verification of GENESIS for the project reach. Section 3 presents the results of several model simulations of design alternatives and relevant discussion.

Description of the Shoreline Change Model GENESIS

Background

64. The numerical model GENESIS is a one-contour line beach evolution model of the type first introduced by Pelnard-Considere (1956). The acronym GENESIS stands for GENERALized model for SIMulating SHoreline change. GENESIS was developed by Hanson (1987) in a cooperative research project with CERC, and sponsored through the U.S. Army Research, Development, and Standardization Group, United Kingdom. GENESIS is a generalized system of numerical models and computer subroutines which allows simulation of long-term shoreline change under a wide variety of user-specified conditions.

65. GENESIS calculates the longshore sand transport rate and resulting plan shape of the modeled coast at short time intervals over the course of the simulation period. The effect of coastal structures such as seawalls, groins, and beach fills on the longshore sand transport rate is incorporated in the model by use of appropriate boundary conditions and constraints. Wave diffraction at detached breakwaters and long groins is represented around and behind these structures in the shoreline change calculation.

66. GENESIS can use two types of wave inputs depending on the available data and degree of computational effort required. A single offshore wave condition can be input, and the breaking wave model within GENESIS will calculate the breaking wave conditions along the modeled reach. The wave model in GENESIS is based on linear wave theory and the assumption of a uniformly sloping bottom with parallel contours. Wave refraction and shoaling are iteratively calculated using Snell's Law, and the principle of wave energy

conservation is used to satisfy a breaking criterion. Diffraction is included in the calculation of breaking waves for grid cells located in the lee of structures. Alternatively, a more sophisticated wave transformation model (such as RCPWAVE) which describes wave propagation over a digitized offshore bathymetry can be used to perform the required wave transformations from offshore to shallow water. In this case, GENESIS retrieves the nearshore wave characteristics (output from RCPWAVE) from a user-defined data base and performs local refraction, diffraction, and shoaling calculations to obtain a breaking wave height and angle with respect to the shoreline. In either case, once the breaking wave field along the modeled reach is available, longshore sand transport rates can be calculated and the shoreline position updated.

Shoreline model theory

67. The goal of shoreline change modeling is to describe long-term evolution in shoreline position, in which the beach profile is assumed to maintain an equilibrium shape. This implies that bottom contours are parallel and that the entire profile is translated either seaward or landward for an accreting or eroding shoreline. Under this assumption, it is necessary to consider the movement of only one contour line, conveniently taken to be the shoreline, as shown in Figure 7. In the present study mean high water (MHW) shoreline positions were digitized from topographic maps of the project area. Seasonal trends in shoreline position change are assumed to be accounted for in an average sense in the verification process.

68. In the model, longshore sand transport is assumed to occur uniformly over the active beach profile down to a critical depth called the depth of closure. No longshore sand transport is assumed at depths greater than the depth of closure. Hence, a change in the shoreline position Δy at a certain point is related to the change in cross-sectional area ΔA at the same point according to Equation 1:

$$\Delta A = \Delta y D \quad (1)$$

where

ΔA = change in cross-sectional beach area (m^2)

Δy = change in shoreline position (m)

D = maximum depth for sand motion (depth of closure) (m)

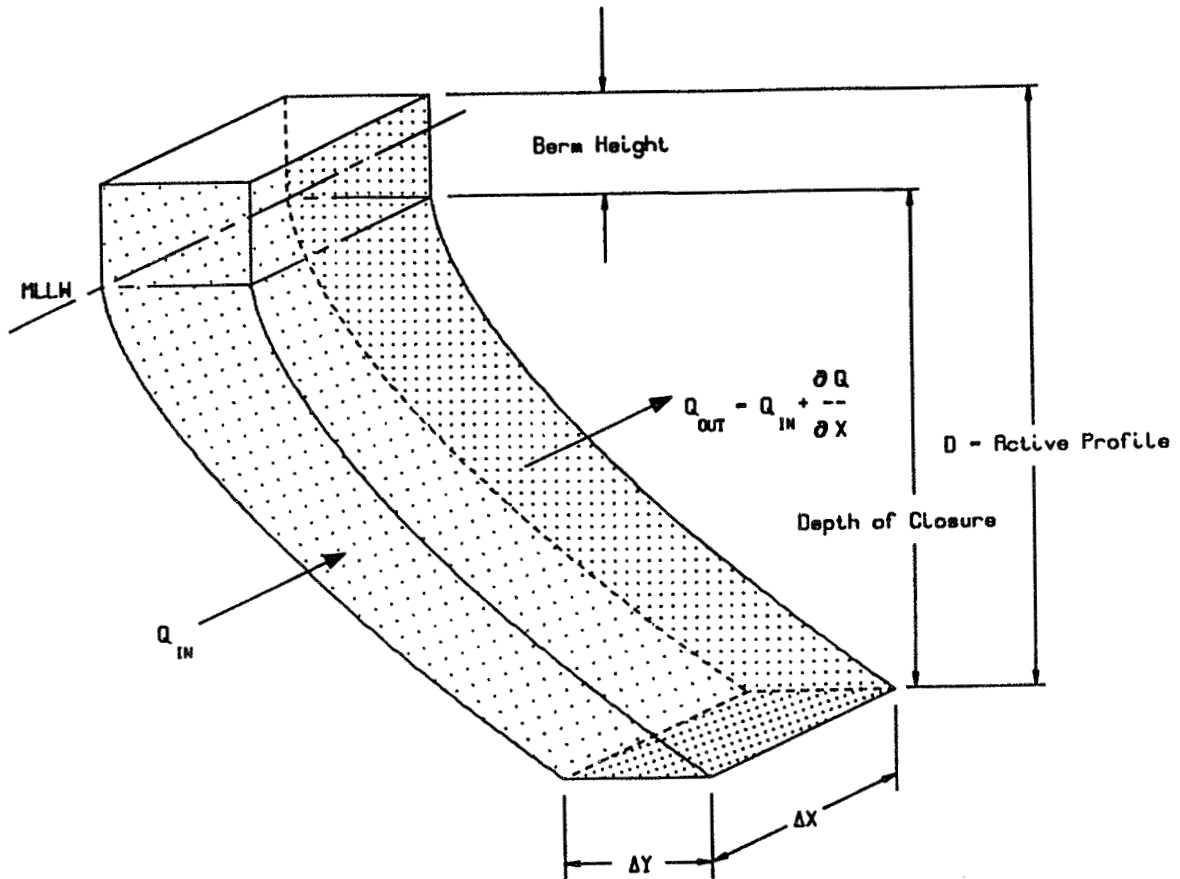


Figure 7. Schematic illustration of an idealized equilibrium beach profile

By considering a control volume of sand and formulating a mass balance during an infinitesimal interval of time, the following differential equation is obtained:

$$\frac{\partial Q}{\partial x} + \frac{\partial A}{\partial t} = 0 \quad (2)$$

where

- Q = longshore sand transport rate (m³/sec)
- A = cross-sectional area of beach (m²)
- x = space coordinate along the axis parallel to the trend of the shoreline (m)
- t = time (sec)

Equation 2 requires that a variation in the longshore sand transport rate be balanced by changes in the shoreline position. Therefore, at a given time step, Δy shown in Figure 6 is equal to $(Q_{in} - Q_{out}) / (D \Delta X)$.

69. In order to solve Equation 2, it is necessary to specify an expression for the longshore sand transport rate. The predictive formula for Q used in the shoreline change model is:

$$Q = \frac{H_b^2 C_{Gb}}{16(S-1)(1-a)} \left[K_1 \sin(2\alpha_{bs}) - 2 \frac{dH_b}{dx} K_2 \cot(\beta) \cos \alpha_{bs} \right] \quad (3)$$

where

- H_b = breaking wave height (ft)
- C_{Gb} = wave group velocity at breaking (ft/sec)
- S = ratio of sediment (quartz) density to water density (S = 2.65)
- a = sediment porosity (a = 0.4)
- α_{bs} = breaking wave angle with respect to the shoreline
- $\cot(\beta)$ = inverse beach slope

The quantities K_1 and K_2 are empirical coefficients and are treated as calibration parameters.

70. The first term in Equation 3 corresponds to the "CERC formula" described in the Shore Protection Manual (SPM) (1984, Chapter 4) and provides an estimate of the sand transport produced by obliquely incident breaking waves. The second term estimates sand transport produced by a longshore current resulting from a variation in the breaking wave height alongshore. The first term is always dominant on an open coast away from diffracting structures; however, the second term provides a significant correction if diffraction enters into the problem (Ozasa and Brampton 1980, Kraus 1983, Kraus and Harikai 1983).

71. The SPM recommends a value of $K_1 = 0.77$ for root mean square wave height in Equation 3 and the coefficient K_2 has been empirically found to lie in the range $0.5 K_1 \leq K_2 \leq 1.5 K_1$

72. Lateral boundary conditions are required in the solution prescribed in Equation 2. Typical boundary conditions are limited sand transport, such as at a long groin or breakwater, and uniform transport, such as at a stable beach. Other boundary conditions may be formulated as required.

Representation of structures in the model

73. As discussed in Part I, several bulkhead seawalls and numerous groins are located along the project reach. The groins and bulkheads were constructed in an attempt to reduce erosion, control the shoreline position, and protect existing infrastructure including roadways, commercial buildings

and private residences landward of the sandy beach. To accurately simulate shoreline change, the influence of these structures on the longshore sand transport rate and shoreline position must be represented in the model.

74. Seawall. In the model, a seawall functions to prevent landward migration of the shoreline. Although only portions of the project shoreline are actually backed by a seawall or bulkhead, a continuous seawall was simulated just seaward of existing infrastructure since erosion would not be permitted beyond these facilities. The position of the effective seawall is located on the baseline of shore protection designs evaluated. If the shoreline erodes to the seawall, the longshore sand transport rate and shoreline position are modified to prohibit erosion of the shoreline landward of the seawall. Implementation of the seawall boundary condition is complex; details of the seawall constraint in the model are given by Hanson and Kraus (1986). The seawall constraint is imposed at the same level of approximation as the assumptions used to derive the one-line model. Wave reflection, scouring, and flanking are not simulated.

75. Groins. The positions and lengths of groins were obtained from April 1987 aerial photographs and corresponding topographic maps. Forty-four groins were represented within the total project area from Asbury Park to Manasquan Inlet. The project area was divided into two model reaches in order to achieve appropriate boundary conditions at the Shark River Inlet. Hereafter, the shoreline extending from Asbury Park to Shark River Inlet will be referred to as the North Model reach, and the shoreline between Shark River Inlet and Manasquan Inlet as the South Model. Thirteen groins were placed in the 2.7-mile-long North Model reach and thirty-one groins were placed in the approximately 6-mile-long South Model reach. Groins judged to be efficient at trapping sand were entered in the model; very short groins and remnants of non-functioning groins were not included. Only four groins of rubble type construction within the project area were classified as non-functioning, whereas several timber groins were determined to be ineffective, according to visual inspection.

76. Bypassing at groins. If only longshore sand transport is considered, in principle and in the model, a high-crested groin extending well beyond the surf zone will completely block the movement of sand. In practice,

most groins are of such length that the surf zone often extends beyond the groin tip. Rip currents and complex circulation patterns within groin compartments also act to remold the shoreline position and to move sand around a groin. During high tides and severe wave conditions, sand may be bypassed over the groin crest or landward of the groin. Furthermore, if a groin contains voids, sand moving alongshore can pass through the groin. An inspection of the groins within the project reach (Coastal Planning & Engineering/URS, 1987) documents evidence of sand transport landward, over, and through groins within the project reach. In the present study, the transport of sand alongshore beyond the groin tip is called bypassing and sand transported over, through, or landward of the groin is called transmission.

77. Bypassing and transmission of sand alongshore at groins within the project area definitely occurs and is represented in the model. Transmission of sand past a groin in GENESIS is represented by specifying a "permeability factor" which may range from 0 (no sand transmission) and 1 (complete sand transmission, no groin). Through the course of this study the implementation of the permeability factor in GENESIS was reformulated. In the new formulation the longshore sand transport rate across a groin cell by transmission is calculated as a fraction of the potential sand transport rate (the transport rate calculated as if no groin were present) (Hanson and Kraus 1980). Formally, the longshore sand transport rate at a groin cell by transmission was determined as a fraction of the sand transport rate at the adjacent updrift cell. The new formulation provides a more realistic time dependant sensitivity to the assigned groin permeability factor. Gravens and Kraus (1989) discuss and evaluate the two methods of implementing groin permeability in one-line shoreline change models. Unfortunately, there are no data sets available to directly estimate groin permeability. Consequently, groin permeability becomes, in effect, part of the calibration process.

78. Bypassing of groins in GENESIS is determined at each time step based on the depth of longshore sand transport pertaining to the wave conditions which exist at the particular time step. For the purpose of determining if groin bypassing will occur, an expression given by Hallermeier (1979, 1983) is used:

$$D_{LT} = 2.28 H - 10.9 \frac{H^2}{L} \quad (4)$$

in which H is the significant wave height in deep water and L is the deepwater wavelength. For calculating the distribution of the longshore sand transport rate and shoreline change the depth of closure was held constant at 6 m (approximately 20 ft). The "bypassing factor," BYP, is calculated assuming a rectangular distribution of the longshore sand transport rate as follows:

$$BYP = \begin{cases} 1 - \frac{D_g}{D_{LT}} & , D_{LT} > D_g \\ 0 & , D_{LT} \leq D_g \end{cases} \quad (5)$$

In which D_g is the depth at the seaward end of the groin. A rectangular distribution of the transport rate provides a reasonable approximation to available field data sets (Kraus and Dean 1987).

79. A theoretically complete analysis of sand transport past a groin be it by transmission or bypassing would require knowledge of the cross-shore and vertical distribution of the longshore sand transport rate as well as the horizontal circulation and transport pattern. Although knowledge of the later is beyond the present state of the art, the permeability factor allows the modeler to tune the model to best represent longshore sand transport processes and shoreline change near groins. For the former, there is not enough field data to estimate the vertical distribution of the longshore sand transport rate. Theoretical expressions exist to predict the cross-shore distribution of the longshore transport rate, however, all pertain to idealized conditions and none have been verified. In light of these circumstances, the simplest assumptions that produce reasonable results as described above are appropriate.

Model Calibration and Verification

Introduction

80. The standard calibration procedure for GENESIS is to determine the magnitude of the transport parameters K_1 and K_2 by reproducing known shoreline change that occurred at the project between two surveys. If sufficient data are available, the calibrated model is then used to simulate known shoreline change over a time interval not spanned by the calibration simulation. The

purpose of a two-part calibration and verification is to verify that the calibration constants assigned in the calibration and held constant in the verification are independent of the time interval. Since measured wave data are not available for the project site, a representative 3-year-long time history of hindcast wave conditions selected as discussed in PART II, provided the required wave input to drive the model during the calibration and verification.

81. In the present study, the calibration and verification deviated from the standard procedure because of the large number of coastal structures that exist within the project area and the unknown time history of their construction. Instead, GENESIS was calibrated for the 2.4 km (1.5 mi) reach centered about Manasquan Inlet. The time period of the calibration (1929 to 1932) concurred with the construction of jetties for the stabilization of Manasquan Inlet. The purpose of the calibration was to: first, adjust the calibration constants K_1 and K_2 to achieve longshore transport rates on the order of those reported historically; second, to produce appropriate shoreline response to the stabilization of Manasquan Inlet; and finally to verify that the procedure used to account for systematic variations in the incident wave climate would produce differential longshore transport rates along the project coast. After calibration, verification simulations were performed for the 10-year time period 1977 to 1987 for both the North and South Models. During the verification simulations, the calibration constants K_1 and K_2 were held constant and permeability factors for each of the groins in the model reach were varied to achieve appropriate shoreline changes.

82. In the calibration and verification procedures, visual comparisons were made by plotting surveyed and calculated shoreline changes as well as the calculated average longshore sand transport rate. Because the magnitude of the longshore sand transport rates were assumed to be of primary importance in this study, calculation of a numerical fitting criterion for shoreline change to assess the calibration and verification results was not performed. In shoreline modeling it is important to realize that a given amount of shoreline change for a specific time period can be achieved with widely varying longshore transport rates provided that the change in the transport rates across the grid are sufficient to produce the known shoreline change.

Therefore, achieving the correct order of magnitude of the longshore sand transport rate is the most critical consideration.

Calibration

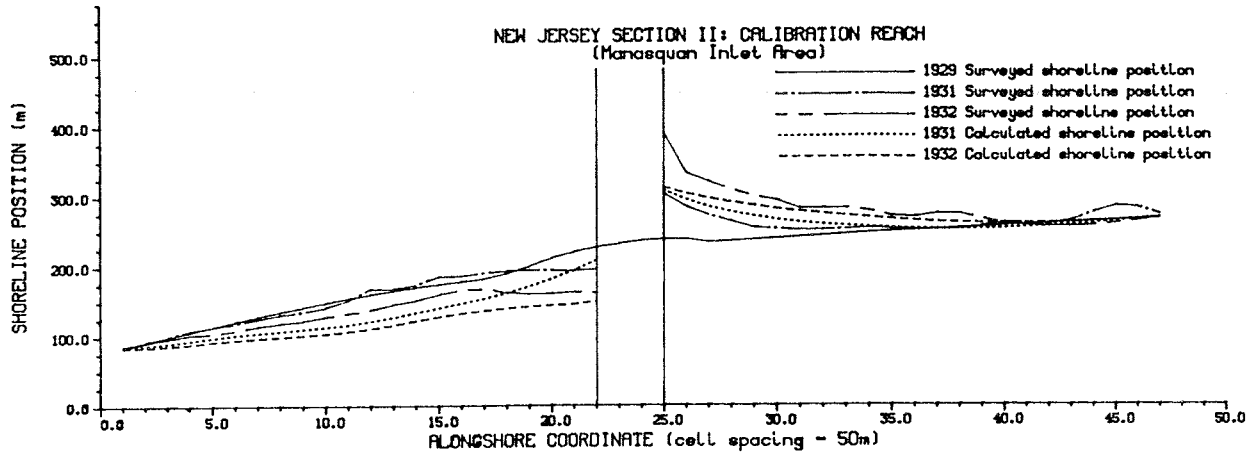
83. The calibration was performed using surveyed shorelines in the vicinity of Manasquan Inlet for 1929, 1931, and 1932. Maps of the shoreline surveys were digitized from plate 6 of House Document No. 71, "Beach Erosion at Manasquan Inlet and Adjacent Beaches" (1937), for input to the shoreline change model. The month in which the various surveys were made is not given in the report. Consequently, consideration of the seasonal compatibility of the surveys was impossible. Normally, the calibration and verification would be performed over a period of time beginning and ending in the same season to avoid possible contamination due to seasonal shoreline changes. The simulation of shoreline change for this 3-year calibration period was performed with the 3-year-long representative time history of wave conditions providing input wave conditions and the initial shoreline position given by the 1929 surveyed shoreline. The positions of the simulated 1931 and 1932 were then compared with the measured 1931 and 1932 shorelines.

84. The configuration of GENESIS for the calibration simulations consisted of 47 alongshore calculation cells with a spacing of 50 m. A "fixed-beach" boundary condition was imposed on the lateral boundaries of the calibration reach. This boundary condition requires uniform sand transport rates on the boundaries which results in a pinned or fixed shoreline position at the boundary. The north and south jetties of Manasquan Inlet, located at grid cells 22 and 25, were modeled as long diffracting groins which served to completely block the movement of sand alongshore. No other structures were modeled in the calibration.

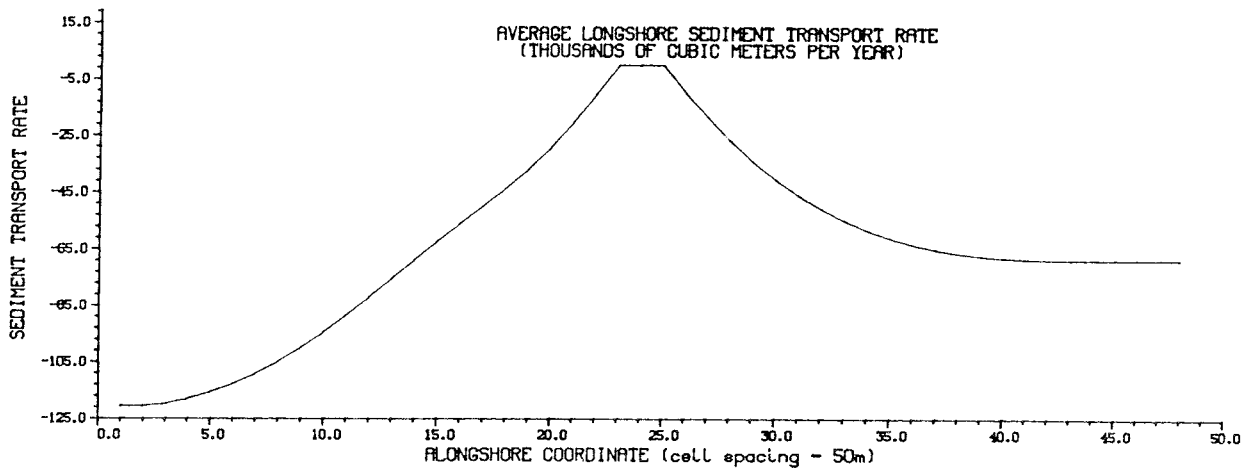
85. Numerous trial calibration runs were made, in each case different values were assigned to the transport parameters K_1 and K_2 . Figure 7 shows the calculated shoreline positions for 1931 and 1932 compared to the measured 1931 and 1932 shoreline positions, along with the average longshore sand transport rate for the calibration period. As a result, the values $K_1 = 0.7$ and $K_2 = 0.3$ were judged to most appropriately estimate expected longshore sand transport rates and reproduce surveyed shoreline change in the Manasquan Inlet area.

86. As shown in Figure 8b, the calculated average annual longshore sand transport rates south of the Inlet between alongshore coordinates 40 and 47 are approximately 68,000 m³/year (89,000 yd³/year). Caldwell estimated the longshore transport rate entering the Manasquan Inlet to Asbury Park reach to be approximately 74,000 yd³/year. The average of the longshore transport rates for all 22 calculation cells south of the Inlet is 55,000 m³/year (72,000 yd³/year) which is very close to Caldwell's estimate. A net annual difference in the sand transport rates (or a differential longshore sand transport rate) of approximately 50,000 m³/year is shown across the calibration reach, which extends approximately 1.1 kilometer (0.7 miles) north and south of Manasquan Inlet. Because the inlet jetties were simulated as complete littoral barriers, sand transport rates at the jetties are zero and increase in both directions away from the jetties.

87. The calculated and measured shoreline positions shown in Figure 8a south of the inlet agree well considering that a representative wave climate was used to drive the model. On the north side of the inlet, however, the agreement between the calculated and surveyed shoreline positions is not as good. The model results indicate erosion at all calculation cells north of the inlet between 1929, 1931, and 1932, whereas the survey shows erosion in only the first three cells immediately adjacent to the inlet and then little or no shoreline change for the period 1929 to 1931. From 1931 to 1932 the surveys indicate shoreline erosion from approximately 35 m adjacent to inlet tapering to no shoreline change at cell number 2. An explanation for this apparent disagreement between the calculated and surveyed shoreline positions north of the inlet may be found in House Document 71, which states that in anticipation of shoreline erosion north of the newly stabilized inlet, material dredged from between the inlet jetties to create the new entrance channel was placed on the beaches north of the inlet. Unfortunately, the quantity of material placed was not stated, precluding the specification of a beach fill north of the inlet in the model during the calibration simulations. It is noted that the calculated average erosion north of the inlet is 15 m between 1931 and 1932 whereas the average surveyed erosion is 18 m north of the inlet for the same period. Therefore, the calculated volumetric erosion north of the inlet for the time period 1931 to 1932 is close to the surveyed erosion.



(a) calculated and measured shoreline position



(b) average annual longshore sand transport rates

Figure 8. Calibration results

Verification

88. The verification of GENESIS for the project study area was independently performed for both the North Model reach (Asbury Park to Shark River Inlet) and the South Model reach (Shark River Inlet to Manasquan Inlet). In this phase of preparing the model for design alternative evaluation, the calibration parameters K_1 and K_2 were held at the previously obtained values, and only the permeability factors for each of the groins within the modeled reaches were varied to achieve the appropriate shoreline change. The verification period was from July 1977 to April 1987. Two preliminary verification simulations were performed. In the first, all groin permeabilities were assigned the value of 0.0; this simulation provided an indication of the shoreline change that could be expected if all the groins were sand tight. In the second preliminary verification simulation all groin permeabilities were assigned the value of 1.0; this simulation provided an indication of the shoreline change that could be expected if all the groins were removed. In general, the overall shoreline change (erosion) that resulted from the simulations with 0.0 permeabilities was less than the surveyed shoreline change. Additionally, the offset between the updrift and downdrift calculation cells adjacent to the groins was greater than the surveys indicated. This means that the calculated longshore sand transport rate at groin cells was too small and that an increase would be required to produce the surveyed shoreline change. The results of the simulations with groin permeabilities of 1.0 indicated more shoreline change (erosion) than the surveys.

North Model grid and boundary conditions

89. The North Model was configured as follows for the verification runs. A fixed-beach boundary condition was assigned at the northern boundary. At this location, a groin which has a 120 m (400 ft) long shore parallel extension at its seaward end protects the Asbury Park Convention Center and acts as a seawall. This boundary condition allows sand to across the model boundary in either direction restricted only by the seawall around the convention center. The northern jetty of the Shark River Inlet provided the southern boundary condition. The jetty was modeled as a 5 percent permeable diffracting groin with a 50-m long breakwater extending to the north from its

seaward end. This condition allowed 5 percent of the calculated sand transport that is not bypassed beyond the jetty tip to move across the boundary in either direction. The modeled reach consisted of eighty-eight calculation cells spaced 50 m apart and 13 groins including the north Shark River Inlet jetty. Numerous verification simulations were performed and the groin permeabilities were adjusted in successive test runs to better represent known shoreline changes. The final verification results for the North Model are given in Figure 9. The solid line is the July 1977 surveyed shoreline position which was input to the model as the initial shoreline position. The dotted line is the April 1987 surveyed shoreline position and the dashed line is the predicted 1987 shoreline position as calculated by the model.

90. Reasonably good agreement between the calculated and surveyed 1987 shoreline position was obtained for the North Model verification. However, because all the groins except for the Shark River Inlet jetty were simulated as non-diffracting groins, the predicted shorelines within groin compartments are essentially straight and not crescentic as shown in the surveys. This results from neglecting the diffractive effect the groins have on small short period waves which act to remold the shoreline within groin compartments. This is important when interpreting model results of design alternative simulations.

91. Average annual longshore sand transport rates calculated by the model for the verification period (July 1977 to April 1987) are given in Figure 10. The transport rates increase from south to north, from about 75,000 m³/year (98,000 yd³/year) at Shark River Inlet to about 135,000 m³/year (177,000 yd³/year) at Asbury Park. The differential longshore sand transport rate caused by the shadowing of wave energy by Long Island is approximately 60,000 m³/year (79,000 yd³/year) for the reach between Asbury Park and Shark River Inlet.

South Model grid and boundary conditions

92. The South Model extends from the south jetty of Shark River Inlet to the north jetty of Manasquan Inlet. The South Model reach contains 192 calculation cells spaced 50 m apart and 31 groins including the jetties at the two inlets which define the boundaries of the model. A diffracting groin boundary condition was applied at both ends of the model reach. The

NORTH MODEL: VERIFICATION SHORELINES
 (Asbury Park to Shark River Inlet)

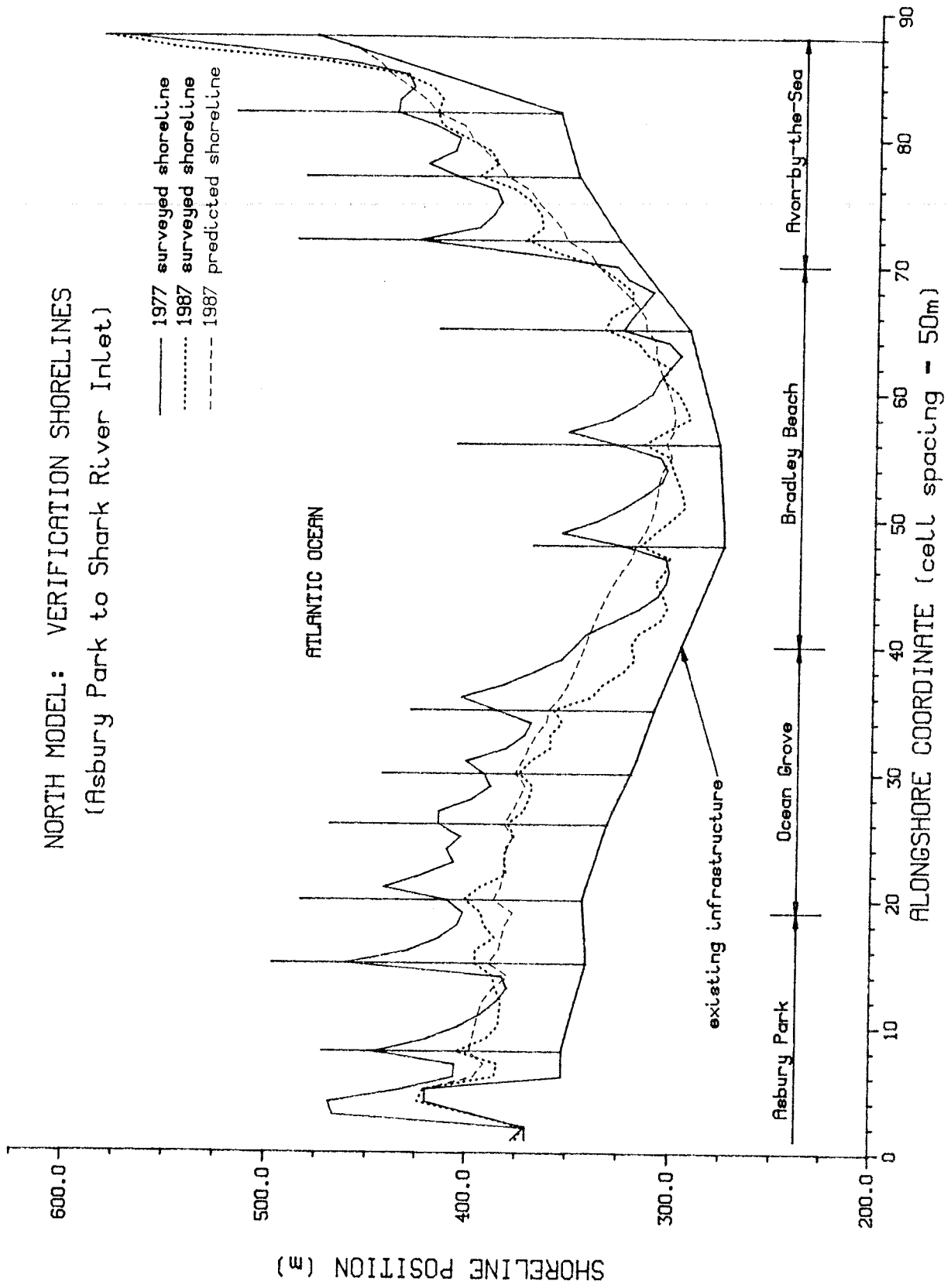


Figure 9. Final verification, North Model

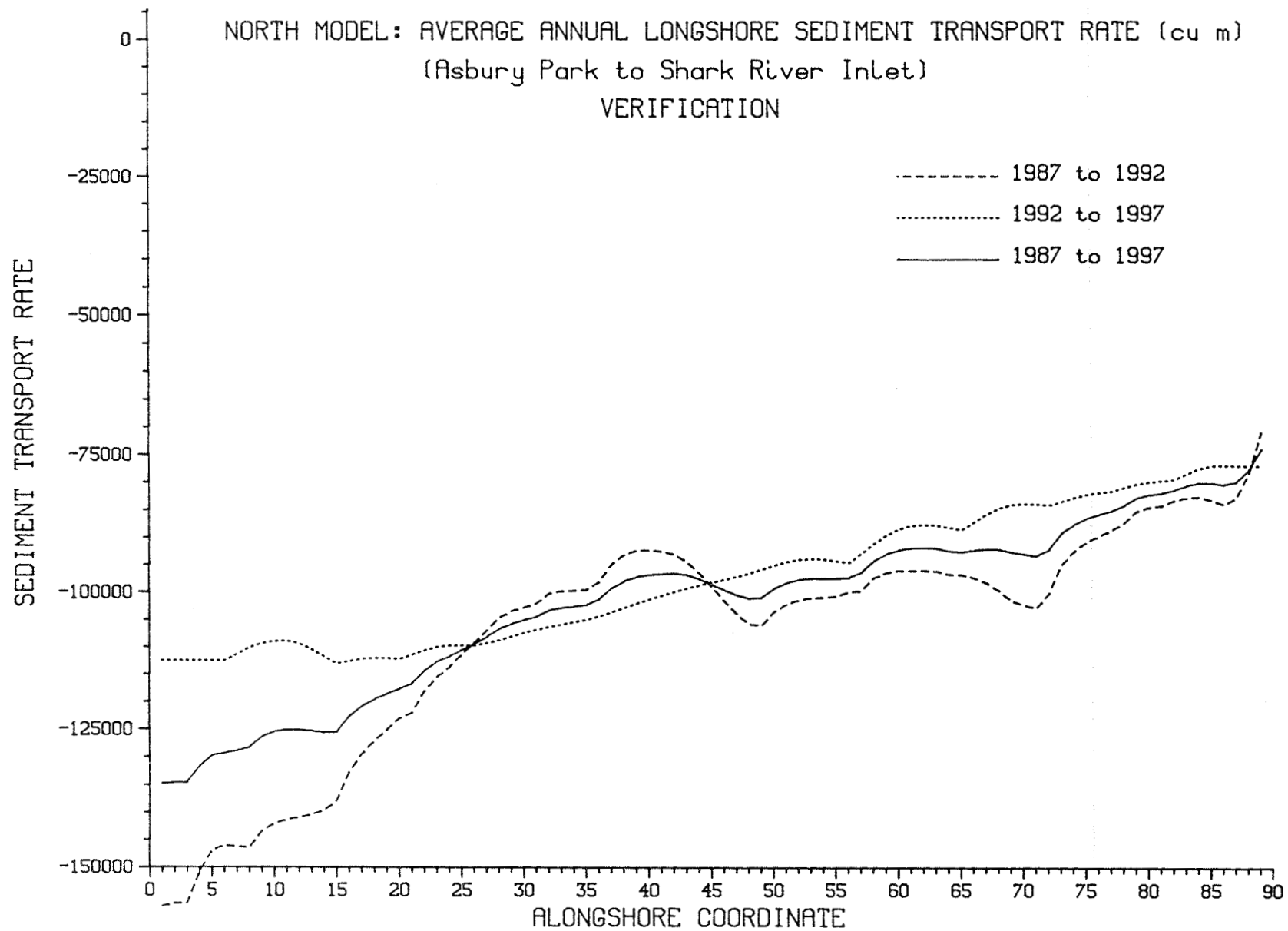


Figure 10. Average annual longshore sand transport rate, North Model

permeability for the south Shark River Inlet jetty was assigned the value of 0.3, which means that 30 percent of the calculated longshore sand transport that is not bypassed seaward of the jetty moves across the boundary in either direction. Similarly, the north Manasquan Inlet jetty was modeled as a diffracting groin with 5 percent permeability. This boundary condition allows 5 percent of the calculated sand transport which is not naturally bypassed to move across the boundary in either direction. As described for the North Model, numerous verification simulations were performed in which the groin permeabilities were varied to best approximate the surveyed shoreline change over the verification period. The final verification results for the south model are given in Figure 11. The solid line is the July 1977 surveyed shoreline position and was input to the model as the initial shoreline position. The dotted line is the April 1987 surveyed shoreline position, and the dashed line is the 1987 shoreline position as calculated by the model.

93. The verification of GENESIS for the south model reach is considered good. The calculated 1987 shoreline position agrees reasonably well with the surveyed 1987 shoreline position except in the region immediately adjacent to the south jetty of Shark River inlet in the township of Belmar. It is believed that the poor agreement in this region is the result of our present inability to model the deflection of littoral drift material into deeper water caused by the Shark River Inlet jetties. Consequently, in the model the calculated longshore sand transport rate decreases in approach to Shark River Inlet and accretion of the shoreline occurs. It is probable that the stream of littoral drift is diverted seaward around the inlet jetties, resulting in relatively stable shoreline. Sediment transport processes in the vicinity of tidal inlets are highly complex and the subject of much research; however, the present state of the art has not progressed to a point of application in shoreline change models such as GENESIS. So long as these limitations are understood and sound judgement used in interpreting model results, significant qualitative and quantitative information can be obtained through the use of shoreline change models for the evaluating shore protection design alternatives.

94. Average annual net longshore sand transport rates calculated by the model for the verification period are given in Figure 12. The net sand

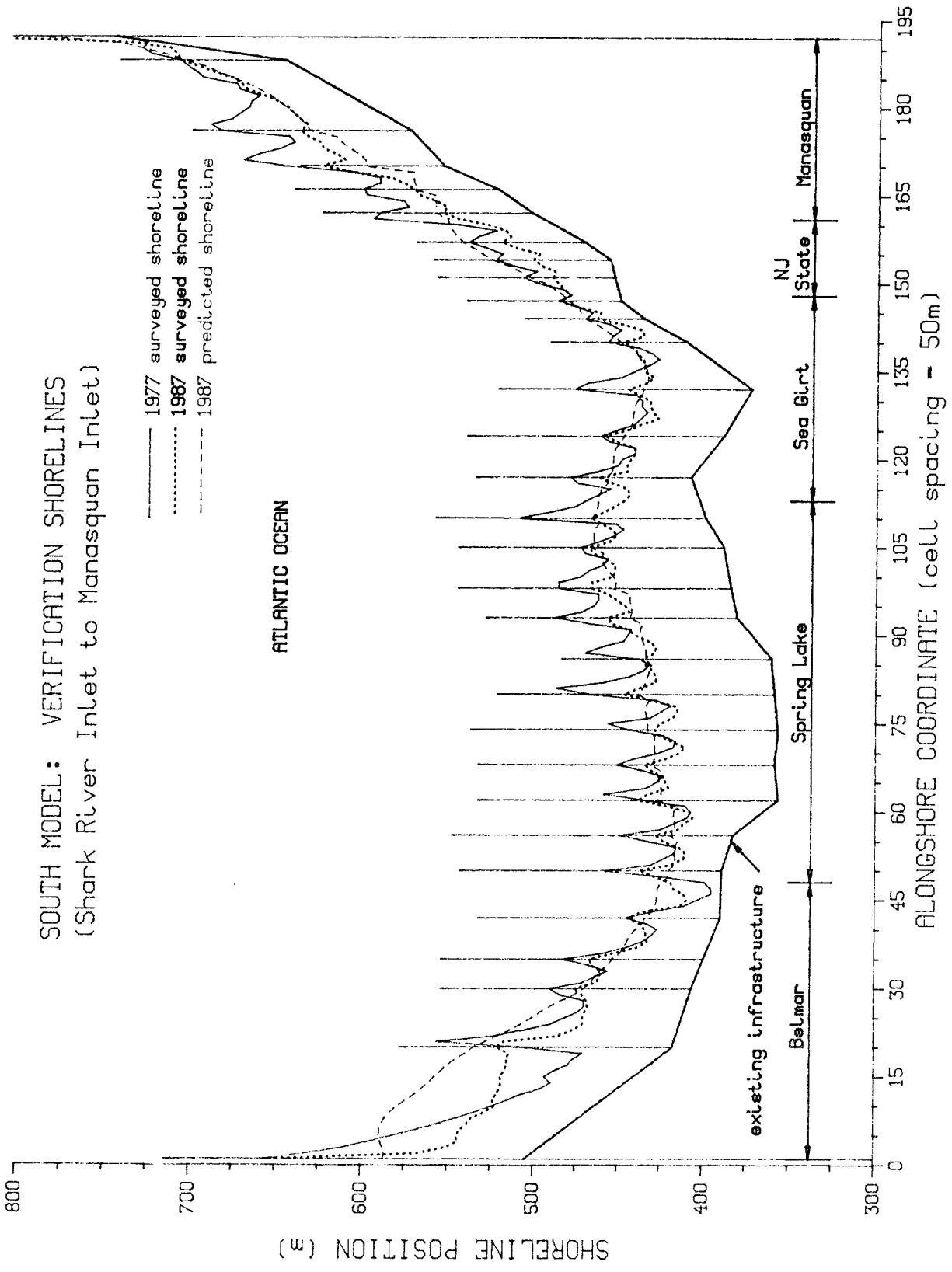


Figure 11. Final verification, South Model

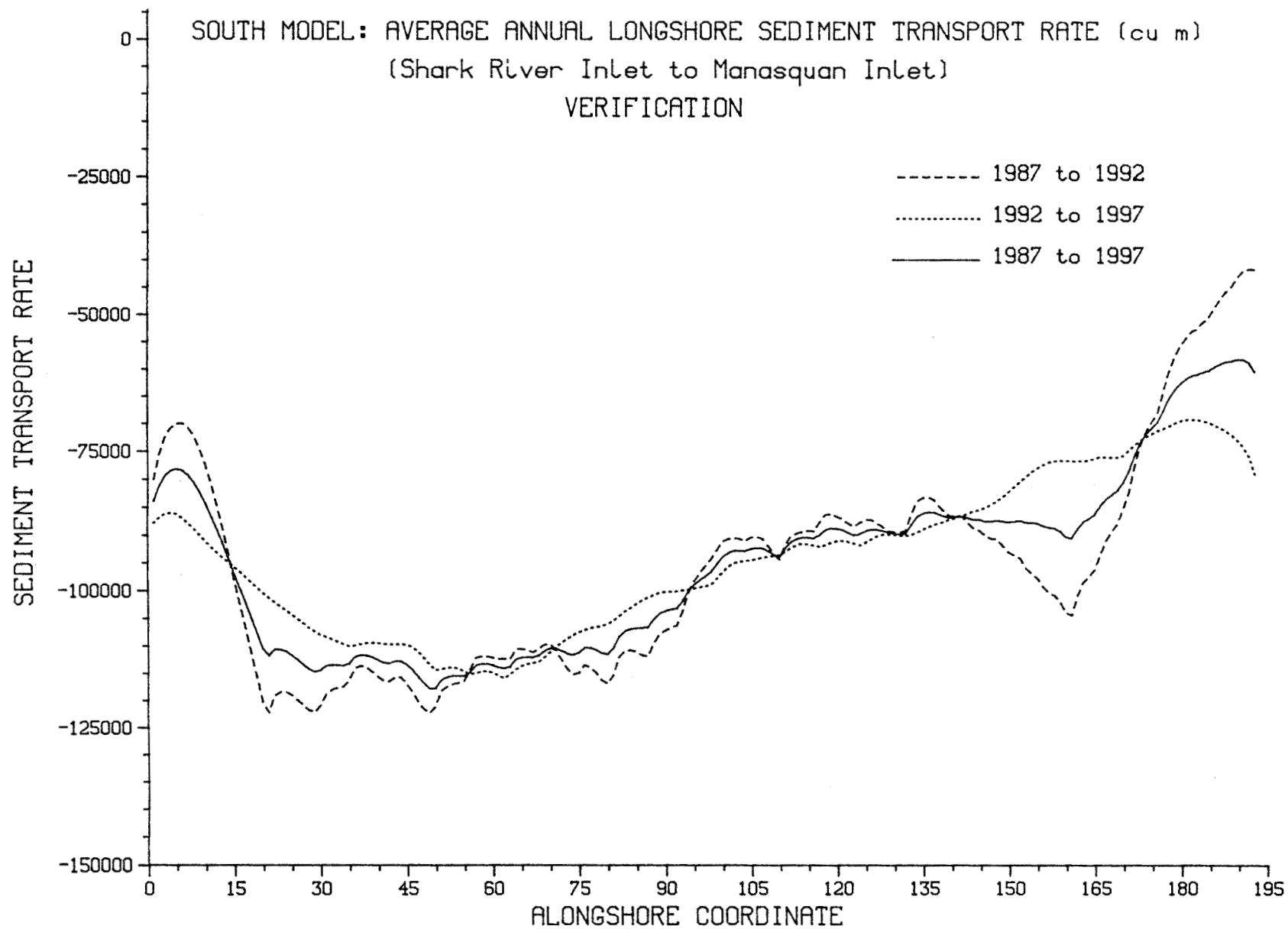


Figure 12. Average annual longshore sand transport rate, South Model

transport rates are directed to the north and in general increase in magnitude from south to north as expected. Transport rates range from about 65,000 to 115,000 m³/year (85,000 to 150,000 yd³/year). The net sand transport deficit or the differential transport rate across the south model reach is on the order of 25,000 m³/year (33,000 yd³/year). However, considering the previous discussion about sand transport rates adjacent to Shark River Inlet, this deficit could more realistically be estimated to be on the order of 50,000 m³/year (65,000 yd³/year).

95. Discussion. The shoreline change model GENESIS was successfully calibrated for the approximately 2.4-km (1.5 mi) reach centered about Manasquan Inlet. The calibration period (1929 to 1932) coincided with the stabilization of Manasquan Inlet which included the construction of inlet jetties and the dredging of a new entrance channel. This time period was selected because the new jetties completely blocked the longshore movement of sand northward along the coast, and allowed model calibration to the impoundment of sand updrift of the inlet. The direction and magnitude of calculated longshore sand transport rates updrift of the inlet agreed well with transport rates inferred from long-term shoreline change Caldwell (1966).

96. Verification of GENESIS was performed for the shoreline reaches where the proposed shore protection designs are being considered. The calibration coefficients were held constant in the verification simulations and the permeability factors were varied to achieve the known (surveyed) shoreline changes. Tables 9 and 10 provide a listing of the groin permeabilities as determined in the verification simulations.

97. Before discussing the results of the design alternative simulations, an introduction to methods of interpreting model results is provided. Successful verification of the model for the actual coastal reach where engineered coastal protection is planned allows a range to be established about the predicted shoreline positions. This range, hereafter referred to as the variability range, is determined with respect to how well the model predicted known shoreline change at any given position in the modeled reach. The variability range is determined from the final verification and is numerically equal to the difference between the surveyed shoreline change and the calculated shoreline change over the simulation

Table 9.

North Model Groin Permeabilities

<u>Model Groin No.</u>	<u>CENAN Groin No.</u>	<u>Permeability (%)</u>
1	107	20
2	108	5
3	109	10
4	110	20
5	111	30
6	112	40
7	115	60
8	117	10
9	119	10
10	121	10
11	122	20
12	123	10
13*	124	5

* Shark River Inlet north jetty.

Table 10.

South Model Groin Permeabilities

<u>Model Groin No.</u>	<u>CENAN Groin No.</u>	<u>Permeability (%)</u>
1*	125	30
2	128	60
3	129	60
4	130	40
5	131	60
6	134	20
7	135	20
8	136	10
9	137	20
10	138	50
11	140	20
12	141	40
13	143	20
14	146	10
15	147	20
16	148	20
17	150	30
18	154	30
19	157	40
20	160	60
21	161	60
22	163	60
23	166	60
24	169	70
25	172	70
26	174	20
27	176	10
28	178	0
29	180	10
30	186	60
31**	187	5

* Shark River Inlet south jetty.

** Manasquan Inlet north jetty.

period. Hence, the variability range at a given calculation cell may be either positive (indicating that the calculated shoreline position was located landward of the surveyed shoreline position) or negative (indicating that the calculated shoreline position was located seaward of the surveyed shoreline position). Figures 13 and 14 respectively show the variability range graphically for the North Model and South Model. In these figures, shoreline change from the 1977 surveyed shoreline position to: (1) the 1987 surveyed shoreline position and; (2) the calculated 1987 shoreline position; is plotted versus the alongshore coordinate. The shaded area (between the 1977-1987 surveyed and calculated shoreline change curves) is the variability range.

98. The variability range provides a quantified estimate of the potential variation about predicted shoreline positions. It is important to remember that GENESIS is a deterministic model and that its application in a predictive mode, requires that the factors responsible for beach change (primarily the waves) be assumed. Furthermore, the effect of groins on longshore sand transport rates and shoreline change is not well understood. In light of the complexity and variability of coastal processes, it is clear that a single answer obtained through a deterministic simulation must be viewed as a representative result that has been smoothed over a large number of unknown and highly variable conditions. Therefore, interpreting the predicted results of design alternative simulations using the variability range produces a more realistic assessment of the expected evolution of the design alternatives.

Evaluation of Alternative Shore Protection Plans

99. Two generic types of design alternatives were evaluated using the verified shoreline change model, the beach-fill only alternative, and the beach fill and groin construction alternative. In both alternatives, 50-, 100-, and 150-ft berm width designs were evaluated. In addition, to provide a baseline for comparison a without-project simulation was performed. Each design alternative was simulated twice, once using nearshore wave conditions refracted over the existing bathymetry and a second time using nearshore wave conditions refracted over a hypothetical bathymetry which contained three excavated sand borrow holes in the nearshore bathymetry as discussed in

NORTH MODEL: VERIFICATION
 (Asbury Park to Shark River Inlet)

SHORELINE CHANGE FROM 1977 SURVEY TO:

— 1987 Survey
 1987 Prediction

▨ Variability

ACCRETION

EROSION

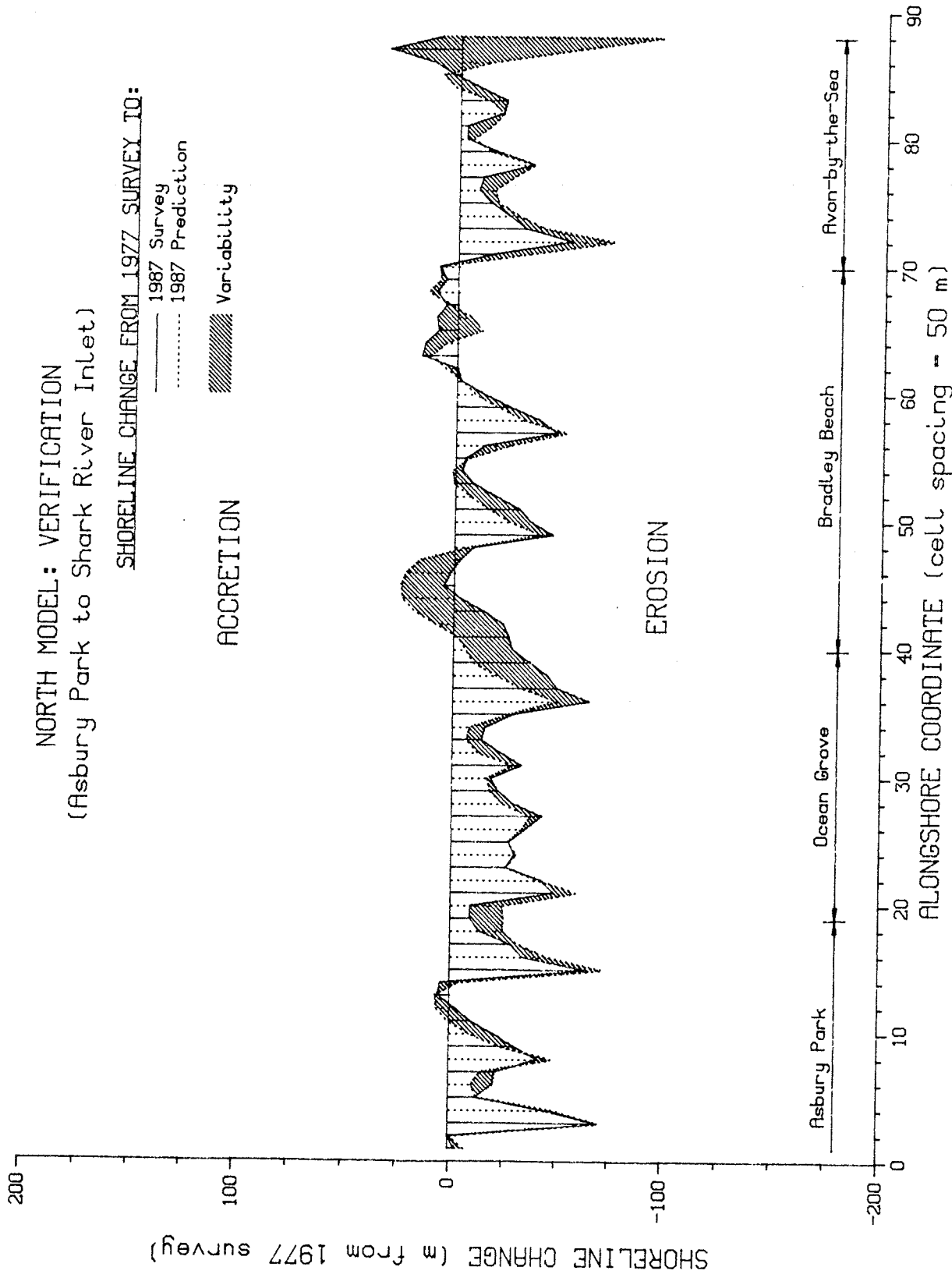


Figure 13. Variability range, North Model

SOUTH MODEL: VERIFICATION
 (Shark River Inlet to Manasquan Inlet)

SHORELINE CHANGE FROM 1977 SURVEY TO:

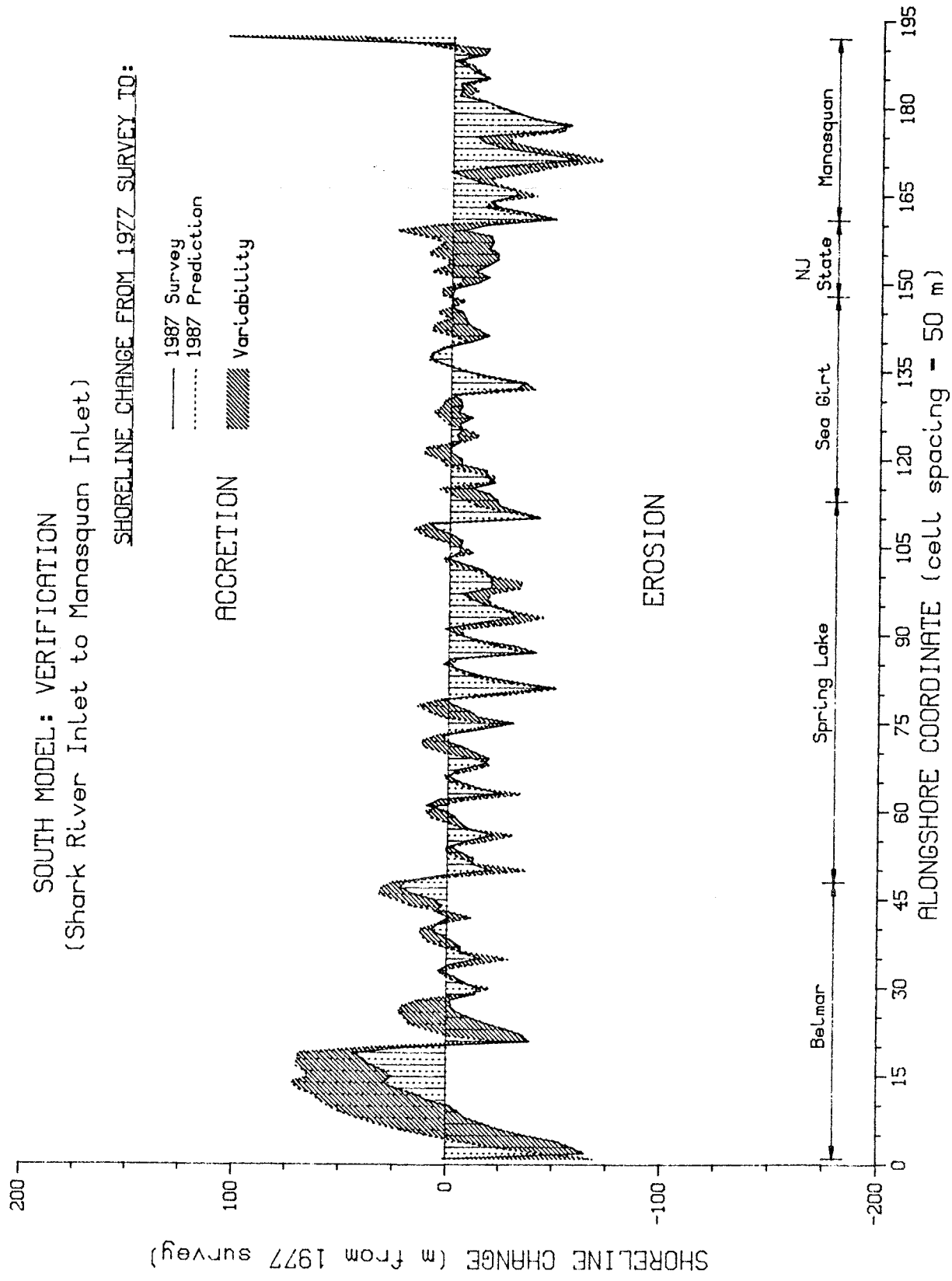


Figure 14. Variability range, South Model

PART II. All design alternatives were simulated for a 10-year period assuming that the shore protection design was implemented on the 1987 surveyed shoreline position. The evaluation of the proposed design alternatives proceeded as described below.

100. Twenty-six model simulations were performed initially. These simulations consisted of modeling the performance of the six basic design alternatives using both nearshore wave data sets and performing the without-project simulation for the North and South model reaches. At this stage the results were reported to CENAN for evaluation and design alternative refinement. CENAN responded by revising the configuration of the 100- and 150-ft berm width design alternatives for both the beach fill only and beach fill and groin construction alternative. The 50-ft berm width design alternatives were determined to be insufficient to achieve the desired shore protection and consequently were not revised for additional evaluation. The revised 100- and 150-ft berm width design alternatives were then simulated again using both nearshore wave data sets. Sixteen revised design alternative simulations were made. A grand total of 42 model simulations were made for the purpose of evaluating the long-term performance of proposed shore protection alternatives. The results of the initial design alternative simulations are included in Appendix D. The results of the without-project and the revised design alternative simulations are presented and discussed below.

101. Without-project simulations. Results of the without-project simulations for the North and South model reaches are given in Figures 15 and 16, respectively. These simulations were performed to quantify the expected evolution of shorelines within the project area without the benefit of proposed shore protection plans. The surveyed 1987 shoreline position was input to the model for the initial shoreline position. In Figures 15 and 16, the solid line is the initial (1987 surveyed) shoreline position, the dotted line is the predicted shoreline position after 5 years (1992 predicted shoreline position), and the dashed line is the predicted shoreline position after ten years (1997 predicted shoreline position). The variability range as discussed above is represented in the figures with cross-hatched shading and was applied to the predicted 1997 shoreline position. As indicated in Figures

15 and 16, continued shoreline erosion can be expected to occur all along the project reach if a shore protection plan is not implemented. In general, erosion on the order of 10 m can be expected in the next 10 years over most of the North Model reach; however, in the southern portion of Ocean Grove and northern portion of Bradley beach, shoreline erosion on the order of about 20 m is indicated. This erosion would place the shoreline dangerously close to parking lots and roadways which back this stretch of shoreline.

102. In the South Model, the 10-year average shoreline erosion is again on the order of about 10 m along most of the reach. Maximum shoreline erosion is indicated from between the southern portion of Sea Girt to the north part of Manasquan. If this maximum erosion were to occur, several private residences in south Sea Girt and northern Manasquan would be placed in jeopardy.

103. Revised 100-ft beach fill plan. This plan calls for the placement of approximately 1.9 million cubic meters of beach sand along the project reach. Of this total volume 1.1 million cubic meters of sand is specified to be placed on the North Model reach and 800 thousand cubic meters of sand is specified to be placed on the South Model reach. The results of the revised 100-ft beach fill design alternative simulations are given in Figures 17 and 18. In Figures 17 and 18, the diamond shaded area represents the shore protection plan as implemented on the April 1987 surveyed shoreline, in this case the revised 100-ft beach fill plan. This shoreline was input to the model as the initial shoreline position. The predicted shoreline position after the 10-year model simulation using nearshore wave conditions refracted over the existing bathymetry is shown as the dotted line. The dashed line is the predicted shoreline position that results from using the nearshore wave conditions that were refracted over the hypothetical dredged bathymetry. The area between the dotted and dashed lines represents the difference in the expected shoreline change due to the use of different incident wave climates. This area denoted in the figures with slashed shading will be referred to as the predicted range. Because natural infilling of the beach fill borrow sites is expected to occur with the passage of time, the actual shoreline position is expected to be located between the two predicted shoreline positions. The variability range was applied to the landward most predicted shoreline be it

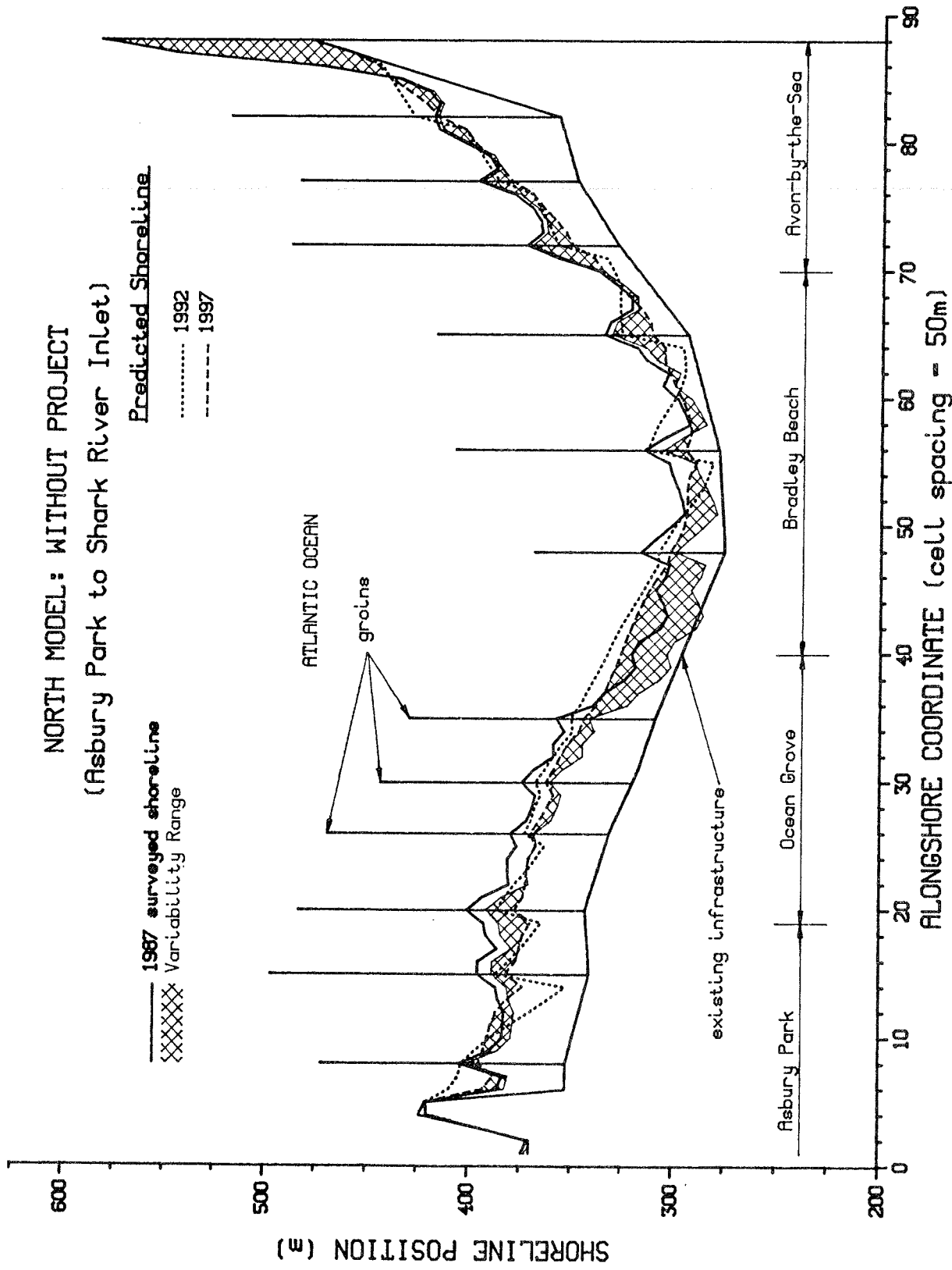


Figure 15. North Model, without-project simulation

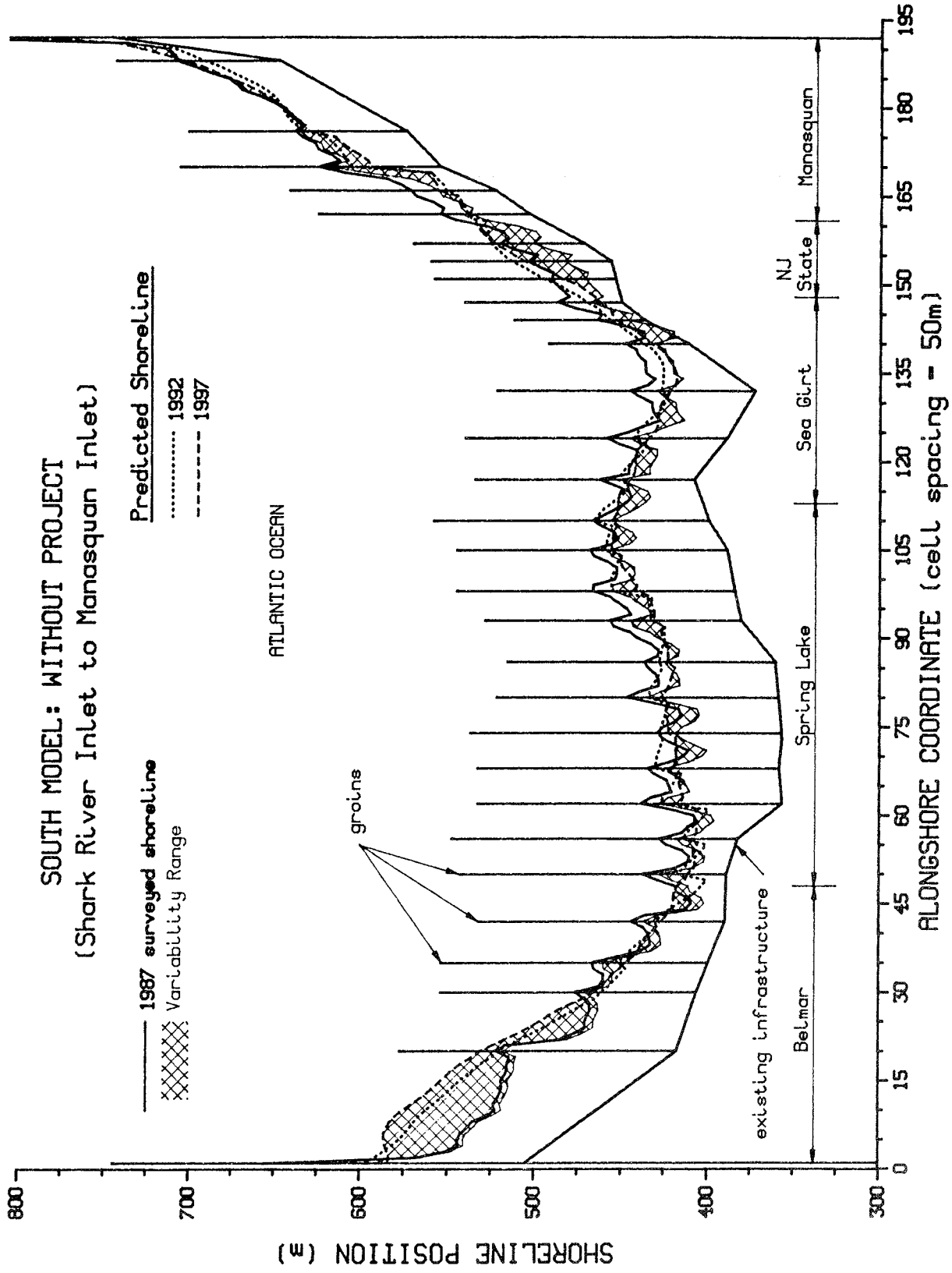


Figure 16. South Model, without-project simulation

NORTH MODEL: REVISED 100 ft BEACH FILL PLAN
 (Asbury Park to Shark River Inlet)

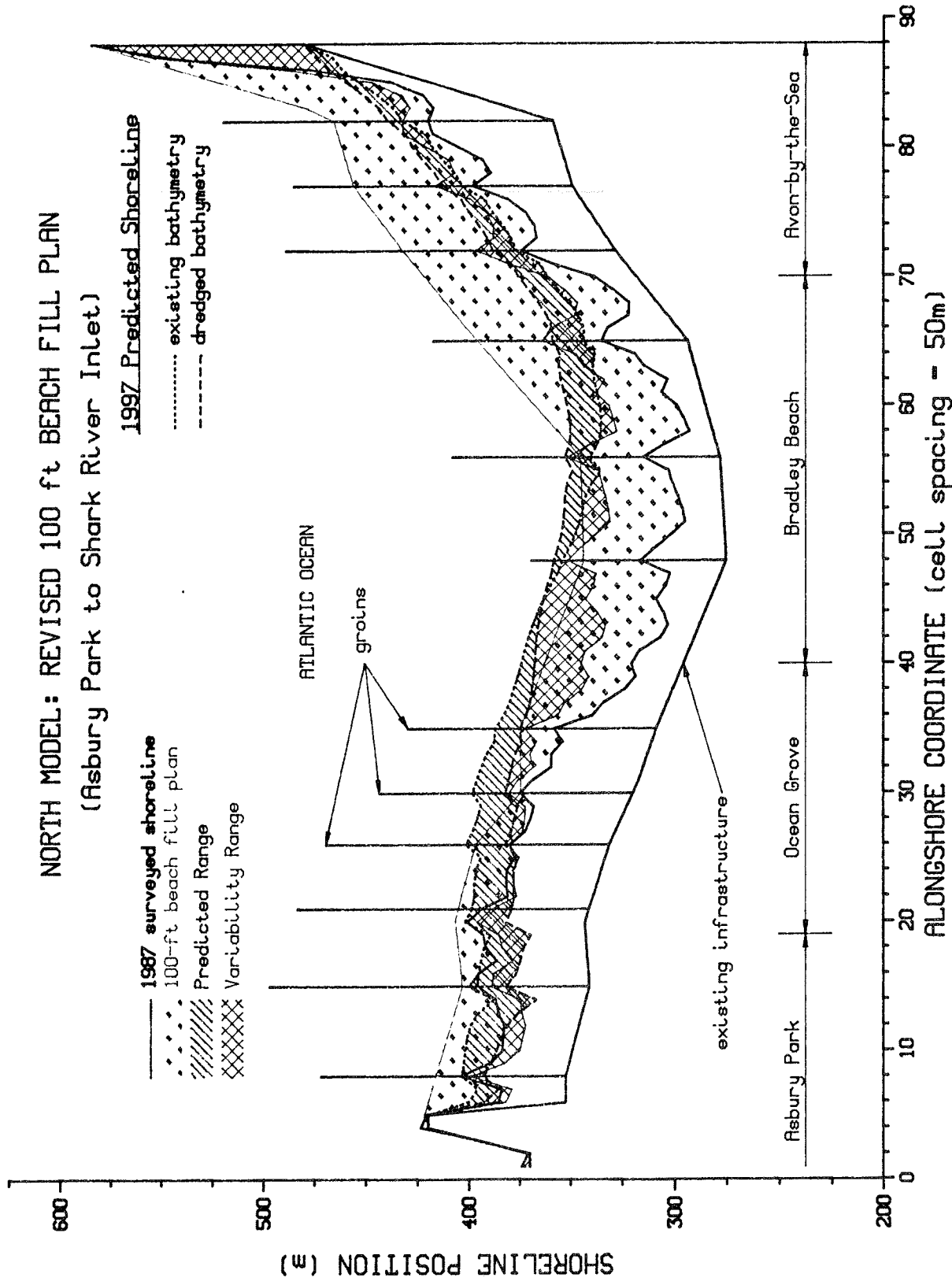


Figure 17. North Model, revised 100-ft beach fill plan simulation

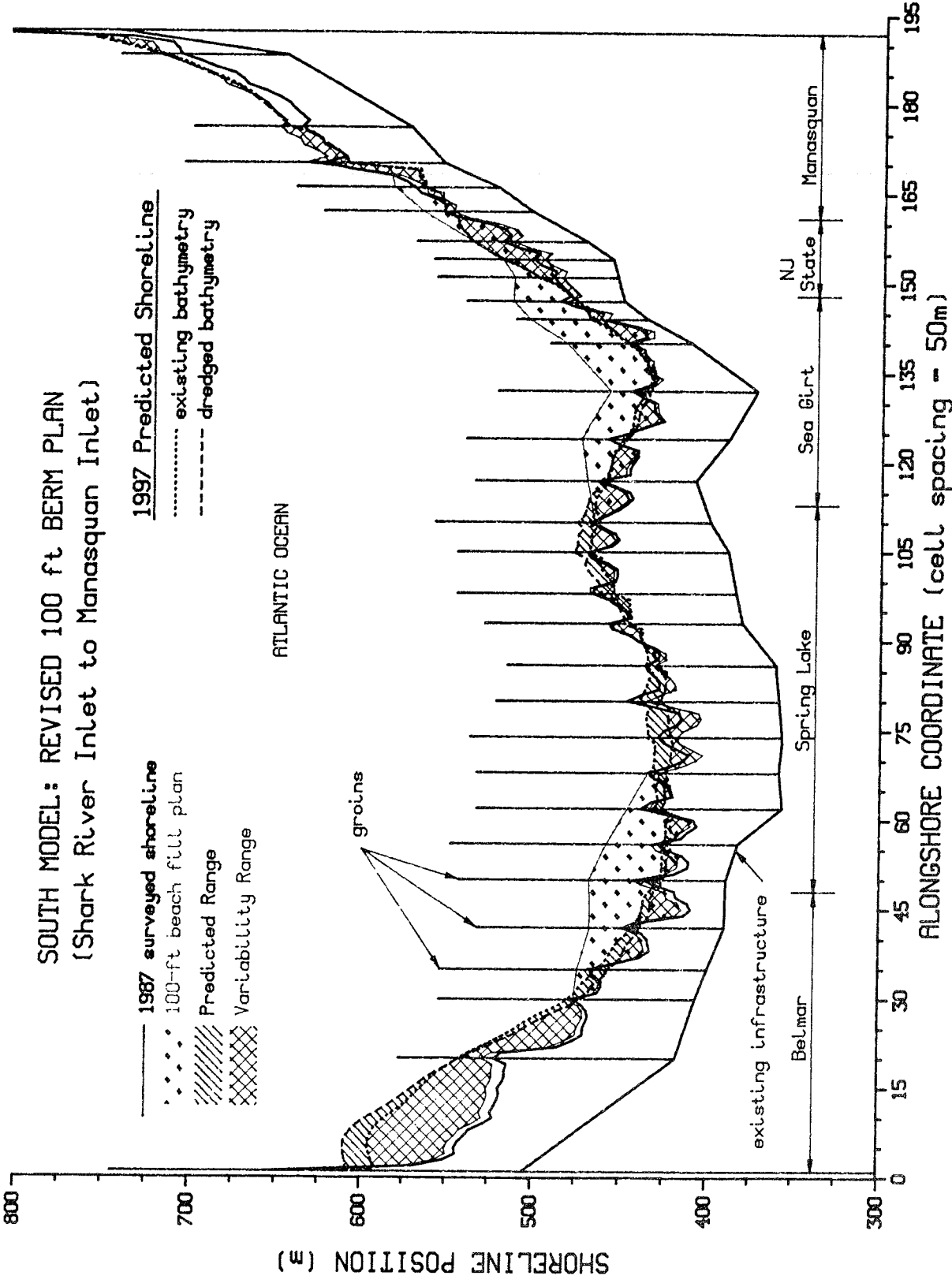


Figure 18. South Model, revised 100-ft beach fill plan simulation

resulting from the existing or dredged bathymetry simulation. The variability range is depicted in the figures by the cross-hatched shading.

104. The predicted range shown in Figures 17 and 18 indicates that excavation of the nearshore beach fill borrow sites will produce both erosion and accretion along the project coast. In the North Model, increased shoreline erosion is indicated from Asbury Park to Bradley Beach. Less shoreline erosion is indicated from Bradley Beach to Shark River Inlet. In the South Model reach, the magnitude of the effect of the excavation of nearshore beach fill borrow sites is somewhat less than in the North Model. Increased shoreline erosion is indicated from northern Belmar to about the middle of Spring Lake, and a slight decrease in shoreline erosion is noted in the southern third of Spring Lake. South of Spring Lake almost no shoreline change due to the nearshore beach fill borrow sites is indicated in the model results.

105. The overall performance of the revised 100-ft beach fill plan for the North Model reach is reasonably good. Volumetric calculations were made to estimate the longevity of the placed beach fill material. After 5 years about 70 percent of the placed beach fill material was still within the model reach and after 10 years more than 50 percent remained in the modeled reach. After the 10-year simulation period the calculated shoreline position with the variability range added to it is located seaward of the 1987 surveyed shoreline position from about the middle of Ocean Grove to Shark River Inlet. In the Asbury Park region, shoreline erosion of about 10 to 15 m is indicated; however, it is important to realize that this area is very sensitive to the effects of the nearshore beach fill borrow sites (i.e., the predicted range is large, on the order of 20 m) and that this erosion is likely to be less than predicted due to infilling of the borrow sites.

106. In the South Model reach, the overall performance of the 100-ft beach fill plan is good. With the addition of the variability range, the predicted shoreline position after 10 years is everywhere within 10 m of the 1987 surveyed shoreline position. Volumetric calculations indicate that about 85 percent of the placed beach fill material was still within the model reach after 5 years and 75 percent after 10 years. This design alternative appears to effectively maintain the shoreline position at the 1987 surveyed shoreline

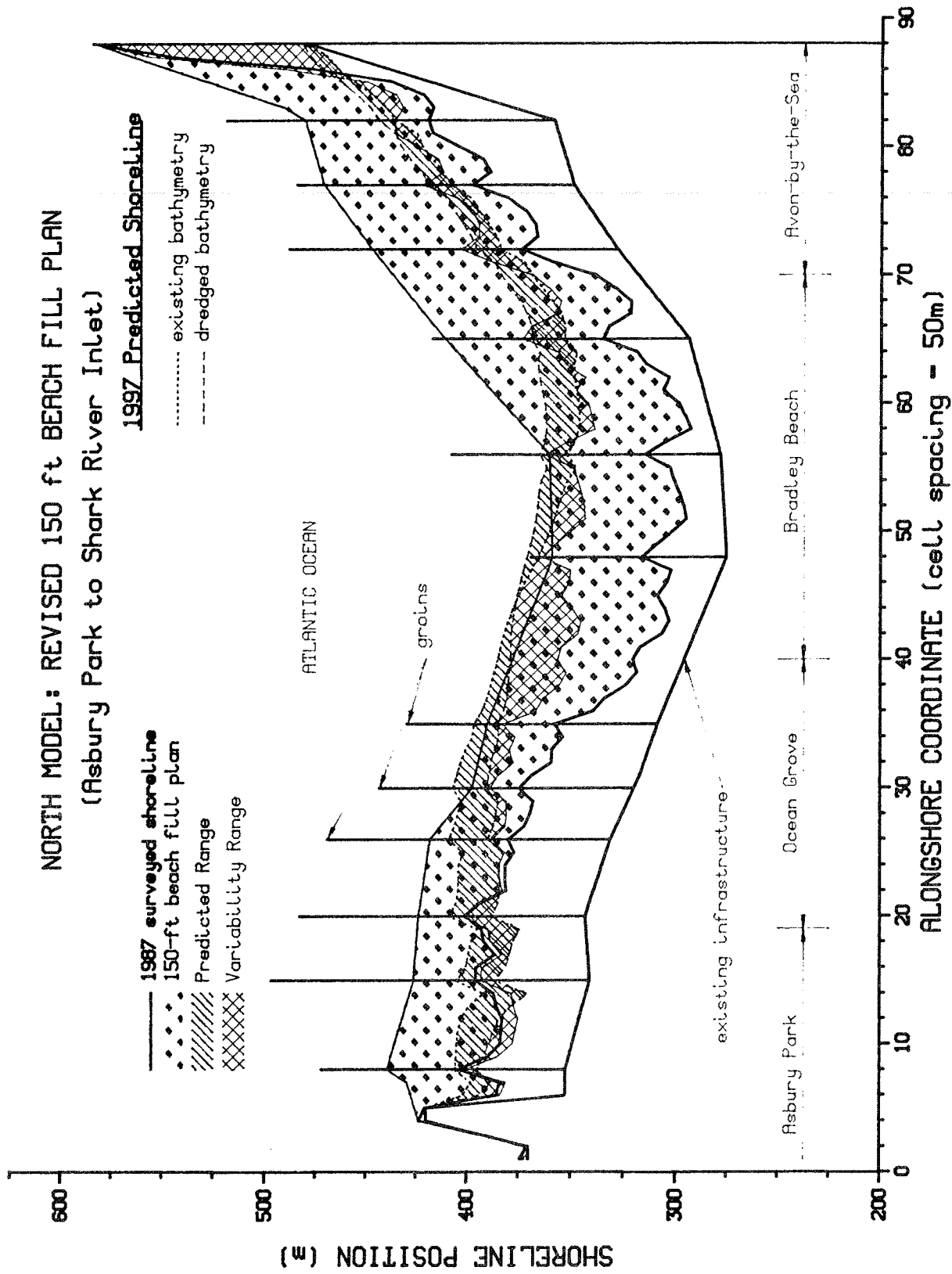
position, at least for the 10-year simulation period.

107. Revised 150-ft beach fill plan. This design alternative calls for the placement of approximately 3.0 million cubic meters of beach sand on the project shorelines. Of this total volume 1.4 million cubic meters of sand is specified to be placed on the North Model reach and 1.6 million cubic meters of sand on the South Model reach. The results of the 150-ft beach fill design alternative simulations are given in Figures 19 and 20. The line and shading designation is the same as given for the 100-ft beach fill plan shown in Figures 17 and 18.

108. It is interesting to note that the predicted range for this design alternative is nearly identical to the predicted range given for the 100-ft beach fill plan shown in Figures 17 and 18. This result could have been anticipated in that the two different sets of nearshore wave conditions each possess a given potential for the transport of sand alongshore. Since both design alternatives have a sufficient amount of sand available for transport the difference between the two predicted shoreline positions is logically the same.

109. The performance of the 150-ft beach fill design alternative is only marginally better than the 100-ft beach fill design alternative in the North Model reach. Shoreline erosion landward of the 1987 surveyed shoreline position by approximately 5 to 10 m is indicated in the Asbury Park region after the 10 year simulation period, while the predicted shoreline position everywhere else in the model reach is seaward of the 1987 surveyed shoreline position. In fact, in the Bradley Beach area the predicted shoreline is in excess of 25 m seaward of the 1987 survey. Average annual longshore sand transport rates calculated by the model provide an explanation for the marginally better performance of the 150-ft beach fill design alternative. Plots of the average longshore sand transport rates for the first 5 years of the model simulation show that transport rates for the 150-ft beach fill plan are about 35,000 m³/year greater than for the 100-ft beach fill plan in the Asbury Park area. In contrast, for the last 5 years of the model simulation, the average longshore sand transport rates are only about 15,000 m³/year greater for the 150-ft beach fill plan than for the 100-ft beach fill plan. This occurs because the effective lengths of the groins are reduced due to the

NORTH MODEL: REVISED 150 ft BEACH FILL PLAN
 (Asbury Park to Shark River Inlet)



1997 Predicted Shoreline

- 1987 surveyed shoreline
- 150-ft beach fill plan
- ▨ Predicted Range
- ▩ Variability Range

- - - - - existing bathymetry
- — — — — dredged bathymetry

Figure 19. North Model, revised 150-ft beach fill plan simulation

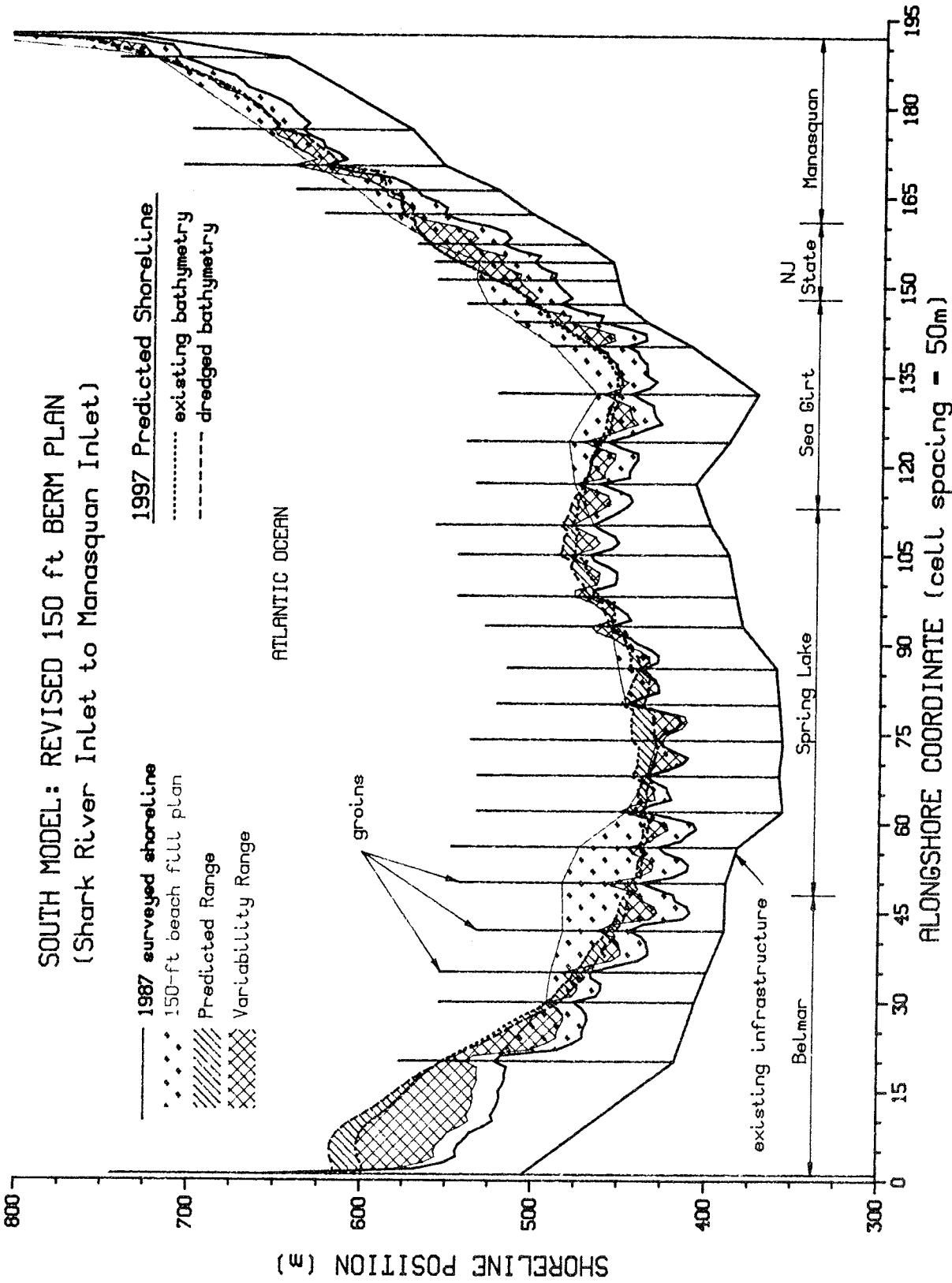


Figure 20. South Model, revised 150-ft beach fill plan simulation

placement of an additional 400,000 m³ of sand in the 150-ft beach fill plan. Consequently, sediment transport around the groins increases due to bypassing, resulting in increased initial shoreline erosion. Volumetric calculations indicate that after 5 years about 70 percent of the placed beach fill remained inside the model reach and after 10 years about 50 percent of the placed beach fill remained in the model reach. These percentages are essentially the same as for the 100-ft beach fill design alternative; however, the absolute losses are greater because the initial fill is greater for the 150-ft beach fill.

110. The performance of the 150-ft beach fill plan for the South Model reach is significantly better than the performance of the 100-ft beach fill plan. Volumetric calculations show that approximately 90 percent of the initial fill volume is still within the South Model reach after 5 years and 85 percent after 10 years. This is a 5 percent improvement (in the retention of the placed beach fill) after 5 years and a 10 percent improvement after 10 years over the 100-ft beach fill plan. The predicted shoreline position after the 10-year simulation period indicates an overall progradation of the shoreline from the 1987 surveyed shoreline position.

111. Revised 100-ft groin and beach fill plan. This design alternative calls for the placement of approximately 2.7 million cubic meters of beach sand on the project shorelines with 1.3 million cubic meters placed on the North Model reach and 1.4 million cubic meters placed on the South Model reach. Additionally, the construction of three new groins and the extension of one existing groin is specified in the North Model reach. In the South Model reach seven new groins and the extension of seven existing groins is specified. The results of the 100-ft groin and beach fill design alternative simulations are given in Figures 21 and 22. The line and shading designation in Figures 21 and 22 is the same as given before.

112. The construction of the groins in this design alternative significantly reduces shoreline erosion in the Asbury Park, Ocean Grove, and Bradley Beach areas of the North Model (see Figure 21). Longshore sand transport rates are effectively decreased by 5,000 to 15,000 m³/year north of Avon. This decrease in the longshore sand transport rates is a result of improved retention of the placed beach fill. Volumetric calculations indicate that 75 percent of the placed beach fill remains in the North Model reach

after 5 years and 65 percent after 10 years.

113. In the South Model reach the 100-ft groin and beach fill design alternative results in less shoreline erosion south of Belmar but increased erosion in Belmar, compared to the 100-ft and 150-ft beach fill design alternatives. Again this is primarily due to the placement of new groins and the extension of existing groins within the South Model reach.

114. Revised 150-ft groin and beach fill plan. This design alternative calls for the placement of approximately 4.6 million cubic meters of beach sand on the project shorelines with 1.8 million cubic meters placed on the North Model reach and 2.8 million cubic meters on the South Model reach. In addition to this beach fill, 5 new groins and 1 groin extension are specified in the North Model reach and 11 new groins and 9 groin extensions are specified in the South Model reach. The results of the 150-ft groin and beach fill design alternative simulations are given in Figures 23 and 24.

115. The predicted shoreline positions in the North Model reach (Figure 23) for this design alternative are in excess of 25 m seaward of the 1987 surveyed shoreline position between Asbury Park and Avon. The performance of this alternative in terms of retention of the placed beach fill material is expected to be lower than for the 100-ft groin and beach fill plan. Volumetric calculations indicate that approximately 70 percent of the placed beach fill is retained within the modeled reach after 5 years and about 55 percent after 10 years. This is about 5 percent less retention after 5 years and 10 percent less retention after 10 compared to the 100-ft groin and beach fill plan. The poorer performance of this design alternative compared to the 100-ft groin and beach fill plan is attributable the reduced effective length of the groins caused by the massive beach fill.

116. The predicted shoreline positions in the South Model reach (Figure 24) for this design alternative are generally about 25 m seaward of the 1987 surveyed shoreline position but vary between 10 and 50 m seaward of the 1987 shoreline position.

117. Summary and Conclusions. The model results of without-project simulations (Figures 15 and 16) give a clear indication that the shorelines within the project area are eroding and that a shore protection plan which includes beach nourishment is required to impede the present rate of shoreline

**NORTH MODEL: REVISED 100 FT GROIN AND BEACH FILL PLAN
(Asbury Park to Shark River Inlet)**

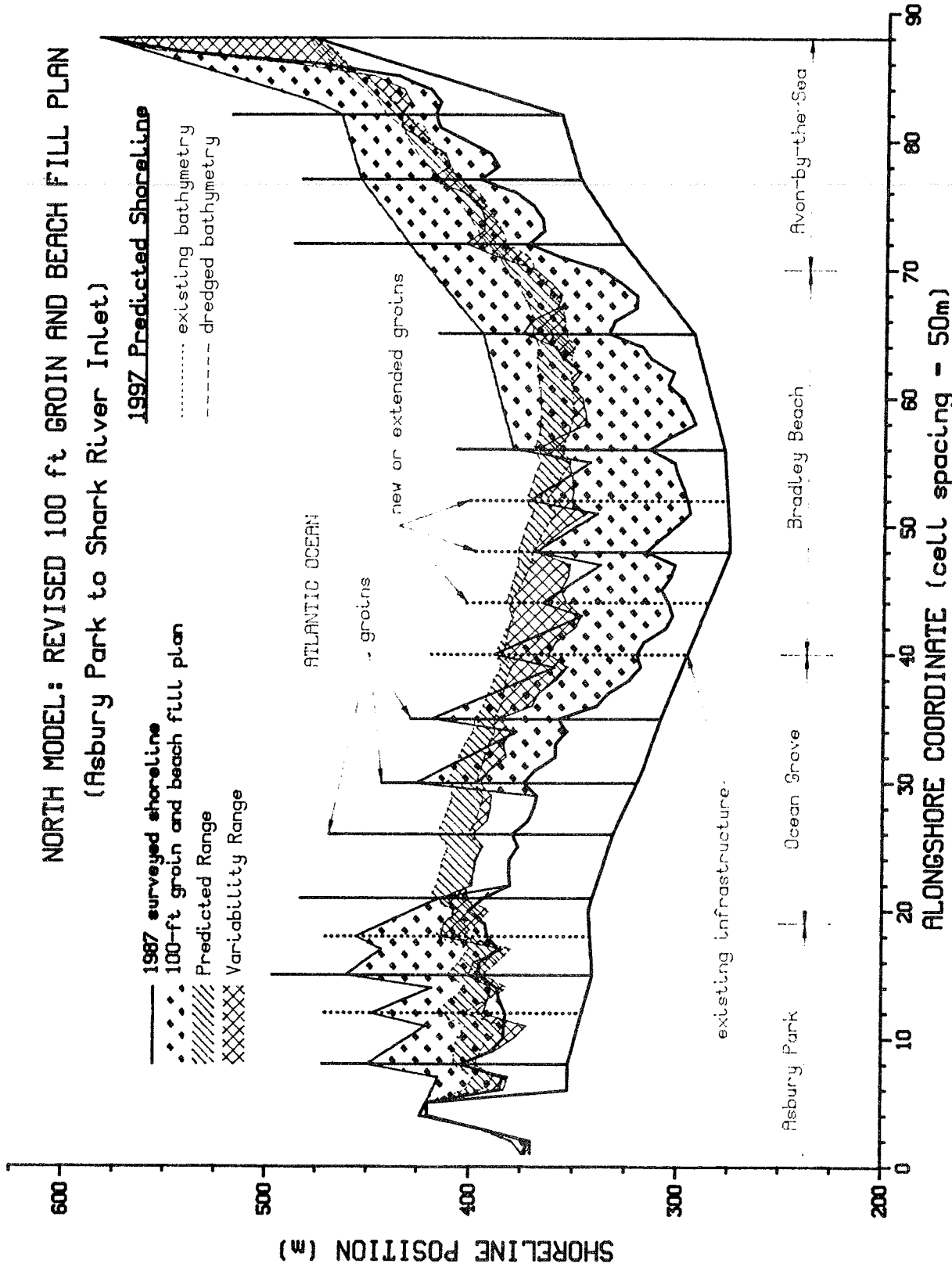


Figure 21. North Model, revised 100-ft groin and beach fill plan simulation

**SOUTH MODEL: REVISED 100 FT GROIN AND BEACH FILL PLAN
(Shark River Inlet to Manasquan Inlet)**

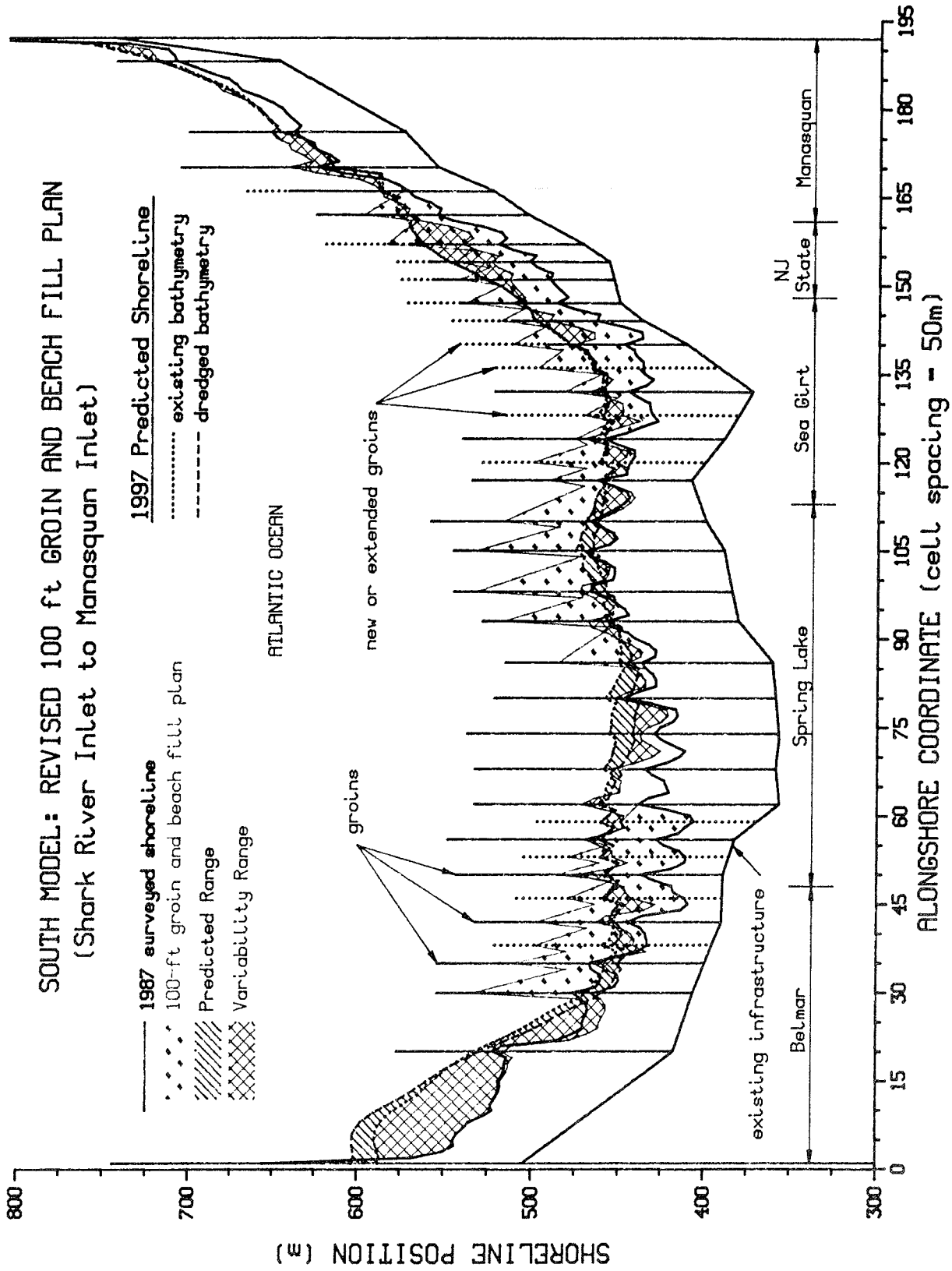


Figure 22. South Model, revised 100-ft groin and beach fill plan simulation

NORTH MODEL: REVISED 150 FT GROIN AND BEACH FILL PLAN
 (Asbury Park to Shark River Inlet)

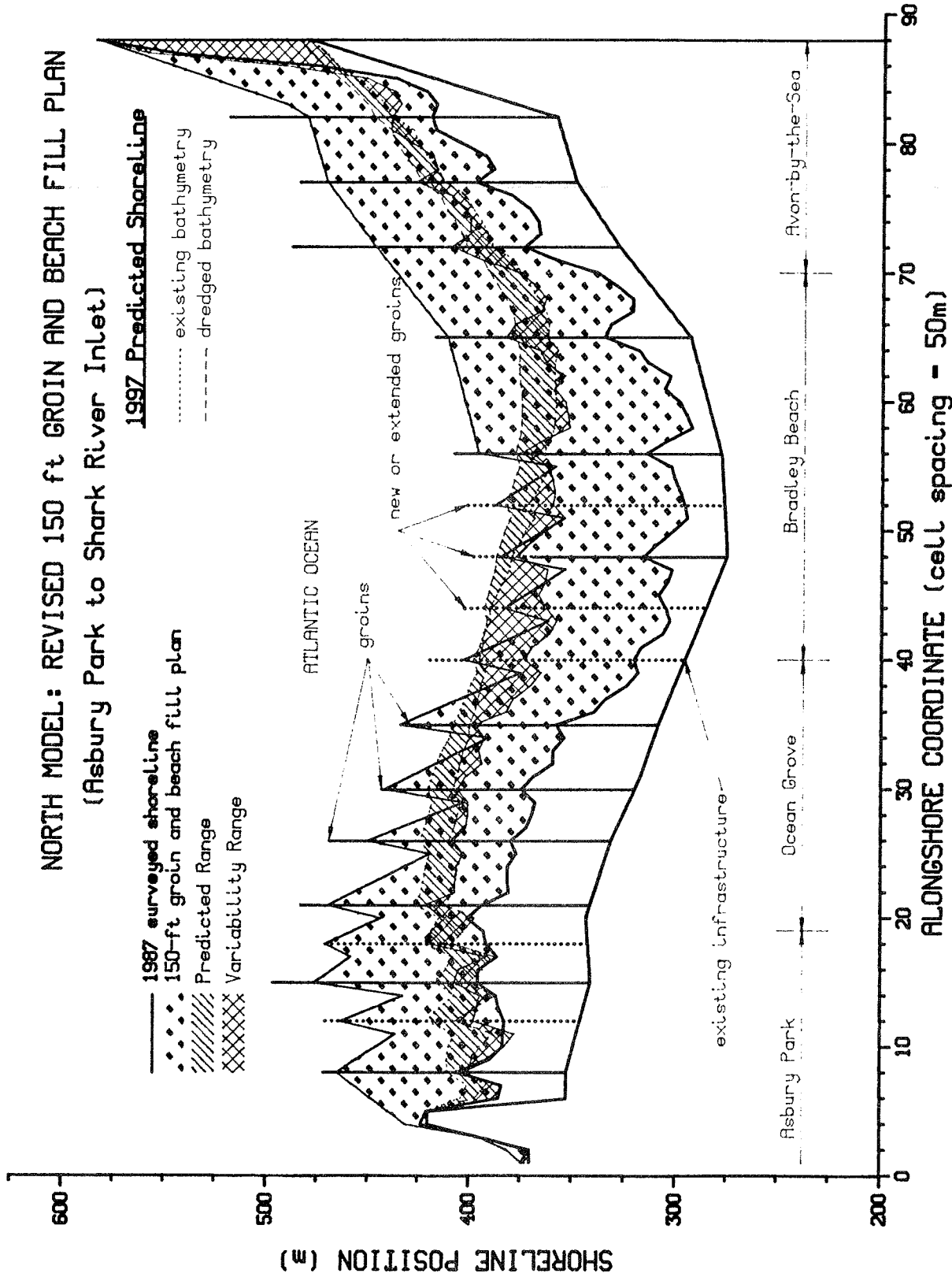


Figure 23. North Model, revised 150-ft groin and beach fill plan simulation

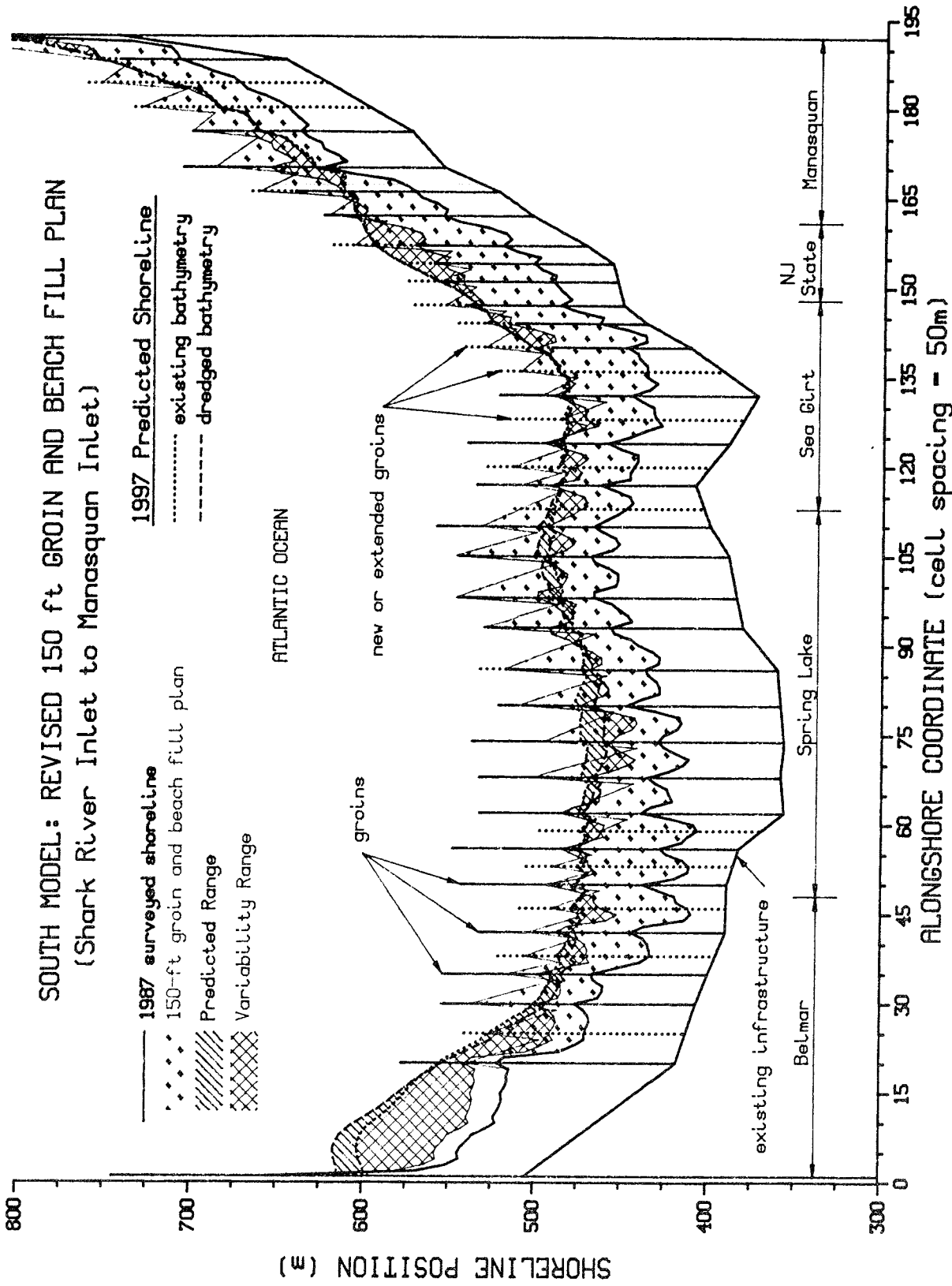


Figure 24. South Model, revised 150-ft groin and beach fill plan simulation

erosion and to provide protection of existing upland infrastructure. The costs associated with the construction of the various shore protection design alternatives will play an important part in the selection of the final design alternative which will be implemented based on an economic cost/benefit analysis. However, the cost/benefit analysis, part of NAN's overall comprehensive shore protection plan, was not performed in the present study. Recommendations made herein are based on predictions of longshore sand transport rates, and related changes in shoreline position. It is important to note that if the beach is nourished, benefits will extend beyond the physical limits of the project reach.

118. In the North Model reach, the results of the long-term shoreline change model indicate that the generic beach fill and groin construction plan will provide a greater level of protection than the beach fill-only plan. The southern Asbury Park region erodes landward of the 1987 surveyed shoreline position in both the 100- and 150-ft beach fill only design alternatives (Figures 17 and 19). In the 100- and 150-ft groin and beach fill design alternatives, the construction of two new groins are specified in this region and the results indicate that these groins decrease longshore sand transport rates and the rate of shoreline erosion (see Figures 21 and 23). Three other new groins and one groin extension are specified in the Bradley Beach region of the North Model reach but do not appear to be required based on the results of the beach fill-only design alternatives. The recommended proposed design alternative for the North Model reach, therefore, is a variation of the 100-ft groin and beach fill plan, in which only the new groins in the Asbury Park region will be implemented.

119. In the South Model reach, the results of the long-term shoreline change model indicate that construction of new groins or the extension of existing groins is not required to protect adjacent coastal properties (compare Figures 18 and 20 to 22 and 24). The 150-ft beach fill-only plan appears to adequately nourish the beaches and provides the desired coastal protection in this modeled reach. In this design alternative, the 1997 predicted shoreline position is located seaward of the surveyed 1987 shoreline position everywhere within the South Model reach.

PART IV: STAGE-FREQUENCY RELATIONSHIPS

Introduction

120. Water level at the coast is an important parameter affecting coastal processes. Water level is measured with respect to a specified datum or fixed reference level. In this study, the National Geodetic Vertical Datum (NGVD) is used as the reference datum. The NGVD is a fixed, level, geodetic surface established over the United States and Canada in 1929. Because there are many physical processes (astronomical, meteorological, and geological) affecting sea level, and because the geodetic datum represents a best fit over a broad area, the relationship between the geodetic datum and local mean sea level is not consistent from one location to another in either time or space. In this study, the local mean sea level between Asbury Park and Manasquan, New Jersey, is taken as 0.5 ft above NGVD as given by Meyers (1970) and listed in Table 4 of Harris (1981). This is the same value used in determining water levels in the Section I (Seabright to Ocean Township) study (Kraus et al., 1988), which was based on a previous CERC study for the Long Island, New York region (Butler et al. in prep.)

121. The task of this part of the study is to develop a relationship between the maximum still water level along the study section and the interval in time between the expected recurrence of this water level. This is referred to as a stage-frequency relationship. Stage information is used in a subsequent task to numerically model storm-induced dune erosion, discussed in PART V. A stage-frequency curve can be estimated from observed water levels at a point over many years or by simulating water levels at a point using a numerical model. In the latter approach, one has to associate a recurrence or frequency interval with the calculated water levels. This is usually done through the meteorological parameters describing a storm. A probability per year is assigned to each parameter, and this probability is estimated from the historical record at the location. The total probability is then the product of the individual parameter probabilities assuming they are independent of each other. In the present case, observed water levels are not available at

the desired point over a sufficiently long time interval so the numerical approach is used. This was the approach taken in the Seabright to Ocean Township study (Kraus et al. 1988) and the Long Island study (Butler et al. in prep.). In the present work, results from these previous studies are correlated with those from past studies (which resulted in stage-frequency curves for nearby locations to the south of the project) to infer the stage-frequency relationship for the project area.

122. The product of this portion of the study is a stage-frequency curve which relates the elevation of flood waters to the average waiting time between floods of equal or greater severity. The ordinate of this curve is stage, measured in feet above NGVD, and the abscissa is return period expressed in years.

123. Flooding in the study area is caused by the combination of storm-induced water level and astronomical tide. The storm-induced water level has two main components, storm surge and wave-induced water level. Storm surge is composed of the combined effects of storm winds piling water up along the shoreline and low barometric pressure raising the water surface. The wave component of the water level is caused by waves breaking along the shoreline. A portion of the momentum of the waves is transformed into both a longshore current and a rise in water level called wave setup. This study estimates the still water level due to the combined effects of storm surge and tide and, with less assurance, the wave setup component.

124. Two distinct classes of storms that result in storm surge in the study area are northeasters and hurricanes. Northeasters, named after the predominate direction of winds, are large-scale low pressure disturbances which usually occur from late September through April. The wind speed of a northeaster is not usually as great as that of a hurricane. Although wind gusts can reach hurricane strength in a very severe northeaster, sustained wind speeds are rarely greater than 50 kn. The flood damage caused by the typical northeaster is often a function of its duration as well as its intensity. Longer-duration storms have more opportunity to destroy both natural and engineered flood protection features. Also, since a northeaster can persist for two or three days, it is more probable for a spring tide to occur during the storm. If this does happen, flood damage will be greater

than if the storm had acted during a period of lower high tides.

125. Hurricanes are a rarer occurrence in the study area. By the time hurricanes approach the latitudes of the northern New Jersey coast, they are usually in a state of rapid decay and are far out to sea on a path that is curving away from the coast. Despite their infrequent occurrence, hurricanes have the potential to cause devastating flooding in the study area because of the large storm surge produced by the high wind speeds and low pressures and, possibly, the funneling effect of the New York Bight near the northern part of the study area.

Methodology

126. The previous studies used to infer a stage-frequency relationship for the present area, Asbury Park to Manasquan, New Jersey, are: a CERC study of the Long Island, New York region (Butler et al. in prep.) which resulted in a stage-frequency relation for Sandy Hook, New Jersey; a CERC study of the Seabright to Ocean Township region (Kraus et al. 1988) which resulted in a stage-frequency relation for Monmouth Beach, New Jersey; and a U.S. Weather Bureau study (Meyers 1970) which resulted in a stage-frequency relation for Long Beach Island, New Jersey.

127. In the target regions of the previous CERC studies, the scarcity of historical water level records necessitated a synthetic modeling approach to generate the water levels needed for the construction of stage-frequency curves. For hurricanes the joint probability method (Meyers 1970) was used to create synthetic storms. An individual hurricane can be represented by five parameters: central pressure deficit, forward speed, radius of maximum winds, track angle, and landfall point. Representative values are chosen for each parameter, and an ensemble of synthetic storms is formed by combining values of the five parameters. Probability is assigned to an individual storm by determining the probability of each parameter value in that storm. If the parameters are independent, then the probability of occurrence of the storm is the product of the probability of the component parameters.

128. For the Long Island Study, 918 hurricanes were simulated resulting in a stage-frequency curve at Sandy Hook for hurricanes. All of these storms

plus an additional 54 storms were used to derive the stage-frequency curve at Monmouth Beach for hurricanes. The report of Meyers (1970) summarizes information on hurricanes impacting the south New Jersey coast over the time interval 1900-1956. Central pressures were in the range of 938-992 mb; forward speeds 15-46 mph landfalling and 19-57 mph alongshore; and radius of winds 22-56 nm.

129. Northeasters are more difficult to parameterize than are hurricanes; therefore, an historical approach was used to establish a northeaster storm ensemble for the Long Island Study. Twenty-seven historical storms were chosen which were representative of the 41-year period, 1940 through 1980. Historical data, after the subtraction of predicted tide, were used to develop a partial duration stage-frequency curve of northeaster surge levels at Sandy Hook. Probabilities were assigned to the 27-member storm ensemble according to the portion of this stage-frequency curve they represented. Due to the large spatial extent of northeasters, the 27 historical northeasters from the Long Island study were also judged to be adequate for the Monmouth Beach site. These 27 storms were used as a basis for creating synthetic events which were used to develop stage-frequency relations for surge plus tide at Sandy Hook and Monmouth Beach for northeasters.

130. The study by Meyers (1970) employed the same joint probability approach to generating a stage-frequency relation. In fact, his was the first published application of this approach. Thus the stage-frequency curve at Long Beach Island was derived using the same approach as the CERC studies although the details of execution were different. For example, the number of values for the parameters characterizing the hypothetical storms were different, the number of hypothetical storms generated from combinations of the parameters was different, and the surge model used to estimate water level for each storm was different.

131. The basic approach of combining the surge with the astronomical tide to obtain the total water level is the same in the studies by Meyers and CERC. That is, a number of tidal signals of different amplitudes and phases are combined with the calculated surge time histories to produce a set of total water levels. The manner in which the tide signals are estimated and

combined with the surge time histories is different in the two studies but both are considered acceptable.

132. At present there is not an accepted methodology to estimate the storm-induced wave setup component of water level at the coast together with the surge and tide components to produce a combined three-component stage-frequency curve. The reason for this is that wave conditions along a coast have not normally been calculated as part of storm surge studies in the past, and the wave setup component is generally considered to be less than the separate effects of wind, pressure, and tide in producing the total water level. Thus engineers have been conservative in their estimates of surge and tide, assuming wave setup would not affect the results. However, as surge models continue to become more detailed and accurate, the magnitude of the wave setup component may exceed the accuracy of the surge models and so should be considered explicitly. CERC will soon begin a research program which will consider this problem and develop a methodology for practical application. In the meantime, for studies such as this where the dynamics of the beach are as important as flood protection, some estimate of wave setup should be included. However, it can only be included in a gross sense since we lack the detailed wave and surge models of the area to produce a more accurate result.

133. Wave setup can be influenced by local bathymetry on a scale smaller than would affect surge. It is also highly dependent on wave height, period, and direction near the coast, all of which can vary considerably in the case of a hurricane. The nature of the land-sea boundary is also a factor. On a low flat coast wave energy and water level will spread out quickly over a broad area. On a non-flooding coast, increased water level and wave energy will be concentrated on the land water boundary. It is seen from the above that along a given section of coast wave setup may be important in some areas and negligible in others. The phenomena is also a time-dependent process, developing as the incident wave field increases in energy until an equilibrium is reached between the transfer of energy from the wave field to setup of the mean water level at the shore and or generation of a longshore current. For a hurricane, the nearshore wave field can build and decay over a few hours. Thus wave setup may be present at a site for a limited time, usually being the greatest with the closest approach of the storm and maximum

surge. When this equilibrium exists, the mean water level is increased and is related to a statistical or spectral wave height. There may also be rapid and potentially large elevation changes at the shore due to individual waves, termed wave runup.

134. Considering the above, it is concluded that incorporation of wave setup in a storm surge calculation to the best of our ability is an extremely complex task. However, if one makes simplifying assumptions, it is possible to obtain an estimate for use in applications. For this study, we assume: the beach is non-flooding (in the sense of overtopping onto a flood plain); the waves approach normal to shore; and the bathymetric contours offshore are straight, shore parallel, and equally spaced. At the mean sea level shoreline, the beach is assumed to change slope to a value larger than the offshore. Incident waves on top of surge plus tide are assumed to break at this slope discontinuity at mean sea level and be limited in height to the total water depth. A breaking wave height to water depth ratio of unity is used to provide a conservative scale for the upper range of breaking wave indices. The maximum setup at the shoreline is assumed to be equal to 0.1 times the breaking wave height. Under these assumptions wave setup becomes equal to 10 percent of the total water level. Some evidence is provided by Tancreto (1958) that wave height is linearly related to surge level. Model studies (Battjes 1974, Battjes and Janssen 1978) have indicated a linear relationship between wave setup and wave height. Field measurements (Hubertz, Jensen, and Abel, 1987) have also indicated that in one case wave setup was on the order of 10% of the total water level; thus, there is some foundation for the assumed relationship between surge and setup used in this study.

Results

135. Previously calculated stage-frequency curves for Sandy Hook, Monmouth Beach, and Long Beach Island are presented in Figure 25. They indicate that there is less than 1/2 foot difference between the stage-frequency at Monmouth Beach and Long Beach Island, which bracket the

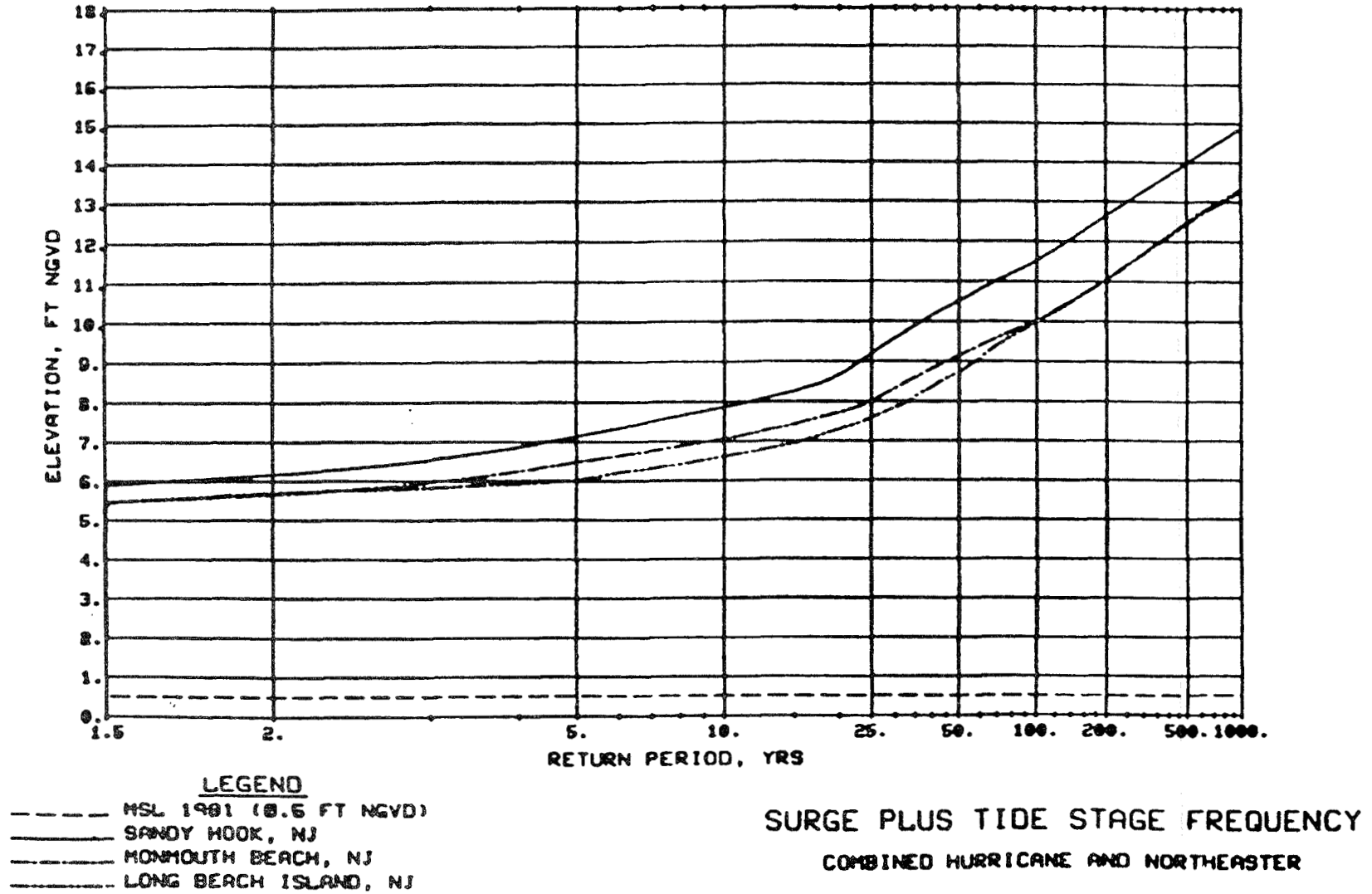


Figure 25. Stage frequency curves for Sandy Hook, Monmouth Beach, and Long Beach Island, NJ

study area. This is encouraging in the sense that along an approximately 50-mile segment of coast, employing the same approach but using different numerical models results in approximately the same stage frequency curve. Review of these data indicate that interpolation of the available stage-frequency curves for Monmouth and Long Beach can be used to arrive at a stage-frequency curve for the present project reach.

136. The stage-frequency curve for the open coast area from Asbury Park to Manasquan is shown in Figure 26. It is derived from an interpolation between stage-frequency curves for Monmouth and Long Beach, and represents the combined effects of hurricanes and northeasters. Separate curves for hurricanes and northeasters are given in Figure 27 and Figure 28, respectively. Northeasters dominate the combined curve up to a return period of approximately 25 years, after which hurricanes are the dominant cause of the rise in water level at the coast. The contribution to the mean still water level by wave setup is shown by the dashed line and results from the assumption that it equals 10 percent of the surge plus tide level.

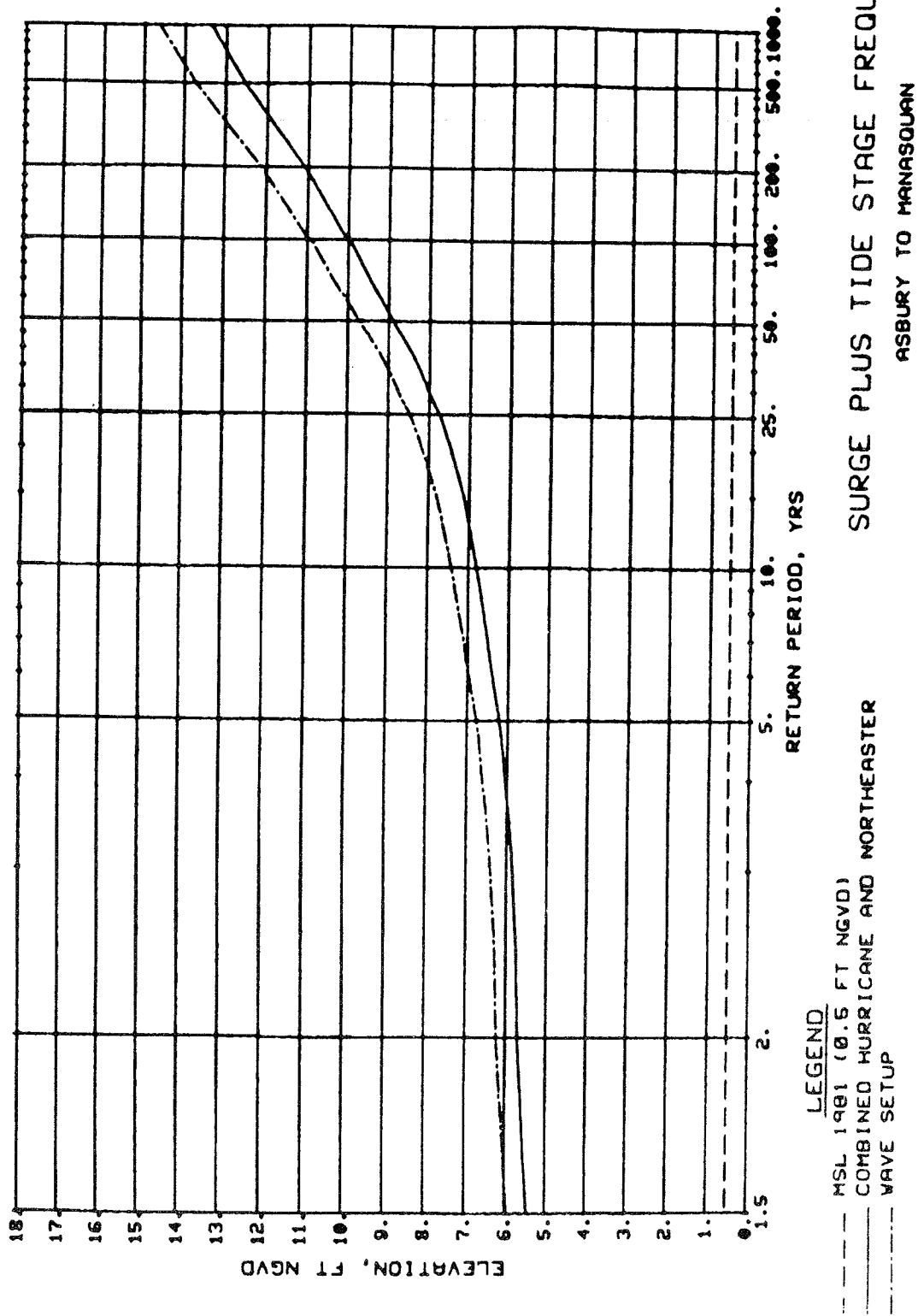
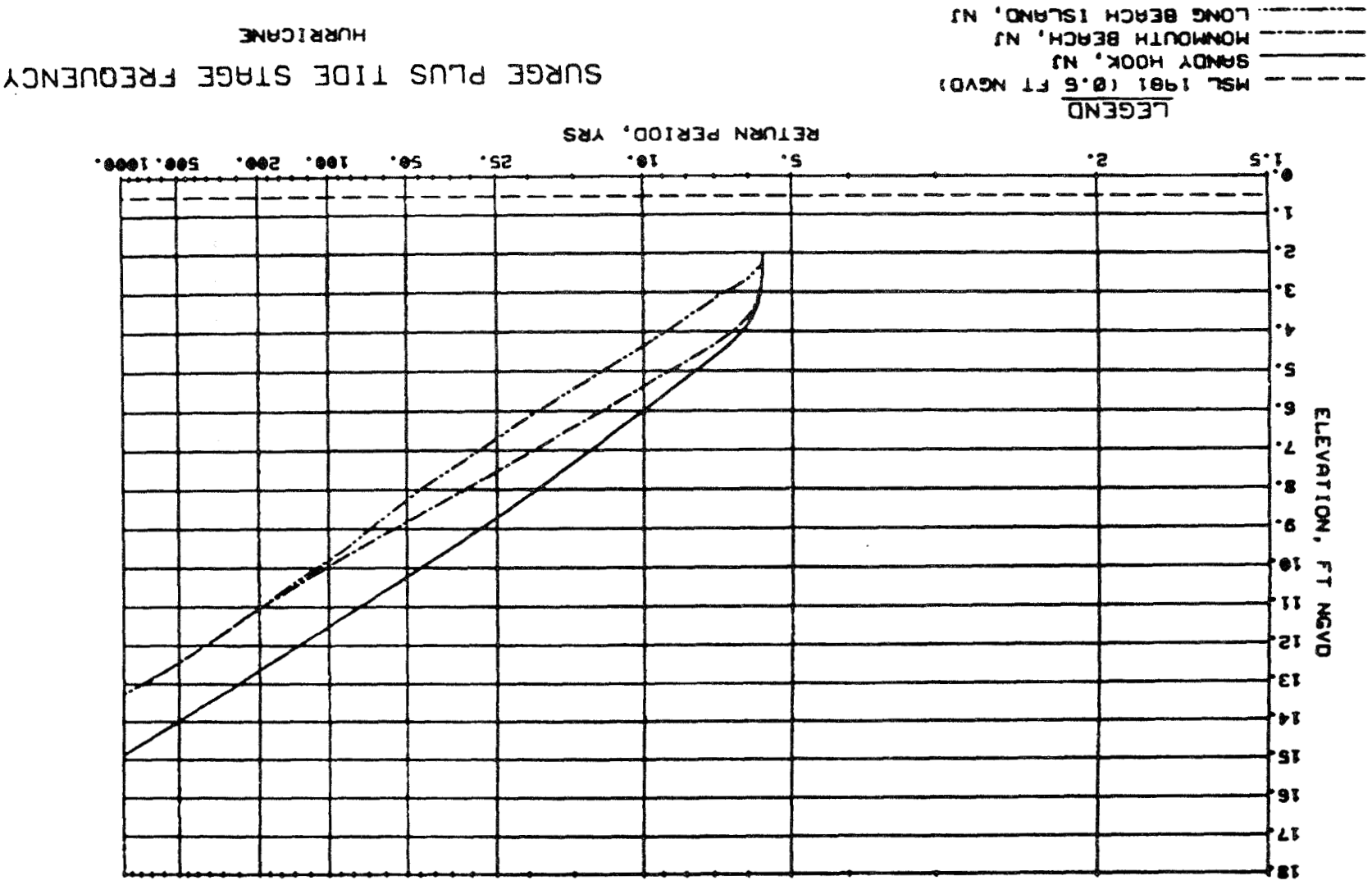


Figure 26. Stage frequency curves for Asbury Park to Manasquan, NJ

Figure 27. Stage frequency curves for hurricanes: Asbury Park to Manasquan, Monmouth Beach, and Long Beach Island, NJ



NORTHEASTER

SURGE PLUS TIDE STAGE FREQUENCY

LEGEND

- MSL 1981 (0.5 FT NGVD)
- SANDY HOOK, NJ
- MONMOUTH BEACH, NJ
- LONG BEACH ISLAND, NJ

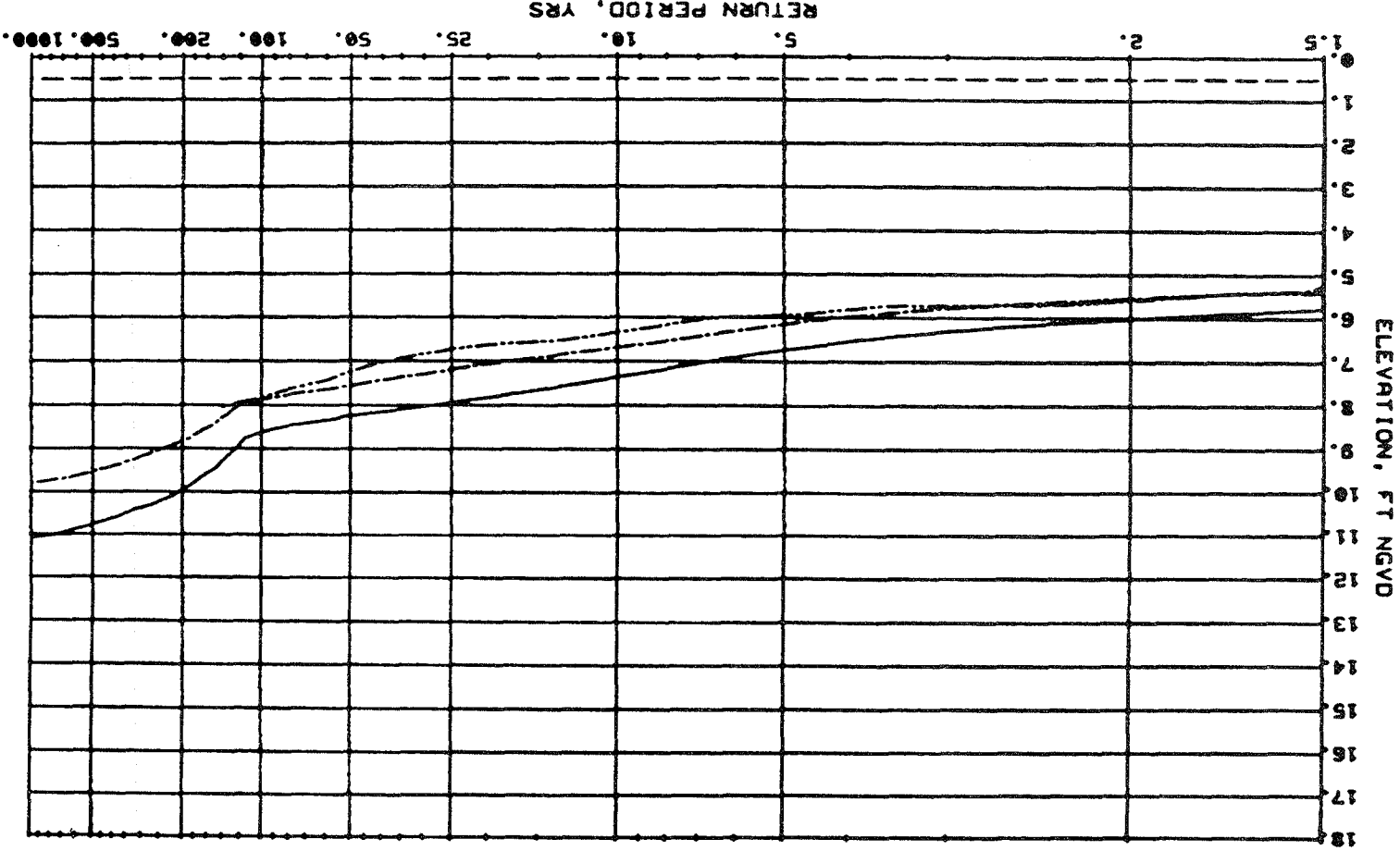


Figure 28. Stage frequency curves for northeasters: Asbury Park to Manasquan, Monmouth Beach, and Long Beach Island, NJ

PART V: NUMERICAL MODELING OF STORM-INDUCED DUNE EROSION

Introduction

137. The objective of the numerical modeling of storm-induced dune erosion task of this study was to determine the potential impact of storm-induced erosion on the coastal area between Asbury Park to Manasquan Inlet, New Jersey. This goal was approached in two phases, the first of which was to evaluate existing conditions in the subject area for the purpose of documenting the necessity of providing additional storm protection measures. The results were used by NAN to design beach fill configurations which would provide adequate storm protection for the areas in which additional protection was indicated. The second phase of this task was to evaluate the effectiveness of each of the proposed beach fill designs.

138. The dune erosion numerical modeling technique employed to accomplish this task is similar to that developed for the Section I study Sea Bright to Ocean Township, New Jersey (Kraus, et. al. 1988). It is based on the modified Kriebel-Dean dune erosion model which computes dune erosion as a function of a single storm surge hydrograph. A technique for evaluation storm protection as a function of frequency of occurrence was developed at CERC which utilized an existing data base of hurricane and northeaster storm events. Volumes of erosion and associated dune recession values were computed for each of these storm events. The indicators of storm associated damage are related to a frequency of occurrence through the use of stage-frequency relationships (see Part IV) developed for the local area. The following sections present a brief overview of the numerical model, define the model input requirements, and present the results of the storm simulations for both the existing conditions and the proposed remedial designs.

The Dune Erosion Model

139. The calculation of dune recession as a function of known storm activity is made with a numerical dune erosion model which employs an empirical relationship to compute the cross-shore sediment transport rate Q_s

as a function of the dissipation of wave energy (i.e., the breaking of waves). This relationship is written as

$$Q_s = k (D - D_{eq}) \quad (6)$$

where k is an empirical coefficient which was determined by Moore (1982) to have a relatively constant value of $2.2 \times 10^{-6} \text{ m}^4/\text{N}$ ($0.001144 \text{ ft}^4/\text{lb}$). The energy dissipation function D is given by

$$D = \frac{1}{h} \frac{\partial F}{\partial x} \quad (7)$$

where h is the depth of flow and F represents the energy flux calculated by linear wave theory. D_{eq} represents the constant value of the parameter D from Equation 7 if the equilibrium profile is specified in the equation arguments. According to this formulation, no transport of sediment occurs if the existing profile is everywhere in equilibrium, i.e., if $D = D_{eq}$. Bathymetric changes below the storm surge level are computed with a one-dimensional continuity equation of the following form:

$$\frac{\partial x}{\partial t} = \frac{\partial Q_s}{\partial h} \quad (8)$$

in which t is time. The temporal change of the distance x to a known contour line at depth h is written as a function of the change in the sediment transport rate with respect to the depth. If a greater amount of sediment enters a region bounded by two contour lines than leaves, sediment accumulates between the two contours and the offshore distance to the respective contour lines increases.

140. Computationally, bathymetric changes computed from Equation 8 are used to determine an offshore sediment budget at each time step throughout the time-varying storm surge event. The primary assumption of the model is that volumetric change computed for the offshore area is in balance with the volumetric change of the dune and berm area according to the results of the sediment budget. For example, excess sediment is equally distributed over the face of the berm if the budget computations indicate an offshore surplus of

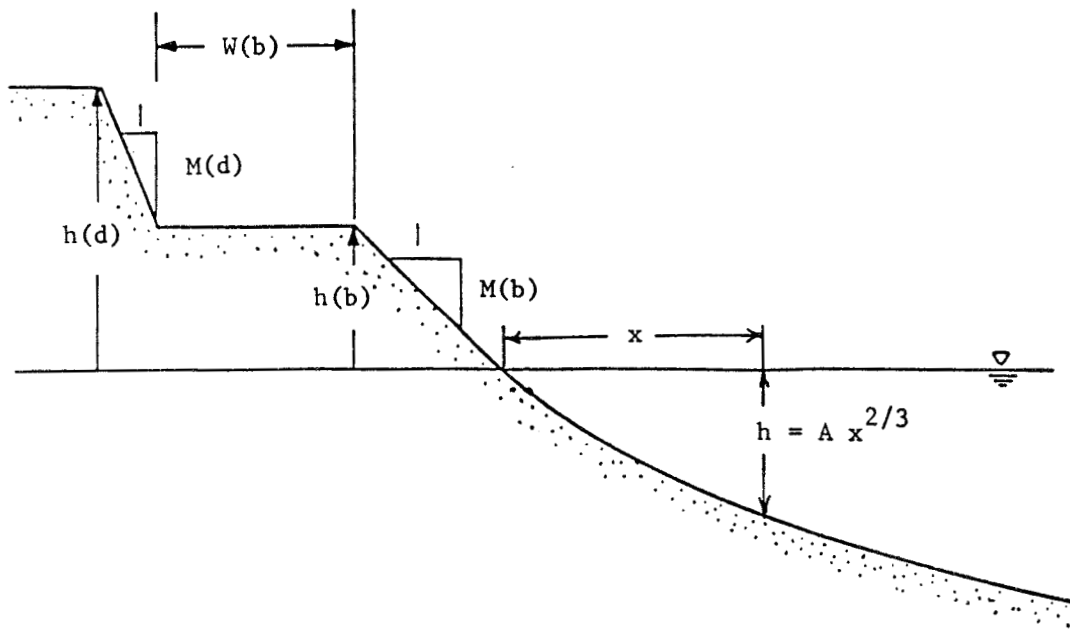
material, i.e., material which is eroded offshore is deposited on the berm face. Conversely, material is uniformly supplied to the offshore contours from the dune and berm faces when the sediment budget indicates offshore transport. In either case, the differentiation between the dune and berm zone and the offshore zone is made at the location of the water line of the temporally varying storm surge. A more thorough description of the model methodology can be found in Kriebel (1984), Birkemeier et al. (1987), and Kraus et al. (1988).

141. Schematization of the onshore and offshore portion of each modeled profile is required as input to the numerical model to ensure that storm event simulations will provide realistic estimates of damage. Shoreward boundary requirements include specification of a dune and berm area of known height and face slope. A schematic diagram of the onshore geometric data required is shown in Figure 29. Note that the schematized profile may or may not contain a flat berm area. The variables $h(b)$ and $h(d)$ refer to the height of the berm or dune, and the variables $M(b)$ and $M(d)$ refer to the slope of the face of the respective berm and dune. $W(b)$ refers to the width of an optional horizontal portion of the berm.

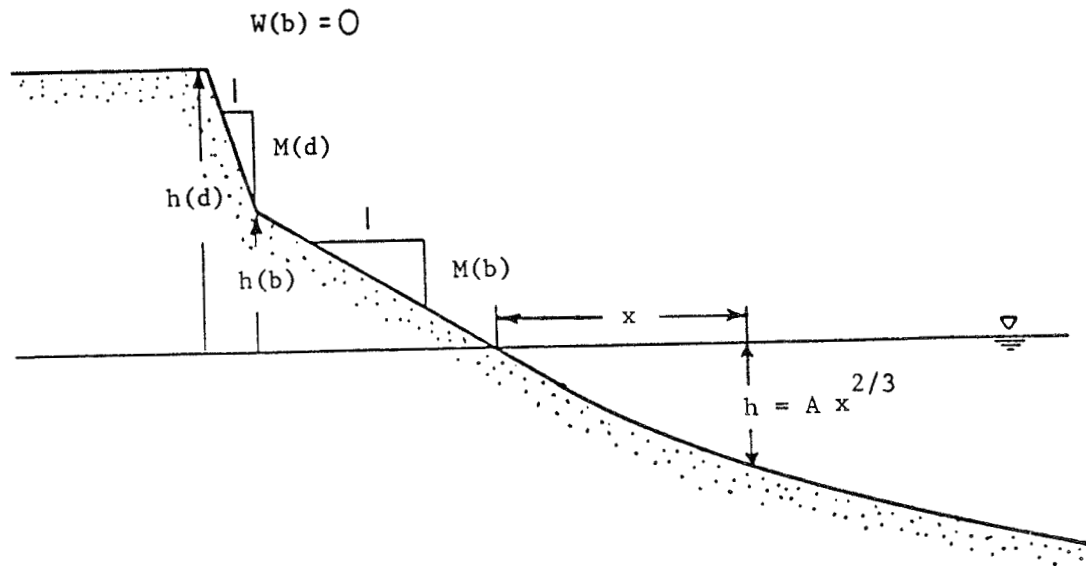
142. The offshore profile is schematized according to an equilibrium profile assumption in which the offshore depth h increases with distance offshore according to the following relationship

$$h = A x^{2/3} \quad (9)$$

in which A is a dimensional equilibrium parameter called the shape coefficient. Comparisons between natural profiles and profiles computed from Equation 9 have shown that the equilibrium concept provides a good description of natural offshore beach profiles characterized by a wide variety of environmental conditions and geometric configurations (Bruun 1954, Dean 1977, Hughes 1978, Moore 1982). Dean's 1977 results showed that this relationship provided an acceptable fit to 502 measured offshore profiles along the



a) with flat berm



b) without flat berm

Figure 29. Schematic dune-beach profile (after Kriebel 1984)

Atlantic coast of the United States. The Section I study (Kraus et al. 1987) also showed good correlation between existing and computed equilibrium profiles.

143. Stage-frequency relationships are not available for the region from Asbury Park to Manasquan Inlet; however, they are available for locations on either side, at Monmouth Beach to the north and Long Beach Island to the south. Analysis of these data sets in Part IV indicates that linear interpolation provides an estimate of a stage-frequency relationship for the Asbury Park to Manasquan Inlet region which is within the limits of accuracy of standard predictive methodologies. Because the subject area is located between Monmouth Beach and Long Beach, a stage-frequency relationship is determined by interpolation between the two bounding curves. The curves developed for both hurricanes and northeasters and their relationship to the Monmouth Beach and Long Beach Island curves are shown in Figures 27 and 28.

Existing Conditions

144. Four profile locations, shown in Figure 30, were selected by CENAN to be representative of beaches along Asbury Park to Manasquan Inlet. The profiles are identified as profile numbers 232, 244, 286, and 290. Plots of the individual profiles are presented in Figures 31 through 34. Included on each plot is the schematic representation of the profile as input to the numerical model.

145. The steepness of the computed offshore profile is determined by the value of the shape coefficient A . Larger values of A produce steeper profiles, a result which would be expected of beaches composed of coarser materials. A correlation between the mean sediment grain diameter D_{50} and the shape coefficient A was made by Moore (1982). This relationship is shown in Figure 35. If detailed bathymetric data are not available, an equilibrium profile can be determined from the sediment characteristics according to this figure. Shape coefficient values determined from best-fit calculations for the selected existing profiles, and their corresponding grain size equivalents, are shown in Table 11.

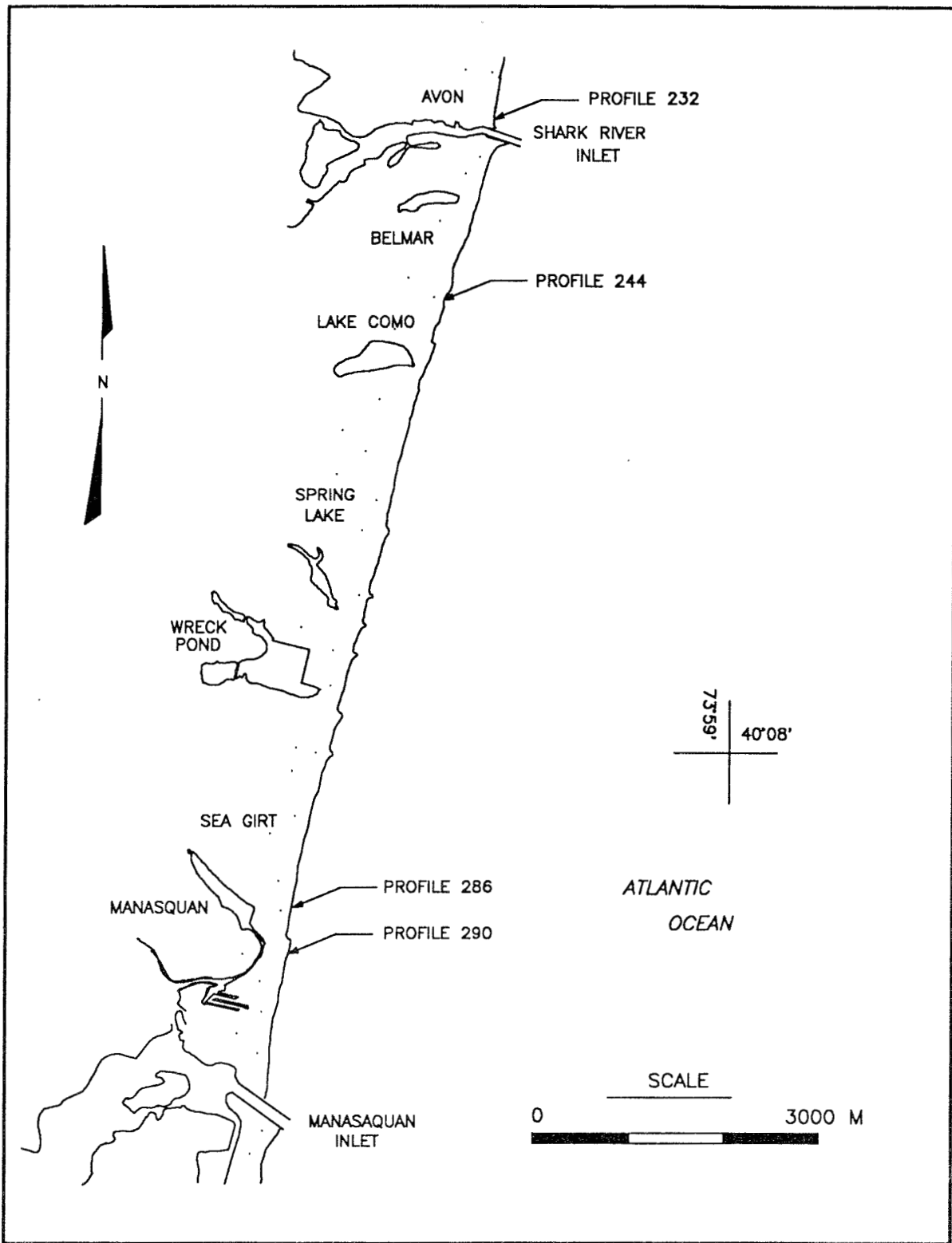


Figure 30. Existing profile locations

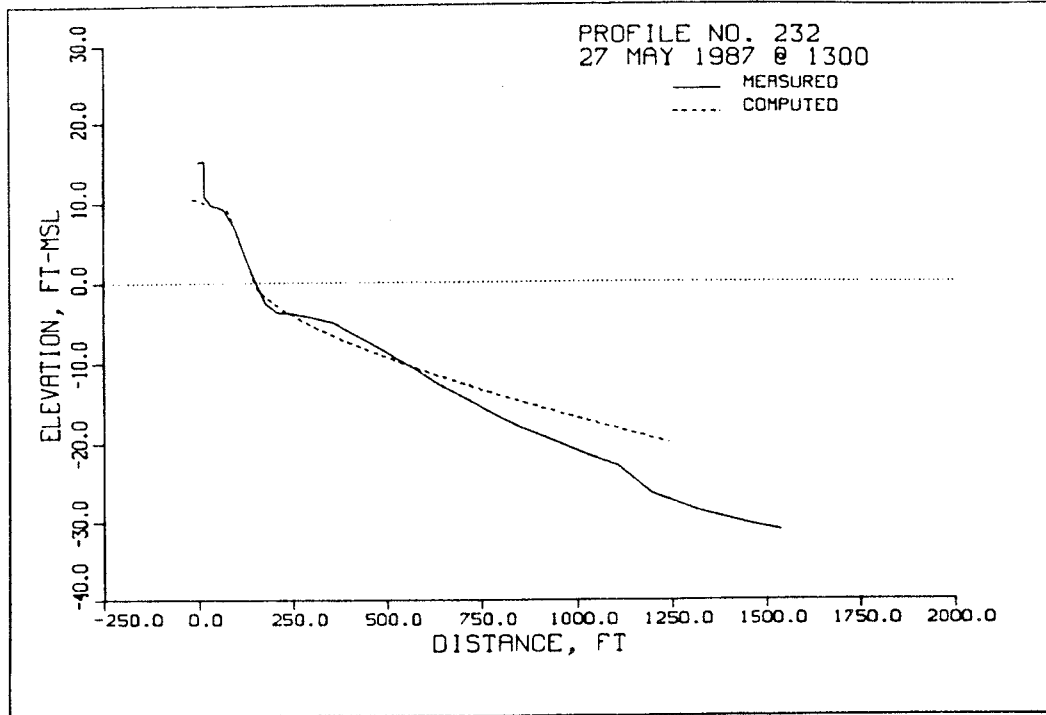


Figure 31. Cross-section of Profile 232

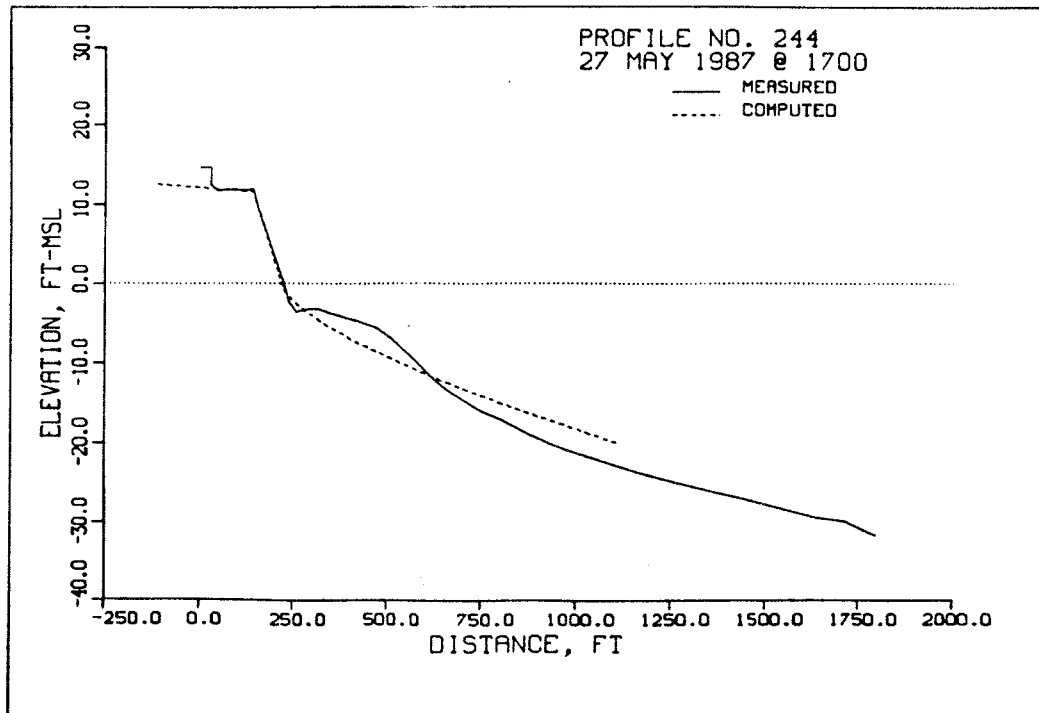


Figure 32. Cross-section of Profile 244

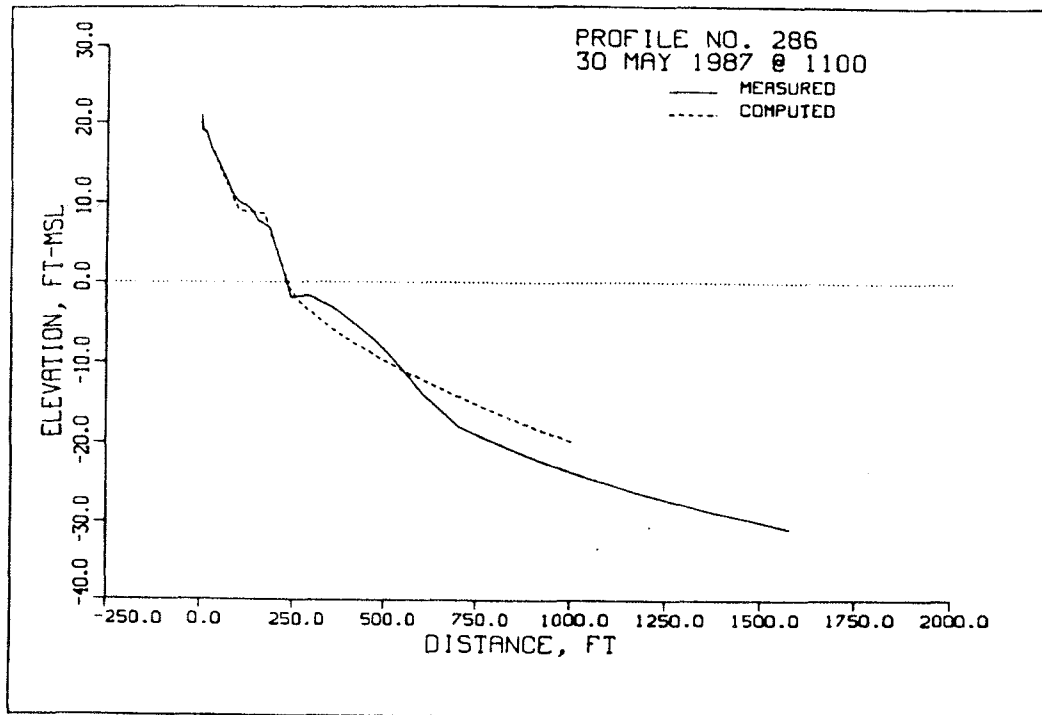


Figure 33. Cross-section of Profile 286

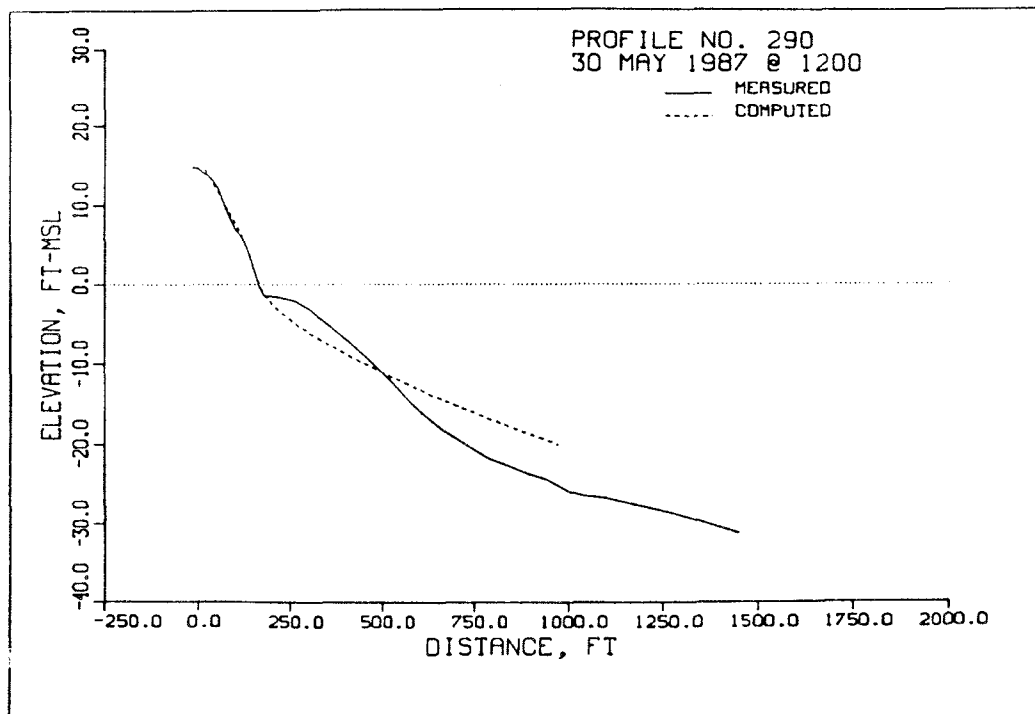


Figure 34. Cross-section of Profile 290

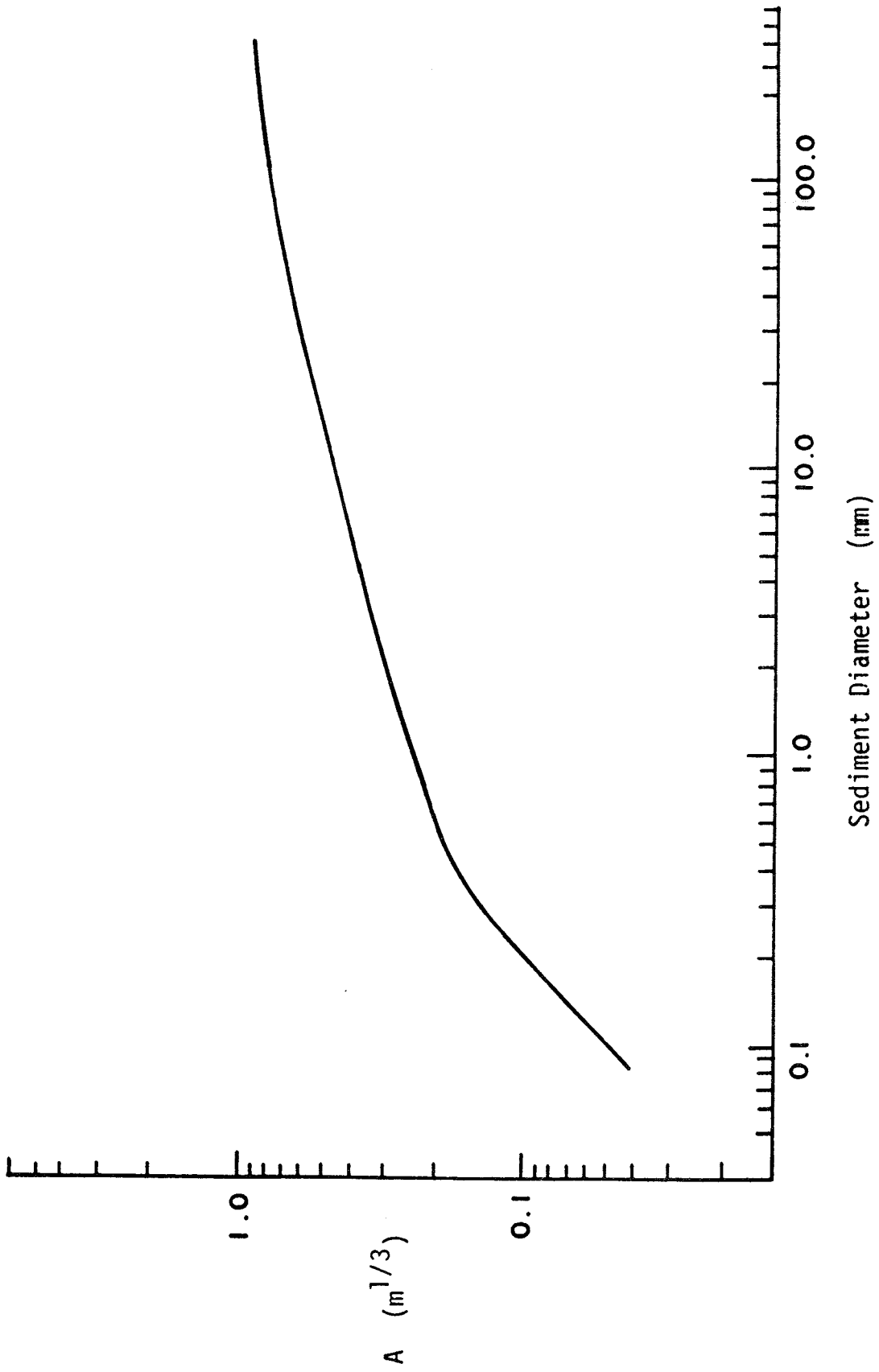


Figure 35. Shape coefficient A versus sediment diameter (from Moore 1982)

Table 11
Existing Profile Characteristics

647X			
<u>Profile</u>	<u>Shape Coefficient</u> <u>ft^{1/3}</u>	<u>m^{1/3}</u>	<u>Median Grain Size</u> <u>D₅₀ (mm)</u>
232	0.188	0.127	0.281
244	0.215	0.145	0.322
286	0.236	0.159	0.355
290	0.230	0.155	0.345

146. A limitation of the basic equilibrium concept is that certain localized features which are known to exist, such as bars and troughs, cannot be explicitly represented. For example, Equation 9 states that the offshore depth monotonically increases with a power law dependence on the distance offshore. This results in an offshore profile which is concave downward in shape as shown in Figure 29. All four of the selected profiles are slightly concave upward in the immediately offshore region, indicative of the presence of a low-relief bar system. The value of the shape coefficient "A", used in the model simulations was computed from best-fit calculations to the active surf zone portion of the profiles. However, the sill feature in the actual profiles shown in Figures 31 to 34, cannot be represented using Equation 9.

147. Table 11 indicates that the median sediment diameters for the present study area range between 0.281 mm and 0.355 mm, these grain sizes are similar to those calculated in a previous study of the adjacent northern reach, Seabright to Ocean Township (Kraus et al. 1988). For example, computed grain sizes for Seabright to Ocean Township ranged between 0.280 mm and 1.400 mm. The representative profiles specified by NAN for use in this task exhibit a predominate offshore bar system or sill area located approximately at an elevation of -3 ft MSL. This characteristic profile shape was not observed in the previous (Seabright to Ocean Township) study area. It is interesting to note that the representative profiles typically change from a convex to a concave shape at about -10 ft MSL elevation. This depth approximately corresponds to depths existing at the tips of the groins within the project area. Presumably, this is a manifestation of the groins ability to trap

sediment in the nearshore zone. Although the computed shape coefficients are numerically comparable for the two regions, the values used in the present study reflect a best fit approximation to the actual profiles. This fit requires the selection of a shape coefficient which best represents the entire profile. For example, the profiles shown in Figures 31 through 34 are less steep nearshore and more steep offshore than can be represented using the equilibrium profile relationship given in Equation 9. The deviation in the computed profiles from the observed profiles is indicated in the figures. This seemingly poor representation of the existing profile is not, however, a significant source of error in the computation of dune recession values since recessions are computed as a function of the total computed volume of sediment which is either deposited on or eroded from the area approximately between the shoreline and the breaker line. Sediment computations for the offshore bar approximation case will indicate a less than anticipated rate of erosion for the nearshore area where the computed profile is at a lower elevation than the observed bar. Conversely, a greater than anticipated volume will be computed offshore where the equilibrium profile is at a higher elevation than the observed profile. The sum of these two calculations does, however, tend to approximate the total average volume of erosion or deposition which is used in the dune recession calculations. Since detailed bathymetric changes are not the purpose of this model, the above approximation methodology for representing the profiles is felt to be adequate.

Existing condition simulations

148. An ensemble of 120 northeasters, corresponding to discrete total surge (storm surge plus tide) elevations from 5.0 to 9.6 ft in 0.2-ft increments, and 275 hurricanes, with total surges from 4.0 to 14.8 ft was produced for input to the model. Due to variability in the duration and shape of the hydrograph of each different storm, two storms of equal total surge elevation do not result in identical computed maximum recession values. A large number of simulations are required in order to produce a sample population from which a reliable interpretation of the overall trend of the data can be made. Too small a population may result in observations which are biased by extreme values. In order to increase the sample size, five separate ensembles of hurricanes and northeasters are used in the simulations. The

envelopes of computed results are shown in the recession-recurrence interval plots for both hurricanes and northeasters for the four existing profiles in Figures 36-43. On each plot, the five sets of plotting symbols refer to the five independent sets of simulations.

149. Separate upper envelope design curves for hurricanes and northeasters are determined for each profile in order to define a maximum expected dune recession which would result from an individual storm event of known frequency of occurrence. A combined hurricane-northeaster design curve is then computed for each existing profile from the two individual curves. The resulting maximum recession-frequency of occurrence relationships indicate the maximum expected recession of the dune corresponding to a given return period. Post-storm recovery of the berm is not incorporated in the plots. The assumption is that maximum recession provides the most meaningful indicator of potential storm-associated damage. These curves are shown in Figures 44-47. An analysis of the impact of the recession-recurrence relationships with respect to the existing profiles is now presented.

150. Profile 232 is characterized by a well developed berm region fronting an asphalt-topped bulkhead. For the purposes of numerical simulation, the bulkhead is considered to be an impermeable, rigid vertical seawall, however, the simulation does not include the effects of scour at the base of the seawall. The distance from the bulkhead to the waterline is approximately 140.0 ft. A gently sloping region extends out from the bulkhead a distance of approximately 50.0 ft, at which point the crest of the berm slopes uniformly to the water line. Recession of this 8.0-ft MSL berm crest to the seawall is indicated to occur on the order of every 80 years for hurricanes and every 25 years for northeasters. The combined curve indicates a recurrence rate of just 20 years. Since recession cannot continue beyond the wall (unless failure of the wall occurs), erosion continues in the form of vertical lowering of the beach in front of the wall. Analysis of several individual extreme storm events (i.e., recurrence intervals on the order of 1000 years) showed vertical erosion of the beach directly in front of the bulkhead by as much as 4.0 ft, thereby removing approximately one-half of the protective beach.

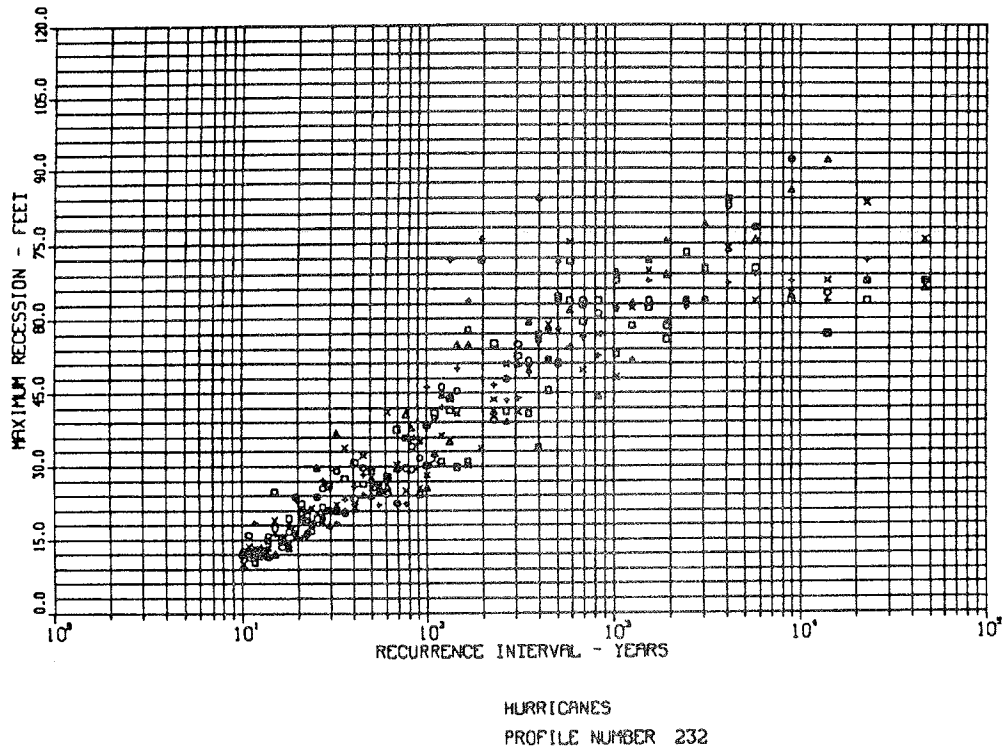


Figure 36. Hurricane recession-recurrence interval simulations for Profile 232

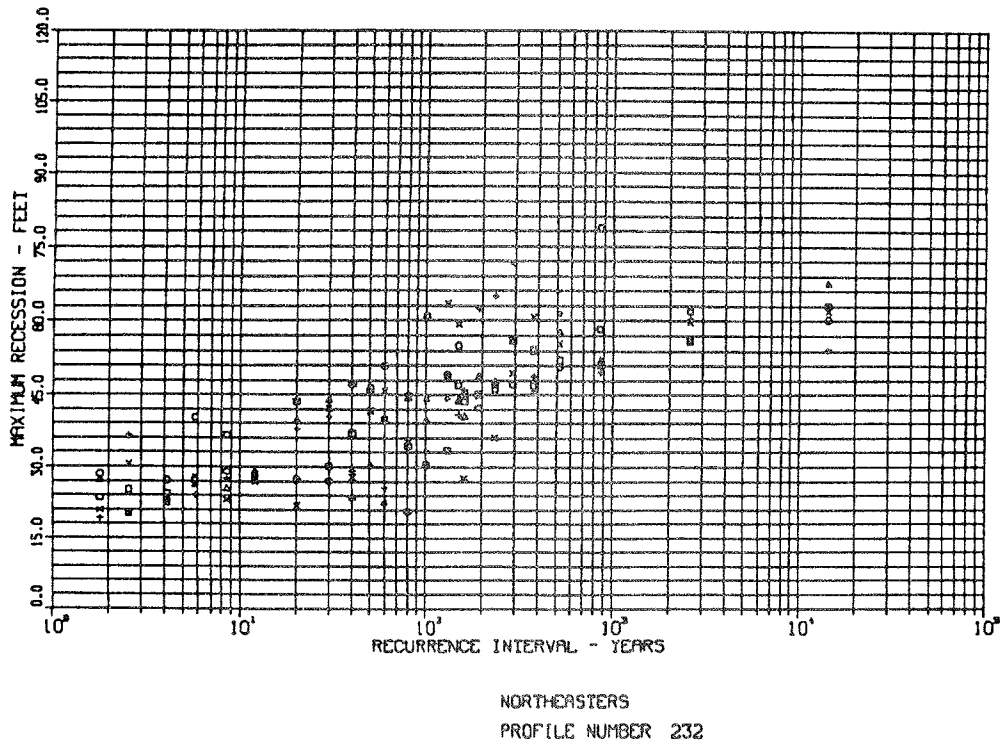


Figure 37. Northeaster recession-recurrence interval simulations for Profile 232

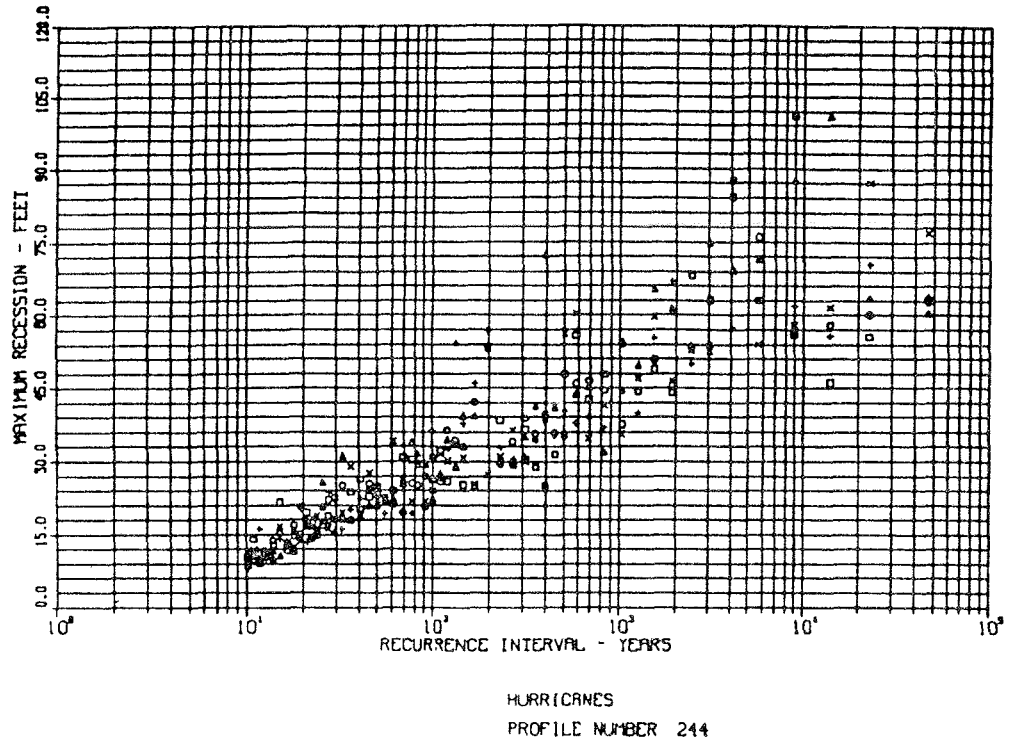


Figure 38. Hurricane recession-recurrence interval simulations for Profile 244

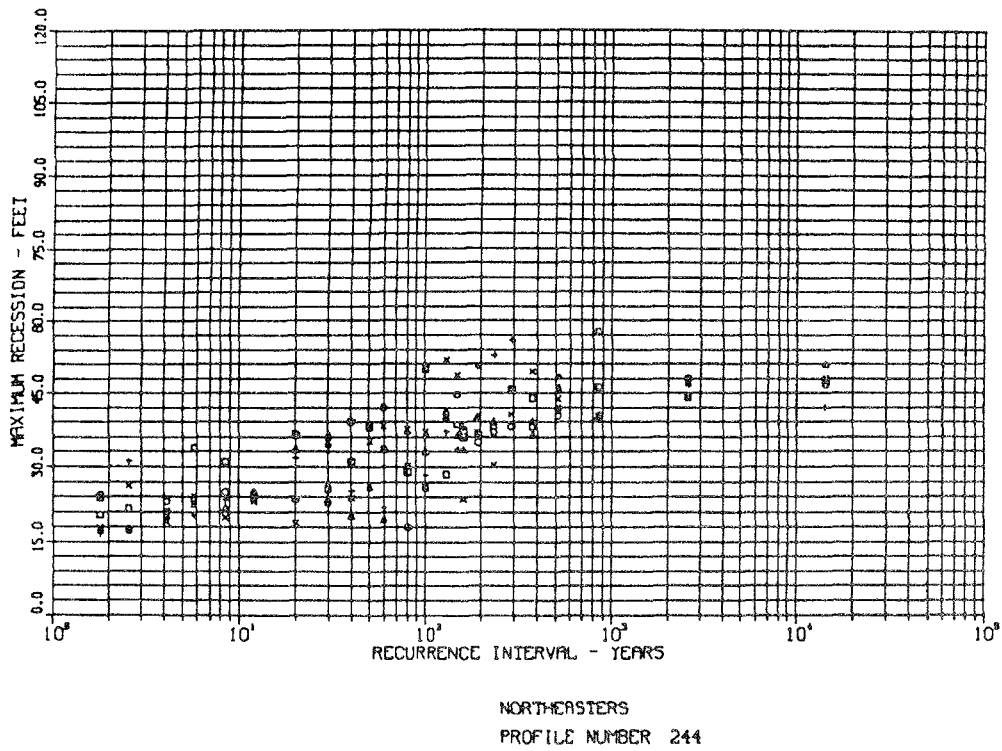


Figure 39. Northeaster recession-recurrence interval simulations for Profile 244

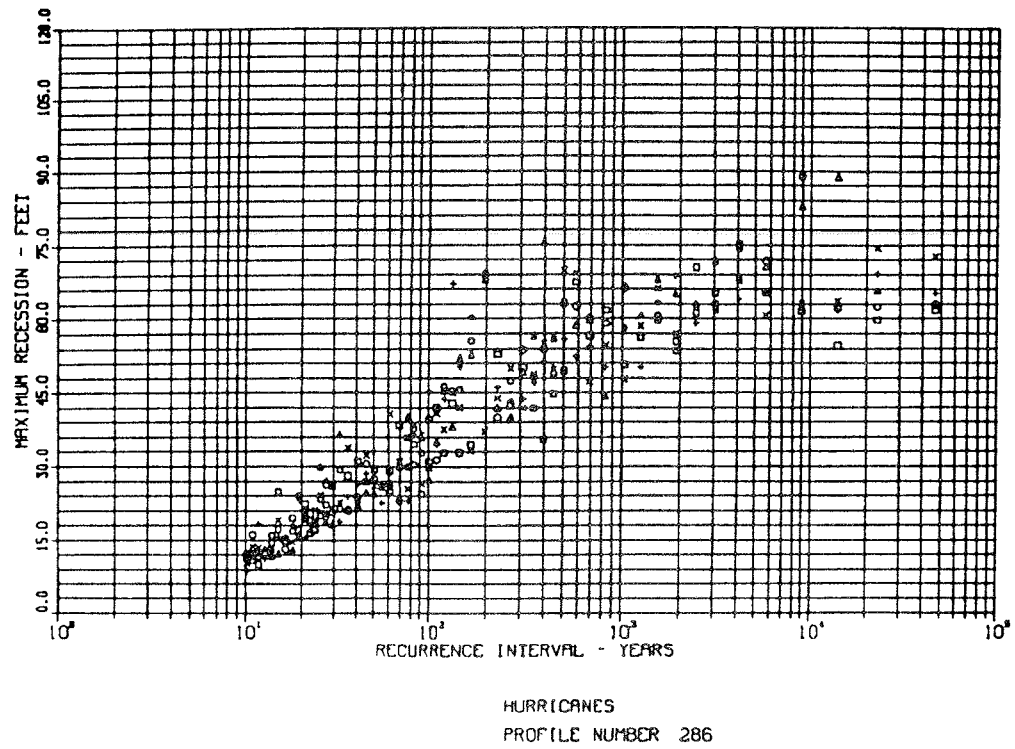


Figure 40. Hurricane recession-recurrence interval simulations for Profile 286

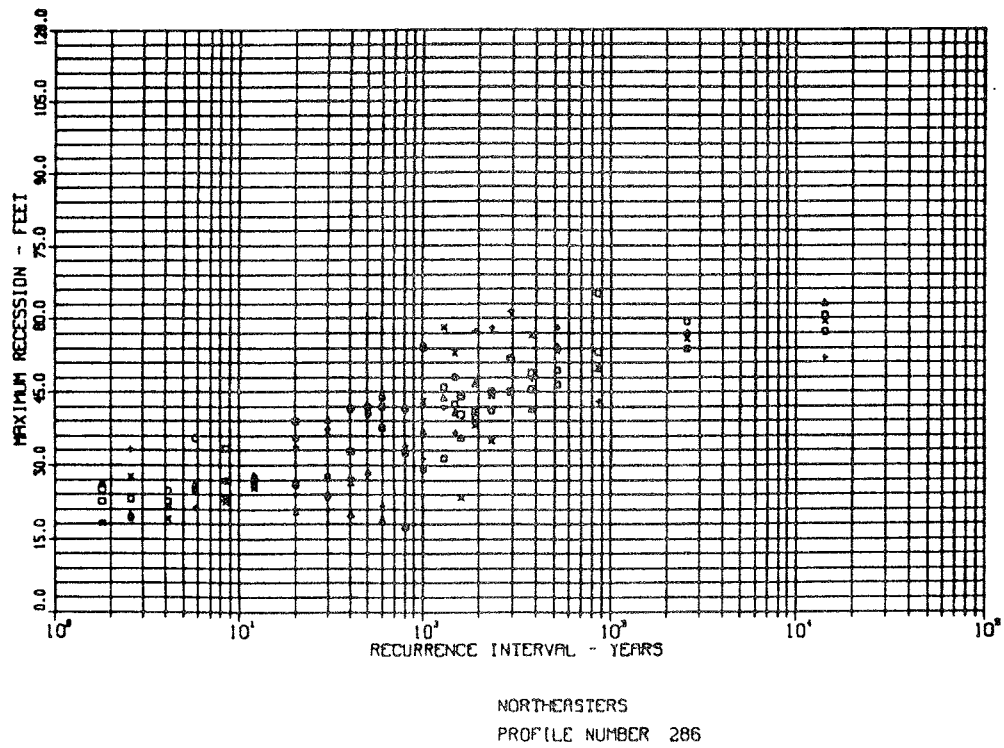


Figure 41. Northeaster recession-recurrence interval simulations for Profile 286

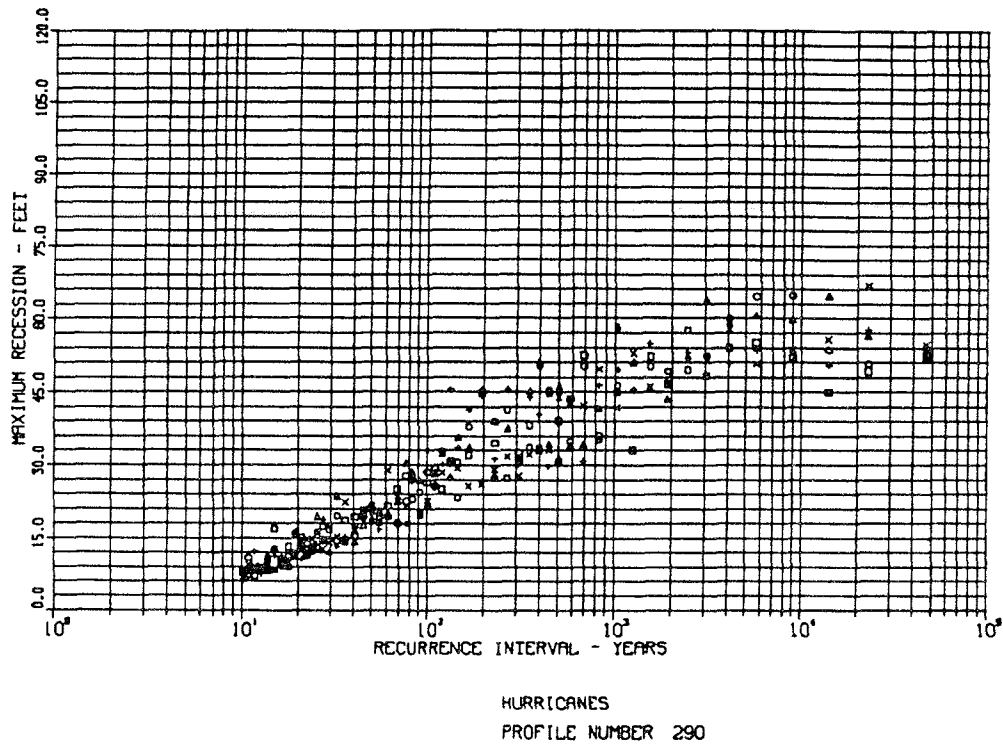


Figure 42. Hurricane recession-recurrence interval simulations for Profile 290

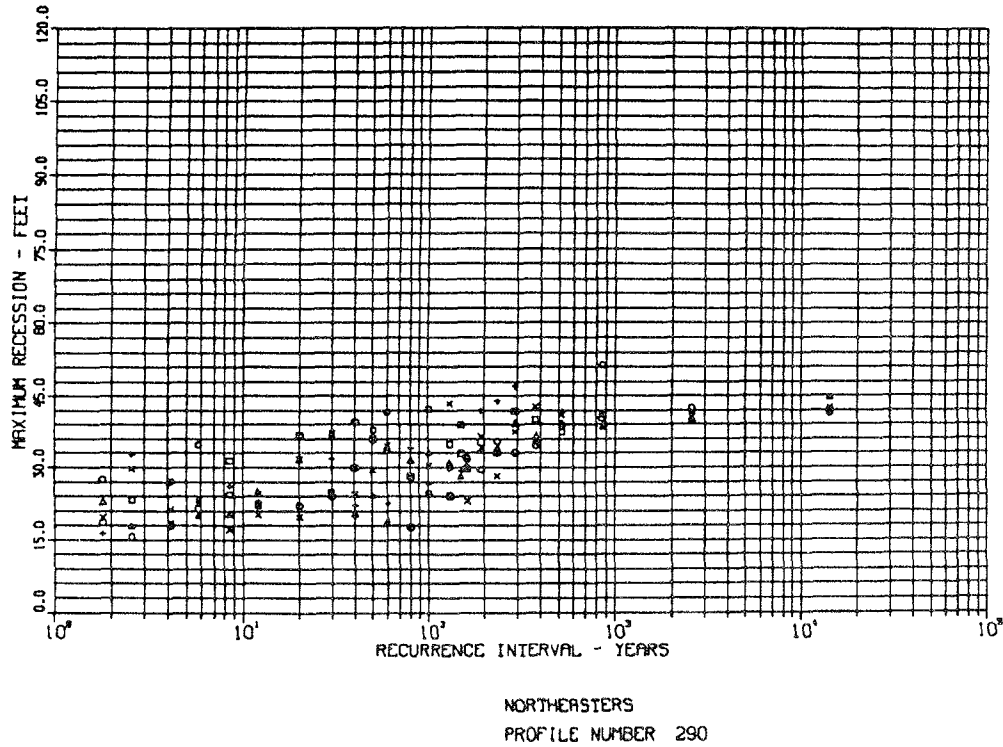


Figure 43. Northeaster recession-recurrence interval simulations for Profile 290

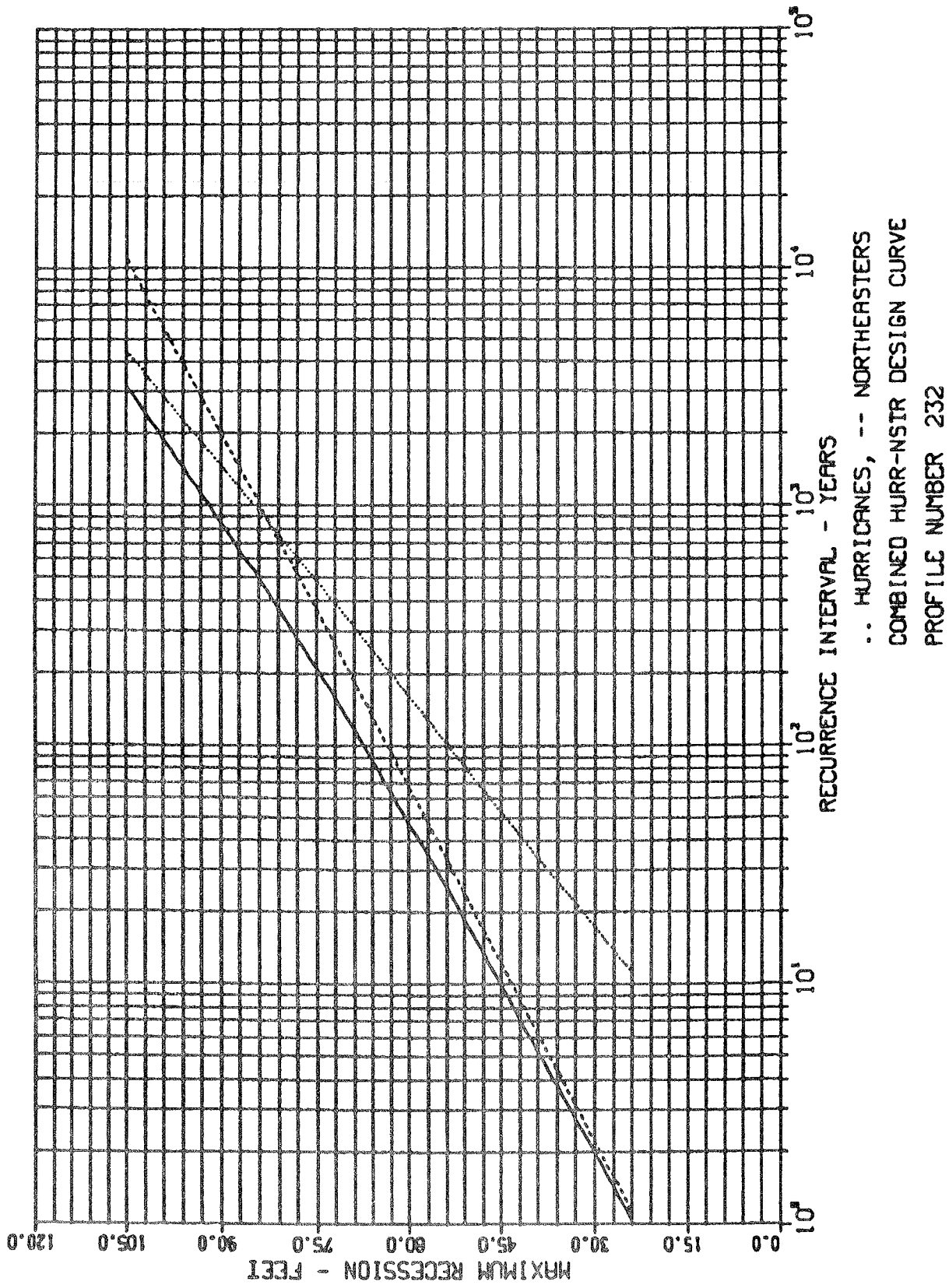


Figure 44. Combined hurricane-northeaster recession-recurrence interval design curve for Profile 232

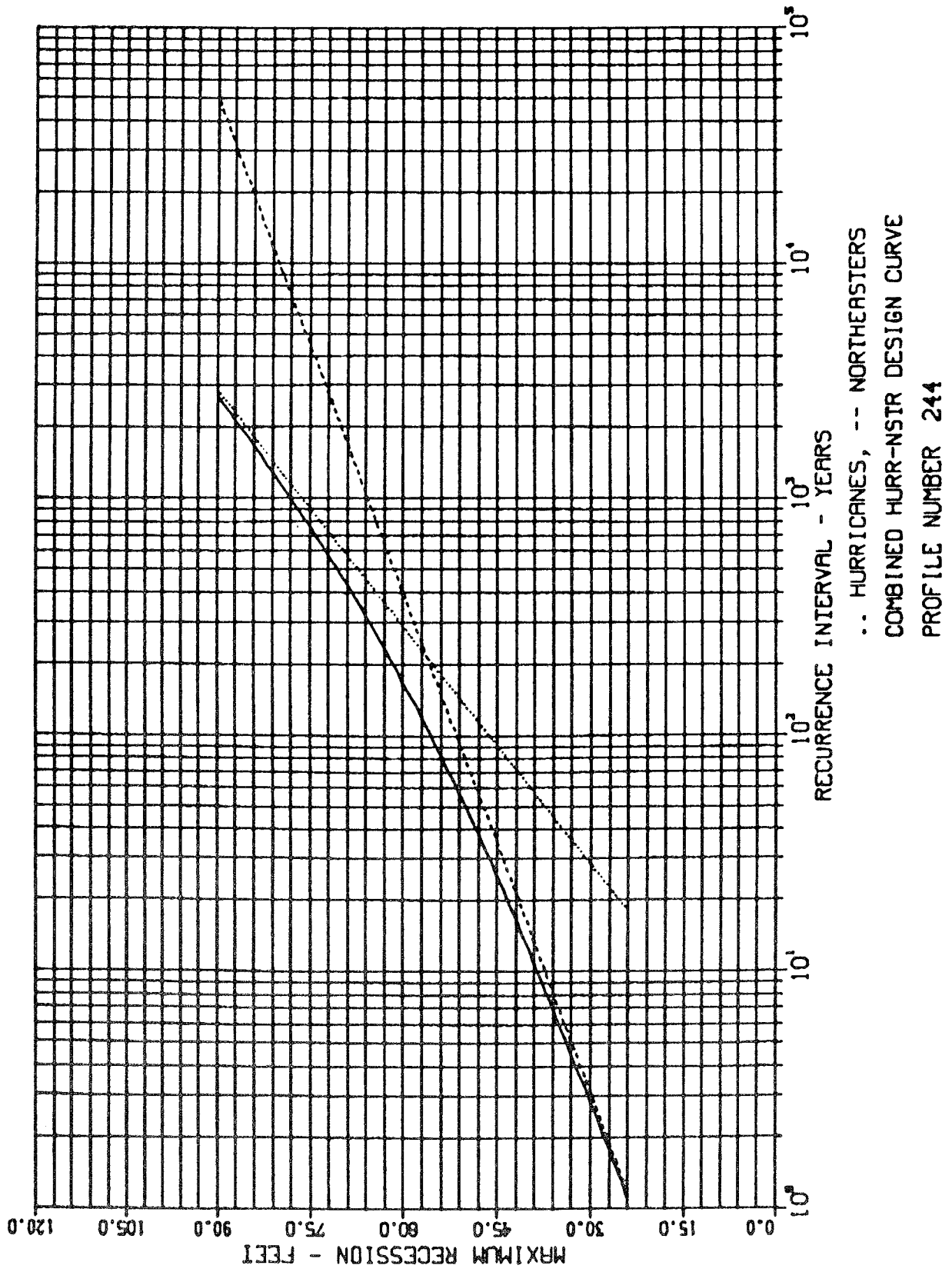


Figure 45. Combined hurricane-northeaster recession-recurrence interval design curve for Profile 244

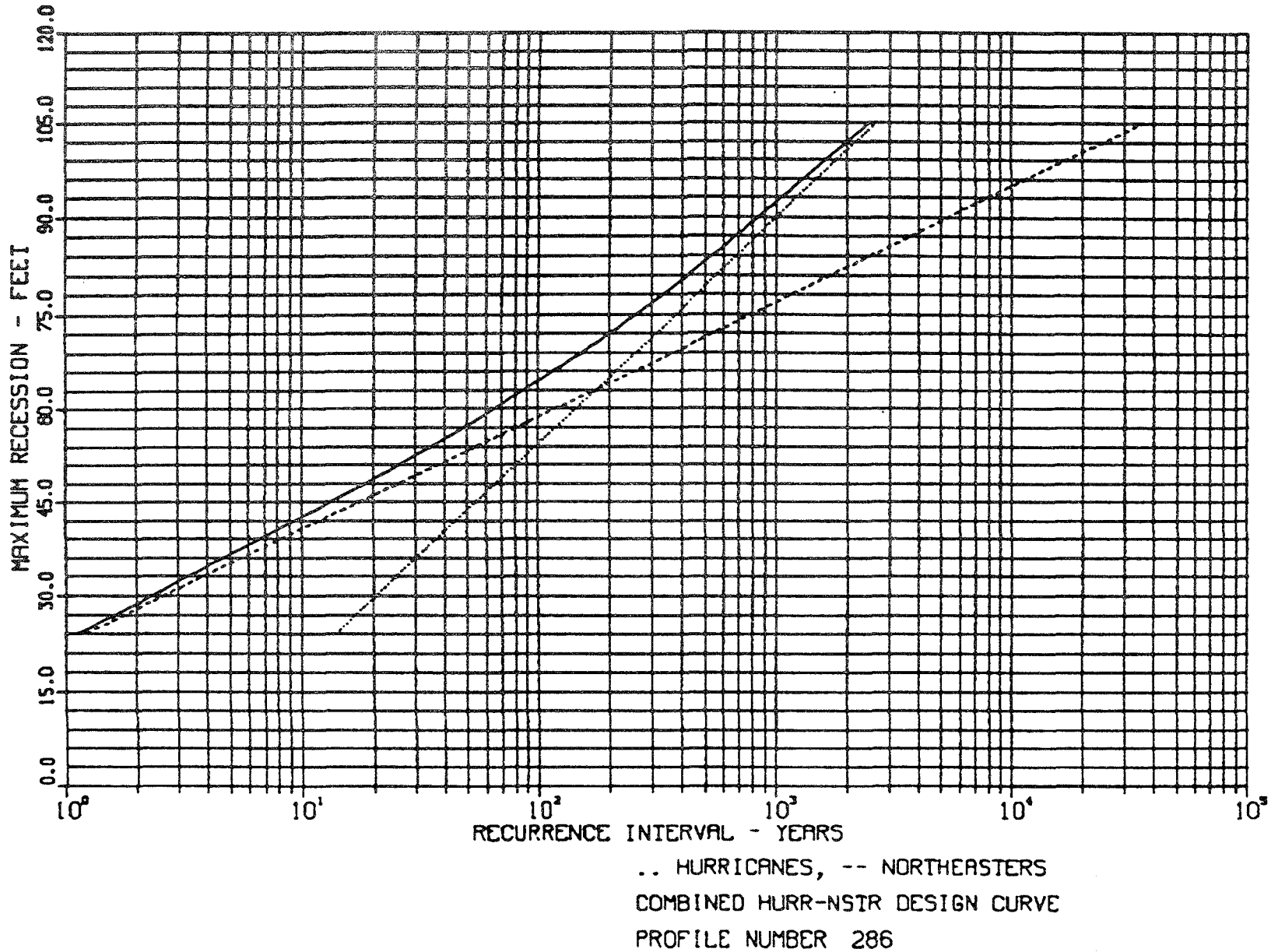


Figure 46. Combined hurricane-northeaster recession-recurrence interval design curve for Profile 286

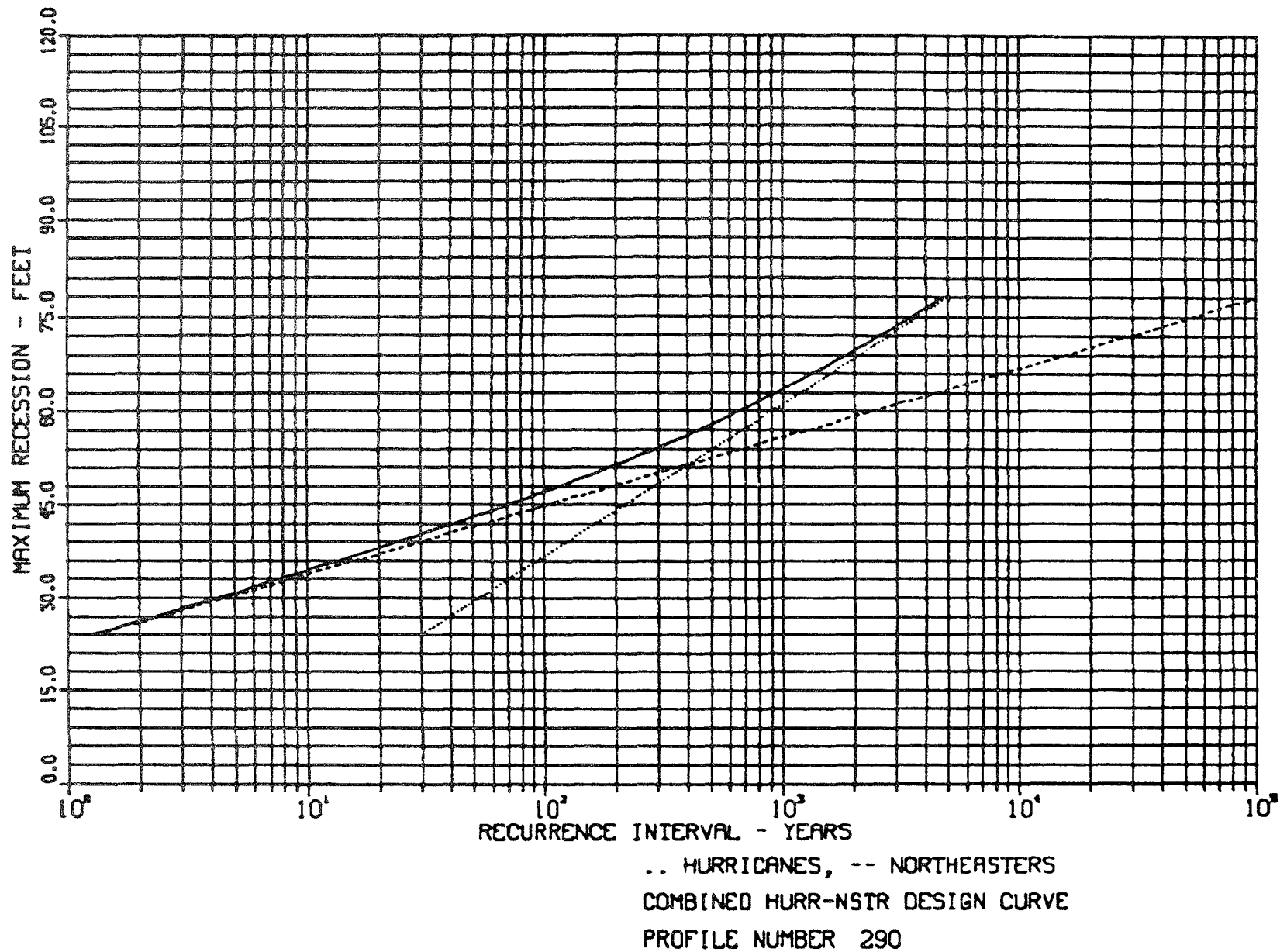


Figure 47. Combined hurricane-northeaster recession-recurrence interval design curve for Profile 290

151. Profile 244 is also characterized by an asphalt-topped bulkhead but with a much greater effective beach width than Profile 232. Approximately 200 ft of beach material separate the bulkhead from the waterline; however, a flat highly protective berm almost 130 ft wide and 11.5 ft MSL high exists before the berm crest slopes to the water. Maximum recessions of the berm crest to the bulkhead are not indicated by model results for any single storm event. For example, numerical simulations show that maximum recessions of only 60.0 ft correspond to recurrence intervals of 300 years for hurricanes and 400 years for northeasters. The combined curve indicates that a return period of over 100 years can be expected for 60.0 ft of erosion.

152. Profile 286 represents a natural-shaped beach profile in which a 20-ft high uniformly sloping dune is separated from an 8.0-ft high, well-defined berm crest by a 65.0-ft flat region. The width of the entire profile, from the dune crest to the water level, is 235.0 ft. Model results show that complete erosion of the flat berm region in front of the base of the dune can be expected to occur on the order of every 100 years, according to the combined design curve. Erosion beyond this point continues at a slower rate because of the large amount of material available in the dune. Analysis of the results of a single storm simulation of a specific extreme hurricane showed that a maximum recession of the berm crest of 75.0 ft was accompanied by a dune crest recession of only 5.0 ft. Storm events with maximum recessions of this order have recurrence intervals of more than 500 years.

153. Profile 290 does not have the protection of a flat berm region separating the base of the dune from the crest of the berm such as that shown in Profile 286. Instead, Profile 290 is characterized as uniformly sloping from the 14.5-ft MSL dune crest to the water line. The distance between dune crest and water line is only 150.0 ft. Maximum recessions of the dune crest of 40.0 ft are indicated for hurricanes with recurrence intervals on the order of 100 years and northeasters with recurrence intervals on the order of 30.0 years. The combined curve indicates 40.0-ft recessions can be expected to occur on the order of every 20.0 years. This high rate of recession is a result of the low dune height and the fact that the dune is not protected by a distinct berm region.

Summary Existing Conditions

154. The numerical model used for this investigation has been tested against various pre- and post-storm survey data sets (Kraus et al. 1988, Birkemeier et al. 1987, and Scheffner 1987) and has been shown capable of yielding acceptable predictions of storm-induced erosion. These comparisons show predictions to range from approximately 50 to 150 percent of measured recessions and volumes of erosion. A natural variation in dune erosion of this magnitude is normal, as has been observed in post-storm surveys from coastal areas which are considered to be uniform. Variations arise from subtle differences in compaction and geometry of the beach and dune material, vegetation, wave refraction and diffraction, wind patterns, and other possible factors. If a conservative approach is applied in which the prediction is 50 percent low, a "variability factor" of 2.0 (i.e., $1.0/0.5$) should be applied to the computed predictions. This value was recommended in the Seabright to Ocean Township study, based on the concept of natural spatial undulations of the shoreline about a straight base line and the effect of these variations on natural erosion. Similar rates of variation are reported by Savage and Birkemeier (1987). If a variability factor of this magnitude is considered, analysis of existing conditions indicates consideration of additional protection for dunes with similar geometries to Profile Nos. 232 and 290. Profiles such as Nos. 244 and 286 appear to provide adequate protection to the dune and seawall due to the high and wide berms.

Beach Fill Design Alternatives

155. Based on the existing conditions analysis six beach fill designs were provided by NAN to CERC for detailed evaluation. These designs, shown in Figure 48, represent three berm widths (50, 100, and 150 ft) for each of two specified berm heights (8 and 10 ft MSL). The design configurations are superimposed on Profile 290, selected as a representative profile for the project area. The slope of the offshore design profile is specified as 1:40, beginning at -3.0 ft National Geodetic Vertical Datum (NGVD). Since dune and berm elevations are specified in the model in increments of 0.5 ft (MSL), this slope break is designated as -3.5 ft MSL.

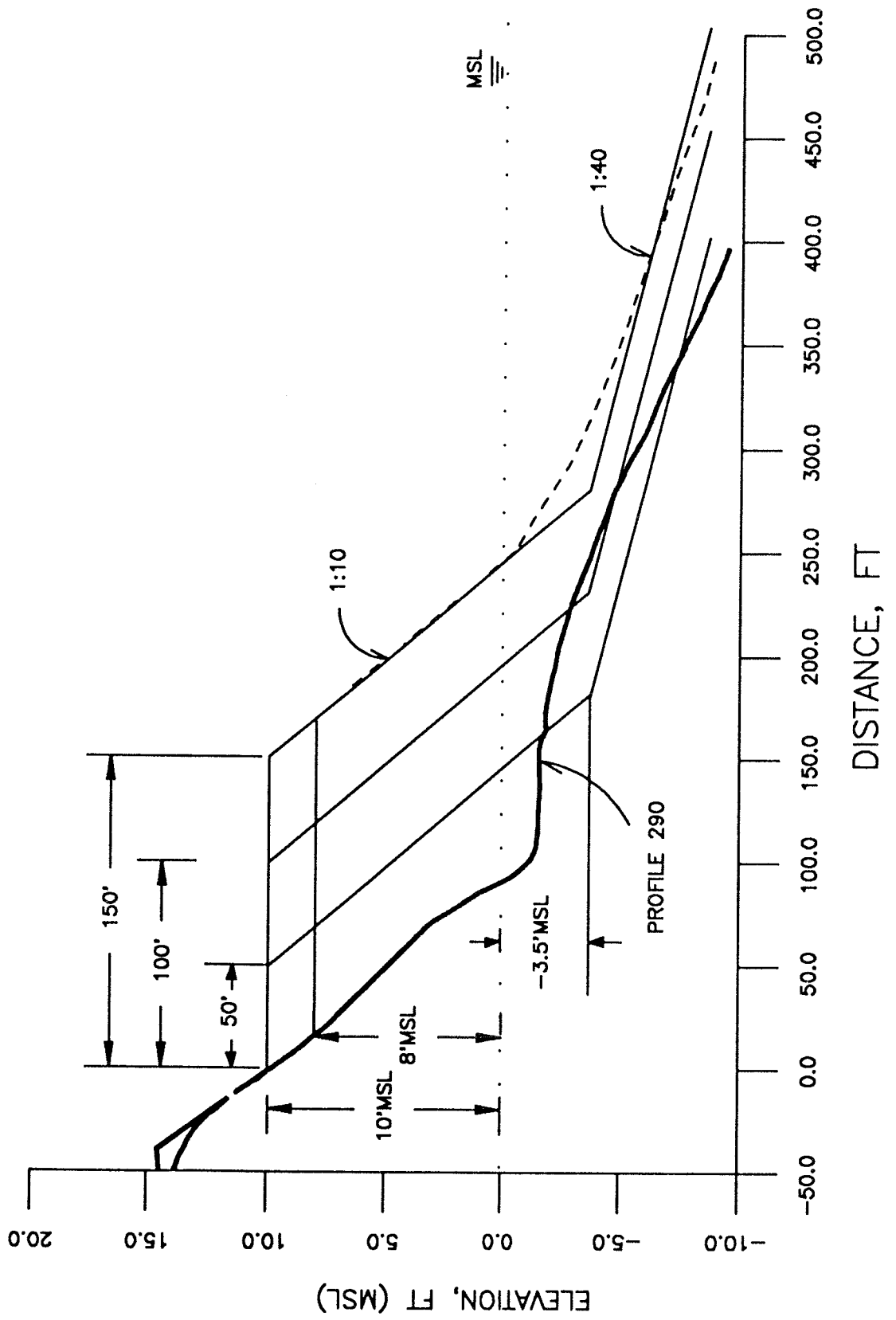


Figure 48. Beach fill design configurations

The relationship between NGVD, MSL, and MLW is

$$\text{NGVD} = \text{MSL} - 0.57 \text{ ft} = \text{MLW} + 1.63 \text{ ft.} \quad (10)$$

This relationship was provided by NAN (as defined by NOAA) and was used in the Seabright to Ocean Township study.

156. Schematization of the offshore profile for input to the numerical model requires the determination of an equilibrium shape coefficient which produces a best representation of the desired profile. A value of $0.235 \text{ ft}^{1/3}$, corresponding to sediment diameter of approximately 0.355 mm, was computed to simulate the specified design slope of 1:40. This value was used in all numerical simulations. The resulting approximation of each design alternative is represented by the dashed line superimposed on the 150-ft width design profile in Figure 48.

Beach fill design simulations

157. Design profiles were subjected to the ensemble of 120 northeaster storm events that were used in the evaluation of existing profiles. Results of the numerical simulation of northeaster storm events are shown in Figures 49 and 50. The recession scatter diagram shown in Figure 49 for the 150-ft wide, 10-ft berm indicates that maximum recession never exceeds 50 ft; therefore, simulations for the 100- and 50-ft widths were not necessary as they would produce identical plots. Results of northeaster simulations for the 150-ft wide, 8-ft berm are shown in Figure 49. All computed recession values were less than 100 ft; therefore the scatter diagram is valid for both the 150- and 100-ft wide, 8-ft berm designs.

158. Since several simulations of the 150/100-ft wide, 8-ft berm design indicated recessions in excess of 50 ft, additional simulations were performed for the 50-ft berm. The results, shown in the scatter diagram of Figure 51, indicate maximum computed recessions which are slightly less than those computed for the 100- and 150-ft widths. This difference is due to the fact that erosion of both the berm and dune face occurs after erosion has eliminated the 50-ft horizontal berm, i.e., maximum horizontal erosion is reduced as vertical erosion is increased. For example, the most severe storm

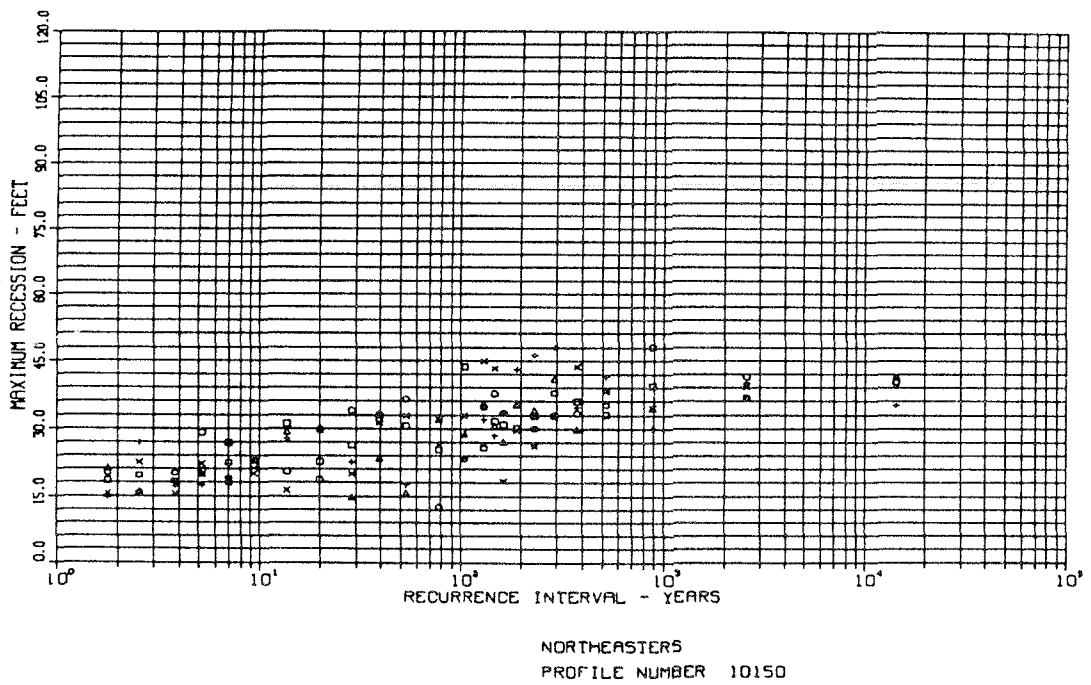


Figure 49. Northeaster recession-recurrence interval simulations for the 150/100/50 ft wide, 10 ft MSL high design berm

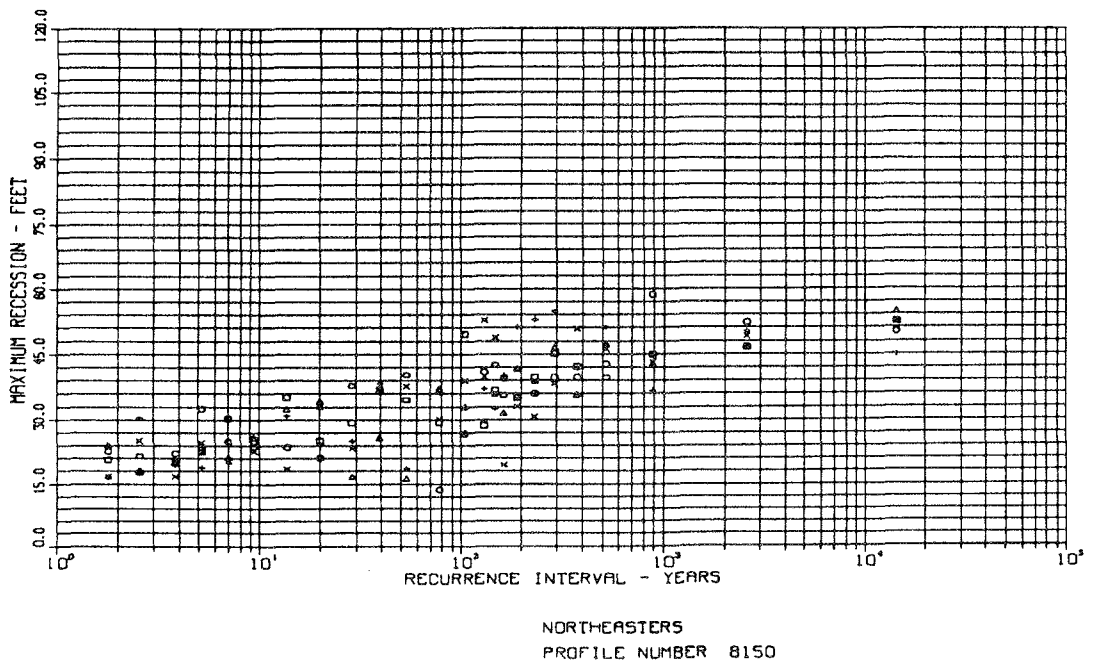


Figure 50. Northeaster recession-recurrence interval simulations for the 150/100 ft wide, 8 ft MSL high design berm

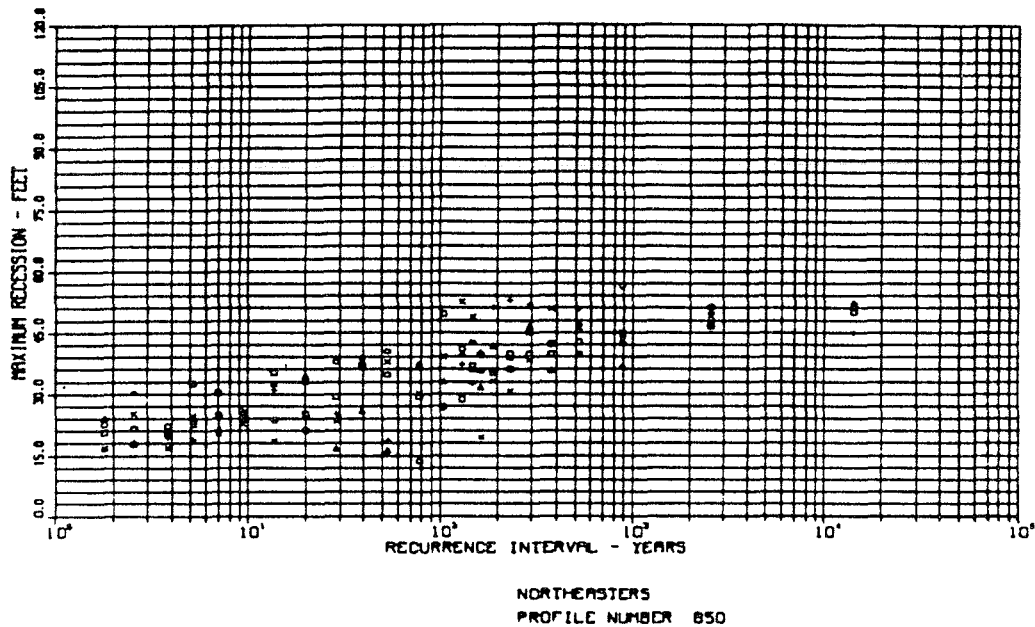


Figure 51. Northeaster recession-recurrence interval simulations for the 50 ft width, 8 ft MSL high design berm

event shown in Figures 49 and 50 was individually rerun for both the 50- and 150/100-ft berm widths. For the 150/100-ft case, a maximum recession of 58 ft was computed, with no erosion of the dune face. Approximately 92 ft of the 150 ft (or 42 ft of the 100 ft) wide, 8 ft high flat berm remained to protect the base of the dune. A maximum recession of 56 ft was computed for 50-ft berm width; however, this figure reflects an accompanying 6-ft recession of the entire dune face, including the crest.

159. Each design profile was subjected to an array of 275 hurricanes to generate recession-frequency of occurrence diagrams similar to those computed for northeasters. Results of simulations for the 150-ft wide, 10-ft berm design are shown in Figure 52. Since maximum berm recessions never exceed 100 ft, the recession-recurrence scatter diagram is equally valid for the 150- and 100-ft wide, 10-ft high designs. Simulations of the 150-ft wide, 8-ft berm design are shown in Figure 53. These results indicate that in only two cases did the computed recession exceed 100 ft, and in these two cases, the recession was only 101 ft. Individual simulations of the two storms for

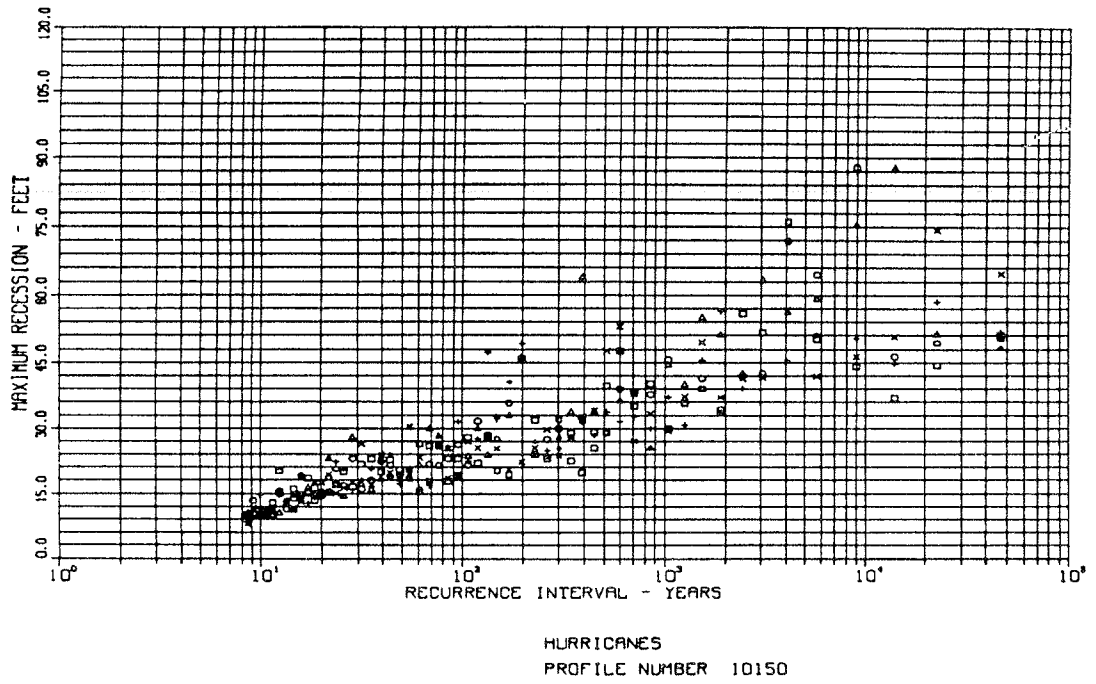


Figure 52. Hurricane recession-recurrence interval simulations for the 150/100 ft wide, 10 ft MSL high design berm

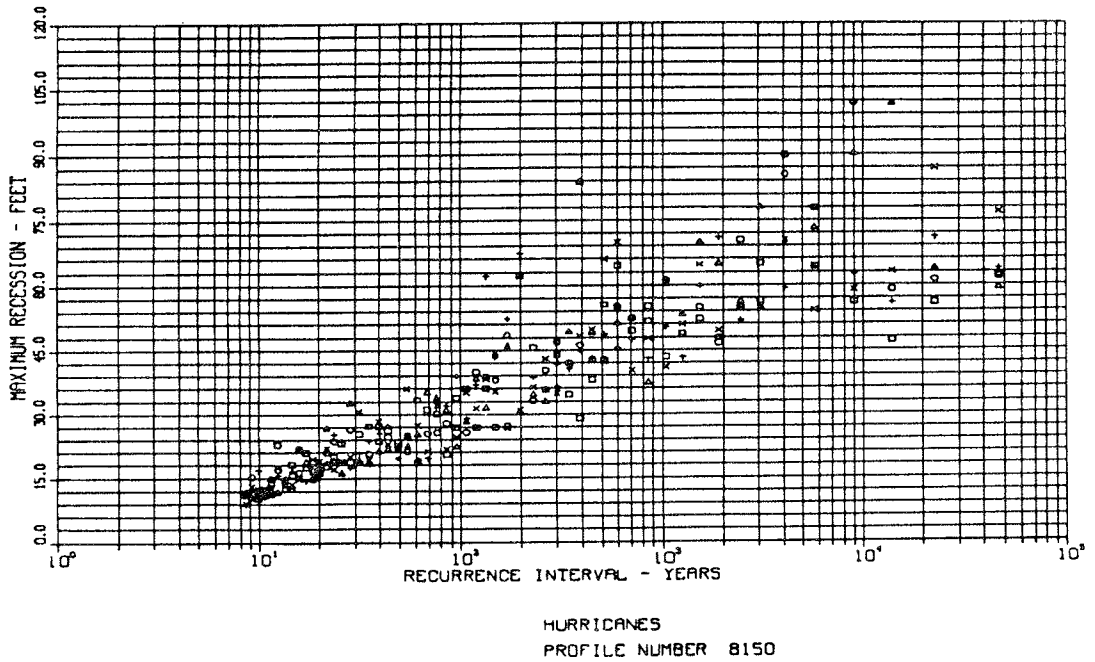


Figure 53. Hurricane recession-recurrence interval simulations for the 150/100 ft wide, 8 ft MSL high design berm

the 8-ft high, 100-ft wide design did not affect recession results; therefore, the relationship in Figure 53 is applicable for both the 150- and 100-ft widths.

160. Because a large number of simulations for both the 10- and 8-ft MSL, 150/100-ft width designs indicated recessions greater than 50 ft, hurricane simulations for the 50-ft wide case were performed. Results for the 10- and 8-ft high, 50-ft wide berms are shown in Figures 54 and 55.

161. Two general observations concerning the scatter diagrams for the different design alternatives should be stated prior to developing and analyzing final design curves. The first is that computed recession values for the 8-ft berm are greater in all cases than those for the 10-ft berm of equal width at each recurrence interval. This result is related to one of the assumptions of the model; alongshore transport is negligible with respect to the cross-shore component during a storm. In order to balance the computed volume of offshore deposition, an equivalent volume of material must be removed from the berm; therefore greater recessions should be expected for lower berms.

162. The second observation concerns the relationship between maximum recession and berm width. A comparison of computed recessions for the 50-ft and 150-ft berm widths of equal height often shows greater maximum recessions for the 150-ft design. An example of this was briefly discussed above for the northeaster simulations of the 8-ft MSL, 50-ft and 150-ft berms. The difference in reported recession occurs because the model is based on the assumption that erosion occurs only on the berm when the berm contains a horizontal plateau, as in the design cases shown in Figure 48. When recession progresses beyond this flat portion, erosion of both the dune and berm face begins. The reduction in calculated maximum recession for the narrower berm width should not be misconstrued as a cost-effective design since this reduction is offset by an equivalent increase in volume of material eroded from the dune face. For example, the two maximum erosion-producing storms (recurrence intervals of approximately 10^4 years) show recessions of approximately 100 ft for the 150-ft berm width. This amount of recession did not affect the dune face; approximately 50 ft of flat berm remained to protect the dune. For the same storms, the computed maximum recession of the 50-ft

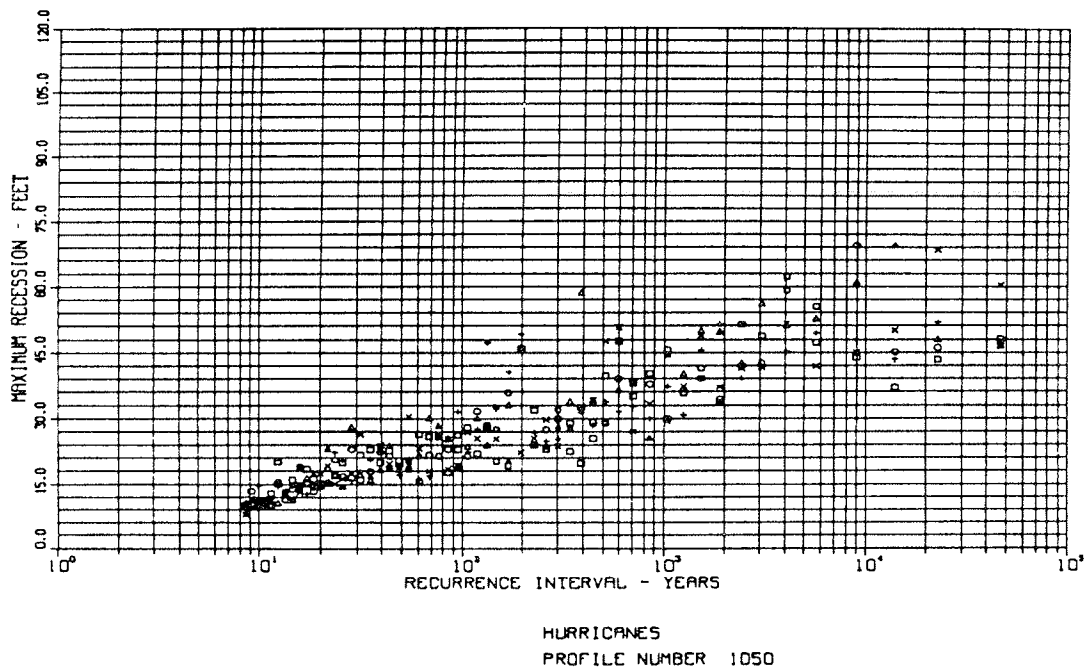


Figure 54. Hurricane recession-recurrence interval simulations for the 50 ft wide, 10 ft MSL high design berm

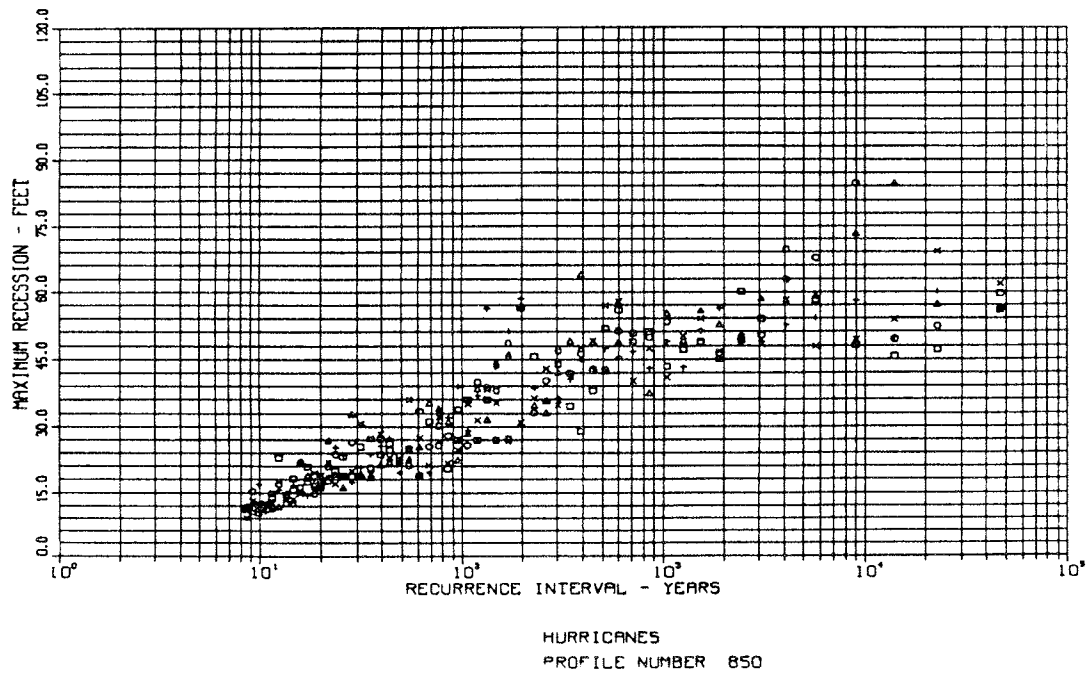


Figure 55. Hurricane recession-recurrence interval simulations for the 50 ft wide, 8 ft MSL high design berm

berm is approximately 85 ft, resulting in complete removal of the horizontal berm and a 15-ft recession of the dune face. For cases in which the width of a dune is narrow, this degree of erosion could result in breaching or overtopping of the entire dune.

163. A curve defining an upper envelope of recession was generated for each of the hurricane and northeaster scatter diagrams. These curves were then used to create an upper limit recession-frequency of occurrence curve for the combined events of a hurricane and northeaster for each design configuration. Results of these computations are shown in Figures 56 through 59.

Summary Design Simulation

164. Incorporation of a variability factor was discussed in the existing conditions section of this report where it was recommended that a factor of 2.0 be considered in design selection. The methodology for using this factor, which would be equally applicable to either seawall-backed beaches or natural duned beaches, involved examining the frequency of occurrence at which maximum recessions are computed to be one-half the design berm width. This approach leads to a conservative estimate of the minimum recurrence interval for complete erosion of the flat portion of the design berm. Continued erosion would be in the form of either lowering of the beach in front of a seawall or recession of the existing dune crest. Table 12 summarizes this data for each of the design alternatives.

165. For the present analysis, in which the design berm configurations are superimposed on Profile 290, horizontal recession of the dune crest will begin following complete erosion of the flat berm. Recession-frequency of occurrence diagrams for Profile 290 indicated the possibility of dune face recessions of 35 ft occurring on the order of every 10 years (not including the variability factor). These values are applicable to the design profiles after the flat design berm has been eroded. Both the 100- and 150-ft wide, 8- and 10-ft berm designs have computed recurrence intervals (Table 12) long enough to allow ample time for reconstruction of storm-related damage to the berm. The 50-ft berm width designs do not provide this degree of protection,

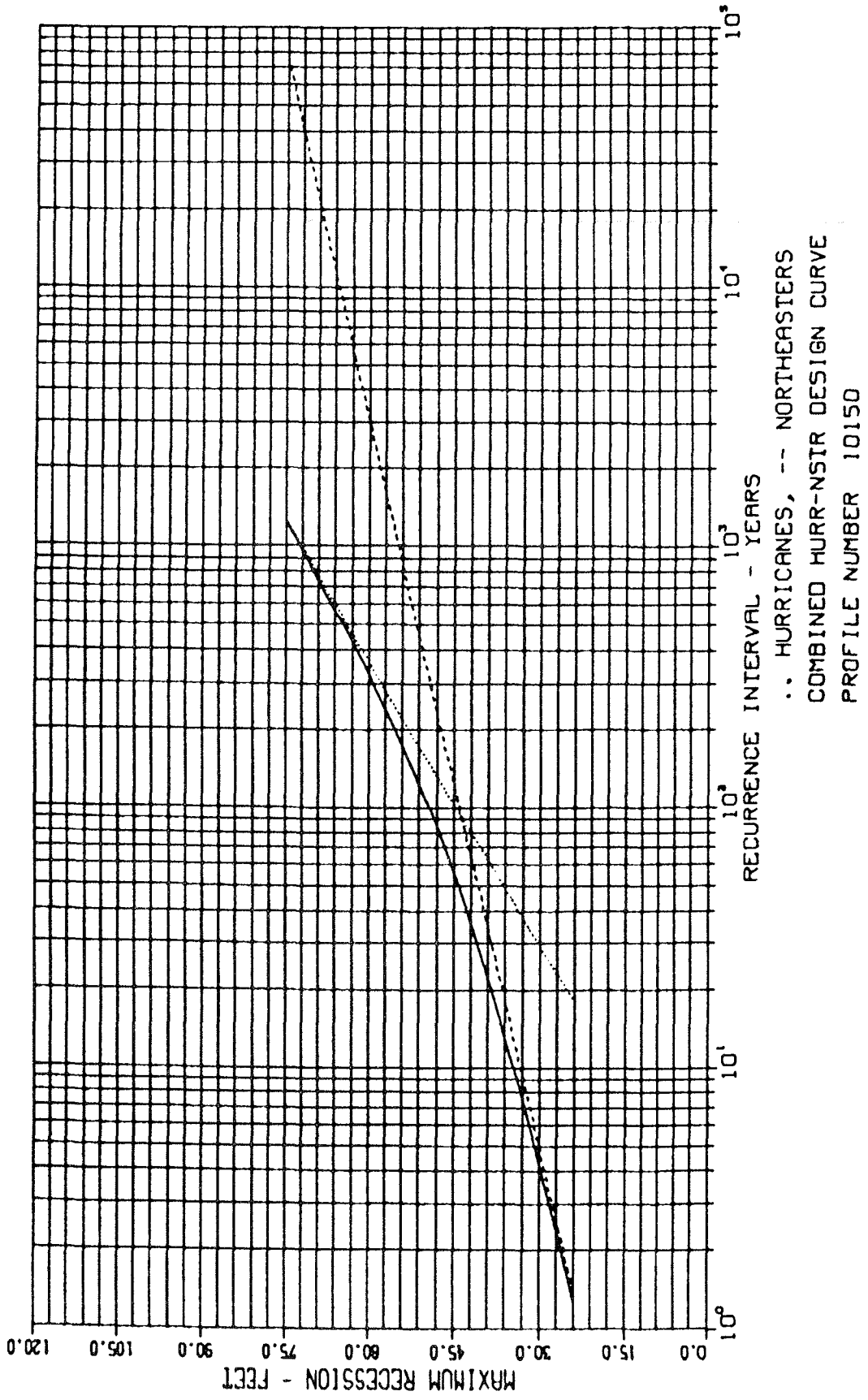


Figure 56. Combined hurricane-northeaster recession-recurrence interval design curve for the 150/100 ft wide, 10 ft MSL high design berm

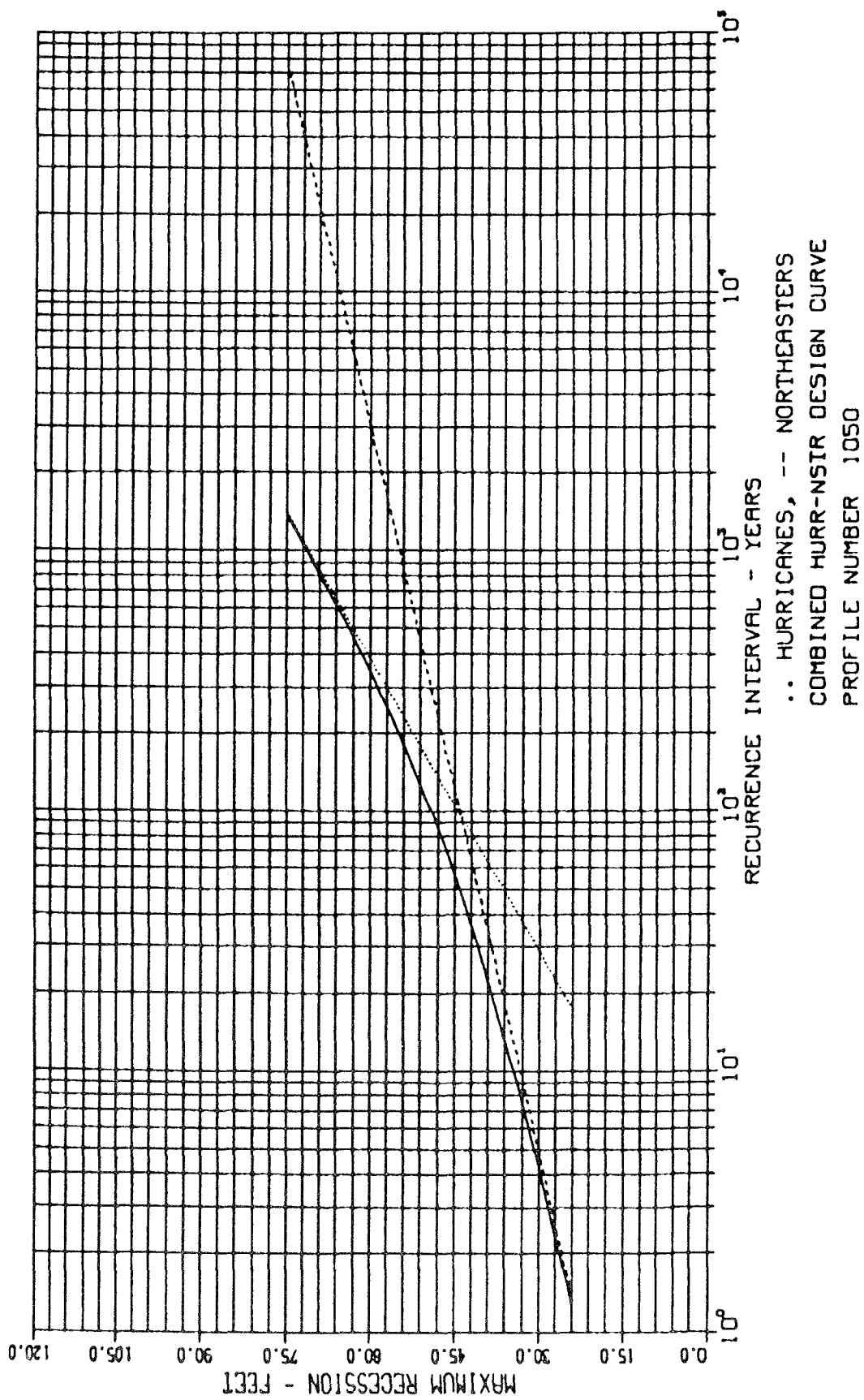


Figure 57. Combined hurricane-northeaster recession-recurrence interval design curve for the 50 ft wide, 10 ft MSL high design berm

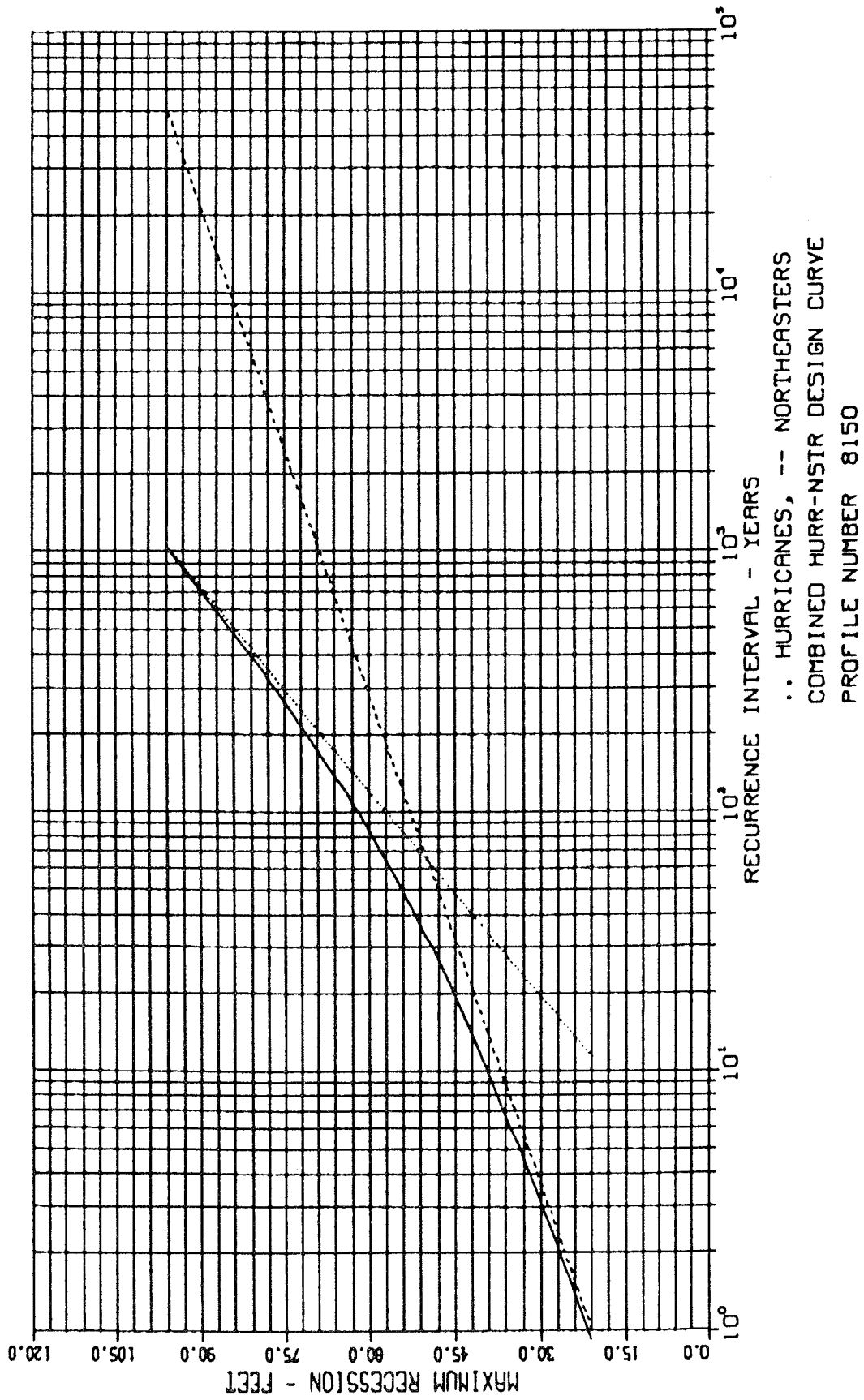


Figure 58. Combined hurricane-northeaster recession-recurrence interval design curve for the 150/100 ft wide, 8 ft MSL high design berm

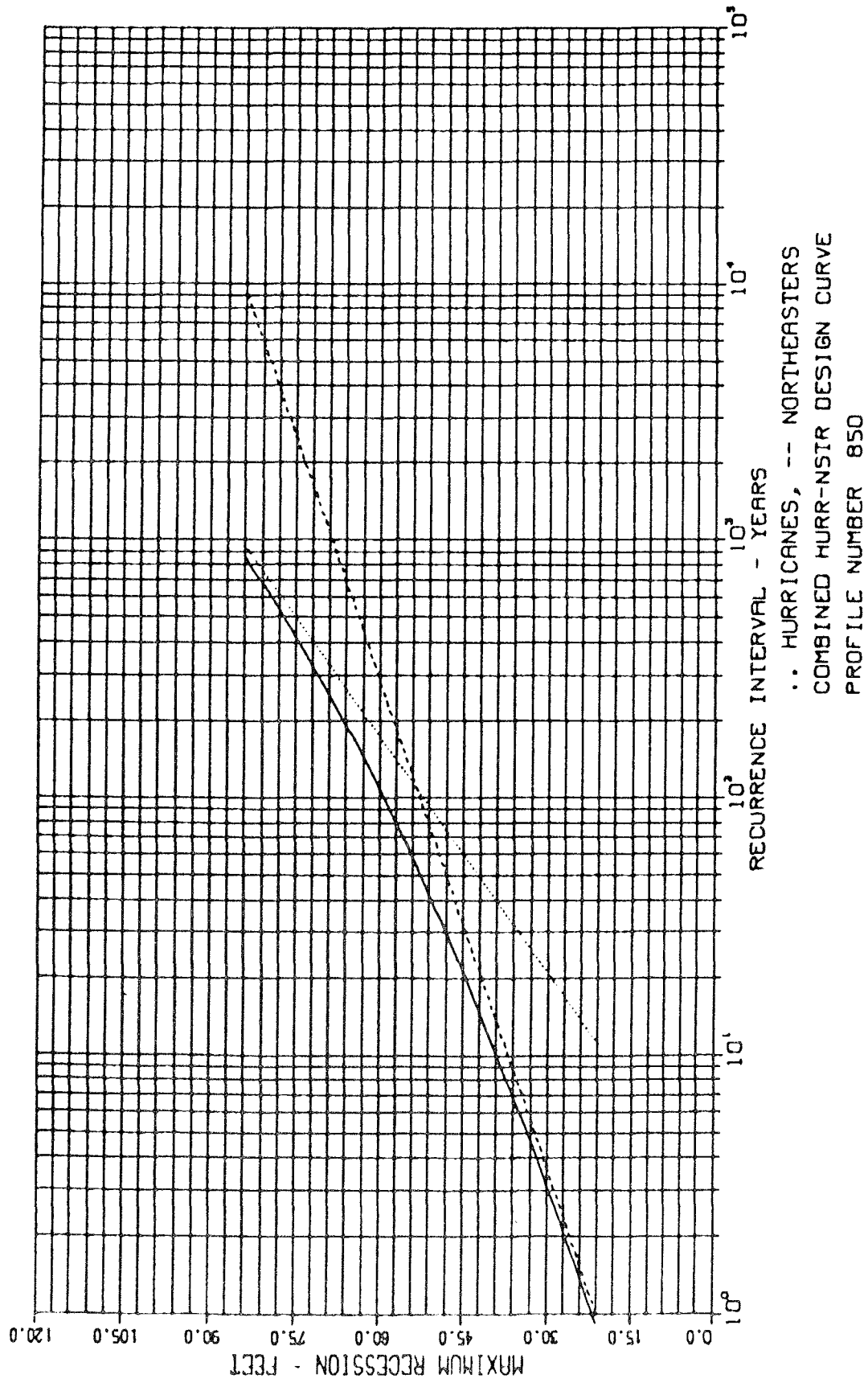


Figure 59. Combined hurricane-northeaster recession-recurrence interval design curve for the 50 ft wide, 8 ft MSL high design curve

and breaching of either the 10-ft or 8-ft (MSL) dunes by storms of intermediate intensity has a reasonable probability of occurring. A recommendation for dune protection is therefore dictated by the relative costs of constructing each of the remaining four designs. The 10-ft MSL, 150-ft wide design provides the most protection; however, it is the most expensive to implement. Since placing material offshore is often more difficult than placing it onshore, the 100-ft wide designs would appear to be more cost effective than the 150-ft wide designs. For areas with low berms (Profile 290), the 10-ft berm appears to provide adequate protection. Dunes with higher crest elevations would be effectively protected by the 8-ft MSL, 100-ft wide design.

Table 12

Recurrence Period (Years) for Storm-Induced Erosion of the Design Berm
(including a 2.0 variability factor)

<u>Berm Height, ft (MSL)</u>	<u>Berm Width, ft</u>		
	<u>50</u>	<u>100</u>	<u>150</u>
10	1.5	120	1200
8	1.5	32	260

166. Following completion of the numerical simulations for the proposed design template, CERC was advised that the location of the break point separating the onshore and offshore design cross-section had been revised from -3.0 NGVD (-3.5 MSL), shown in Figure 48, to -1.5 NGVD (-2.0 MSL). The onshore and offshore slopes of 1:10 and 1:40 respectively remain unchanged. Following the revision, NAN requested CERC to evaluate the potential impact of the new design on the results and conclusions based on the original design. In order to determine the impact of these changes, maximum recession simulations were re-computed for two hurricane and two northeaster events. The selected events represent storms which lie on the upper envelope design curve shown in Figures 56 and 59. A berm width of 150 ft and a berm height of 8.5 ft (NGVD) was assumed in the two simulations. Results are shown in Table 13.

Table 13
Comparison of Recession Simulation for
Old and New Design Cross-Section

<u>Storm ID</u> <u>Increase</u>	<u>Recurrence</u> <u>Interval yrs</u>	<u>Recession ft.</u> <u>Old</u>	<u>Recession ft</u> <u>New</u>	<u>Percent</u>
<u>Hurricanes</u>				
5216904555	28.3	-32.7	-36.0	10.1 %
8776208833	197.4	-67.3	-76.3	13.4 %
<u>Northeasters</u>				
26614452	5.2	-32.4	-37.0	14.2 %
15670268	129.0	-52.6	-59.4	12.9 %

167. Results indicate that computed maximum dune recession values for the revised design template (break point at -1.5 NGVD) increased over the old design (break point -3.0 NGVD) by approximately 10 to 15 percent. This increase results from an effective decrease in the shape coefficient A. For example, the new design is initially less steep immediately offshore and is shallower in depth at fixed distances offshore than the old design. A lower value of A in the equilibrium profile relationship is required to best fit this new design. For the example Profile 290 used in the original design and in the above comparison computations, this change translates in a change in the shape factor A from $0.235 \text{ ft}^{1/3}$ to $0.206 \text{ ft}^{1/3}$. Physically, this reduced offshore depth indicates a smaller grain size which translates to increased erosion.

168. Conclusions of the evaluation of the new design are that a maximum of 10 to 15 percent increased recession would be experienced over the old design with the -3.0 NGVD break point. This slight increase would not change the overall conclusions reached in the original design analysis.

REFERENCES

- Allen, J. R. 1981. "Beach Erosion as a Function of Variations in the Sediment Budget, Sandy Hook, New Jersey," Earth Sciences Processes, Vol 6, pp 139-150.
- Alpine Ocean Seismic Survey, Inc. 1987. "Delineation of Borrow Areas, Atlantic Coast of New Jersey From Asbury Park to Manasquan," Unpublished Final Report, Prepared for US Army Corps of Engineers, New York District.
- Ashley, G. M., Halsey, S. D., and Buteux, C. B. 1986. "New Jersey's Longshore Current Pattern," Journal of Coastal Research, Vol 2, pp 453-463.
- Battjes, J. A. 1974. "Computations of Setup, Longshore Currents, Runup, Overtopping Due to Wind-Generated Waves," Report 74-2 Delft University of Technology, Delft, The Netherlands.
- Battjes, J. A. and J. P. F. M. Janssen. 1979. "Energy Loss and Setup Due to Breaking of Random Waves," Proceedings 16th Coastal Engineering Conference, American Society of Civil Engineers, 569-000.
- Birkemeier W. A., Kraus, N. C., Scheffner, N. W. and Knowles, S. C. 1987. "Feasibility Study of Quantitative Erosion Models for use by the Federal Emergency Management Agency in the Prediction of Coastal Flooding," Technical Report CERC-87-8, US Army Engineer Waterways Experiment Station, Coastal Engineering Research Center, Vicksburg, MS.
- Brooks, R. M., Corson, W. D. 1984. "Summary of Archived Atlantic Coast Wave Information Study Pressure, Wind, and Water Level Data," Wave Information Study Report 13, US Army Engineer Waterways Experiment Station, Vicksburg, MS.
- Bruun, P. 1954. "Coast Erosion and the Development of Beach Profiles," TM-44, US Army Corps of Engineers, Beach Erosion Board.
- Butler, H.L., and Prater, M. D. 1987. "Innovative Determination of Nearshore Flood Frequency," Proceedings of the 20th Coastal Engineering Conference, American Society of Civil Engineers, pp 2463-2476.
- Butler, H. L., Prater, M. A., and Hardy, T. A. (in prep.). "Fire Island to Montauk Point Storm Surge Study," US Army Engineer Waterways Experiment Station, Coastal Engineering Research Center.
- Caldwell, J. M. 1966. "Coastal Processes and Beach Erosion," Journal of the Society of Civil Engineers, Vol 53, No. 2, pp 142-157. (also reprinted with an abstract and errata as Reprint Report I-67, US Army Coastal Engineering Research Center, Corps of Engineers, 1967.)
- Coastal Planning and Engineering / URS Co. 1987. "Asbury Park to Manasquan, N.J. Beach Erosion Control Project; Detailed Field Observation Report," New York, NY.

Corps of Engineering. 1954. "Atlantic Coast of New Jersey, Sandy Hook to Barnegat Inlet," US Army Engineer District, New York, Beach Erosion Control Report on Cooperative Study (Survey), Serial NO. 38.

Dean, R. G. 1977. "Equilibrium Beach Profiles: U.S. Atlantic and Gulf Coasts," Ocean Engineering Report No. 12, Department of Civil Engineering, University of Delaware, Newark, DE.

Ebersole, B. A., Prater, M. A., and Cialone, M. A. 1986. "Regional Coastal Processes Numerical Modeling System; Report 1 RCPWAVE - A Linear Wave Propagation Model for Engineering Use," Technical Report CERC-86-4, US Army Engineer Waterways Experiment Station, Coastal Engineering Research Center, Vicksburg, Miss.

Fairchild, J. C. 1966. "Correlation of Littoral Transport with Wave Energy Along Shores of New York and New Jersey," Technical Memorandum No. 18, US Army Engineer Waterways Experiment Station, Coastal Engineering Research Center, Vicksburg, Miss.

Gares, P. A. 1981. "Historical Analysis of Shoreline Changes at Sandy Hook Spit," in Assessment of Management Problems and Management Problems and Management Strategies for the Shoreline of Sandy Hook Spit, Gateway National Recreational Area, Vol II, Technical Appendices, Center for Coastal and Environmental Studies, Rutgers University, New Brunswick, N. J., pp 15-50.

Gorman, L. T. 1989. "Geomorphic Development of Northern New Jersey Beaches, Asbury Park to Manasquan, with Anotated Bibliography," US Army Engineer Waterways Experiment Station, Coastal Engineering Research Center, Vicksburg, MS.

Gravens, M. B. 1988. "Use of Hindcast Wave Data for Estimation of Longshore Sediment Transport," Proc. Symposium on Coastal Water Resources, American Water Resources Association.

_____. (in prep.) "Estimation of Potential Longshore Sand Transport Rates," US Army Engineer Waterways Experiment Station, Coastal Engineering Research Center, Vicksburg, MS.

Gravens, M. B., and Kraus 1989. "Representation of Groins in Numerical Models of Shoreline Response," Proceedings of XXIII Congress, Hydraulics and the Environment, International Association for Hydraulic Research, in press.

Hallermeier, R. F. 1979. "Uses for a Calculated Limit depth to Beach Erosion," Proceedings of 16th Coastal Engineering Conference, American Society of Civil Engineers, pp.1943-1512.

_____. 1983. "Sand Transport Limits in Coastal Structure Designs," Proceedings Coastal Structures '83, American Society of Civil Engineers, pp 703-716.

- Hanson, H. 1987. "GENESIS - A Generalized Shoreline Change Numerical Model for Engineering Use," PhD Dissertation, Department of Water Resources Engineering, Lund University, Lund, Sweden.
- Hanson H. and Kraus N. C. 1980. "Numerical Model for Studying Shoreline Change in the Vicinity of Coastal Structures," Report No. 3040, Department of Water Resources Engineering, Lund University, Lund, Sweden.
- _____. 1986. "Seawall Boundary Condition in Numerical Models of Shoreline Evolution," US Army Waterways Experiment Station, Vicksburg, MS
- Hanson, H., Kraus, N. C., and Gravens, M. B. 1988 (in press). "Prototype Applications of a Shoreline Prediction Model," Proceedings 21st Coastal Engineering Conference, American Society of Civil Engineers.
- Harris, D. L. 1981. "Tides and Tidal Datums in the United States," Special Report No. 7, US Army Corps of Engineers, Coastal Engineering Research Center.
- Hubertz, J. M., R. E. Jensen, C. E. Abel. 1987. "A Hindcast of Winds, Waves, Water Levels and Currents During Hurricane Gloria," Proceedings of the International Symposium on Natural and Man-Made Hazards, D. Reidel Pub. Co., Dordrecht, The Netherlands.
- Hughes, S. A. 1978. "The Variation in Beach Profiles When Approximated by a Theoretical Curve," Unpublished M.S. Thesis, Department of Coastal and Oceanographic Engineering, University of Florida, Gainesville, FL.
- Jensen, R.E. 1983a. "Atlantic Coast Hindcast, Shallow-Water Significant Wave Information," Wave Information Study Report 9, U.S. Army Engineer Waterways Experiment Station, Vicksburg, MS.
- _____. 1983b. "Methodology for the Calculation of a Shallow-Water Wave Climate," Wave Information Study Report 8, U.S. Army Engineer Waterways Experiment Station, Vicksburg, MS.
- Kondolf, G. M. 1978. "Genesis and Development of Sandy Hook, New Jersey," unpublished Senior Thesis, Department of Geological and Geophysical Sciences, Princeton University, Princeton, N. J.
- Kraus, N. C. 1983. "Applications of a Shoreline Prediction Model," Proceedings Coastal Structures '83, American Society of Civil Engineers, pp. 632-645.
- Kraus, N. C. and Dean, J. L. 1987. "Longshore Sediment Transport Rate Distributions Measured by Trap," Proceedings Coastal Sediments '87, American Society of Civil Engineers, pp 881-896.
- Kraus, N. C., and Harikai, S. 1983. "Numerical Model of the Shoreline Change at Oarai Beach," Coastal Engineering, Vol. 7, No. 1 pp. 1-28.

- Kraus, N. C., Gingerich, K. J., and Rosati, J. D. 1988 (in press). "Toward an Improved Empirical Formula for Longshore Sand Transport," Proceedings of 21st Coastal Engineering Conference, American Society of Civil Engineers.
- Kraus, N. C., Gravens, M. B., and Mark, D. J. 1988. Vol 2, "Coastal Processes at Sea Bright to Ocean Township, New Jersey," US Army Engineer Waterways Experiment Station, Coastal Engineering Research Center, Vicksburg, MS.
- Kraus N. C., Hanson, H. and Larson, M. 1988. "Threshold of Longshore Sediment Transport and the Shoreline Change Simulation Model," Symposium on Mathematical Modeling of Sediment Transport in the Coastal Zone, International Association of Hydraulic Research, pp.117-126.
- Kraus, N. C., Scheffner, N. W., and Hanson, H., Chou, L. W., Cialone, M. A., Smith, J. M., and Hardy, T. A. 1988. Vol 1, "Coastal Processes at Sea Bright to Ocean Township, New Jersey," US Army Engineer Waterways Experiment Station, Coastal Engineering Research Center, Vicksburg, MS.
- Kriebel, D. L. 1984. "Beach Erosion (EBEACH) Users Manual, Volume II: Theory and Background," Beaches and Shores Technical and Design Memorandum No. 84-5-II, Division of Beaches and Shores, Florida Department of Natural Resources, Tallahassee, FL.
- Meyers, V. A. 1970. "Joint Probability Method of Tide Frequency Analysis Applied to Atlantic City and Long Beach Island, NJ," ESSA Technical Memo. WBTM HYDRO 11, U.S. Department of Commerce, ESSA, Weather Bureau.
- Moore, B. 1982. "Beach Profile Evolution in Response to Changes in Water Level and Wave Height," Unpublished M.S. Thesis, Department of Civil Engineering, University of Delaware, Newark, DE.
- Ozasa, H., and Brampton, A. H. 1980. "Mathematical Modeling of Beaches Backed by Seawalls," Coastal Engineering, Vol 4, No. 1, pp. 47-64.
- Phillips, J. D. 1985. "Headland-Bay Beaches Revisited: An Example from Sandy Hook, New Jersey," Marine Geology, Vol 65, pp 21-31.
- Phillips, J. D., Psuty, N. P., and McCluskey, J. M. 1984. "The Impact of Beach Nourishment at South Beach, Sandy Hook, New Jersey," Final Report, Center for Coastal and Environmental Studies, Rutgers University, New Brunswick, N. J., 30 pp.
- Pelnard-Considere, R. 1956. "Essai de Th'eorie de l'Evolution des Forms de Rivages en Plage de Sable et de Galets," 4th Journees de l'Hydraulique, les Energies de la Mer, Question III, Rapport No. 1, pp 289-298.
- Savage, R. J. and Birkemeier, W. A. 1987. "Storm Erosion Data from the United States Atlantic Coast," Proceedings of Coastal Sediments '87, American Society of Civil Engineers, pp. 1445-1459.

Scheffner, N. W. 1987. Unpublished comparisons of offshore profiles to computed equilibrium profiles, US Army Engineer Waterways Experiment Station, Coastal Engineering Research Center, Vicksburg, MS.

Shore Protection Manual. 1984. 4th ed., 2 Vols. US Army Engineer Waterways Experiment Station, Coastal Engineering Research Center, US Government Printing Office, Washington, DC.

Tancreto, A. E. 1958. "A Method for Forecasting the Maximum Surge at Boston due to Extratropical Storms," Monthly Weather Review, Vol 86, No. 6, pp 197-200.

US Congress 1937. "Beach Erosion at Manasquan Inlet and Adjacent Beaches," House Document No. 71.

APPENDIX A: NOTATION

a	Sand porosity
A	Parameter determining equilibrium beach shape
BYP	Sand bypassing factor
C_{gb}	Wave group velocity at breaking given by linear wave theory
$\cot(\beta)$	Inverse beach slope
D	Wave energy dissipation in the surf zone
D_c	Depth of closure
D_{eq}	Equilibrium wave energy dissipation in the surf zone
D_g	Depth at seaward end of groin
DLT	Depth of littoral transport
F	Wave energy flux by linear wave theory
h	Water depth
H	Wave height
H_b	Breaking wave height
H_{mo}	Energy-based wave height
H_s	Significant wave height
H_{savg}	Average significant wave height
H_{smax}	Maximum significant wave height
k	Empirical coefficient in cross-shore transport rate equation
K_1, K_2	Calibration parameters in shoreline contour model
Q	Volume rate of longshore sand transport
Q_s	Volume rate of cross-shore sand transport
S	Ratio of sand density to water density
t	time
T_p	Peak spectral wave period
x	Coordinate direction
y	Coordinate direction
α_{bs}	Breaking wave angle to the shoreline

APPENDIX B: STATISTICS OF THE WAVE HINDCAST DATA BASE

WIS Hindcast Summary

1. This appendix provides information on the Wave Information Study (WIS) Phase III hindcast wave data. Included is a summary of wave statistics for the 20-year period 1956-1975 for the two stations used in this study (Stations 55 and 56). Tables B1 and B2 give the statistics categorized by wave approach angle in degrees for Stations 55 and 56 respectively. Values in the direction tables represent the percent of the 20 years that waves occur from the specified direction bands for the indicated height and period ranges. The values have been multiplied by 1,000 to allow more accuracy with less printing space. Summations are provided in the last column and row of each table. Table B3 is a summary of the same data for waves from all directions for both stations. Values in Table B3 are multiplied by 100, and the parameters listed in the last line of the all-direction tables are derived from the directional tables given in Tables B1 and B2.

Representative Time History of Wave Conditions

2. The procedure used to select a 3-year-long representative time history of wave conditions for use with the shoreline contour model GENESIS is described below. A time history of wave conditions is required in order to utilize GENESIS in a predictive mode to assess the long-term performance of proposed shore protection design alternatives. The selected representative wave conditions were used in all model simulations including the calibration and verification as well as in the design alternative evaluation simulations.

3. Simple statistics of wave height and percent occurrence categorized by angle band and year were used to select 3 years of representative wave conditions for use in this study. Tables B4 and B5 give the average significant wave height and number of occurrences for both sea and swell wave conditions categorized by angle band and year, for Stations 55 and 56 respectively. These data were averaged (between the two stations) and compared to the averages of the entire 20-year hindcast (for both stations).

Table B1

Wave Statistics Categorized by Wave Approach Angle (Station 55)

NEW JERSEY, SECTION II, ASBURY PARK TO MANASQUAN
 ATLANTIC PHASE III WAVE INFORMATION
 STATION 55 20 YEARS WAVE APPROACH ANGLE(DEGREES)= 0. - 11.24
 WAVE APPROACH ANGLES RELATIVE TO TRUE NORTH
 WATER DEPTH = 18.60 METERS
 PERCENT OCCURRENCE(X1000) OF HEIGHT AND PERIOD BY DIRECTION

HEIGHT(METERS)	PERIOD(SECONDS)										TOTAL
	0.0- 1.9	2.0- 3.9	4.0- 5.9	6.0- 7.9	8.0- 9.9	10.0- 11.9	12.0- 13.9	14.0- 15.9	16.0- 17.9	18.0- LONGER	
0.0 - 0.49	0
0.50 - 0.99	0
1.00 - 1.49	0
1.50 - 1.99	0
2.00 - 2.49	0
2.50 - 2.99	0
3.00 - 3.49	0
3.50 - 3.99	0
4.00 - 4.49	0
4.50 - 4.99	0
5.00 - GREATER	0
TOTAL	0	0	0	0	0	0	0	0	0	0	0

AVERAGE HS(M) = 0. LARGEST HS(M) = 0. ANGLE CLASS % = 0.

NEW JERSEY, SECTION II, ASBURY PARK TO MANASQUAN
 ATLANTIC PHASE III WAVE INFORMATION
 STATION 55 20 YEARS WAVE APPROACH ANGLE(DEGREES)= 11.25 - 33.74
 WAVE APPROACH ANGLES RELATIVE TO TRUE NORTH
 WATER DEPTH = 18.60 METERS
 PERCENT OCCURRENCE(X1000) OF HEIGHT AND PERIOD BY DIRECTION

HEIGHT(METERS)	PERIOD(SECONDS)										TOTAL
	0.0- 1.9	2.0- 3.9	4.0- 5.9	6.0- 7.9	8.0- 9.9	10.0- 11.9	12.0- 13.9	14.0- 15.9	16.0- 17.9	18.0- LONGER	
0.0 - 0.49	0
0.50 - 0.99	0
1.00 - 1.49	0
1.50 - 1.99	0
2.00 - 2.49	0
2.50 - 2.99	0
3.00 - 3.49	0
3.50 - 3.99	0
4.00 - 4.49	0
4.50 - 4.99	0
5.00 - GREATER	0
TOTAL	0	0	0	0	0	0	0	0	0	0	0

AVERAGE HS(M) = 0. LARGEST HS(M) = 0. ANGLE CLASS % = 0.

NEW JERSEY, SECTION II, ASBURY PARK TO MANASQUAN
 ATLANTIC PHASE III WAVE INFORMATION
 STATION 55 20 YEARS WAVE APPROACH ANGLE(DEGREES)= 33.75 - 56.24
 WAVE APPROACH ANGLES RELATIVE TO TRUE NORTH
 WATER DEPTH = 18.60 METERS
 PERCENT OCCURRENCE(X1000) OF HEIGHT AND PERIOD BY DIRECTION

HEIGHT(METERS)	PERIOD(SECONDS)										TOTAL
	0.0- 1.9	2.0- 3.9	4.0- 5.9	6.0- 7.9	8.0- 9.9	10.0- 11.9	12.0- 13.9	14.0- 15.9	16.0- 17.9	18.0- LONGER	
0.0 - 0.49	0
0.50 - 0.99	0
1.00 - 1.49	0
1.50 - 1.99	0
2.00 - 2.49	0
2.50 - 2.99	0
3.00 - 3.49	0
3.50 - 3.99	0
4.00 - 4.49	0
4.50 - 4.99	0
5.00 - GREATER	0
TOTAL	0	0	0	0	0	0	0	0	0	0	0

AVERAGE HS(M) = 0. LARGEST HS(M) = 0. ANGLE CLASS % = 0.

(Continued)

(Sheet 1 of 3)

Table B1 (Continued)

NEW JERSEY, SECTION II, ASBURY PARK TO MANASQUAN
 ATLANTIC PHASE III WAVE INFORMATION
 STATION 55 20 YEARS WAVE APPROACH ANGLE(DEGREES)= 56.25 - 78.74
 WAVE APPROACH ANGLES RELATIVE TO TRUE NORTH
 WATER DEPTH = 18.60 METERS
 PERCENT OCCURRENCE(X1000) OF HEIGHT AND PERIOD BY DIRECTION

HEIGHT(METERS)	PERIOD(SECONDS)										TOTAL
	0.0- 1.9	2.0- 3.9	4.0- 5.9	6.0- 7.9	8.0- 9.9	10.0- 11.9	12.0- 13.9	14.0- 15.9	16.0- 17.9	18.0- LONGER	
0.0 - 0.49	56	1584	2438	746	118	10	4952
0.50 - 0.99	.	6	1057	386	61	8	1526
1.00 - 1.49	.	.	143	287	15	446
1.50 - 1.99	.	.	5	100	6	111
2.00 - 2.49	.	.	.	11	1	12
2.50 - 2.99	0
3.00 - 3.49	0
3.50 - 3.99	0
4.00 - 4.49	0
4.50 - 4.99	0
5.00 - GREATER	0
TOTAL	56	1590	3643	1530	201	18	0	0	0	0	0

AVERAGE HS(M) = 0.39 LARGEST HS(M) = 2.29 ANGLE CLASS % = 7.0

NEW JERSEY, SECTION II, ASBURY PARK TO MANASQUAN
 ATLANTIC PHASE III WAVE INFORMATION
 STATION 55 20 YEARS WAVE APPROACH ANGLE(DEGREES)= 78.75 - 101.24
 WAVE APPROACH ANGLES RELATIVE TO TRUE NORTH
 WATER DEPTH = 18.60 METERS
 PERCENT OCCURRENCE(X1000) OF HEIGHT AND PERIOD BY DIRECTION

HEIGHT(METERS)	PERIOD(SECONDS)										TOTAL
	0.0- 1.9	2.0- 3.9	4.0- 5.9	6.0- 7.9	8.0- 9.9	10.0- 11.9	12.0- 13.9	14.0- 15.9	16.0- 17.9	18.0- LONGER	
0.0 - 0.49	56	1190	34	2215	975	335	191	.	.	.	4996
0.50 - 0.99	.	349	1399	1466	1401	946	130	.	.	.	5711
1.00 - 1.49	.	1	771	562	171	59	59	.	.	.	2169
1.50 - 1.99	.	.	65	622	270	18	18	.	.	.	1034
2.00 - 2.49	.	.	.	154	177	33	15	.	.	.	249
2.50 - 2.99	.	.	.	30	35	5	1	.	.	.	69
3.00 - 3.49	8	.	3	.	.	.	61
3.50 - 3.99	8	.	3	.	.	.	14
4.00 - 4.49	1	.	3	.	.	.	4
4.50 - 4.99	8	.	.	.	13
5.00 - GREATER	8	.	.	.	0
TOTAL	56	1540	2269	5423	3549	1564	435	0	0	0	0

AVERAGE HS(M) = 0.84 LARGEST HS(M) = 6.86 ANGLE CLASS % = 14.9

NEW JERSEY, SECTION II, ASBURY PARK TO MANASQUAN
 ATLANTIC PHASE III WAVE INFORMATION
 STATION 55 20 YEARS WAVE APPROACH ANGLE(DEGREES)= 101.25 - 123.74
 WAVE APPROACH ANGLES RELATIVE TO TRUE NORTH
 WATER DEPTH = 18.60 METERS
 PERCENT OCCURRENCE(X1000) OF HEIGHT AND PERIOD BY DIRECTION

HEIGHT(METERS)	PERIOD(SECONDS)										TOTAL
	0.0- 1.9	2.0- 3.9	4.0- 5.9	6.0- 7.9	8.0- 9.9	10.0- 11.9	12.0- 13.9	14.0- 15.9	16.0- 17.9	18.0- LONGER	
0.0 - 0.49	42	829	.	665	954	386	3	.	.	.	2879
0.50 - 0.99	.	521	876	222	272	333	1	.	.	.	2232
1.00 - 1.49	.	1	650	56	70	63	840
1.50 - 1.99	.	.	66	177	35	13	291
2.00 - 2.49	.	.	.	159	17	6	182
2.50 - 2.99	.	.	.	106	22	1	129
3.00 - 3.49	.	.	.	34	46	80
3.50 - 3.99	.	.	.	1	13	14
4.00 - 4.49	1	0
4.50 - 4.99	0
5.00 - GREATER	0
TOTAL	42	1351	1592	1427	1430	802	4	0	0	0	0

AVERAGE HS(M) = 0.75 LARGEST HS(M) = 4.09 ANGLE CLASS % = 6.7

(Continued)

(Sheet 2 of 3)

Table B1 (Concluded)

NEW JERSEY, SECTION II, ASBURY PARK TO MANASQUAN
 ATLANTIC PHASE III WAVE INFORMATION
 STATION 55 20 YEARS WAVE APPROACH ANGLE(DEGREES)= 123.75 - 146.24
 WAVE APPROACH ANGLES RELATIVE TO TRUE NORTH
 WATER DEPTH = 18.60 METERS
 PERCENT OCCURRENCE(X1000) OF HEIGHT AND PERIOD BY DIRECTION

HEIGHT(METERS)	PERIOD(SECONDS)										TOTAL
	0.0-1.9	2.0-3.9	4.0-5.9	6.0-7.9	8.0-9.9	10.0-11.9	12.0-13.9	14.0-15.9	16.0-17.9	18.0-LONGER	
0.0 - 0.49	46	1132		3196	2041	658	66				7139
0.50 - 0.99		609	959	708	621	114					3011
1.00 - 1.49		1	583	154	82						828
1.50 - 1.99			82	177	13						289
2.00 - 2.49				145	13						183
2.50 - 2.99				65	41						119
3.00 - 3.49				23	32						60
3.50 - 3.99				1	13						14
4.00 - 4.49					1						1
4.50 - 4.99											0
5.00 - GREATER											0
TOTAL	46	1742	1624	4469	2866	831	66	0	0	0	

AVERAGE HS(M) = 0.56 LARGEST HS(M) = 4.31 ANGLE CLASS % = 11.7

NEW JERSEY, SECTION II, ASBURY PARK TO MANASQUAN
 ATLANTIC PHASE III WAVE INFORMATION
 STATION 55 20 YEARS WAVE APPROACH ANGLE(DEGREES)= 146.25 - 168.74
 WAVE APPROACH ANGLES RELATIVE TO TRUE NORTH
 WATER DEPTH = 18.60 METERS
 PERCENT OCCURRENCE(X1000) OF HEIGHT AND PERIOD BY DIRECTION

HEIGHT(METERS)	PERIOD(SECONDS)										TOTAL
	0.0-1.9	2.0-3.9	4.0-5.9	6.0-7.9	8.0-9.9	10.0-11.9	12.0-13.9	14.0-15.9	16.0-17.9	18.0-LONGER	
0.0 - 0.49	59	2164		9560	4317	465					16565
0.50 - 0.99		744	1726	2722	2263	386					7841
1.00 - 1.49			790	759	492	73					2114
1.50 - 1.99			56	527	219	39					841
2.00 - 2.49				301	111	10					422
2.50 - 2.99				73	54	1					128
3.00 - 3.49				5	8						13
3.50 - 3.99					3						3
4.00 - 4.49											0
4.50 - 4.99											0
5.00 - GREATER											0
TOTAL	59	2908	2572	13947	7467	974	0	0	0	0	

AVERAGE HS(M) = 0.57 LARGEST HS(M) = 3.98 ANGLE CLASS % = 27.9

NEW JERSEY, SECTION II, ASBURY PARK TO MANASQUAN
 ATLANTIC PHASE III WAVE INFORMATION
 STATION 55 20 YEARS WAVE APPROACH ANGLE(DEGREES)= 168.75 - 193.00
 WAVE APPROACH ANGLES RELATIVE TO TRUE NORTH
 WATER DEPTH = 18.60 METERS
 PERCENT OCCURRENCE(X1000) OF HEIGHT AND PERIOD BY DIRECTION

HEIGHT(METERS)	PERIOD(SECONDS)										TOTAL
	0.0-1.9	2.0-3.9	4.0-5.9	6.0-7.9	8.0-9.9	10.0-11.9	12.0-13.9	14.0-15.9	16.0-17.9	18.0-LONGER	
0.0 - 0.49	135	6463	5532	3133	3						15266
0.50 - 0.99		203	3591	675	3						4472
1.00 - 1.49			244	465	20						729
1.50 - 1.99			1	90	8						99
2.00 - 2.49				13							13
2.50 - 2.99											0
3.00 - 3.49											0
3.50 - 3.99											0
4.00 - 4.49											0
4.50 - 4.99											0
5.00 - GREATER											0
TOTAL	135	6666	9368	4376	34	0	0	0	0	0	

AVERAGE HS(M) = 0.37 LARGEST HS(M) = 2.49 ANGLE CLASS % = 20.6

Table B2 (Continued)

NEW JERSEY, SECTION II, ASBURY PARK TO MANASQUAN
 ATLANTIC PHASE III WAVE INFORMATION
 STATION 57 20 YEARS WAVE APPROACH ANGLE(DEGREES)= 56.25 - 78.74
 WAVE APPROACH ANGLES RELATIVE TO TRUE NORTH
 WATER DEPTH = 18.60 METERS
 PERCENT OCCURRENCE(X1000) OF HEIGHT AND PERIOD BY DIRECTION

HEIGHT(METERS)	PERIOD(SECONDS)										TOTAL
	0.0-1.9	2.0-3.9	4.0-5.9	6.0-7.9	8.0-9.9	10.0-11.9	12.0-13.9	14.0-15.9	16.0-17.9	18.0-LONGER	
0.0 - 0.49	82	1933	2547	2684	343	35	7624
0.50 - 0.99	.	20	1163	1358	407	49	2997
1.00 - 1.49	.	.	121	845	164	11	1141
1.50 - 1.99	.	.	.	492	102	5	599
2.00 - 2.49	.	.	.	164	82	5	251
2.50 - 2.99	.	.	.	6	22	3	1	.	.	.	32
3.00 - 3.49	3	3
3.50 - 3.99	0
4.00 - 4.49	0
4.50 - 4.99	0
5.00 - GREATER	0
TOTAL	82	1953	3831	5549	1123	108	1	0	0	0	

AVERAGE HS(M) = 0.54 LARGEST HS(M) = 3.22 ANGLE CLASS % = 12.7

NEW JERSEY, SECTION II, ASBURY PARK TO MANASQUAN
 ATLANTIC PHASE III WAVE INFORMATION
 STATION 57 20 YEARS WAVE APPROACH ANGLE(DEGREES)= 78.75 - 101.24
 WAVE APPROACH ANGLES RELATIVE TO TRUE NORTH
 WATER DEPTH = 18.60 METERS
 PERCENT OCCURRENCE(X1000) OF HEIGHT AND PERIOD BY DIRECTION

HEIGHT(METERS)	PERIOD(SECONDS)										TOTAL
	0.0-1.9	2.0-3.9	4.0-5.9	6.0-7.9	8.0-9.9	10.0-11.9	12.0-13.9	14.0-15.9	16.0-17.9	18.0-LONGER	
0.0 - 0.49	30	1134	11	1309	1098	585	224	.	.	.	4391
0.50 - 0.99	.	414	1421	898	2236	669	174	.	.	.	5812
1.00 - 1.49	.	.	77	405	682	112	15	.	.	.	1990
1.50 - 1.99	.	.	95	487	280	73	935
2.00 - 2.49	.	.	.	487	31	23	641
2.50 - 2.99	.	.	.	205	157	18	380
3.00 - 3.49	.	.	.	17	124	6	3	.	.	.	150
3.50 - 3.99	22	6	1	.	.	.	29
4.00 - 4.49	6	5	1	.	.	.	12
4.50 - 4.99	3	3	6	.	.	.	9
5.00 - GREATER	10	.	.	.	13
TOTAL	30	1548	2303	3008	4739	1500	434	0	0	0	

AVERAGE HS(M) = 0.89 LARGEST HS(M) = 6.66 ANGLE CLASS % = 14.4

NEW JERSEY, SECTION II, ASBURY PARK TO MANASQUAN
 ATLANTIC PHASE III WAVE INFORMATION
 STATION 57 20 YEARS WAVE APPROACH ANGLE(DEGREES)= 101.25 - 123.74
 WAVE APPROACH ANGLES RELATIVE TO TRUE NORTH
 WATER DEPTH = 18.60 METERS
 PERCENT OCCURRENCE(X1000) OF HEIGHT AND PERIOD BY DIRECTION

HEIGHT(METERS)	PERIOD(SECONDS)										TOTAL
	0.0-1.9	2.0-3.9	4.0-5.9	6.0-7.9	8.0-9.9	10.0-11.9	12.0-13.9	14.0-15.9	16.0-17.9	18.0-LONGER	
0.0 - 0.49	41	788	860	450	3287	254	4820
0.50 - 0.99	.	521	1	181	847	13	3	.	.	.	2425
1.00 - 1.49	.	.	633	168	70	1	733
1.50 - 1.99	.	.	71	157	20	1	243
2.00 - 2.49	.	.	.	152	18	170
2.50 - 2.99	.	.	.	15	21	109
3.00 - 3.49	1	56
3.50 - 3.99	10	11
4.00 - 4.49	1	1	2
4.50 - 4.99	0
5.00 - GREATER	0
TOTAL	41	1310	1564	1110	4316	271	3	0	0	0	

AVERAGE HS(M) = 0.63 LARGEST HS(M) = 4.32 ANGLE CLASS % = 8.6

(Continued)

(Sheet 2 of 3)

Table B2 (Concluded)

NEW JERSEY, SECTION II, ASBURY PARK TO MANASQUAN
 ATLANTIC PHASE III WAVE INFORMATION
 STATION 57 20 YEARS WAVE APPROACH ANGLE(DEGREES)= 123.75 - 146.24
 WAVE APPROACH ANGLES RELATIVE TO TRUE NORTH
 WATER DEPTH = 18.60 METERS
 PERCENT OCCURRENCE(X1000) OF HEIGHT AND PERIOD BY DIRECTION

HEIGHT(METERS)	PERIOD(SECONDS)										TOTAL
	0.0-1.9	2.0-3.9	4.0-5.9	6.0-7.9	8.0-9.9	10.0-11.9	12.0-13.9	14.0-15.9	16.0-17.9	18.0-LONGER	
0.0 - 0.49	18	1019		2164	171	1019	29				4420
0.50 - 0.99		614	900	518	73	391					2496
1.00 - 1.49			593	87	27	69					773
1.50 - 1.99			68	205	10	34					317
2.00 - 2.49			1	148	8	22					170
2.50 - 2.99				71	41	10					122
3.00 - 3.49				18	47	8					68
3.50 - 3.99					13	1					14
4.00 - 4.49						1					1
4.50 - 4.99											0
5.00 - GREATER											0
TOTAL	18	1633	1562	5211	390	1547	29	0	0	0	0

AVERAGE HS(M) = 0.67 LARGEST HS(M) = 4.37 ANGLE CLASS % = 8.4

NEW JERSEY, SECTION II, ASBURY PARK TO MANASQUAN
 ATLANTIC PHASE III WAVE INFORMATION
 STATION 57 20 YEARS WAVE APPROACH ANGLE(DEGREES)= 146.25 - 168.74
 WAVE APPROACH ANGLES RELATIVE TO TRUE NORTH
 WATER DEPTH = 18.60 METERS
 PERCENT OCCURRENCE(X1000) OF HEIGHT AND PERIOD BY DIRECTION

HEIGHT(METERS)	PERIOD(SECONDS)										TOTAL
	0.0-1.9	2.0-3.9	4.0-5.9	6.0-7.9	8.0-9.9	10.0-11.9	12.0-13.9	14.0-15.9	16.0-17.9	18.0-LONGER	
0.0 - 0.49	42	1925	6	8511	3206	17					13707
0.50 - 0.99		679	2073	2031	1899	88					6770
1.00 - 1.49		1	781	737	338	23					1880
1.50 - 1.99			37	545	193	10					805
2.00 - 2.49				222	106	1					329
2.50 - 2.99				47	35						82
3.00 - 3.49				1	5						6
3.50 - 3.99											0
4.00 - 4.49											0
4.50 - 4.99											0
5.00 - GREATER											0
TOTAL	42	2605	2897	12094	5782	139	0	0	0	0	0

AVERAGE HS(M) = 0.57 LARGEST HS(M) = 3.46 ANGLE CLASS % = 23.6

NEW JERSEY, SECTION II, ASBURY PARK TO MANASQUAN
 ATLANTIC PHASE III WAVE INFORMATION
 STATION 57 20 YEARS WAVE APPROACH ANGLE(DEGREES)= 168.75 - 190.00
 WAVE APPROACH ANGLES RELATIVE TO TRUE NORTH
 WATER DEPTH = 18.60 METERS
 PERCENT OCCURRENCE(X1000) OF HEIGHT AND PERIOD BY DIRECTION

HEIGHT(METERS)	PERIOD(SECONDS)										TOTAL
	0.0-1.9	2.0-3.9	4.0-5.9	6.0-7.9	8.0-9.9	10.0-11.9	12.0-13.9	14.0-15.9	16.0-17.9	18.0-LONGER	
0.0 - 0.49	78	5876	6505	758	13						13230
0.50 - 0.99		133	2926	812	51						3922
1.00 - 1.49			123	333	5						511
1.50 - 1.99				32							33
2.00 - 2.49				1							1
2.50 - 2.99											0
3.00 - 3.49											0
3.50 - 3.99											0
4.00 - 4.49											0
4.50 - 4.99											0
5.00 - GREATER											0
TOTAL	78	6009	9554	1926	69	0	0	0	0	0	0

AVERAGE HS(M) = 0.34 LARGEST HS(M) = 2.21 ANGLE CLASS % = 17.7

Table B3

Wave Statistics for the 20-Year Period (1956-1975)

NEW JERSEY, SECTION II, ASBURY PARK TO MANASQUAN
 ATLANTIC PHASE III WAVE INFORMATION
 STATION 55 20 YEARS FOR ALL DIRECTIONS
 WAVE APPROACH ANGLES RELATIVE TO TRUE NORTH
 WATER DEPTH = 18.60 METERS
 PERCENT OCCURRENCE(X100) OF HEIGHT AND PERIOD FOR ALL DIRECTIONS

HEIGHT(METERS)	PERIOD(SECONDS)										TOTAL
	0.0- 1.9	2.0- 3.9	4.0- 5.9	6.0- 7.9	8.0- 9.9	10.0- 11.9	12.0- 13.9	14.0- 15.9	16.0- 17.9	18.0- LONGER	
0.0 - 0.49	39	1336	800	1951	841	185	26	.	.	.	5178
0.50 - 0.99	.	243	961	620	462	178	13	.	.	.	2477
1.00 - 1.49	.	.	318	228	130	31	5	.	.	.	712
1.50 - 1.99	.	.	27	169	56	12	1	.	.	.	265
2.00 - 2.49	.	.	.	99	29	6	1	.	.	.	135
2.50 - 2.99	.	.	.	39	3	61
3.00 - 3.49	.	.	.	9	12	21
3.50 - 3.99	3	3
4.00 - 4.49	1	1
4.50 - 4.99	0
5.00 - GREATER	0
TOTAL	39	1579	2106	3115	1553	415	46	0	0	0	
AVE HS(M) = 0.50		LARGEST HS(M) = 6.86		TOTAL CASES =		58440					

NEW JERSEY, SECTION II, ASBURY PARK TO MANASQUAN
 ATLANTIC PHASE III WAVE INFORMATION
 STATION 57 20 YEARS FOR ALL DIRECTIONS
 WAVE APPROACH ANGLES RELATIVE TO TRUE NORTH
 WATER DEPTH = 18.60 METERS
 PERCENT OCCURRENCE(X100) OF HEIGHT AND PERIOD FOR ALL DIRECTIONS

HEIGHT(METERS)	PERIOD(SECONDS)										TOTAL
	0.0- 1.9	2.0- 3.9	4.0- 5.9	6.0- 7.9	8.0- 9.9	10.0- 11.9	12.0- 13.9	14.0- 15.9	16.0- 17.9	18.0- LONGER	
0.0 - 0.49	29	1267	907	1587	812	191	25	.	.	.	4818
0.50 - 0.99	.	238	934	580	551	121	17	.	.	.	2441
1.00 - 1.49	.	.	303	252	128	21	1	.	.	.	705
1.50 - 1.99	.	.	27	192	60	12	291
2.00 - 2.49	.	.	.	117	34	5	156
2.50 - 2.99	.	.	.	41	27	3	71
3.00 - 3.49	.	.	.	5	22	1	28
3.50 - 3.99	4	1	5
4.00 - 4.49	0
4.50 - 4.99	0
5.00 - GREATER	1	.	.	.	1
TOTAL	29	1505	2171	2774	1638	355	44	0	0	0	
AVE HS(M) = 0.50		LARGEST HS(M) = 6.66		TOTAL CASES =		58440					

Table B4

Comparison of Annual Average Wave Height and Wave Events
Categorized by Year and Approach Angle for Station 55 (Asbury Park)

Year	Angle Band									Calm
	1	2	3	4	5	6	7	8	9	
1956										
Events	0	0	0	475	781	404	137	1510	1277	1272
Heights	0.	0.	0.	.48	.95	.66	.73	.48	.39	
1957										
Events	0	0	0	429	560	618	404	1194	1187	1448
Heights	0.	0.	0.	.47	.77	.52	.55	.57	.38	
1958										
Events	0	0	0	375	470	883	352	680	1085	2067
Heights	0.	0.	0.	.41	1.07	.64	.42	.60	.35	
1959										
Events	0	0	0	384	448	445	325	876	1344	2012
Heights	0.	0.	0.	.35	.65	.68	.66	.64	.28	
1960										
Events	0	0	0	379	721	365	359	748	1215	2069
Heights	0.	0.	0.	.39	.75	.90	.53	.69	.32	
1961										
Events	0	0	0	342	788	223	267	1457	1206	1557
Heights	0.	0.	0.	.51	.77	1.05	.67	.53	.39	
1962										
Events	0	0	0	560	714	237	392	828	1100	2009
Heights	0.	0.	0.	.38	.94	.80	.81	.59	.33	
1963										
Events	0	0	0	439	389	483	458	849	1202	2020
Heights	0.	0.	0.	.34	.90	.82	.52	.57	.35	
1964										
Events	0	0	0	358	600	315	439	1243	1226	1675
Heights	0.	0.	0.	.51	.88	.74	.52	.60	.38	
1965										
Events	0	0	0	347	501	412	212	1377	1261	1703
Heights	0.	0.	0.	.40	.68	.69	.49	.48	.40	
1966										
Events	0	0	0	563	413	387	464	1158	1156	1699
Heights	0.	0.	0.	.26	.84	.81	.50	.50	.38	
1967										
Events	0	0	0	492	631	375	323	1276	1159	1584
Heights	0.	0.	0.	.52	.85	.59	.81	.59	.39	
1968										
Events	0	0	0	450	366	765	295	1192	1041	1747
Heights	0.	0.	0.	.34	.84	.56	.53	.52	.34	
1969										
Events	0	0	0	855	917	197	332	1090	1000	1719
Heights	0.	0.	0.	.43	.80	.96	.62	.61	.34	
1970										
Events	0	0	0	437	607	404	506	1013	1007	1866
Heights	0.	0.	0.	.35	.79	1.08	.45	.51	.38	
1971										
Events	0	0	0	419	507	339	567	1273	1009	1726
Heights	0.	0.	0.	.42	.95	.87	.50	.57	.43	
1972										
Events	0	0	0	490	550	451	331	952	1085	1897
Heights	0.	0.	0.	.36	1.02	.74	.62	.67	.41	
1973										
Events	0	0	0	417	570	153	700	1038	1147	1815
Heights	0.	0.	0.	.50	.80	1.17	.57	.70	.37	
1974										
Events	0	0	0	529	461	257	351	1323	1013	1906
Heights	0.	0.	0.	.34	.75	.72	.62	.61	.39	
1975										
Events	0	0	0	615	414	312	452	1307	891	1849
Heights	0.	0.	0.	.29	.82	.68	.61	.53	.40	

Table B5
Comparison of Annual Average Wave Height and Wave Events
Categorized by Year and Approach Angle for Station 56 (Bay Head)

Year	Angle Band									Calm
	1	2	3	4	5	6	7	8	9	
1956										
Events	0	0	0	679	780	140	138	1435	1100	1584
Heights	0.	0.	0.	.61	1.06	.85	.72	.48	.39	
1957										
Events	0	0	0	570	474	497	519	1062	980	1738
Hdights	0.	0.	0.	.54	.87	.61	.53	.56	.38	
1958										
Events	0	0	0	520	470	932	235	498	936	2249
Heights	0.	0.	0.	.59	1.15	.47	.66	.66	.37	
1959										
Events	0	0	0	556	537	193	275	872	1120	2287
Heights	0.	0.	0.	.45	.65	.70	.83	.64	.27	
1960										
Events	0	0	0	513	746	326	299	705	985	2282
Heights	0.	0.	0.	.66	.84	.72	.62	.67	.30	
1961										
Events	0	0	0	442	665	198	252	1383	1020	1880
Heights	0.	0.	0.	.69	.88	.95	.85	.53	.35	
1962										
Events	0	0	0	816	499	213	396	809	868	2239
Heights	0.	0.	0.	.57	1.12	.89	.86	.57	.33	
1963										
Events	0	0	0	579	370	464	455	627	964	2381
Heights	0.	0.	0.	.46	1.00	.43	.66	.59	.32	
1964										
Events	0	0	0	526	782	316	171	979	1034	2048
Heights	0.	0.	0.	.64	.82	.63	.85	.64	.35	
1965										
Events	0	0	0	560	509	153	171	1410	1027	2039
Heights	0.	0.	0.	.50	.65	.86	.81	.46	.37	
1966										
Events	0	0	0	750	334	408	332	1190	972	1854
Heights	0.	0.	0.	.37	.94	.60	.58	.47	.35	
1967										
Events	0	0	0	642	478	206	502	1123	943	1946
Heights	0.	0.	0.	.58	.86	.62	.68	.58	.34	
1968										
Events	0	0	0	645	312	1301	206	657	891	1844
Heights	0.	0.	0.	.44	1.06	.50	.62	.60	.32	
1969										
Events	0	0	0	753	825	135	360	932	838	1997
Heights	0.	0.	0.	.61	.82	.79	.85	.55	.31	
1970										
Events	0	0	0	560	766	270	467	948	799	2030
Heights	0.	0.	0.	.57	.76	1.02	.58	.50	.35	
1971										
Events	0	0	0	554	533	304	598	1133	764	1954
Heights	0.	0.	0.	.55	1.01	.75	.56	.57	.43	
1972										
Events	0	0	0	776	429	378	241	865	8387	2329
Heights	0.	0.	0.	.44	1.14	.58	.88	.67	.37	
1973										
Events	0	0	0	567	425	134	768	764	1016	2166
Heights	0.	0.	0.	.62	.87	1.14	.56	.75	.33	
1974										
Events	0	0	0	683	439	242	332	1175	872	2097
Heights	0.	0.	0.	.43	.81	.60	.64	.61	.37	
1975										
Events	0	0	0	723	734	278	376	1061	761	1907
Heights	0.	0.	0.	.52	.68	.73	.53	.57	.39	

A scoring system was established in which if the statistic of interest (i.e., the average wave height or number of events in angle band 5 for 1963) was within plus or minus one and a half standard deviations of the mean for entire hindcast (i.e., the average wave height or number of events in angle band 5 for all 20-years) then one point was given to the year otherwise a score of zero was entered. Table B6 gives the scores for the average wave height analysis. Similarly, Table B7 gives the scores for the number of events analysis. The 7 years with a total score (sum of the scores given in Tables B6 and B7) of 13 or greater were selected for further investigation.

4. In the second phase of the selection process consideration was given to storm events. The 250 largest wave heights ranked in descending order, together with the corresponding date, expected return period, wave period, and wave direction measured counter-clockwise from the trend in the shoreline orientation, are tabulated in Tables B8 and B9. Individual storm events in the listings are signified in the tables by a series of asterisks followed by the rank of the storm. As can be seen in Table B8, 74 individual storm events are represented in the 250 largest wave heights at Asbury Park (Station 55). Seventy storms were identified in the 250 largest wave heights at Bay Head (Station 56), see Table B9. Table B10 provides a summary of the storm events at each of the stations and a listing of 60 storms which occurred at both stations together with the average wave height. Table B11 categorizes these 60 storm events which represent the 60 most severe storms in the 20-year hindcast record with the year in which they occurred. A simple average would predict that an "typical year" would contain 2 of the 60 most severe storms. However, the actual number of storms for a given year in the hindcast record ranges from zero to in 1963 to six in 1962 again proving the profound variability in coastal processes. The years of interest (those with a total score of 13 or greater from the previous analysis) are denoted with an asterisk in Table B11. The years 1957, 1967, and 1969 were discounted because of there lack of a significant number of storm events and the relatively low rank of those storms which did occur. In the final analysis two relatively stormy years (1972 and 1974) and one typical year (1970) were selected for use as input to the shoreline change model, and were assumed to be representative of the long-term wave climate within the project area.

Table B6
Annual Average Wave Height Analysis

Year	Angle Band						All Directions	Score
	4	5	6	7	8	9		
1956	1	1	1	1	1	1	0	6
1957	1	1	1	1	1	1	2	8
1958	1	0	0	1	1	1	2	6
1959	1	0	0	1	1	0	0	3
1960	0	1	1	1	0	0	2	5
1961	0	1	0	0	1	1	2	5
1962	1	0	1	0	1	1	2	6
1963	1	1	1	1	1	1	0	6
1964	0	1	1	0	1	1	2	6
1965	1	1	1	1	0	1	0	5
1966	0	1	1	1	0	1	0	4
1967	1	1	1	1	1	1	2	8
1968	1	1	1	1	1	1	0	6
1969	1	1	1	0	1	1	2	7
1970	1	1	0	1	1	1	2	7
1971	1	1	1	1	1	0	2	7
1972	1	0	1	0	1	1	2	6
1973	1	1	0	1	0	1	2	6
1974	1	1	1	1	1	1	2	8
1975	0	1	1	1	1	0	2	6

Table B7
Annual Average Events Analysis

Year	Calm	Angle Band						Score	Total Score
		4	5	6	7	8	9		
1956	0	1	0	1	0	0	0	2	8
1957	0	1	1	1	1	1	1	6	14
1958	1	1	1	0	1	0	1	5	11
1959	0	1	1	1	1	1	0	5	8
1960	0	1	0	1	1	0	1	4	9
1961	1	0	0	1	1	0	1	4	9
1962	1	0	1	1	1	1	1	6	12
1963	0	1	0	1	1	0	1	4	10
1964	1	1	1	1	1	1	1	7	13
1965	1	1	1	1	0	0	1	5	10
1966	1	1	0	1	1	1	1	6	10
1967	1	1	1	1	1	1	1	7	15
1968	1	1	0	0	1	1	1	5	11
1969	1	1	0	1	1	1	1	6	13
1970	1	1	1	1	1	1	1	7	14
1971	1	1	1	1	0	1	0	5	12
1972	1	1	1	1	1	1	1	7	13
1973	1	1	1	1	0	1	1	6	12
1974	1	1	1	1	1	1	1	7	15
1975	1	0	1	1	1	1	0	5	11

Table B8

Largest 250 Wave Heights in 20-Year Hindcast, Station 55 (Asbury Park)

RANK	COUNT	DATE	HEIGHT	RETURN	PERIOD	DIRECTION
*****	1	1	1	1	1	1
1	1	62030618	6.86	21.00	10.00	102.02
2	2	62030703	6.11	10.50	13.00	97.95
3	3	62030700	6.04	7.00	13.00	99.76
4	4	62030615	6.02	5.25	10.00	102.36
5	5	62030706	5.73	4.20	13.00	97.95
6	6	62030621	5.53	3.50	10.00	105.96
7	7	62030709	5.43	3.00	13.00	97.95
8	8	62030712	5.17	2.63	13.00	97.95
9	9	62030715	4.99	2.33	13.00	97.95
10	10	62030718	4.62	2.10	13.00	97.95
*****	2	2	2	2	2	2
11	11	72021918	4.61	1.91	9.00	93.03
12	12	62030609	4.31	1.75	9.00	105.91
*****	3	3	3	3	3	3
13	13	73120921	4.31	1.62	9.00	62.72
14	14	62030803	4.28	1.50	13.00	99.76
15	15	62030721	4.24	1.43	13.00	97.95
16	16	62030806	4.21	1.31	13.00	99.76
*****	4	4	4	4	4	4
17	17	74120203	4.20	1.24	9.00	96.03
18	18	74120206	4.15	1.17	9.00	96.58
19	19	62030800	4.14	1.11	13.00	98.55
20	20	74120209	4.12	1.05	9.00	91.76
21	21	73120918	4.09	1.00	8.00	80.85
22	22	74120200	4.03	0.95	9.00	95.48
23	23	73121000	3.98	0.91	9.00	46.48
24	24	74120212	3.97	0.88	9.00	79.35
25	25	62030809	3.87	0.84	13.00	100.36
*****	5	5	5	5	5	5
26	26	75031921	3.85	0.81	9.00	57.42
27	27	62030612	3.84	0.78	9.00	106.30
28	28	74120121	3.76	0.75	8.00	97.02
*****	6	6	6	6	6	6
29	29	66012321	3.76	0.72	9.00	73.46
30	30	75032000	3.72	0.70	9.00	56.16
31	31	75031918	3.68	0.68	9.00	60.64
*****	7	7	7	7	7	7
32	32	69122621	3.68	0.66	8.00	72.85
*****	8	8	8	8	8	8
33	33	64011321	3.67	0.64	9.00	106.30
*****	9	9	9	9	9	9
34	34	75121000	3.66	0.62	8.00	76.85
*****	10	10	10	10	10	10
35	35	60121203	3.66	0.60	7.00	88.31
*****	11	11	11	11	11	11
36	36	73102918	3.65	0.58	8.00	89.12
*****	12	12	12	12	12	12
37	37	74033103	3.63	0.57	8.00	97.02
38	38	74120215	3.63	0.55	8.00	61.11
39	39	73120915	3.60	0.54	8.00	95.84
40	40	73102921	3.60	0.52	8.00	85.40
*****	13	13	13	13	13	13
41	41	62110400	3.60	0.51	8.00	84.64
*****	14	14	14	14	14	14
42	42	70121718	3.59	0.50	9.00	59.95
*****	15	15	15	15	15	15
43	43	69110312	3.54	0.49	8.00	63.37
44	44	62030812	3.54	0.48	13.00	100.96
45	45	70121715	3.53	0.47	9.00	89.85
*****	16	16	16	16	16	16
46	46	73020221	3.53	0.46	8.00	49.22
*****	17	17	17	17	17	17
47	47	60073015	3.52	0.45	7.00	62.45
*****	18	18	18	18	18	18
48	48	73122109	3.52	0.44	9.00	46.48
49	49	73122106	3.50	0.43	9.00	48.54
50	50	66012318	3.50	0.42	8.00	68.86

(Continued)

(Sheet 1 of 5)

Table B8 (Continued)

RANK	COUNT	DATE	HEIGHT	RETURN	PERIOD	DIRECTION
51	51	75032003	3.49	0.41	9.00	55.52
52	52	64011318	3.47	0.40	8.00	105.63
*****	19	19		19	19	
53	53	72020403	3.46	0.40	8.00	55.96
54	54	74033106	3.45	0.39	8.00	71.25
55	55	75032006	3.44	0.38	10.00	68.49
56	56	62110321	3.44	0.38	7.00	101.61
*****	20	20		20	20	
57	57	61020412	3.43	0.37	8.00	103.64
58	58	66012312	3.43	0.36	7.00	94.75
59	59	75121003	3.42	0.36	8.00	72.85
60	60	73122103	3.41	0.35	9.00	53.06
*****	21	21		21	21	
61	61	60021909	3.41	0.34	8.00	82.37
*****	22	22		22	22	
62	62	62122203	3.41	0.34	7.00	79.45
63	63	73122100	3.40	0.33	8.00	54.58
*****	23	23		23	23	
64	64	64020621	3.39	0.33	7.00	70.09
65	65	70121703	3.39	0.32	7.00	78.60
*****	24	24		24	24	
66	66	74121703	3.38	0.32	8.00	58.84
67	67	75120921	3.37	0.31	8.00	80.05
68	68	61020409	3.37	0.31	8.00	98.20
*****	25	25		25	25	
69	69	59030615	3.37	0.30	6.00	49.80
*****	26	26		26	26	
70	70	58110309	3.36	0.30	8.00	81.61
71	71	74120118	3.35	0.30	7.00	98.54
72	72	73122115	3.35	0.29	9.00	40.82
73	73	69122221	3.35	0.29	8.00	86.16
*****	27	27		27	27	
74	74	65012421	3.34	0.28	8.00	77.65
75	75	62110403	3.34	0.28	8.00	58.09
76	76	73103000	3.33	0.28	8.00	81.61
*****	28	28		28	28	
77	77	56011021	3.33	0.27	11.00	101.19
*****	29	29		29	29	
78	78	64012021	3.33	0.27	7.00	63.26
79	79	70121712	3.33	0.27	8.00	84.64
80	80	72022000	3.33	0.26	6.00	25.61
81	81	72021912	3.32	0.26	8.00	99.38
*****	30	30		30	30	
82	82	71021321	3.32	0.26	6.00	60.78
83	83	73122112	3.32	0.25	10.00	51.17
*****	31	31		31	31	
84	84	58102218	3.32	0.25	8.00	92.53
*****	32	32		32	32	
85	85	60022609	3.32	0.25	8.00	59.60
86	86	58102221	3.31	0.24	8.00	89.80
*****	33	33		33	33	
87	87	62031218	3.30	0.24	9.00	65.48
88	88	62031221	3.30	0.24	9.00	64.79
89	89	73102915	3.30	0.24	8.00	91.84
90	90	75120918	3.30	0.23	8.00	84.64
91	91	69122618	3.30	0.23	8.00	76.85
*****	34	34		34	34	
92	92	72031509	3.29	0.23	8.00	90.48
93	93	65012418	3.29	0.23	8.00	83.88
94	94	72021915	3.28	0.22	8.00	109.04
*****	35	35		35	35	
95	95	71030412	3.28	0.22	8.00	38.47
*****	36	36		36	36	
96	96	68110715	3.28	0.22	7.00	94.75
*****	37	37		37	37	
97	97	68031809	3.28	0.22	7.00	105.23
98	98	75031915	3.28	0.21	8.00	61.86
99	99	60022606	3.28	0.21	7.00	67.53
100	100	61020406	3.28	0.21	7.00	94.75

(Continued)

(Sheet 2 of 5)

Table B8 (Continued)

RANK	COUNT	DATE	HEIGHT	RETURN	PERIOD	DIRECTION
*****	38	38	38	38	38	38
101	101	57100621	3.27	0.21	7.00	93.32
102	102	73020218	3.27	0.21	8.00	57.33
103	103	62030815	3.26	0.20	13.00	102.74
104	104	74033100	3.26	0.20	8.00	106.96
*****	39	39	39	39	39	39
105	105	65022512	3.25	0.20	6.00	78.86
*****	40	40	40	40	40	40
106	106	64021615	3.24	0.20	6.00	91.93
107	107	62031215	3.24	0.20	7.00	62.45
108	108	62031300	3.23	0.19	9.00	63.41
109	109	75120915	3.21	0.19	8.00	88.43
*****	41	41	41	41	41	41
110	110	67121121	3.21	0.19	8.00	84.64
*****	42	42	42	42	42	42
111	111	72112612	3.20	0.19	6.00	51.38
112	112	72031512	3.20	0.19	8.00	83.12
*****	43	43	43	43	43	43
113	113	72110821	3.19	0.19	7.00	58.40
114	114	64011312	3.19	0.18	7.00	107.64
115	115	73020300	3.18	0.18	9.00	44.98
*****	44	44	44	44	44	44
116	116	69012121	3.17	0.18	8.00	101.15
117	117	58102215	3.17	0.18	8.00	95.26
118	118	56011100	3.16	0.18	11.00	101.19
119	119	67121118	3.16	0.18	8.00	87.67
*****	45	45	45	45	45	45
120	120	67122818	3.15	0.18	6.00	94.92
121	121	68110800	3.15	0.17	8.00	87.67
122	122	73102912	3.14	0.17	7.00	93.32
123	123	73103003	3.13	0.17	8.00	75.25
124	124	74033018	3.13	0.17	8.00	109.04
125	125	74120218	3.13	0.17	7.00	42.50
126	126	62031309	3.13	0.17	9.00	53.57
127	127	71030409	3.13	0.17	7.00	74.35
128	128	67121115	3.12	0.16	7.00	88.31
*****	46	46	46	46	46	46
129	129	70040215	3.11	0.16	6.00	49.01
*****	47	47	47	47	47	47
130	130	71112518	3.11	0.16	8.00	83.88
131	131	72021903	3.10	0.16	6.00	96.95
132	132	72020400	3.10	0.16	7.00	91.17
*****	48	48	48	48	48	48
133	133	67120321	3.10	0.16	7.00	91.17
134	134	62030606	3.10	0.16	8.00	106.96
135	135	58102212	3.10	0.16	8.00	97.02
136	136	75120912	3.10	0.15	8.00	91.84
137	137	74033109	3.09	0.15	7.00	41.18
138	138	74033015	3.09	0.15	8.00	107.38
139	139	73122021	3.09	0.15	7.00	56.77
140	140	65012500	3.09	0.15	8.00	61.11
*****	49	49	49	49	49	49
141	141	64112603	3.08	0.15	7.00	60.83
142	142	66012315	3.08	0.15	7.00	87.51
*****	50	50	50	50	50	50
143	143	64010115	3.08	0.15	6.00	86.50
144	144	72110900	3.08	0.15	8.00	41.09
145	145	74033021	3.08	0.14	8.00	109.04
146	146	74121700	3.07	0.14	8.00	78.45
147	147	57100700	3.07	0.14	7.00	89.74
148	148	57100618	3.07	0.14	7.00	100.38
149	149	71112515	3.07	0.14	8.00	88.43
*****	51	51	51	51	51	51
150	150	68031306	3.07	0.14	7.00	47.09

(Continued)

(Sheet 3 of 5)

Table B8 (Continued)

RANK	COUNT	DATE	HEIGHT	RETURN	PERIOD	DIRECTION
151	151	67121203	3.07	0.14	7.00	73.50
152	152	65012415	3.06	0.14	8.00	86.92
*****	52	52	52	52	52	52
153	153	68011412	3.06	0.14	6.00	94.17
154	154	69012118	3.06	0.14	7.00	101.00
155	155	58110306	3.06	0.14	7.00	88.31
156	156	58102209	3.06	0.13	8.00	98.79
*****	53	53	53	53	53	53
157	157	59031221	3.06	0.13	7.00	78.60
158	158	60021906	3.06	0.13	8.00	78.45
159	159	60021903	3.06	0.13	7.00	88.31
160	160	60021415	3.06	0.13	8.00	51.83
161	161	73103006	3.06	0.13	8.00	64.12
*****	54	54	54	54	54	54
162	162	58011500	3.05	0.13	7.00	102.13
163	163	68110803	3.05	0.13	8.00	91.16
164	164	73020215	3.05	0.13	7.00	61.64
165	165	65022518	3.05	0.13	7.00	73.50
*****	55	55	55	55	55	55
166	166	69032515	3.04	0.13	7.00	51.45
167	167	58102206	3.04	0.13	8.00	99.38
168	168	73120912	3.04	0.13	7.00	103.16
169	169	74121621	3.03	0.12	7.00	83.51
170	170	75032009	3.03	0.12	10.00	68.49
*****	56	56	56	56	56	56
171	171	60020106	3.03	0.12	7.00	104.20
*****	57	57	57	57	57	57
172	172	62111012	3.03	0.12	7.00	68.38
173	173	72031506	3.03	0.12	8.00	92.53
174	174	69122615	3.02	0.12	7.00	90.46
*****	58	58	58	58	58	58
175	175	70110506	3.02	0.12	7.00	79.45
176	176	67121200	3.02	0.12	8.00	81.61
177	177	64010200	3.01	0.12	8.00	44.31
178	178	62122212	3.01	0.12	8.00	59.60
179	179	62122209	3.01	0.12	7.00	71.80
*****	59	59	59	59	59	59
180	180	59102421	3.01	0.12	8.00	51.14
181	181	57100703	3.01	0.12	8.00	103.03
*****	60	60	60	60	60	60
182	182	56092715	3.01	0.12	8.00	110.75
*****	61	61	61	61	61	61
183	183	72021321	3.00	0.11	7.00	66.68
184	184	70110509	2.99	0.11	8.00	74.45
*****	62	62	62	62	62	62
185	185	68052918	2.99	0.11	7.00	84.31
186	186	68052915	2.99	0.11	8.00	91.84
187	187	69110306	2.99	0.11	8.00	98.20
188	188	58102121	2.99	0.11	7.00	98.54
189	189	59102418	2.99	0.11	8.00	56.65
190	190	58102300	2.98	0.11	8.00	88.43
*****	63	63	63	63	63	63
191	191	62040115	2.98	0.11	8.00	38.94
192	192	62040109	2.98	0.11	8.00	45.54
*****	64	64	64	64	64	64
193	193	61112421	2.98	0.11	7.00	76.90
194	194	75121006	2.98	0.11	10.00	91.51
195	195	73121409	2.98	0.11	7.00	55.96
196	196	69110221	2.98	0.11	7.00	91.89
197	197	69110209	2.98	0.11	6.00	81.44
198	198	70121709	2.98	0.11	7.00	84.31
*****	65	65	65	65	65	65
199	199	63050103	2.98	0.11	8.00	43.24
200	200	64010121	2.97	0.11	7.00	70.09

(Continued)

(Sheet 4 of 5)

Table B8 (Concluded)

RANK	COUNT	DATE	HEIGHT	RETURN	PERIOD	DIRECTION
201	201	69032518	2.97	0.10	8.00	49.84
202	202	71112512	2.97	0.10	7.00	89.74
*****	66	66	66	66	66	66
203	203	74012112	2.97	0.10	6.00	62.56
204	204	75120909	2.97	0.10	8.00	94.57
205	205	56092718	2.97	0.10	7.00	108.51
206	206	62031312	2.97	0.10	10.00	55.19
207	207	58102203	2.97	0.10	8.00	99.38
*****	67	67	67	67	67	67
208	208	61041315	2.96	0.10	8.00	94.57
209	209	61041318	2.96	0.10	8.00	83.88
210	210	72021400	2.96	0.10	8.00	49.22
211	211	65022521	2.96	0.10	8.00	64.12
212	212	67121206	2.96	0.10	7.00	62.45
213	213	67120315	2.96	0.10	6.00	49.01
214	214	65012412	2.95	0.10	7.00	89.02
215	215	68031815	2.95	0.10	7.00	103.16
216	216	57100615	2.95	0.10	7.00	104.72
217	217	56011103	2.95	0.10	11.00	100.49
*****	68	68	68	68	68	68
218	218	75112715	2.95	0.10	7.00	38.90
219	219	75120906	2.94	0.10	7.00	96.08
220	220	68052912	2.94	0.10	8.00	95.84
221	221	71021400	2.94	0.10	7.00	42.50
*****	69	69	69	69	69	69
222	222	72100712	2.94	0.09	8.00	99.97
*****	70	70	70	70	70	70
223	223	71040706	2.93	0.09	8.00	107.79
224	224	69032521	2.93	0.09	8.00	47.38
225	225	64021915	2.93	0.09	8.00	80.85
*****	71	71	71	71	71	71
226	226	56041621	2.93	0.09	7.00	38.90
227	227	59030618	2.93	0.09	7.00	42.50
228	228	60021900	2.93	0.09	8.00	93.21
229	229	61041312	2.93	0.09	7.00	97.92
*****	72	72	72	72	72	72
230	230	58032018	2.92	0.09	8.00	109.90
231	231	73103009	2.92	0.09	8.00	53.20
*****	73	73	73	73	73	73
232	232	74030403	2.92	0.09	6.00	36.24
233	233	69012200	2.92	0.09	8.00	106.55
234	234	69110303	2.92	0.09	8.00	98.20
235	235	69110300	2.91	0.09	8.00	95.84
236	236	73020303	2.91	0.09	9.00	40.82
237	237	64011315	2.91	0.09	7.00	109.37
238	238	62122215	2.91	0.09	8.00	49.84
239	239	74033009	2.91	0.09	7.00	99.77
240	240	73122018	2.91	0.09	8.00	62.61
241	241	62040112	2.91	0.09	8.00	40.55
242	242	62111003	2.91	0.09	7.00	85.11
243	243	73121412	2.90	0.09	8.00	47.38
*****	74	74	74	74	74	74
244	244	63110721	2.90	0.09	7.00	91.89
245	245	71033012	2.89	0.09	8.00	105.63
246	246	58102303	2.89	0.09	8.00	98.71
247	247	58102200	2.89	0.09	8.00	98.79
248	248	72110818	2.88	0.08	7.00	65.82
249	249	72021909	2.88	0.08	7.00	103.68
250	250	65022515	2.87	0.08	7.00	79.45

Table B9

Largest 250 Wave Heights in 20-Year Hindcast, Station 56 (Bay Head)

RANK	COUNT	DATE	HEIGHT	RETURN	PERIOD	DIRECTION
*****	1	1	1	1	1	1
1	1	62030618	6.66	21.00	11.00	107.30
2	2	62030703	5.82	10.50	13.00	102.17
3	3	62030712	5.59	7.00	13.00	102.17
4	4	62030706	5.59	5.25	13.00	101.56
5	5	62030709	5.52	4.20	13.00	102.17
6	6	62030621	5.51	3.50	10.00	107.44
7	7	62030715	5.42	3.00	13.00	102.17
8	8	62030718	5.03	2.63	13.00	102.17
9	9	62030800	4.79	2.33	13.00	105.06
10	10	62030803	4.78	2.10	13.00	103.90
11	11	62030700	4.76	1.91	9.00	110.70
12	12	62030721	4.62	1.75	13.00	103.32
13	13	62030806	4.59	1.62	13.00	103.90
*****	2	2	2	2	2	2
14	14	74120203	4.52	1.50	9.00	96.03
15	15	62030809	4.45	1.40	13.00	106.21
*****	3	3	3	3	3	3
16	16	73120921	4.37	1.31	10.00	64.45
17	17	74120200	4.35	1.24	9.00	95.48
*****	4	4	4	4	4	4
18	18	64011321	4.35	1.17	10.00	97.17
19	19	74120206	4.32	1.11	10.00	95.63
20	20	73120918	4.32	1.05	10.00	82.28
*****	5	5	5	5	5	5
21	21	72021915	4.25	1.00	9.00	72.73
22	22	74120209	4.19	0.95	10.00	91.08
23	23	73120915	4.12	0.91	9.00	94.93
24	24	74120121	4.11	0.88	8.00	95.26
25	25	64011318	4.11	0.84	9.00	99.89
*****	6	6	6	6	6	6
26	26	74033103	3.92	0.81	10.00	94.02
27	27	62030812	3.90	0.78	13.00	106.79
28	28	74120212	3.89	0.75	10.00	77.56
*****	7	7	7	7	7	7
29	29	75031921	3.86	0.72	9.00	55.52
30	30	75031918	3.85	0.70	9.00	59.95
*****	8	8	8	8	8	8
31	31	61020409	3.85	0.68	8.00	93.21
*****	9	9	9	9	9	9
32	32	72020403	3.84	0.66	8.00	57.33
33	33	61020412	3.80	0.64	9.00	98.24
34	34	61020415	3.76	0.62	9.00	106.30
*****	10	10	10	10	10	10
35	35	71040706	3.76	0.60	9.00	62.72
36	36	72021912	3.71	0.58	8.00	95.84
*****	11	11	11	11	11	11
37	37	56092812	3.70	0.57	10.00	106.45
38	38	75032000	3.67	0.55	9.00	54.26
39	39	75031915	3.65	0.54	8.00	60.35
40	40	73120912	3.65	0.52	9.00	101.38
41	41	62030615	3.65	0.51	10.00	104.48
*****	12	12	12	12	12	12
42	42	73102918	3.63	0.50	9.00	89.22
43	43	73102921	3.62	0.49	9.00	85.07
*****	13	13	13	13	13	13
44	44	75120915	3.62	0.48	9.00	92.39
45	45	75121000	3.61	0.47	9.00	81.56
46	46	75120918	3.60	0.46	9.00	89.85
47	47	75120921	3.60	0.45	9.00	86.48
48	48	75120912	3.59	0.44	9.00	94.93
*****	14	14	14	14	14	14
49	49	73122109	3.59	0.43	9.00	45.48
50	50	75121003	3.57	0.42	9.00	77.14

(Continued)

(Sheet 1 of 5)

Table B9 (Continued)

RANK	COUNT	DATE	HEIGHT	RETURN	PERIOD	DIRECTION
51	51	73121000	3.56	0.41	10.00	47.05
52	52	74033100	3.56	0.40	10.00	101.49
53	53	74033021	3.56	0.40	9.00	106.69
*****	15	15	15	15	15	15
54	54	68110721	3.54	0.39	8.00	89.12
*****	16	16	16	16	16	16
55	55	62110400	3.53	0.38	9.00	75.67
56	56	74033106	3.53	0.38	8.00	63.37
57	57	56092718	3.52	0.37	9.00	104.19
*****	17	17	17	17	17	17
58	58	69122221	3.52	0.36	8.00	68.07
59	59	73102915	3.51	0.36	8.00	91.84
60	60	73122106	3.50	0.35	9.00	46.98
61	61	68110800	3.50	0.34	8.00	84.64
*****	18	18	18	18	18	18
62	62	65012418	3.49	0.34	8.00	83.88
63	63	62030815	3.49	0.33	13.00	107.37
64	64	74120215	3.48	0.33	8.00	46.16
*****	19	19	19	19	19	19
65	65	64020621	3.48	0.32	7.00	70.09
*****	20	20	20	20	20	20
66	66	70121712	3.48	0.32	8.00	70.46
67	67	75120909	3.47	0.31	9.00	97.14
68	68	73122103	3.47	0.31	9.00	51.37
*****	21	21	21	21	21	21
69	69	58102218	3.47	0.30	9.00	92.39
*****	22	22	22	22	22	22
70	70	57100621	3.47	0.30	8.00	91.84
71	71	73122115	3.46	0.30	9.00	41.25
*****	23	23	23	23	23	23
72	72	68031809	3.46	0.29	7.00	103.16
*****	24	24	24	24	24	24
73	73	72100715	3.45	0.29	8.00	61.86
*****	25	25	25	25	25	25
74	74	64010115	3.45	0.28	7.00	87.51
75	75	73122112	3.45	0.28	10.00	51.63
76	76	73122100	3.45	0.28	8.00	53.20
*****	26	26	26	26	26	26
77	77	60022609	3.44	0.27	8.00	57.33
78	78	72021918	3.43	0.27	10.00	47.51
79	79	72100712	3.42	0.27	8.00	89.80
80	80	62110321	3.42	0.26	9.00	93.66
81	81	75032003	3.42	0.26	9.00	53.06
82	82	74120118	3.41	0.26	8.00	97.02
83	83	56092715	3.41	0.25	9.00	106.30
84	84	57100700	3.41	0.25	8.00	85.40
*****	27	27	27	27	27	27
85	85	60021415	3.40	0.25	8.00	44.93
*****	28	28	28	28	28	28
86	86	56011118	3.40	0.24	9.00	106.15
*****	29	29	29	29	29	29
87	87	74121703	3.39	0.24	9.00	66.18
88	88	74033018	3.39	0.24	9.00	108.26
89	89	61020406	3.39	0.24	8.00	91.16
*****	30	30	30	30	30	30
90	90	60073015	3.38	0.23	7.00	54.41
*****	31	31	31	31	31	31
91	91	69012121	3.37	0.23	9.00	100.91
*****	32	32	32	32	32	32
92	92	69110309	3.36	0.23	9.00	71.26
93	93	64011315	3.36	0.23	9.00	104.65
*****	33	33	33	33	33	33
94	94	66012315	3.35	0.22	8.00	77.65
*****	34	34	34	34	34	34
95	95	71082809	3.35	0.22	8.00	44.31
96	96	69110303	3.34	0.22	8.00	96.43
*****	35	35	35	35	35	35
97	97	67121121	3.34	0.22	8.00	83.88
98	98	64010121	3.34	0.21	7.00	64.12
99	99	57100703	3.34	0.21	8.00	105.62
100	100	58102215	3.34	0.21	9.00	95.48

(Continued)

(Sheet 2 of 5)

Table B9 (Continued)

RANK	COUNT	DATE	HEIGHT	RETURN	PERIOD	DIRECTION
*****	36	36	36	36	36	36
101	101	73020218	3.34	0.21	8.00	55.96
102	102	73103003	3.33	0.21	8.00	74.45
*****	37	37	37	37	37	37
103	103	60030321	3.33	0.20	6.00	103.68
*****	38	38	38	38	38	38
104	104	59030615	3.33	0.20	6.00	47.42
*****	39	39	39	39	39	39
105	105	71021321	3.33	0.20	6.00	59.91
106	106	69110300	3.32	0.20	8.00	95.84
107	107	58102221	3.32	0.20	9.00	90.49
108	108	58102200	3.32	0.19	8.00	99.38
109	109	74121700	3.31	0.19	8.00	78.45
110	110	70121715	3.31	0.19	9.00	50.80
111	111	67121118	3.30	0.19	8.00	86.92
112	112	57100618	3.30	0.19	9.00	97.14
113	113	58102206	3.28	0.19	9.00	98.24
114	114	60022606	3.28	0.18	8.00	67.27
115	115	57100615	3.27	0.18	9.00	102.31
116	116	75120903	3.27	0.18	8.00	98.79
117	117	73103000	3.27	0.18	9.00	82.27
118	118	73120909	3.27	0.18	8.00	105.63
119	119	69012200	3.27	0.18	9.00	105.91
*****	40	40	40	40	40	40
120	120	71030409	3.27	0.18	8.00	64.88
121	121	73020221	3.26	0.17	9.00	51.37
122	122	75120906	3.26	0.17	9.00	97.69
123	123	58102203	3.26	0.17	9.00	97.69
124	124	58102300	3.26	0.17	8.00	88.43
125	125	58102209	3.25	0.17	9.00	98.24
126	126	56092721	3.25	0.17	9.00	103.72
127	127	74033015	3.25	0.17	9.00	106.30
128	128	65012421	3.25	0.16	9.00	81.56
*****	41	41	41	41	41	41
129	129	65022512	3.25	0.16	6.00	77.96
*****	42	42	42	42	42	42
130	130	62031221	3.24	0.16	9.00	56.79
131	131	58102212	3.23	0.16	9.00	97.14
132	132	66012318	3.23	0.16	9.00	53.06
*****	43	43	43	43	43	43
133	133	68052915	3.23	0.16	8.00	93.21
*****	44	44	44	44	44	44
134	134	72110815	3.23	0.16	7.00	58.40
135	135	72020400	3.22	0.16	8.00	91.16
136	136	67121115	3.22	0.15	7.00	89.02
*****	45	45	45	45	45	45
137	137	58032009	3.22	0.15	8.00	106.55
*****	46	46	46	46	46	46
138	138	61041312	3.22	0.15	7.00	94.75
139	139	74033012	3.22	0.15	8.00	105.63
140	140	56011021	3.22	0.15	8.00	112.73
141	141	56092815	3.21	0.15	10.00	106.45
142	142	60021906	3.21	0.15	8.00	62.61
*****	47	47	47	47	47	47
143	143	67120321	3.21	0.15	8.00	89.80
144	144	65012415	3.21	0.15	8.00	87.67
145	145	67121200	3.20	0.14	8.00	80.05
146	146	69012118	3.20	0.14	8.00	101.15
147	147	60021412	3.20	0.14	7.00	72.65
148	148	58102121	3.20	0.14	8.00	98.79
149	149	56011121	3.19	0.14	9.00	106.15
150	150	69012218	3.19	0.14	9.00	106.69

(Continued)

(Sheet 3 of 5)

Table B9 (Continued)

RANK	COUNT	DATE	HEIGHT	RETURN	PERIOD	DIRECTION
151	151	64011400	3.19	0.14	10.00	109.98
*****	48	48	48	48	48	48
152	152	72031506	3.18	0.14	8.00	75.25
*****	49	49	49	49	49	49
153	153	58012600	3.18	0.14	8.00	85.40
154	154	58012521	3.18	0.14	8.00	78.45
155	155	60021903	3.17	0.14	7.00	81.91
*****	50	50	50	50	50	50
156	156	60020106	3.16	0.13	8.00	107.38
157	157	62030606	3.16	0.13	8.00	106.55
158	158	75121006	3.16	0.13	10.00	99.79
159	159	68052912	3.16	0.13	8.00	96.43
160	160	69110221	3.16	0.13	8.00	91.16
161	161	64011312	3.16	0.13	8.00	106.96
*****	51	51	51	51	51	51
162	162	62111012	3.15	0.13	8.00	65.67
163	163	69012215	3.15	0.13	9.00	107.08
164	164	56092712	3.15	0.13	9.00	108.26
165	165	75031912	3.15	0.13	7.00	60.83
166	166	62031218	3.15	0.13	9.00	58.68
167	167	62030818	3.13	0.13	13.00	107.94
*****	52	52	52	52	52	52
168	168	56102621	3.13	0.13	8.00	101.15
169	169	56011203	3.13	0.12	11.00	99.80
170	170	69110306	3.13	0.12	9.00	91.12
*****	53	53	53	53	53	53
171	171	64021909	3.13	0.12	7.00	74.35
172	172	68110803	3.12	0.12	9.00	80.83
173	173	72100709	3.12	0.12	8.00	97.02
174	174	73020300	3.12	0.12	9.00	42.56
175	175	73122021	3.12	0.12	7.00	55.96
176	176	56102700	3.11	0.12	8.00	98.79
177	177	62031300	3.11	0.12	9.00	51.37
178	178	61041315	3.11	0.12	8.00	89.80
179	179	69122615	3.11	0.12	7.00	73.50
*****	54	54	54	54	54	54
180	180	62122212	3.11	0.12	8.00	61.11
181	181	65012500	3.11	0.12	8.00	58.84
182	182	72031509	3.10	0.12	8.00	49.84
*****	55	55	55	55	55	55
183	183	71112512	3.10	0.11	7.00	73.50
*****	56	56	56	56	56	56
184	184	62112715	3.09	0.11	9.00	107.48
185	185	62111015	3.09	0.11	8.00	56.65
186	186	64011309	3.09	0.11	8.00	108.21
187	187	62031215	3.09	0.11	8.00	63.37
188	188	58032012	3.09	0.11	9.00	106.69
*****	57	57	57	57	57	57
189	189	62040106	3.08	0.11	7.00	40.61
190	190	56092809	3.08	0.11	8.00	109.04
191	191	73102912	3.08	0.11	8.00	93.21
192	192	62112818	3.08	0.11	8.00	110.64
*****	58	58	58	58	58	58
193	193	64112603	3.08	0.11	7.00	57.58
194	194	68052921	3.08	0.11	8.00	100.44
195	195	71040700	3.07	0.11	8.00	107.38
196	196	56102618	3.07	0.11	8.00	103.14
197	197	56011200	3.07	0.11	9.00	105.35
198	198	60020109	3.07	0.11	9.00	106.30
199	199	69012212	3.06	0.11	9.00	108.26
200	200	69012221	3.05	0.11	9.00	106.30

(Continued)

(Sheet 4 of 5)

Table B9 (Concluded)

RANK	COUNT	DATE	HEIGHT	RETURN	PERIOD	DIRECTION
201	201	58102118	3.05	0.10	8.00	99.97
202	202	56102615	3.05	0.10	8.00	104.64
203	203	56092800	3.04	0.10	8.00	106.13
*****	59	59	59	59	59	59
204	204	56031618	3.04	0.10	6.00	94.17
205	205	74121621	3.04	0.10	8.00	83.88
206	206	73103006	3.04	0.10	9.00	68.33
207	207	69012203	3.04	0.10	9.00	108.66
208	208	70121709	3.04	0.10	7.00	78.60
*****	60	60	60	60	60	60
209	209	70040215	3.04	0.10	7.00	46.44
*****	61	61	61	61	61	61
210	210	70110503	3.03	0.10	6.00	64.38
211	211	73020215	3.03	0.10	7.00	62.45
*****	62	62	62	62	62	62
212	212	73042803	3.03	0.10	8.00	58.09
213	213	56102703	3.02	0.10	8.00	97.61
214	214	57100612	3.02	0.10	9.00	105.91
*****	63	63	63	63	63	63
215	215	61052712	3.02	0.10	8.00	97.02
216	216	65022521	3.02	0.10	8.00	61.11
217	217	65012412	3.02	0.10	7.00	89.74
218	218	62122209	3.02	0.10	8.00	73.65
219	219	64010200	3.02	0.10	8.00	37.54
*****	64	64	64	64	64	64
220	220	66092021	3.02	0.10	6.00	94.17
221	221	67121203	3.01	0.10	8.00	71.25
222	222	58012509	3.01	0.09	6.00	94.17
223	223	60021900	3.01	0.09	7.00	89.02
*****	65	65	65	65	65	65
224	224	59102418	3.01	0.09	8.00	56.65
225	225	75120900	3.01	0.09	8.00	98.20
*****	66	66	66	66	66	66
226	226	61030906	3.00	0.09	7.00	92.60
*****	67	67	67	67	67	67
227	227	68011421	3.00	0.09	7.00	85.91
228	228	69012209	3.00	0.09	9.00	109.05
229	229	64011306	3.00	0.09	7.00	109.80
230	230	62112821	3.00	0.09	8.00	111.34
231	231	62111009	3.00	0.09	7.00	76.90
232	232	62110318	3.00	0.09	8.00	105.63
233	233	62122206	2.99	0.09	7.00	80.30
234	234	68011503	2.99	0.09	8.00	75.25
235	235	69122218	2.99	0.09	7.00	55.15
236	236	71112515	2.99	0.09	8.00	51.14
237	237	58102303	2.99	0.09	7.00	85.11
238	238	74121709	2.99	0.09	9.00	68.36
239	239	73121409	2.99	0.09	7.00	49.97
240	240	74033009	2.99	0.09	8.00	101.65
241	241	73042800	2.98	0.09	8.00	68.86
242	242	74121618	2.98	0.09	7.00	86.71
*****	68	68	68	68	68	68
243	243	58110306	2.98	0.09	8.00	54.58
*****	69	69	69	69	69	69
244	244	60121206	2.98	0.09	7.00	96.69
245	245	62031309	2.98	0.09	9.00	48.97
*****	70	70	70	70	70	70
246	246	72111421	2.98	0.09	6.00	95.67
247	247	62112815	2.98	0.09	8.00	110.99
248	248	65022518	2.98	0.08	8.00	71.25
249	249	69122618	2.97	0.08	8.00	45.54
250	250	58032006	2.97	0.08	8.00	106.55

Table B10

Summary of Storm Events In 250 Largest Waves

Storm Rank	Asbury Park (Sta 55)		Bay Head (Sta 56)		Storms 55/56	Averaged	
	Date	Height (m)	Date	Height (m)		Date	Height (m)
1	62030618	6.86	62030618	6.66	1/1	620306	6.76
2	72021918	4.61	74120203	4.52	2/5	720119	4.43
3	73120921	4.31	73120921	4.37	4/2	741202	4.36
4	74120203	4.20	64011321	4.35	3/3	731209	4.34
5	75031921	3.85	72021915	4.25	8/4	640113	4.01
6	66012321	3.76	74033103	3.92	5/7	750319	3.86
7	69122621	3.68	75031921	3.86	12/6	740331	3.78
8	64011321	3.67	61020409	3.85	19/9	720204	3.65
9	75121000	3.66	72020403	3.84	9/13	751210	3.64
10	60121203	3.66	71040706	3.76	11/12	731029	3.64
11	73102918	3.65	56092812	3.70	20/8	610204	3.64
12	74033103	3.63	73102918	3.63	7/17	691224	3.60
13	61110400	3.60	75120915	3.62	18/14	731221	3.56
14	70121718	3.59	73122109	3.59	6/33	660123	3.56
15	69110312	3.54	68110721	3.54	13/16	621104	3.56
16	73020221	3.53	62110400	3.53	14/20	701217	3.54
17	60073015	3.52	69122221	3.52	15/32	691103	3.45
18	73122109	3.52	65012418	3.49	17/30	600730	3.45
19	72020403	3.46	64020621	3.48	16/36	730202	3.44
20	61020412	3.66	70121712	3.48	23/19	640206	3.44
21	60021909	3.41	58102218	3.47	27/18	650124	3.42
22	62122203	3.41	57100621	3.47	21/27	600217	3.42
23	64020621	3.39	68031809	3.46	36/15	681107	3.41
24	74121703	3.38	72100715	3.45	31/21	581022	3.40
25	59030615	3.37	64010115	3.45	24/29	741217	3.38
26	58110309	3.36	60022609	3.44	32/26	600226	3.38
27	65012421	3.34	60021415	3.40	37/23	680318	3.37
28	56011021	3.33	56011118	3.40	38/22	571006	3.37
29	64012021*	3.33	74121703	3.39	28/28	560110	3.36
30	71021321	3.32	60073015	3.38	60/11	560928	3.36
31	58102218	3.32	69012121	3.37	70/10	710407	3.35
32	60022609	3.32	69110309	3.36	25/38	590306	3.35
33	62031218	3.30	66012315	3.35	30/39	710213	3.32
34	72031509	3.29	71082809*	3.35	10/69	601212	3.32
35	71030412	3.28	67121121	3.34	35/40	710304	3.28
36	68110715	3.28	73020218	3.34	41/35	671211	3.28
37	68031809	3.28	60030321*	3.33	44/31	690121	3.27
38	57100621	3.27	59030615	3.33	33/42	620312	3.27
39	65022512	3.25	71021321	3.33	50/25	640101	3.26

(Continued)

(Sheet 1 of 2)

Table B10 (Concluded)

Storm Rank	Asbury Park (Sta 55)		Bay Head (Sta 56)		Storms 55/56	Averaged	
	Date	Height (m)	Date	Height (m)		Date	Height (m)
40	64021615	3.24	71030409	3.27	22/54	621222	3.26
41	67121121	3.21	65022512	3.25	39/41	650225	3.25
42	72112612*	3.20	62031221	3.24	34/48	720315	3.24
43	72110821	3.19	68052915	3.23	43/44	721108	3.21
44	69012121	3.17	72110815	3.23	69/24	721007	3.20
45	67122818*	3.15	58032009	3.22	40/53	640216	3.18
46	70040215	3.11	61041312	3.22	26/68	581103	3.17
47	71112518	3.11	67120312	3.21	48/47	671203	3.16
48	67120321	3.10	72031506	3.18	54/49	580120	3.12
49	64112603	3.08	58012600	3.18	62/43	680529	3.11
50	64010115	3.08	60020106	3.16	47/55	711125	3.10
51	68031306*	3.07	62111012	3.15	57/51	621110	3.09
52	68011412	3.06	56102621*	3.13	67/46	610413	3.09
53	59031221*	3.06	64021909	3.13	56/50	600201	3.09
54	58011500	3.05	62122212	3.11	46/60	700402	3.08
55	69032512*	3.04	71112512	3.10	49/58	641126	3.08
56	60020106	3.03	62112715*	3.09	72/45	580320	3.07
57	62111012	3.03	62040106	3.08	52/67	680114	3.03
58	70110506	3.02	64112603	3.08	63/57	620401	3.03
59	59102421	3.01	56031618	3.04	58/61	701105	3.02
60	56092715	3.01	70040215	3.04	59/65	591024	3.01
61	72021321	3.00	70110503	3.03			
62	68052918	2.99	73042803*	3.03			
63	62040115	2.98	61052712*	3.02			
64	61112421*	2.98	66092021*	3.02			
65	63050103*	2.98	59102418	3.01			
66	74012112*	2.97	61030906*	3.00			
67	61041315	2.96	68011421	3.00			
68	75112715*	2.95	58110306	2.98			
69	72100712	2.94	60121206	2.98			
70	71040706	2.93	72111421*	2.98			
71	56041621*	2.93					
72	58032018	2.92					
73	74030403*	2.92					
74	63110721*	2.90					

* Storm events with un-matched occurrences at other station

Table B11
Rank of Storm Events By Year

<u>Year</u>	<u>Number of Storms</u>	<u>Rank of Storm</u>
1956	2	29,30
1957	1	28
1958	4	24,46,48,56
1959	2	32,60
1960	3	18,26,53
1961	4	11,22,34,52
1962	6	1,15,38,40,51,58
1963	0	
1964	5	5,20,39,45,55
1965	2	21,41
1966	2	14,17
1967	2	36,47
1968	4	23,27,49,57
1969	2	12,37
1970	3	16,54,59
1971	4	31,33,35,50
1972	5	2,8,42,43,44
1973	4	4,10,13,19
1974	3	3,7,25
1975	2	6,9

APPENDIX C: NEARSHORE WAVE REFRACTION (MODEL RESULTS)

1. This appendix contains plots showing the results of the RCPWAVE production runs. Economic and computational restrictions preclude running of the nearshore wave refraction model for every distinct wave condition occurring in the deepwater time series. The standard procedure is to divide the possible angles of wave approach into bands and execute the model with a unit wave height and an angle of approach equal to the central angle of the band. This information is input on the offshore boundary of the bathymetry grid for each of the dominant wave periods. This procedure was followed and, in addition, the wave height and angle were linearly varied across the grid by amounts equal to the gradients calculated from the two WIS stations. These gradients simulate the shadowing effect of Long Island on the incident wave climate at the project area.

2. Nine angle bands were used in this project (Figure 3 of main text). The angle bands are 22.5 degrees wide and correspond to the compass directions of north, north-northeast, northeast, east-northeast, east, east-southeast, southeast, south-southeast, and south. Shadowing by Long Island eliminates all waves in angle bands 1 through 3.

3. The data plotted on the following sheets are the wave heights and angles of approach at a nominal 3-m depth (the location at which they are saved for input to the shoreline change model). The results for the existing bathymetry are plotted as dotted lines, the solid lines represent the result with the dredged bathymetry. The results are plotted across the entire bathymetry grid; however, the RCPWAVE grid extends beyond the project area laterally (from Deal to Mantoloking), whereas the shoreline change model grid is from Asbury Park to Manasquan Inlet. Therefore, only the information from alongshore grid coordinates 45 to 141 were used in the shoreline model, the remaining grid points on the ends provide boundary conditions. The coordinate system of RCPWAVE is such that alongshore coordinate 45 corresponds to Manasquan Inlet to the south and alongshore coordinate 141 corresponds to Asbury Park.

4. The RCPWAVE results for sea conditions are given in Figures C1 through C12. The results for swell wave conditions are given in Figures C13

through C24. Figures C25 and C26 show the effect of the excavation of the nearshore borrow sites on the incident wave height and angle for 4 and 7 second waves.

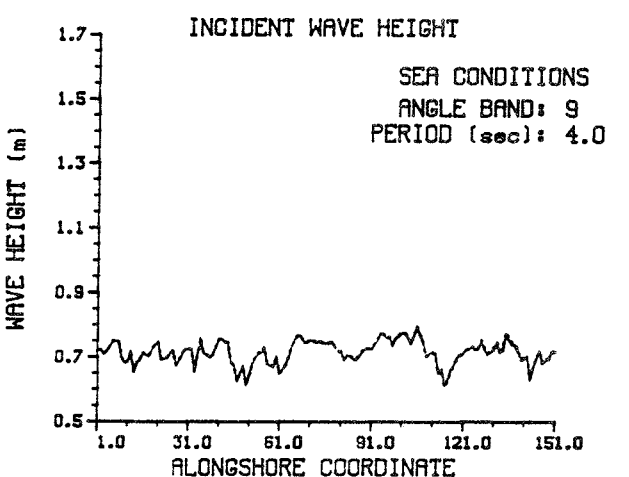
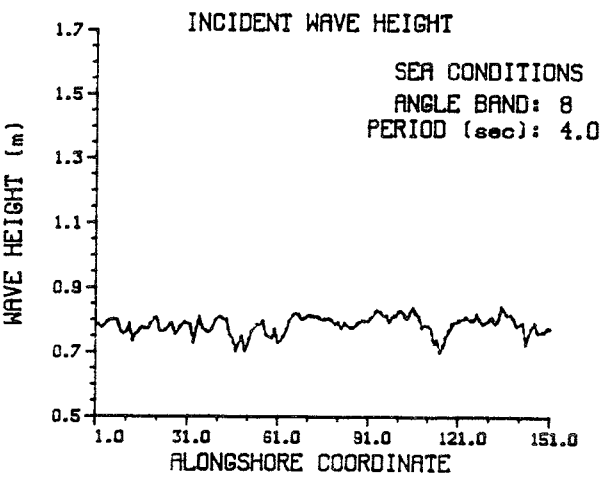
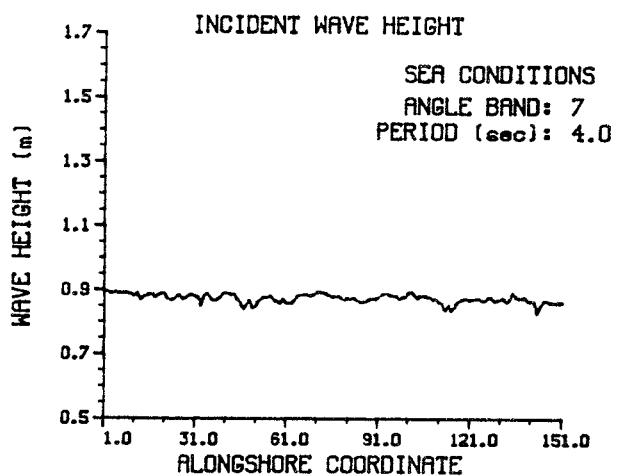
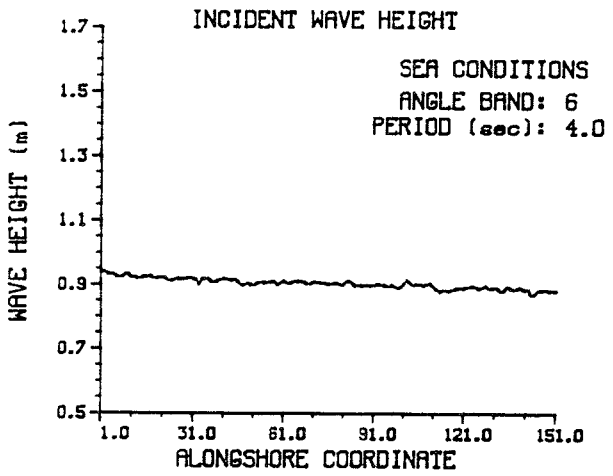
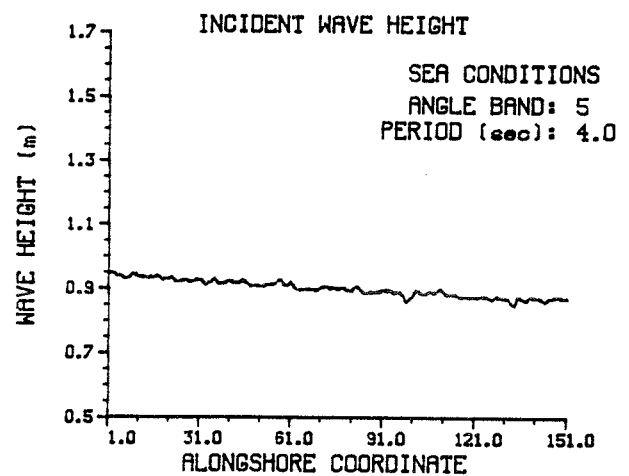
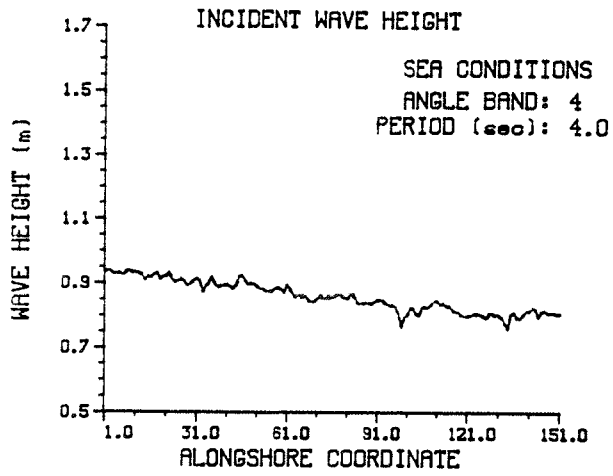


Figure C1. Sea conditions; wave height, T = 4.0 sec

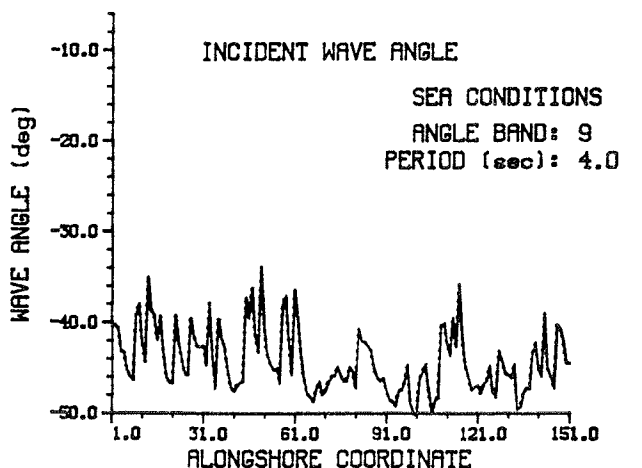
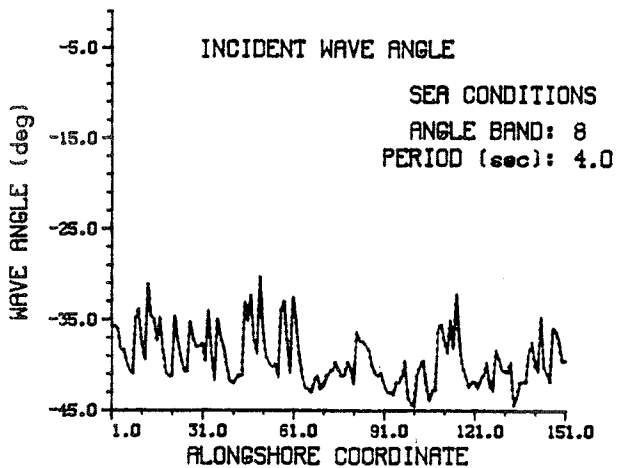
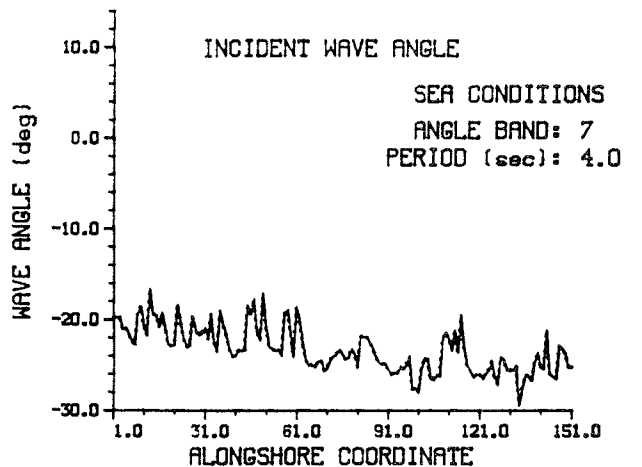
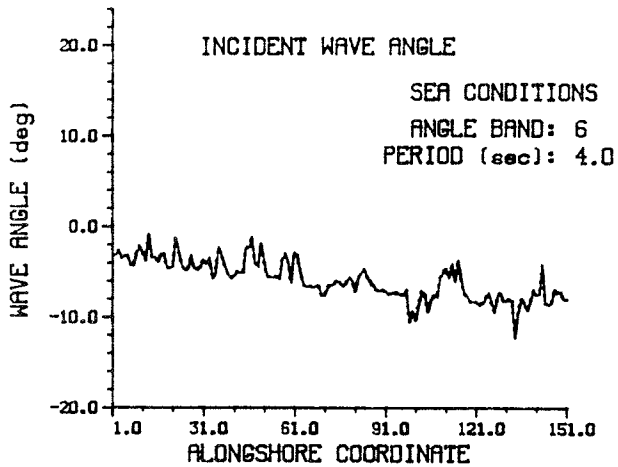
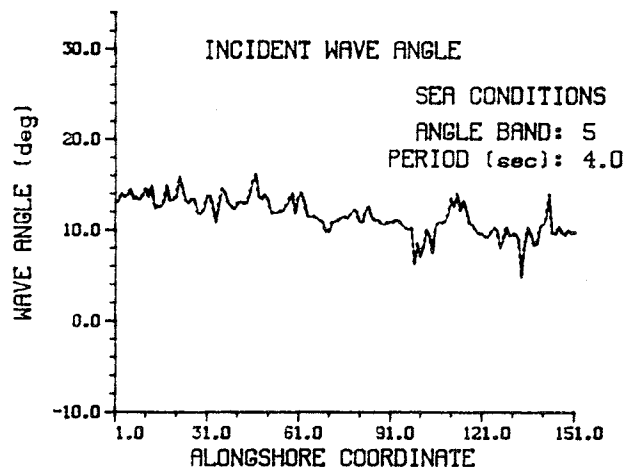
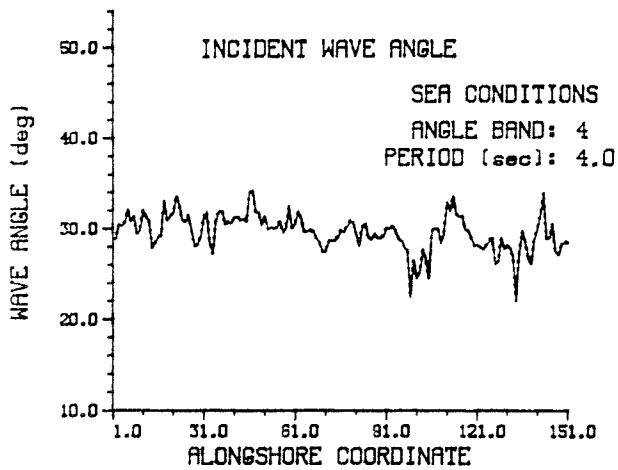


Figure C2. Sea conditions; wave angles, $T = 4.0$ sec

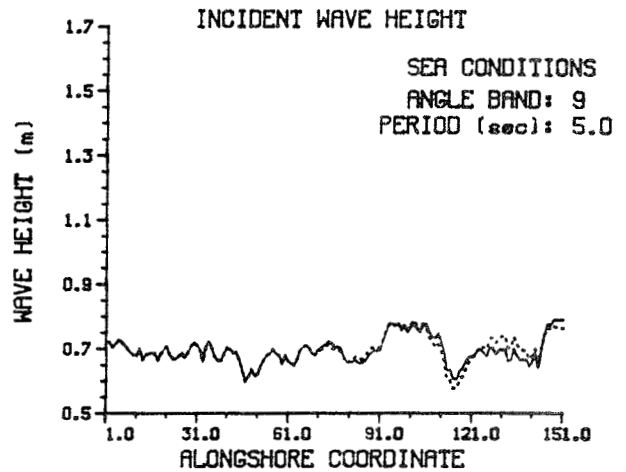
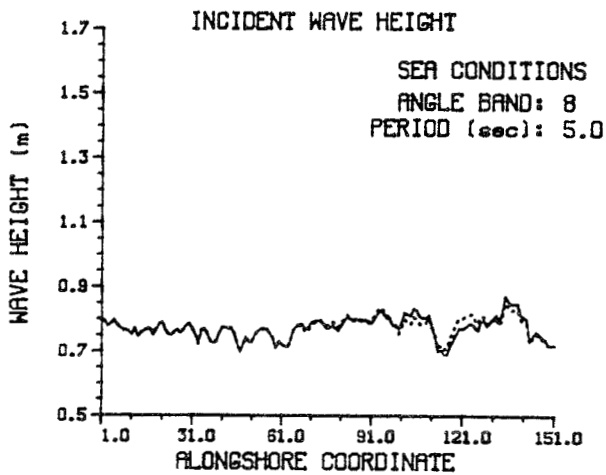
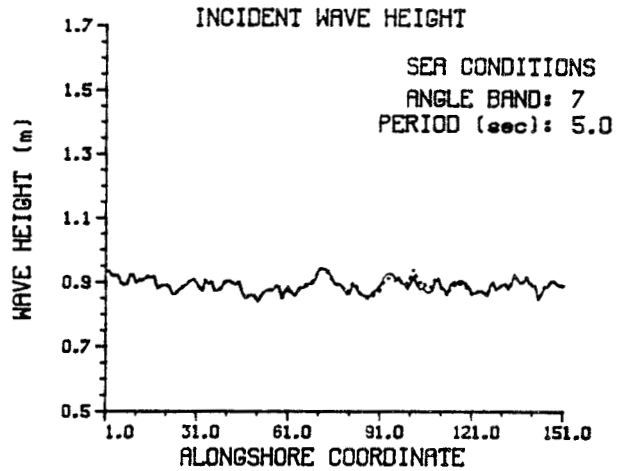
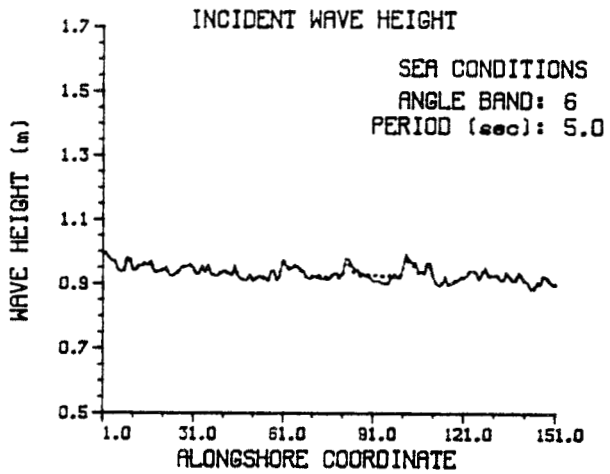
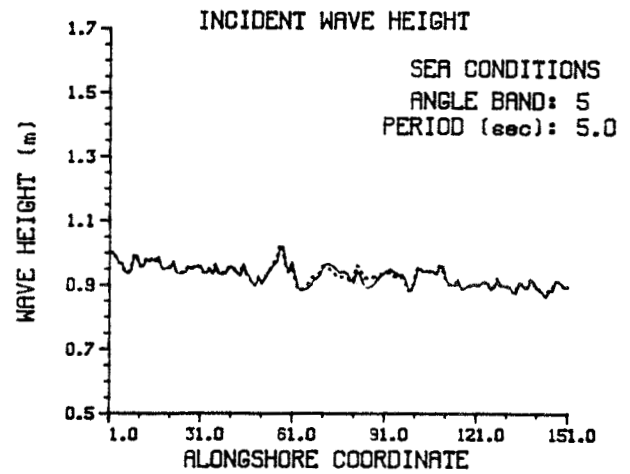
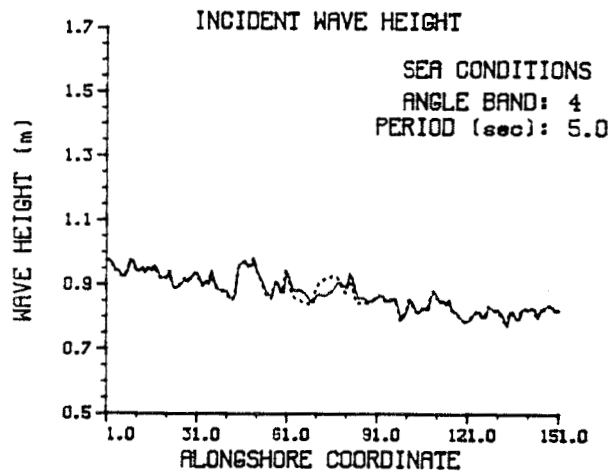


Figure C3. Sea conditions; wave height, $T = 5.0$ sec

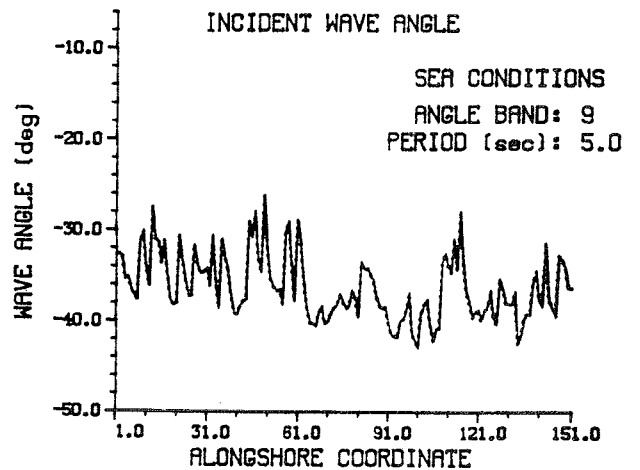
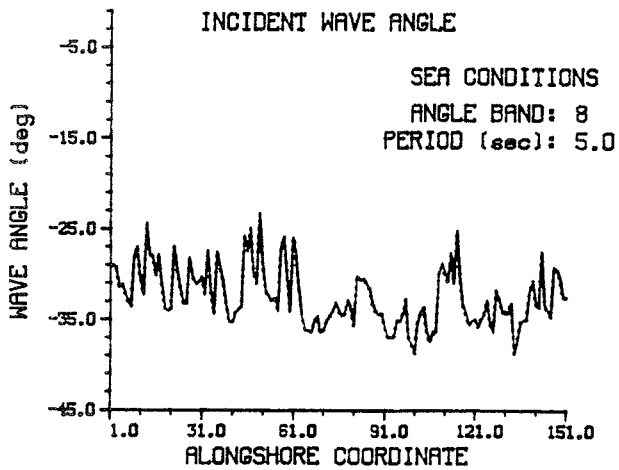
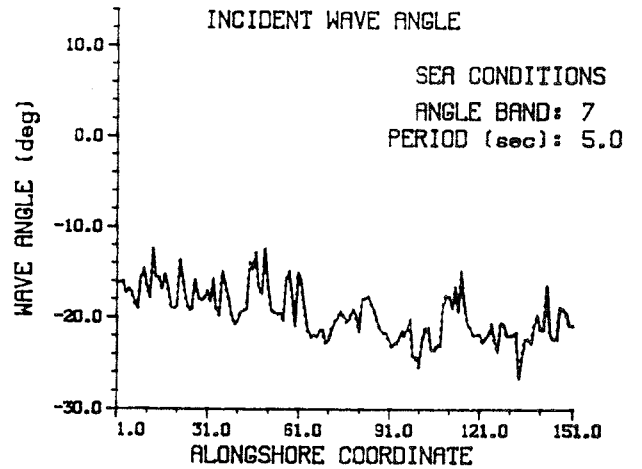
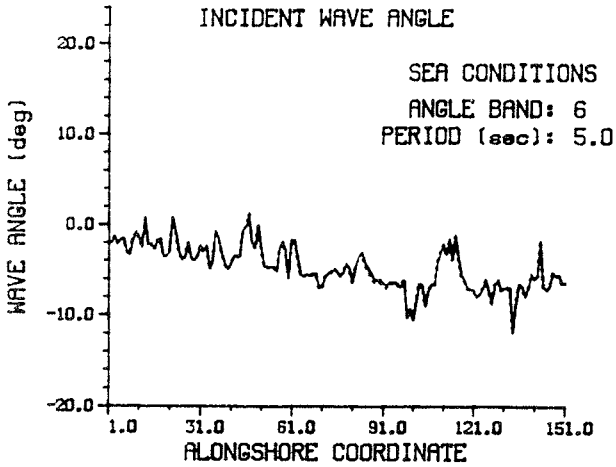
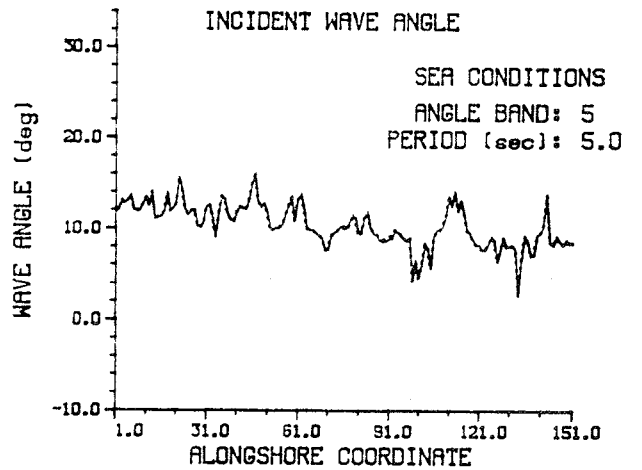
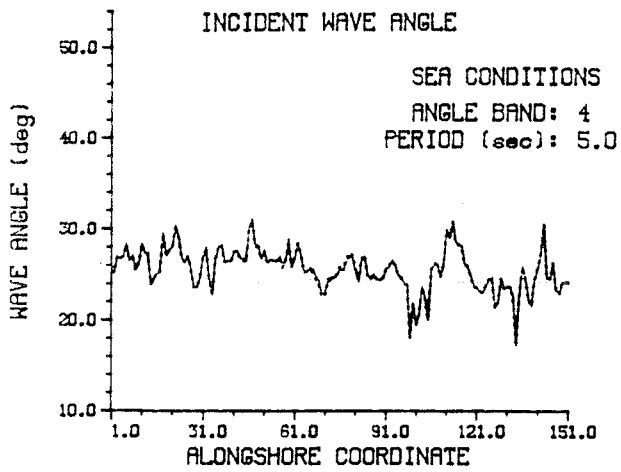


Figure C4. Sea conditions; wave angles, $T = 5.0$ sec

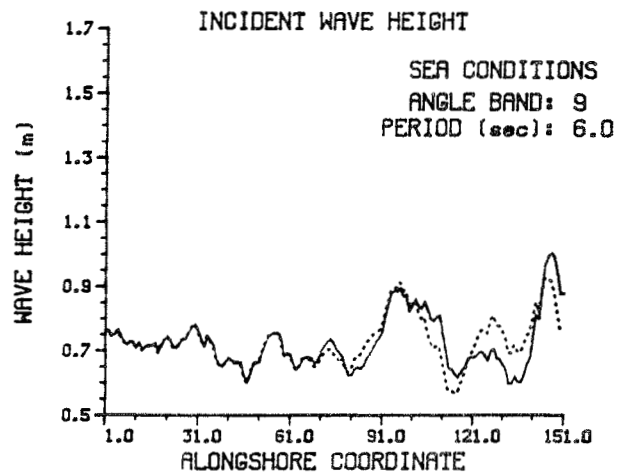
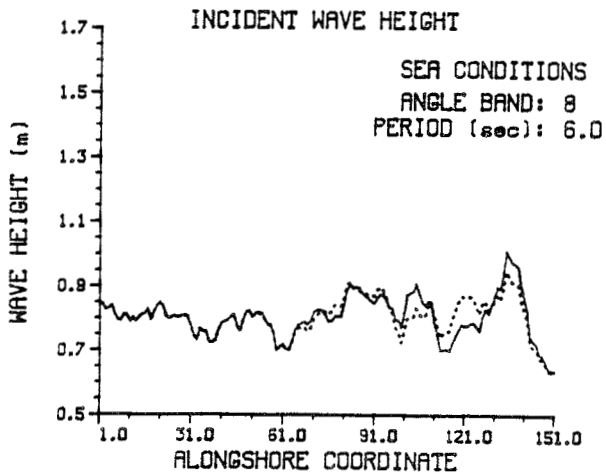
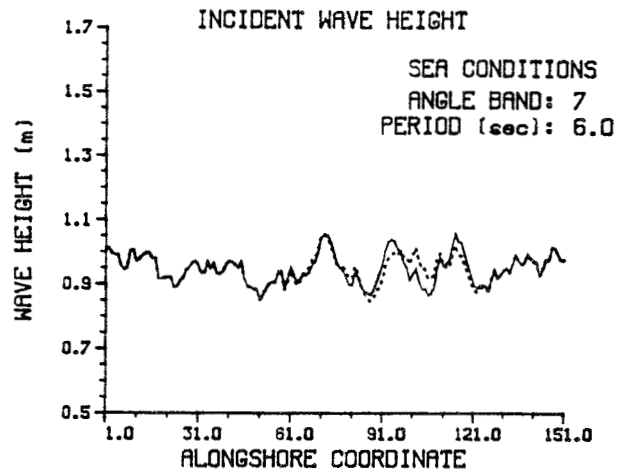
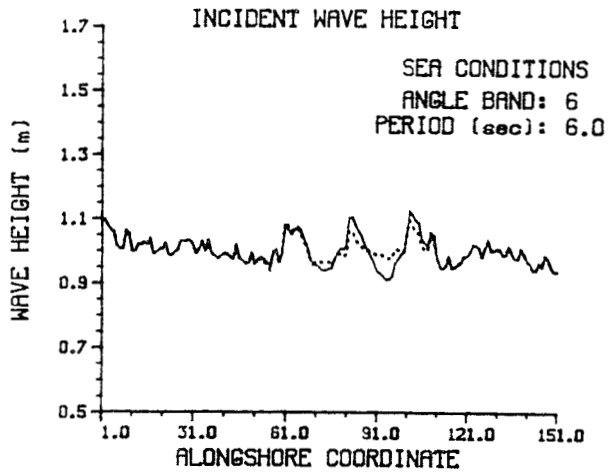
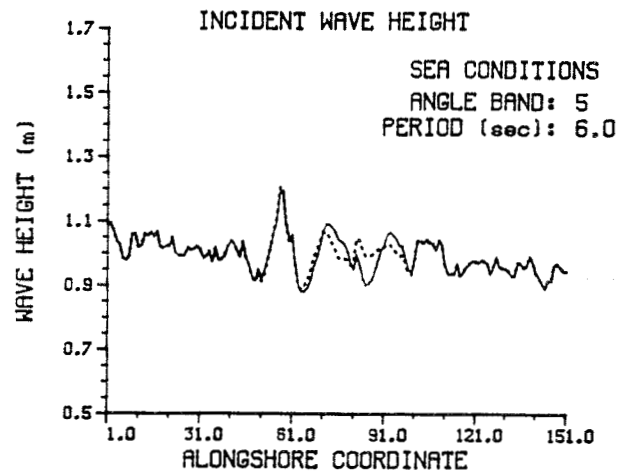
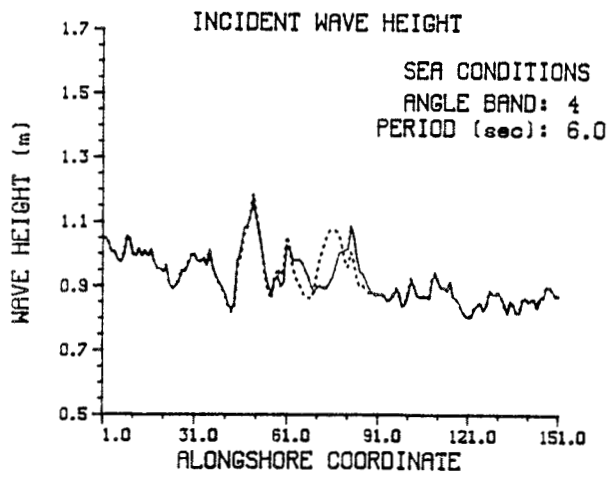


Figure C5. Sea conditions; wave height, $T = 6.0$ sec

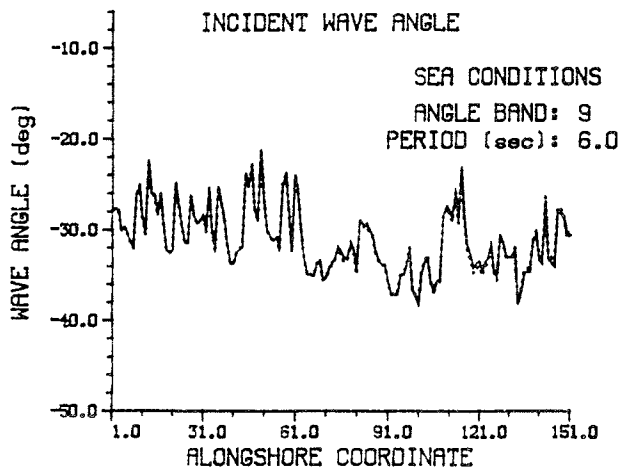
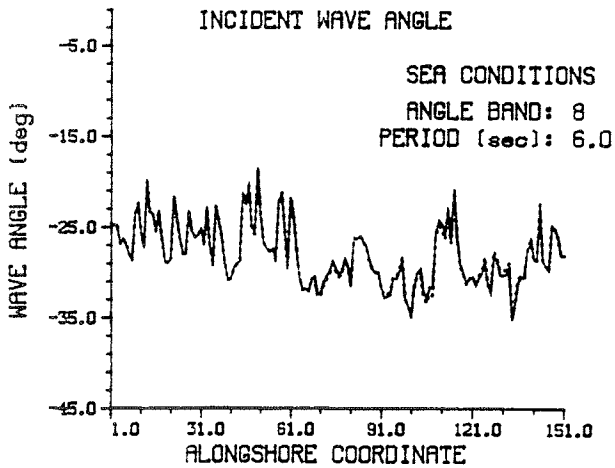
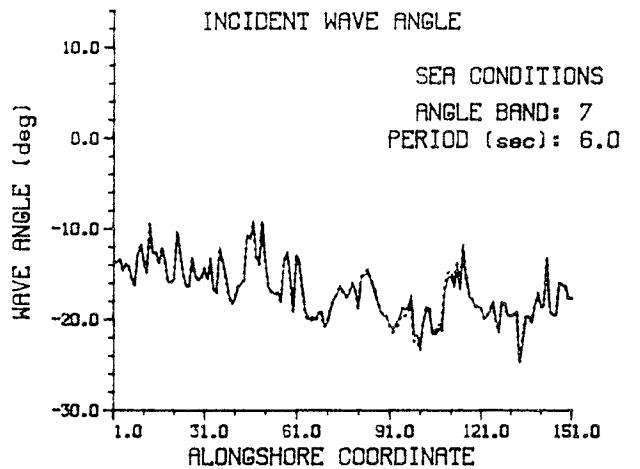
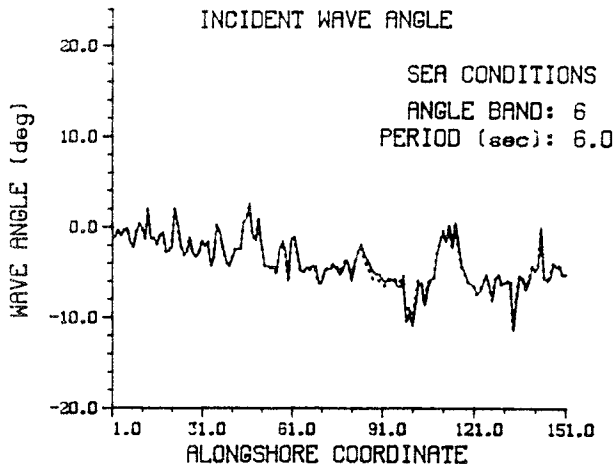
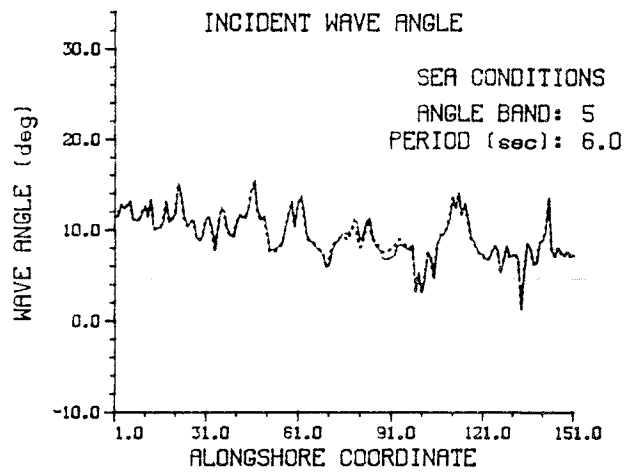
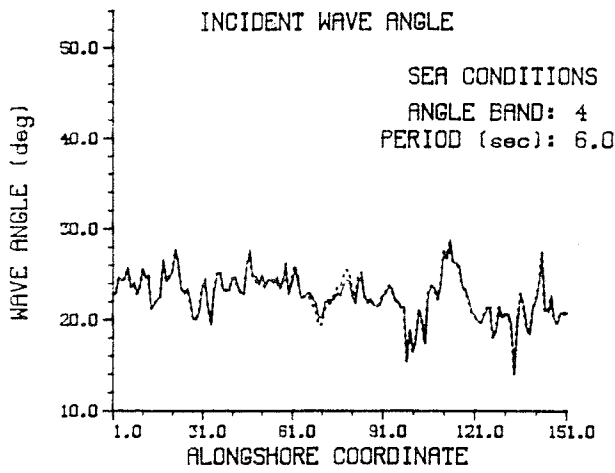


Figure C6. Sea conditions; wave angles, $T = 6.0$ sec

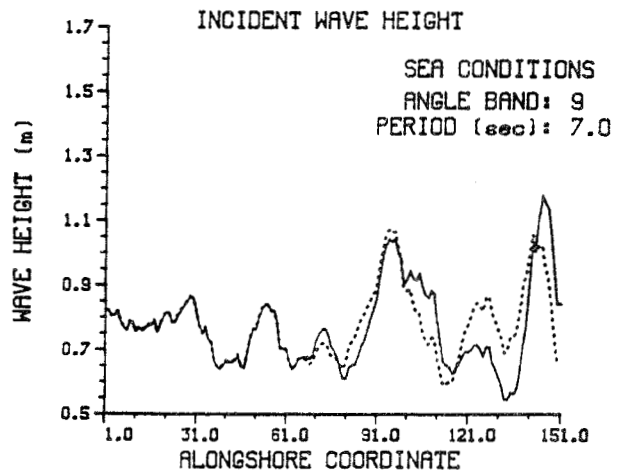
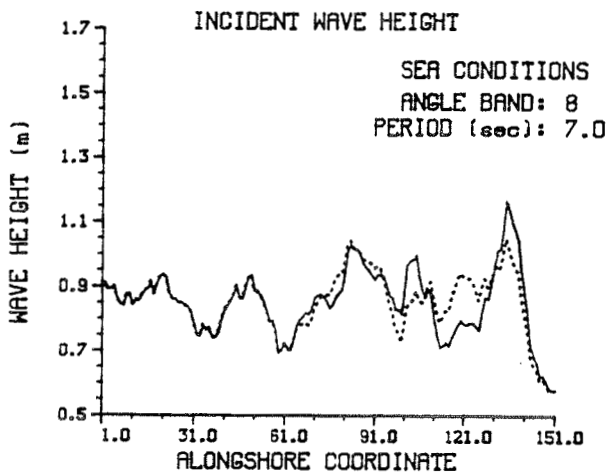
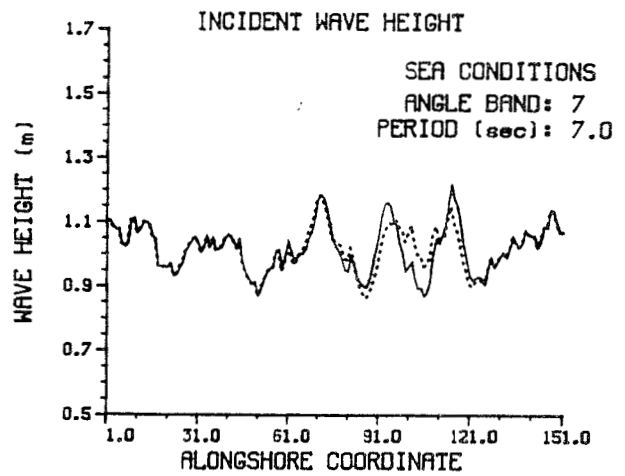
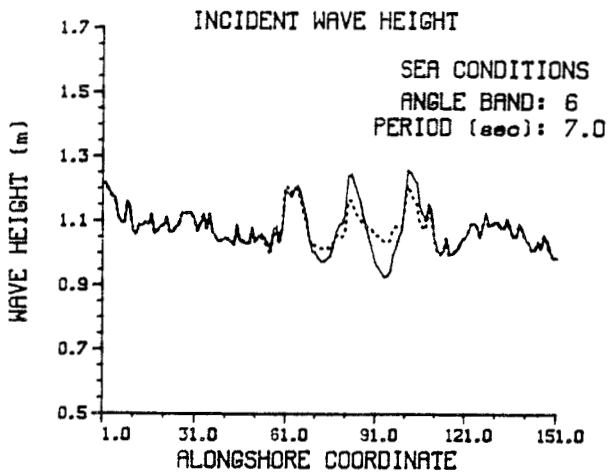
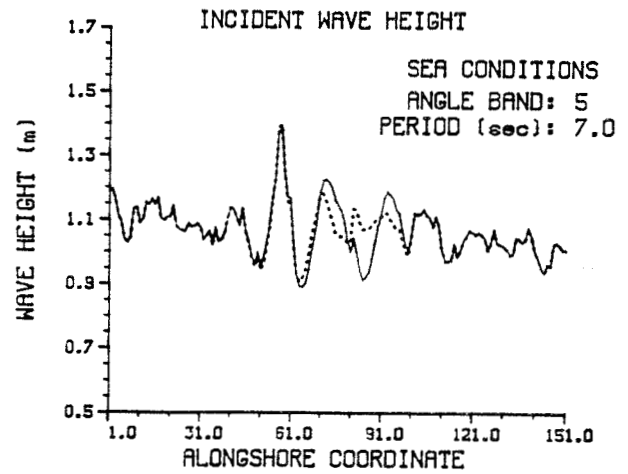
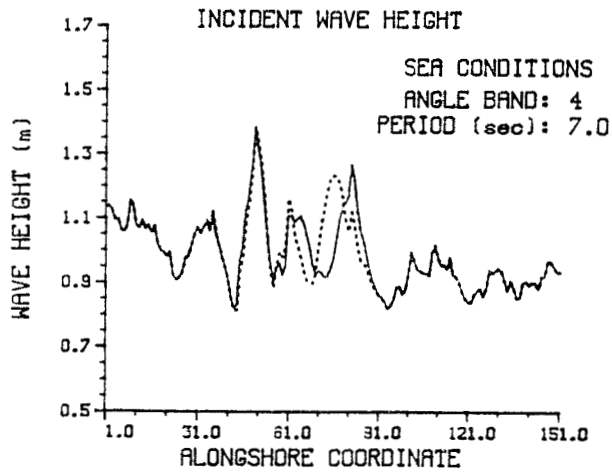


Figure C7. Sea conditions; wave height, $T = 7.0$ sec

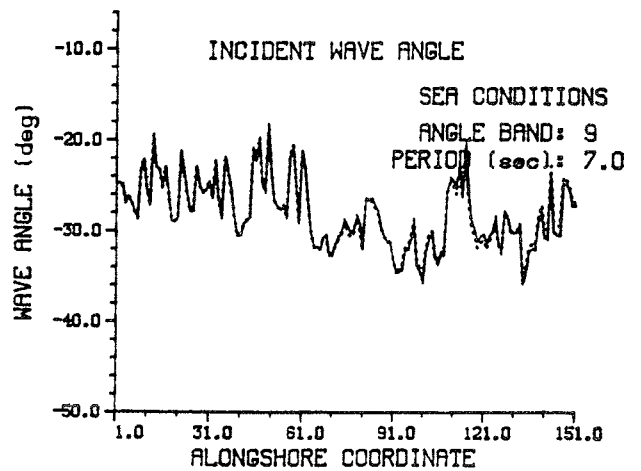
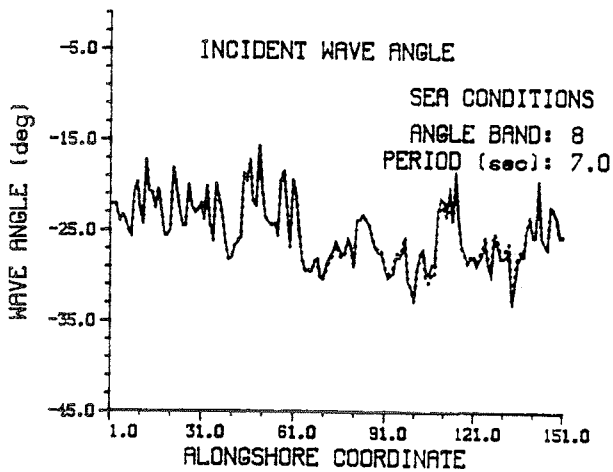
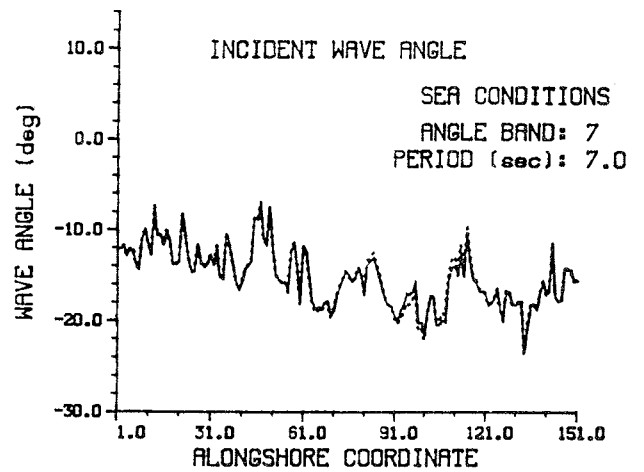
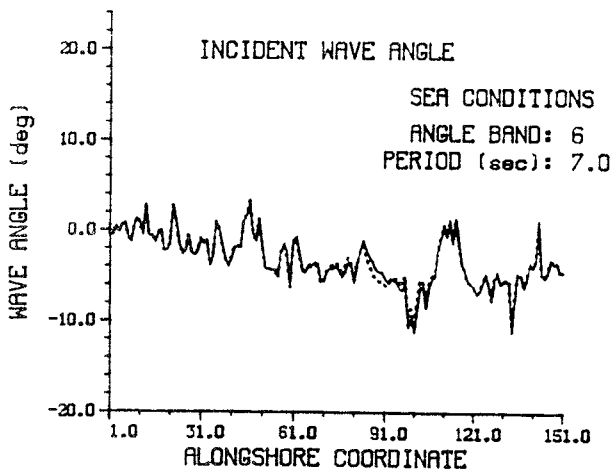
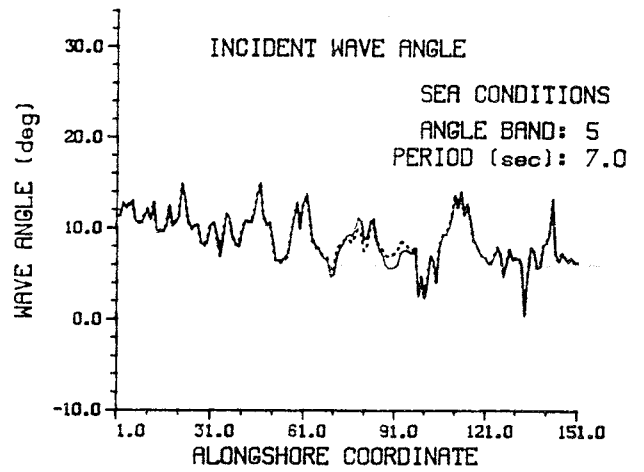
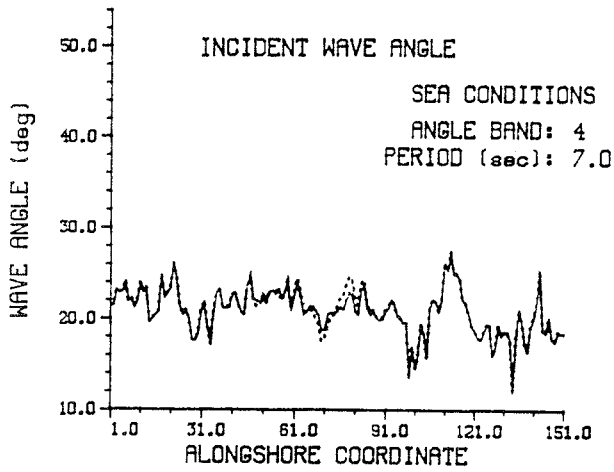


Figure C8. Sea conditions; wave angles, $T = 7.0$ sec

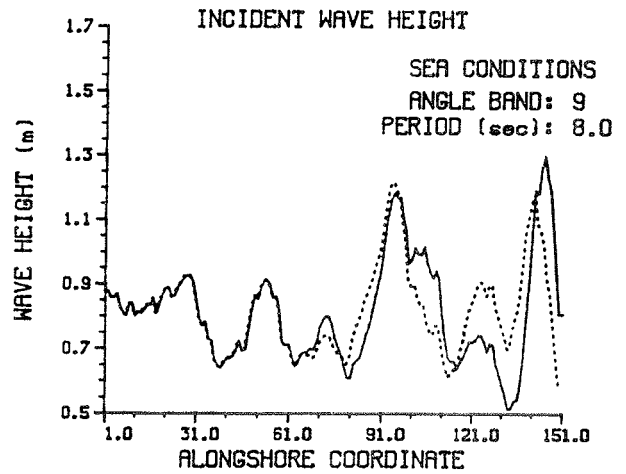
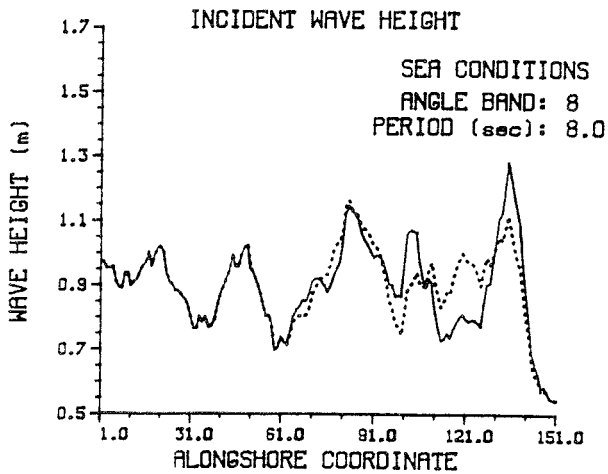
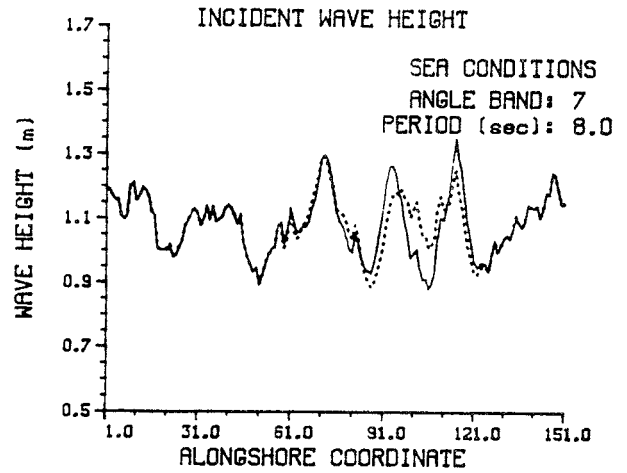
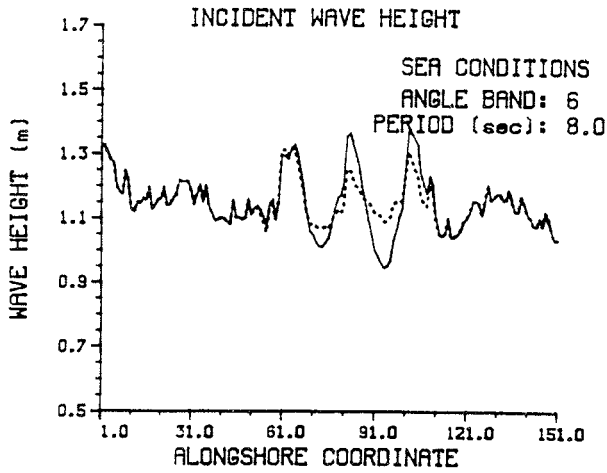
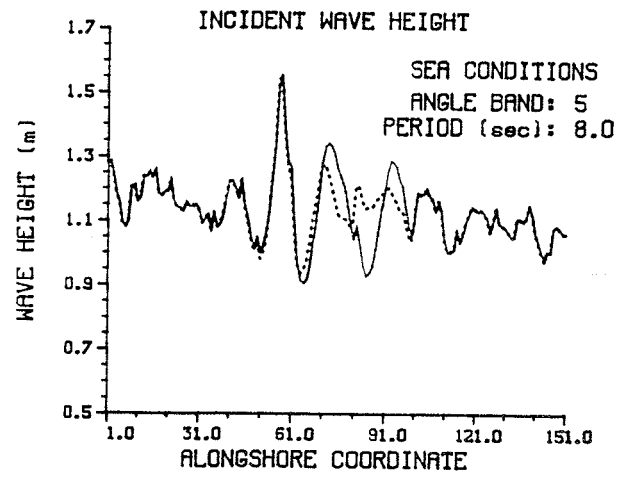
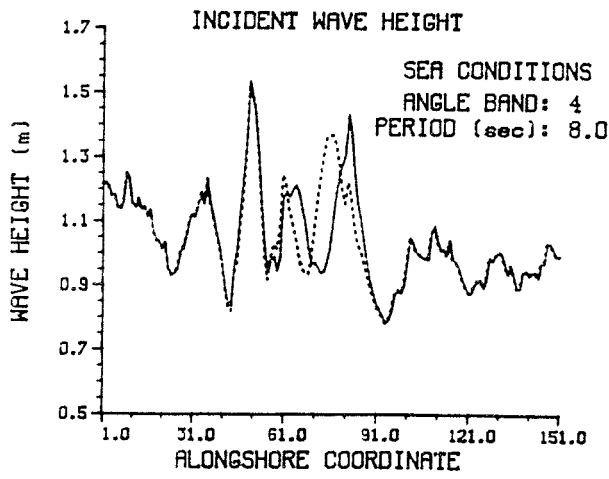


Figure C9. Sea conditions; wave height, $T = 8.0$ sec

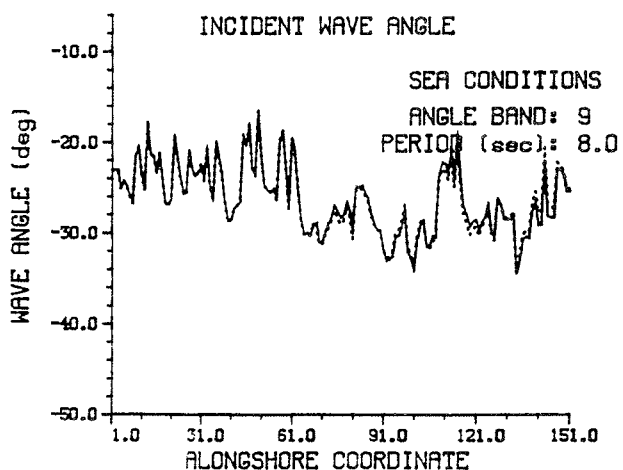
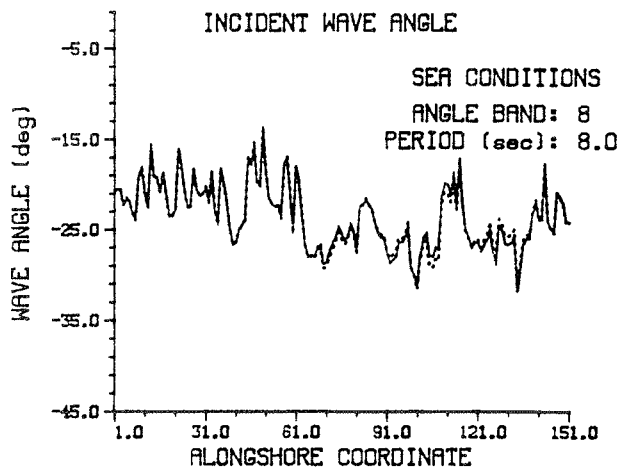
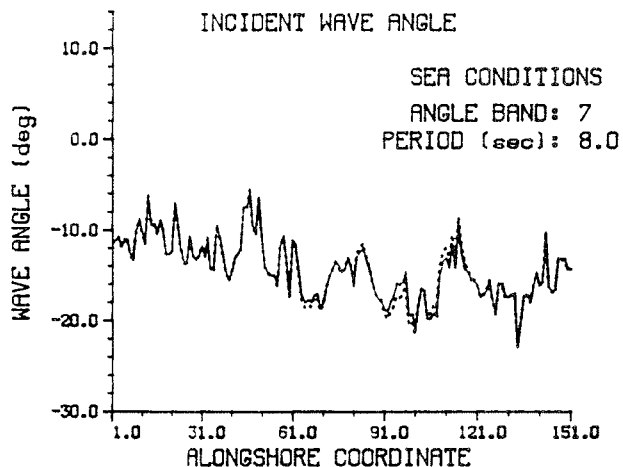
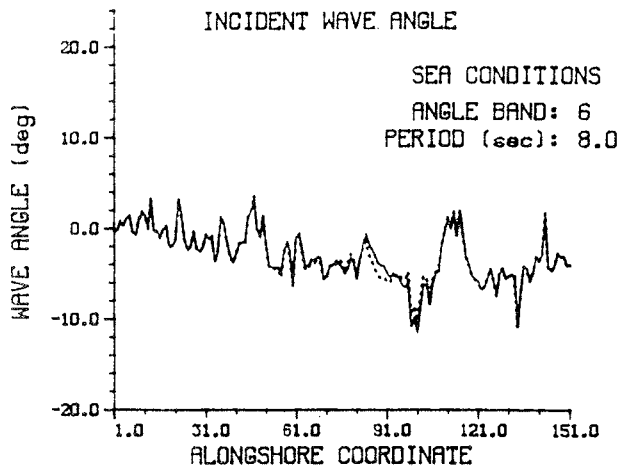
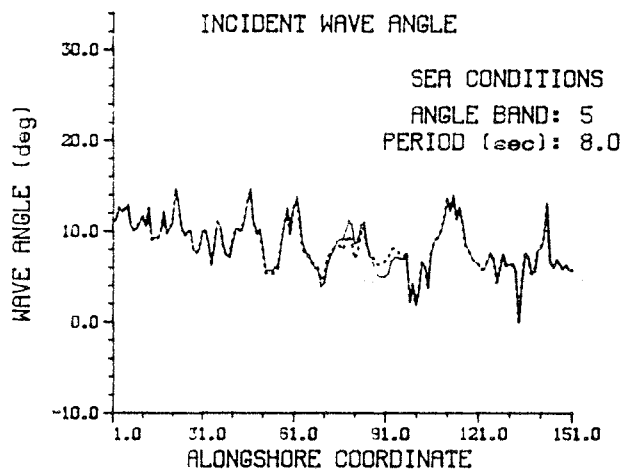
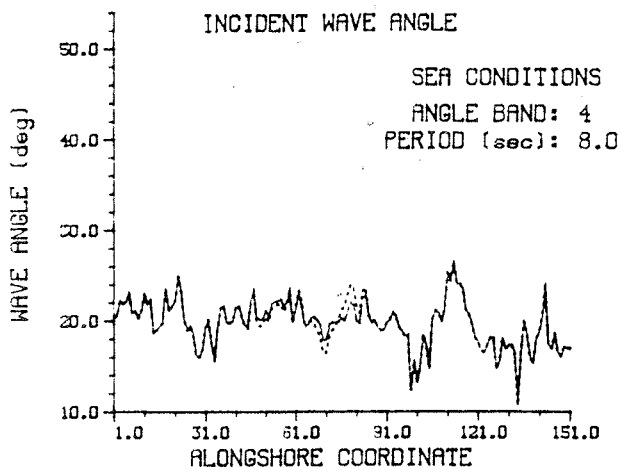


Figure C10. Sea conditions; wave angles, $T = 8.0$ sec

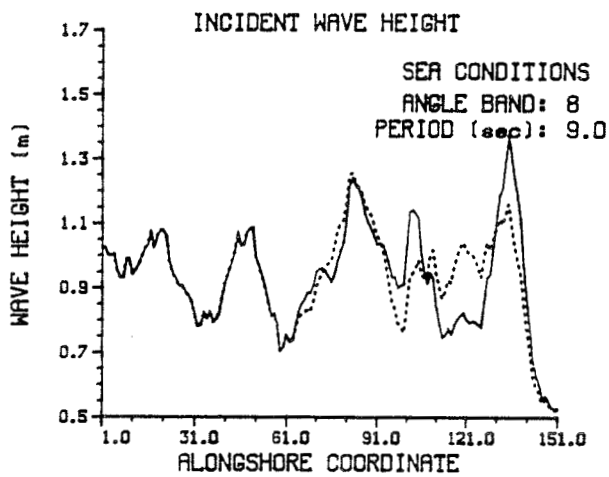
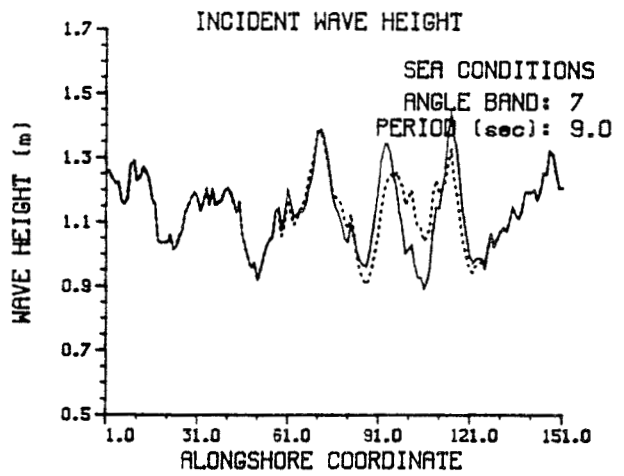
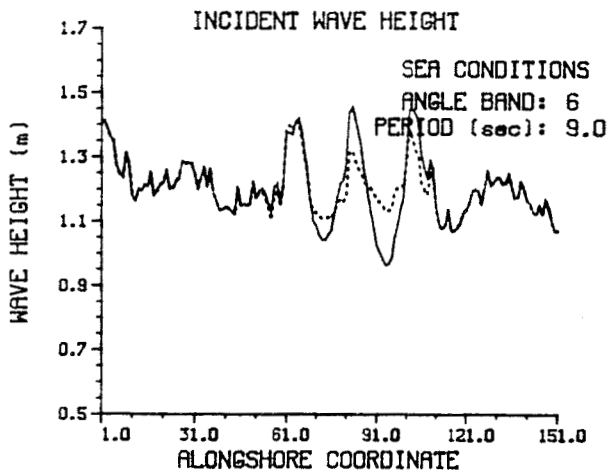
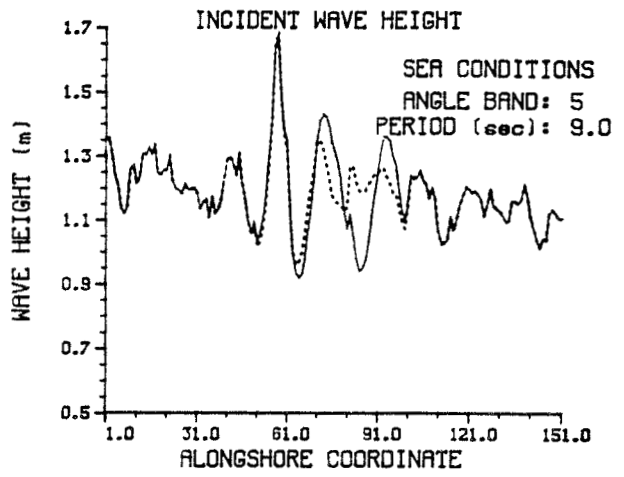


Figure C11. Sea conditions; wave height, $T = 9.0$ sec

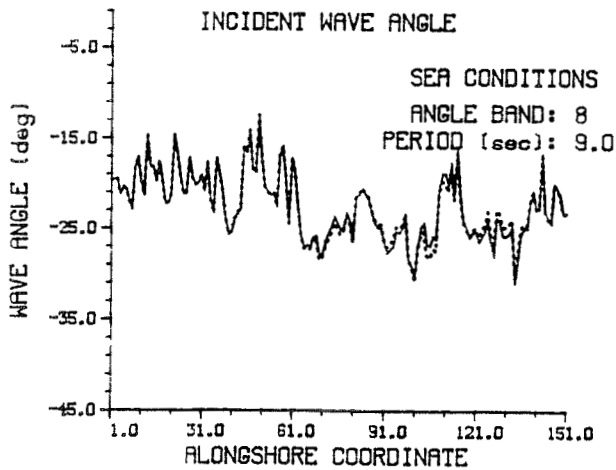
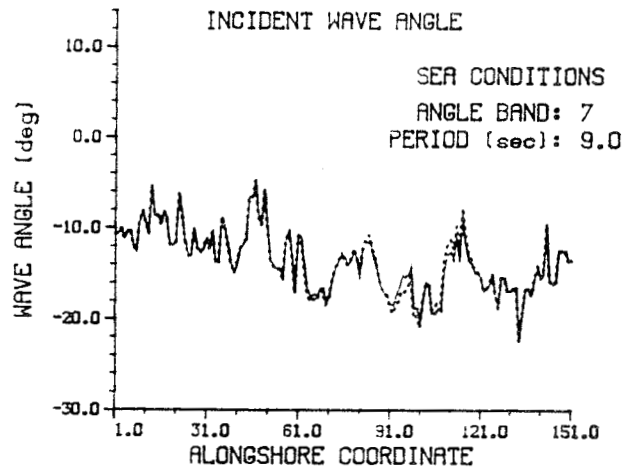
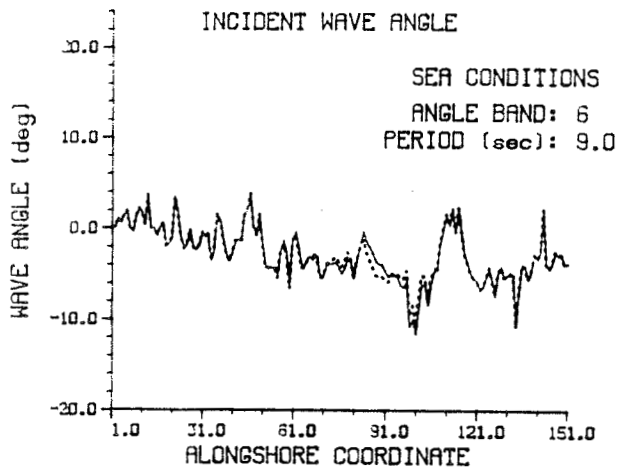
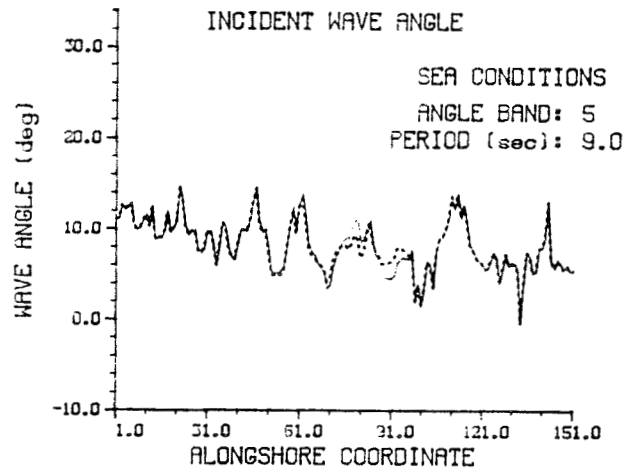


Figure C12. Sea conditions; wave angles, $T = 9.0$ sec

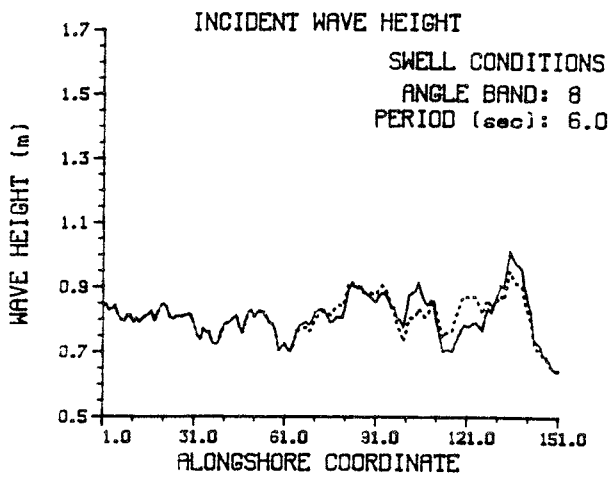
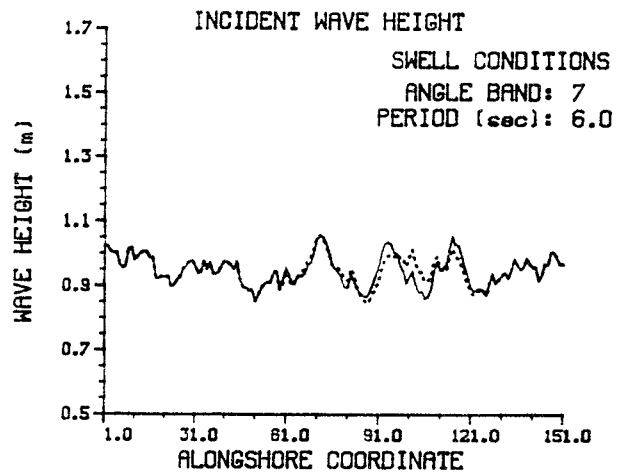
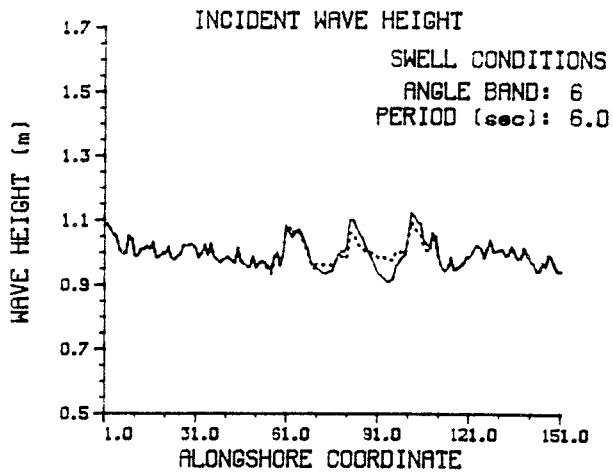
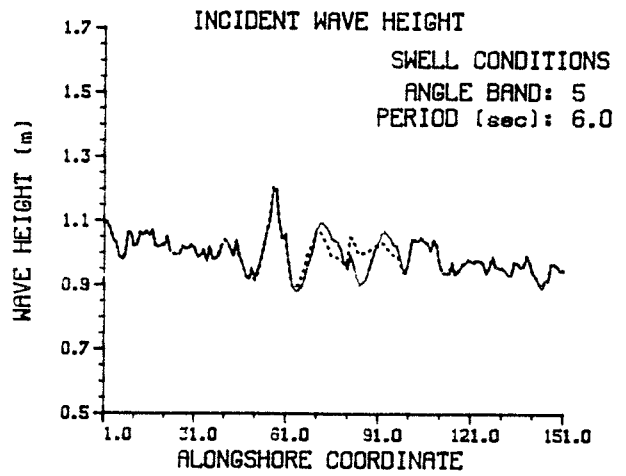
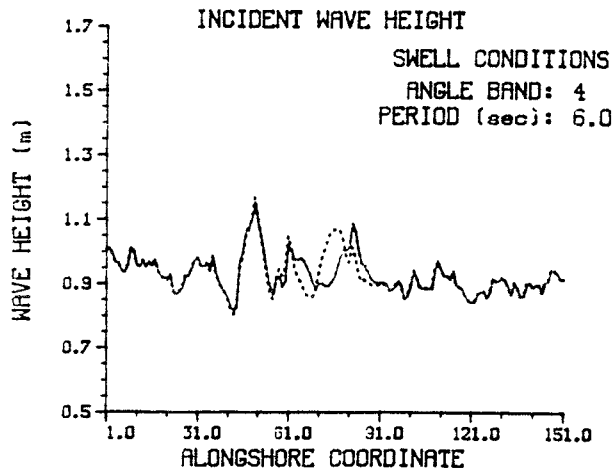


Figure C13. Swell conditions; wave height, $T = 6.0$ sec

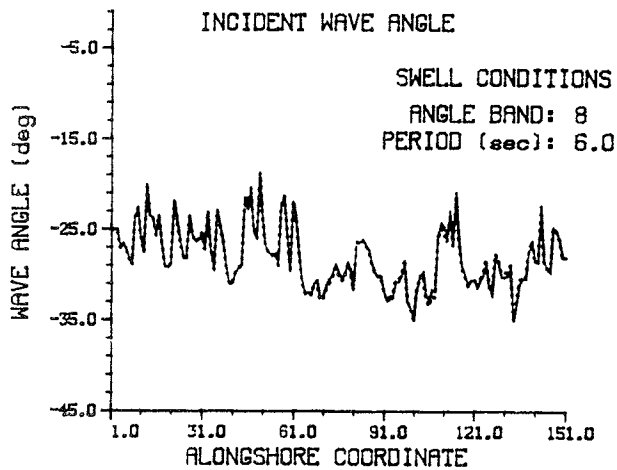
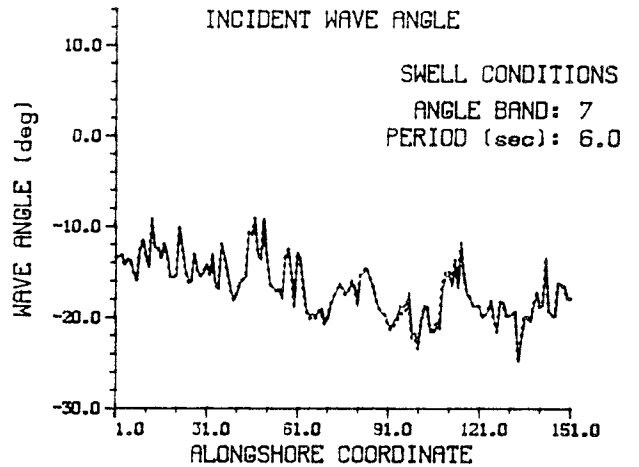
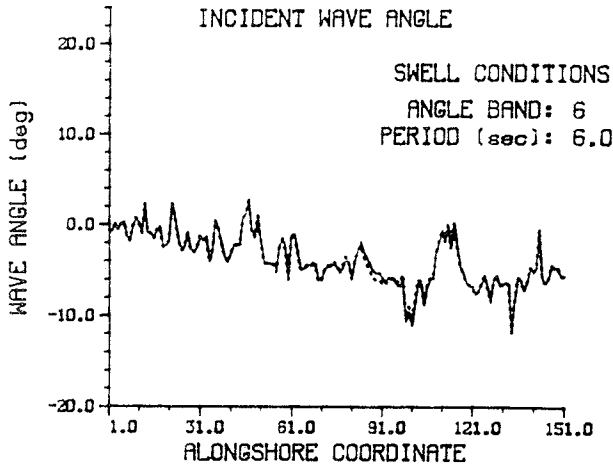
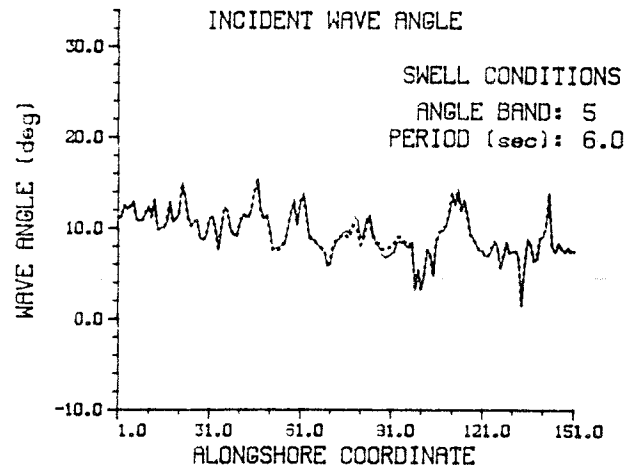
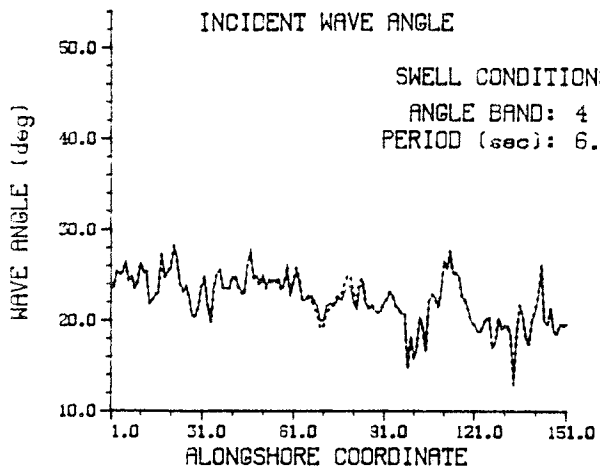


Figure C14. Swell conditions; wave angles, $T = 6.0$ sec

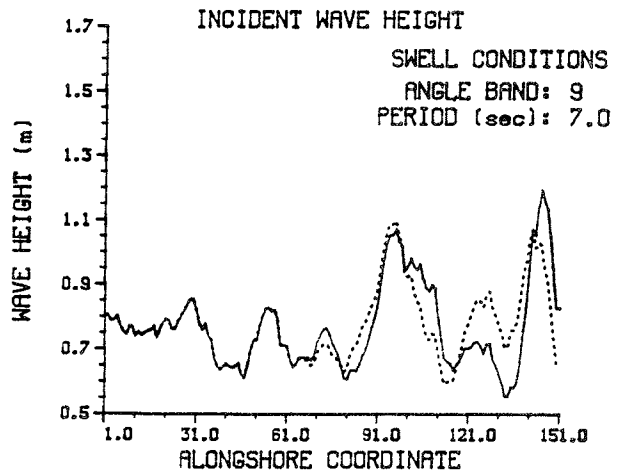
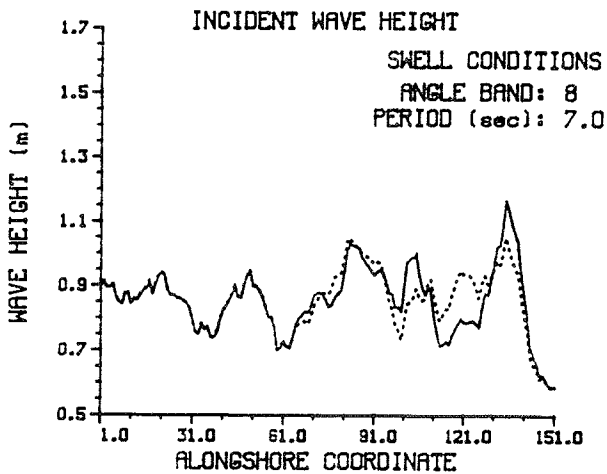
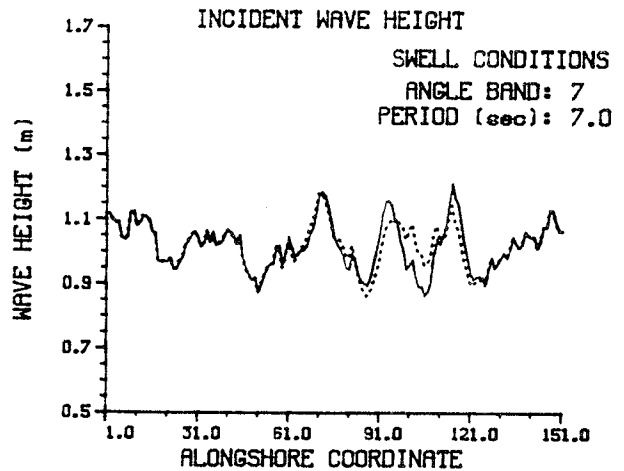
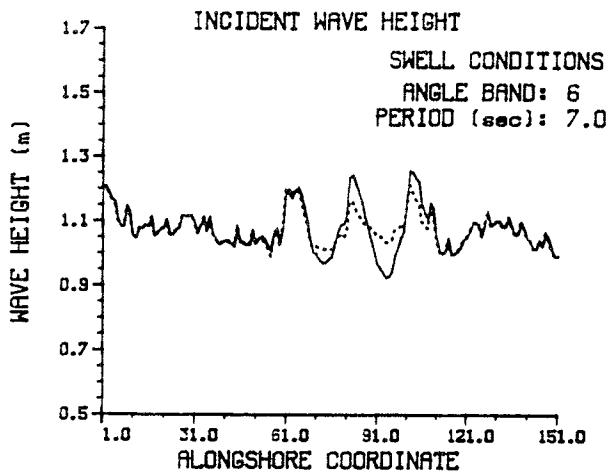
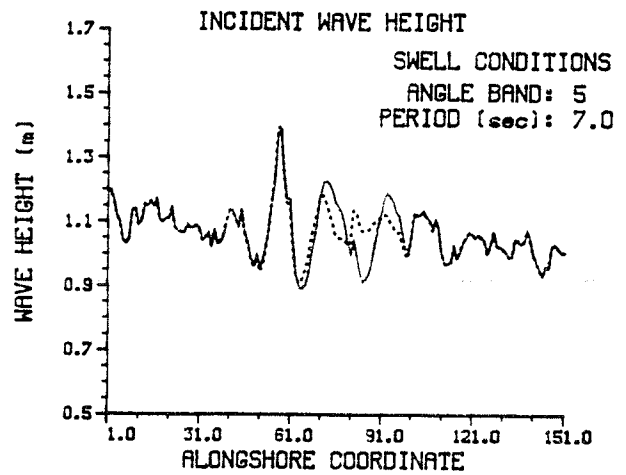
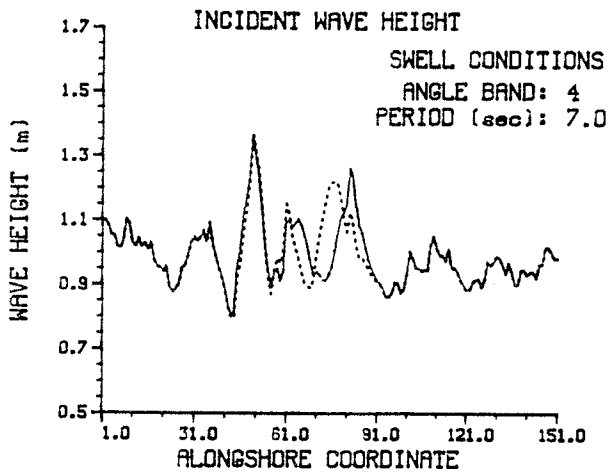


Figure C15. Swell conditions; wave height, $T = 7.0$ sec

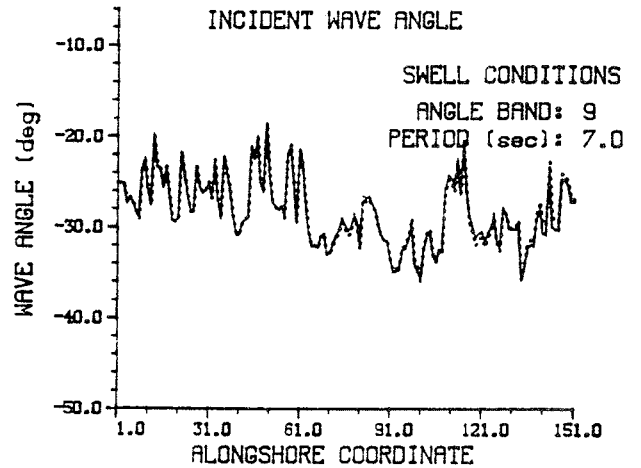
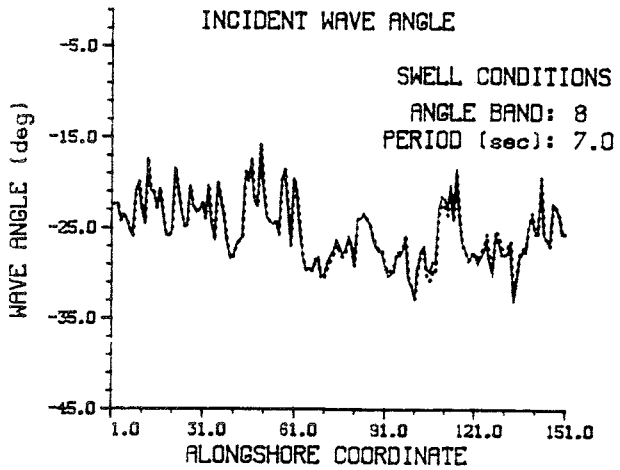
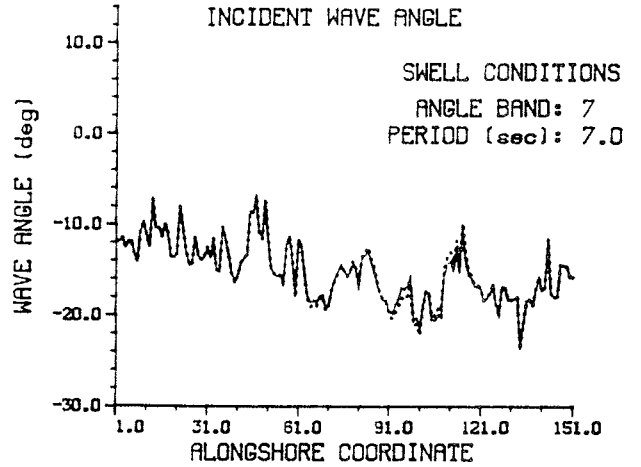
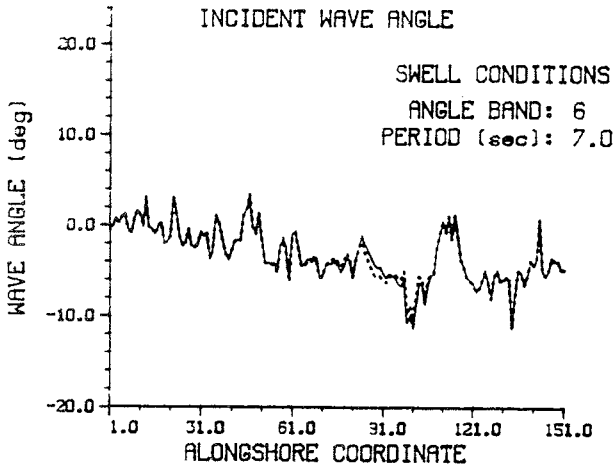
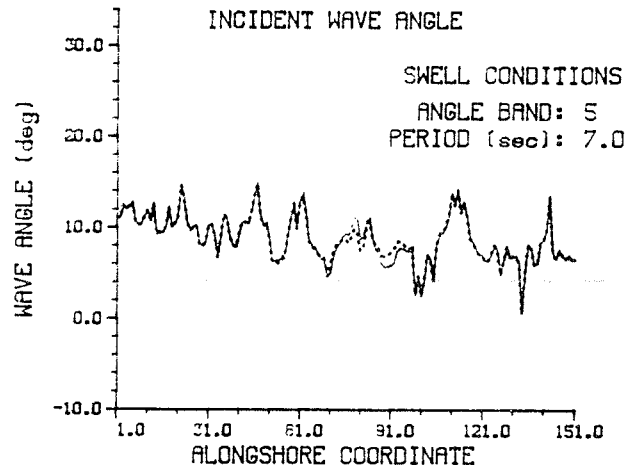
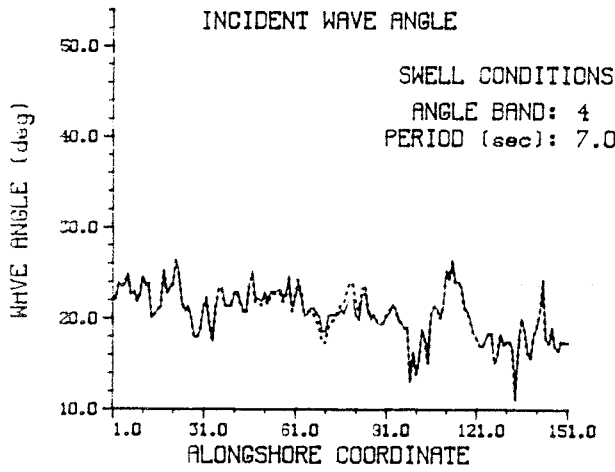


Figure C16. Swell conditions; wave angles, $T = 7.0$ sec

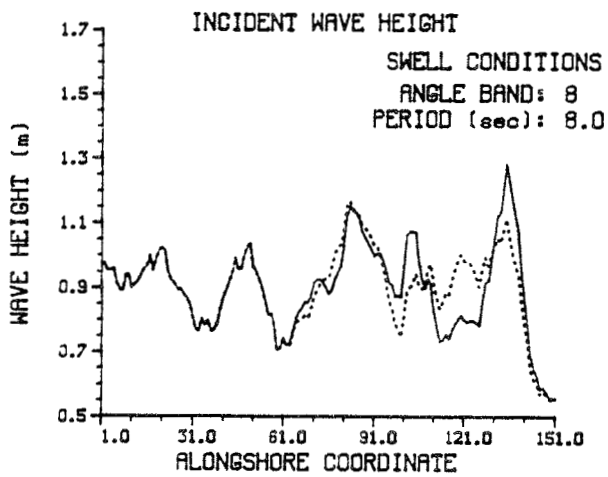
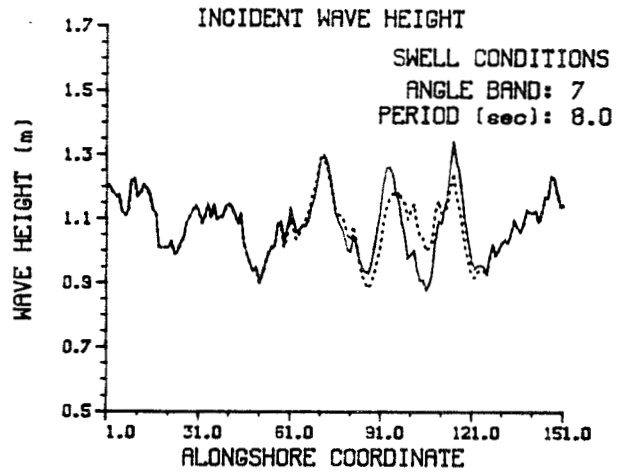
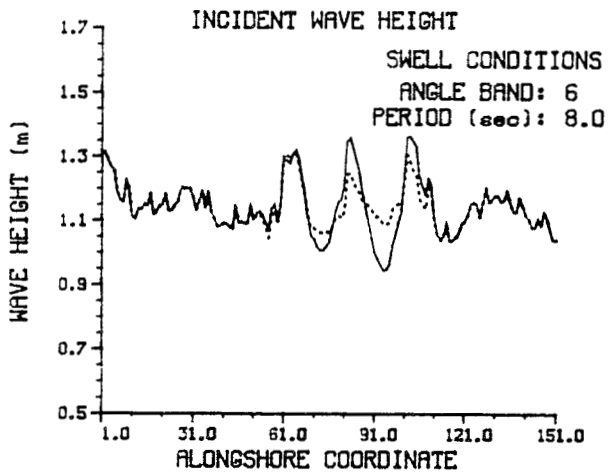
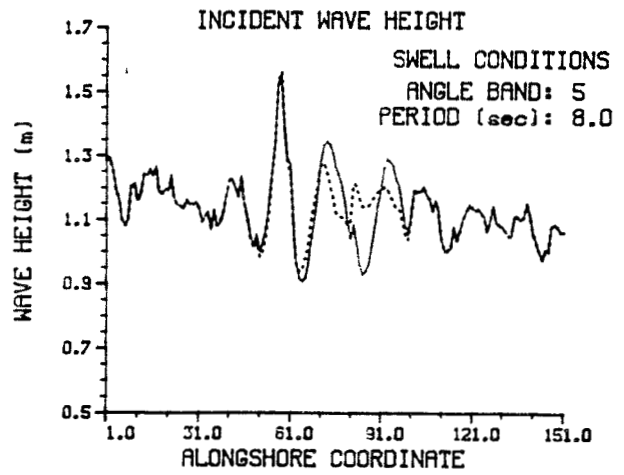
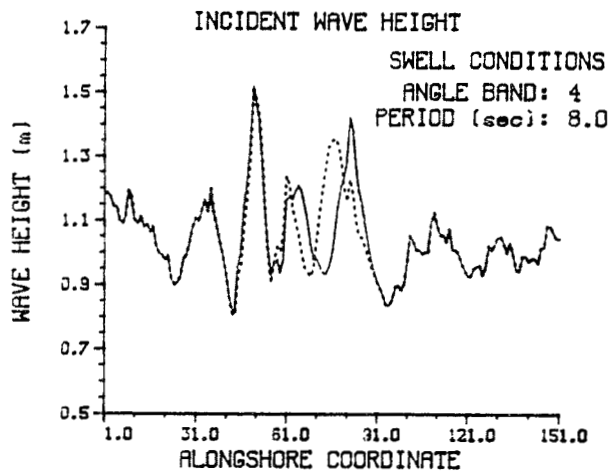


Figure C17. Swell conditions; wave height, $T = 8.0$ sec

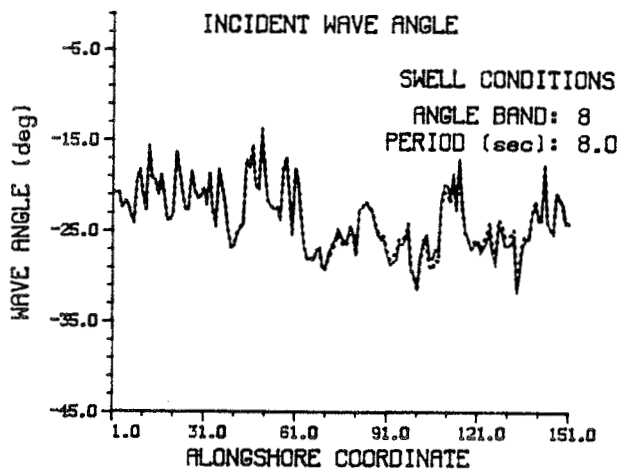
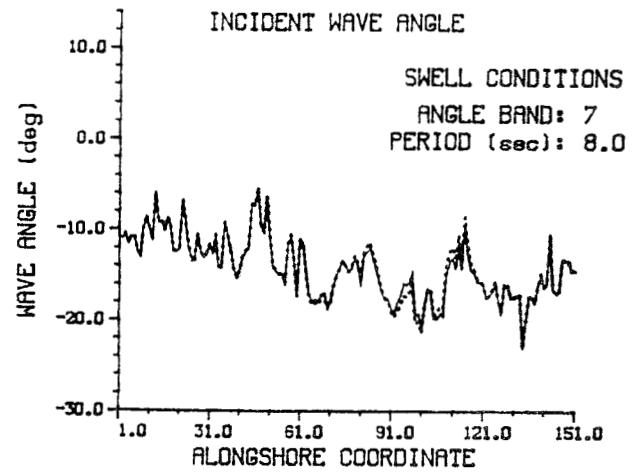
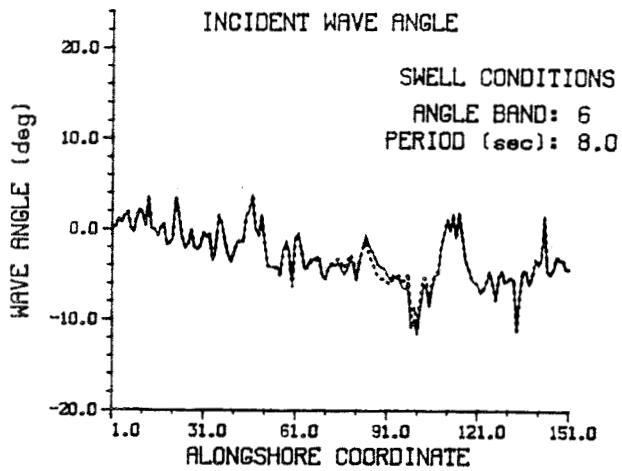
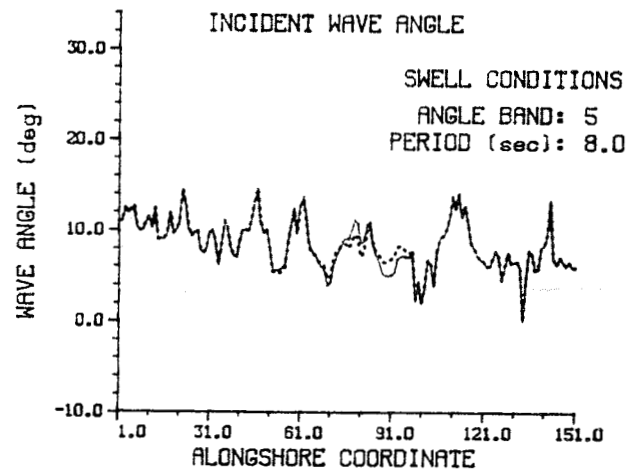
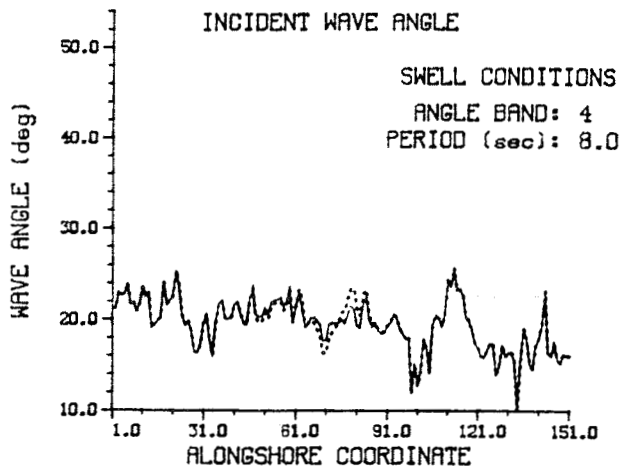


Figure C18. Swell conditions; wave angles, $T = 8.0$ sec

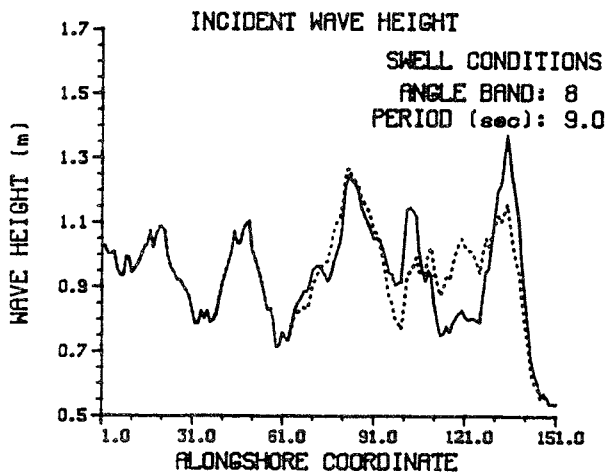
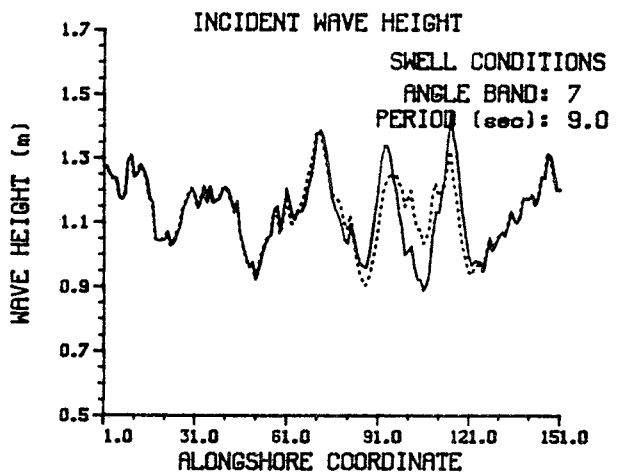
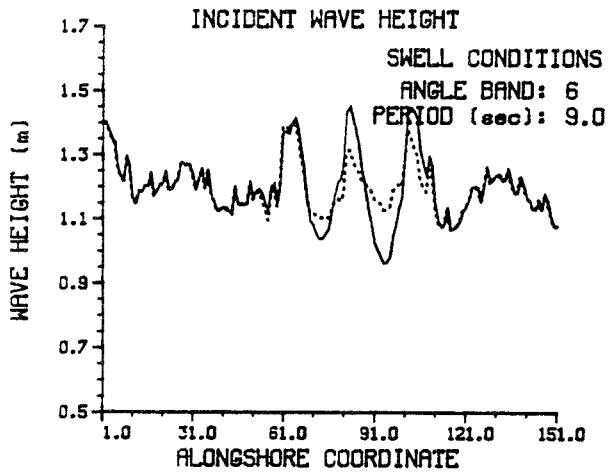
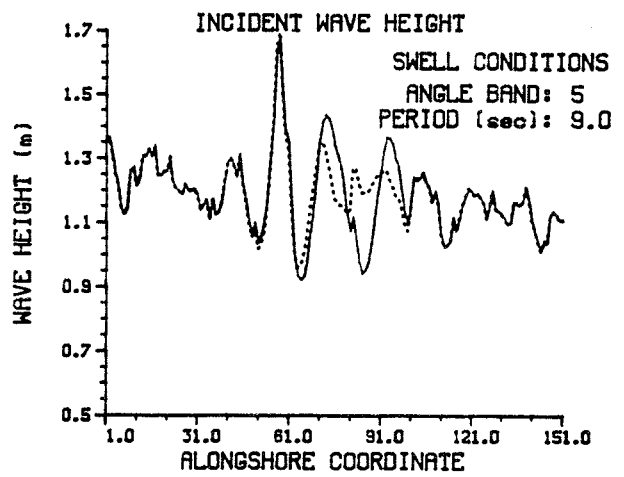
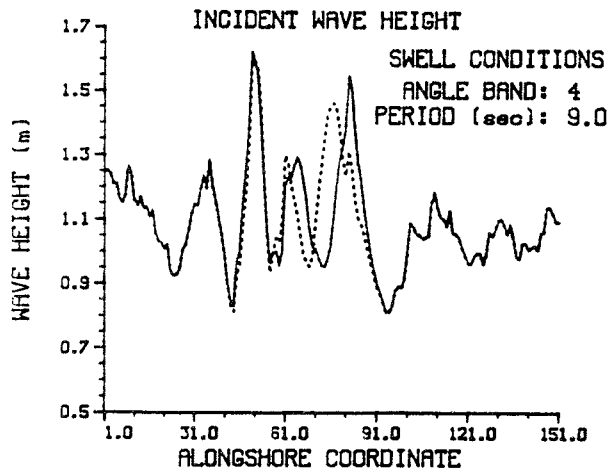


Figure C19. Swell conditions; wave height, $T = 9.0$ sec

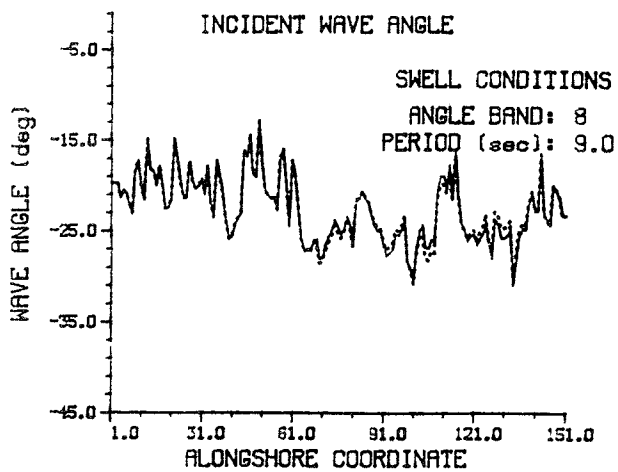
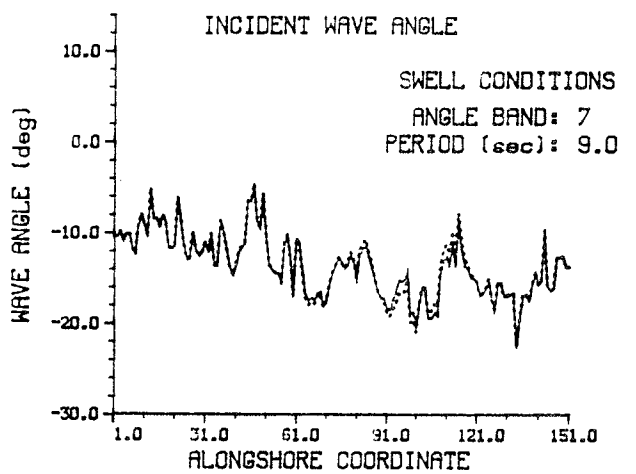
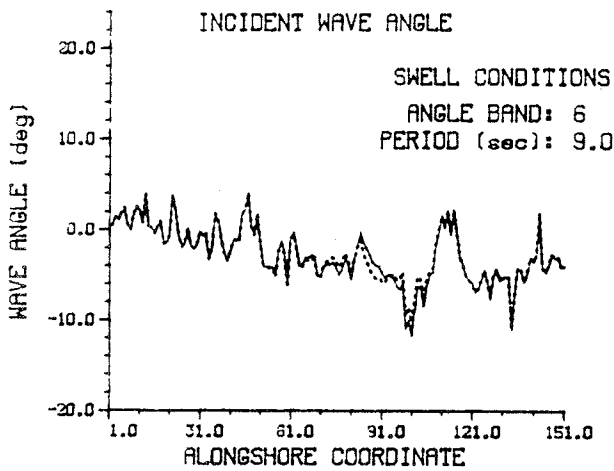
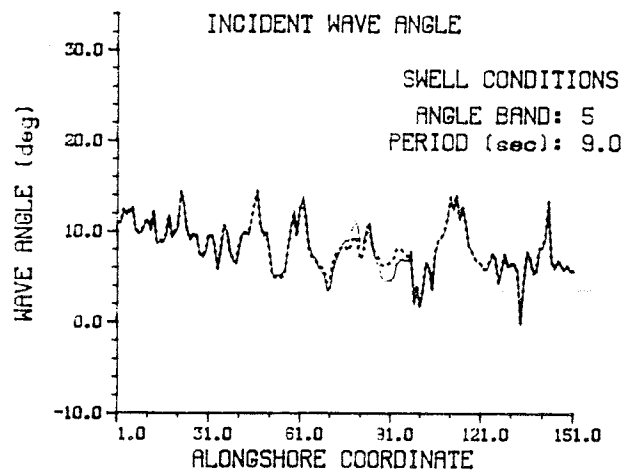
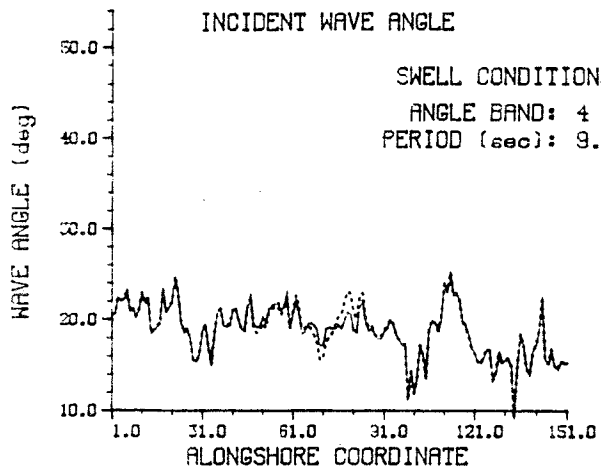


Figure C20. Swell conditions; wave angles, $T = 9.0$ sec

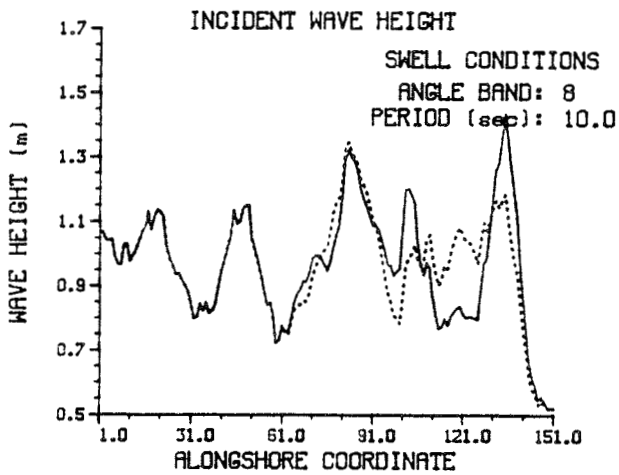
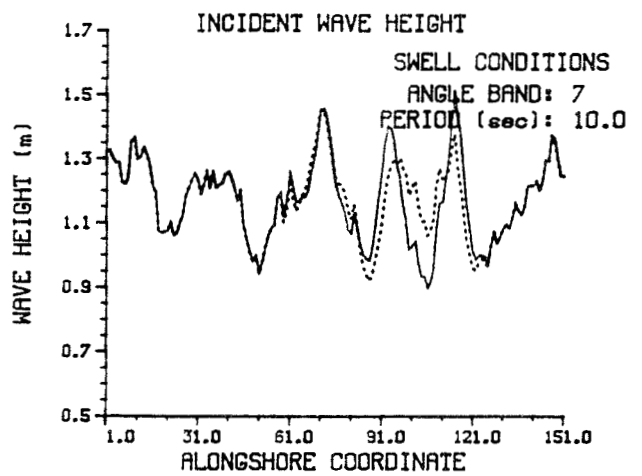
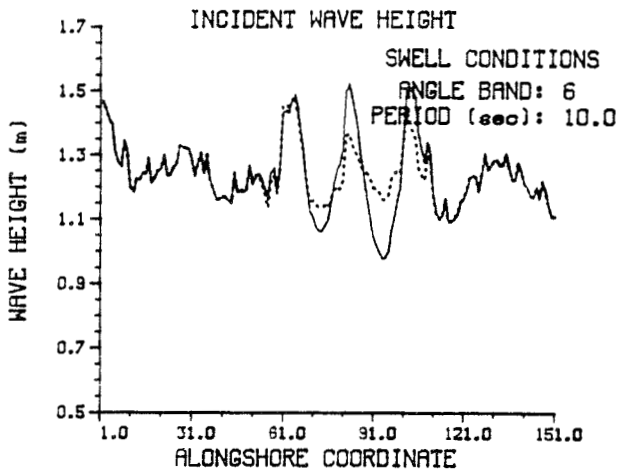
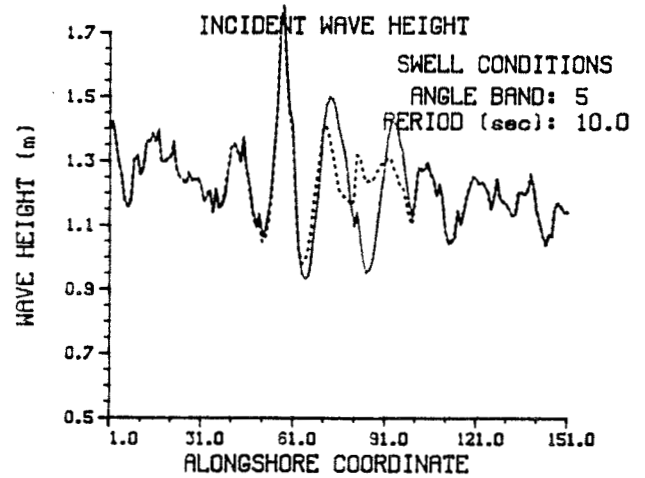
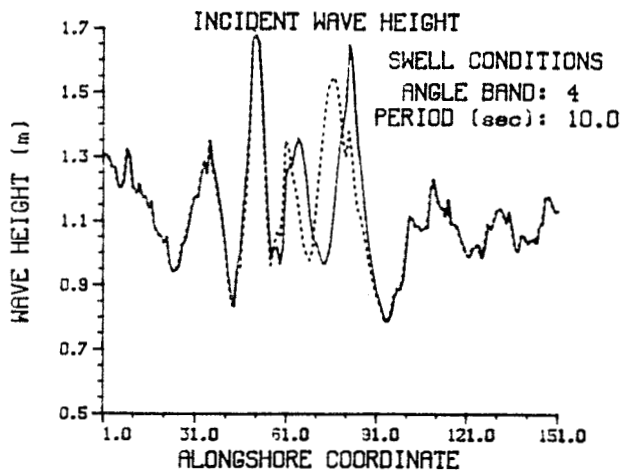


Figure C21. Swell conditions; wave height, $T = 10.0$ sec

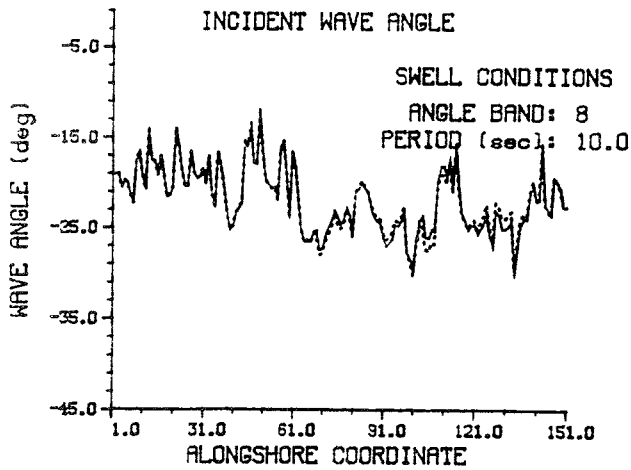
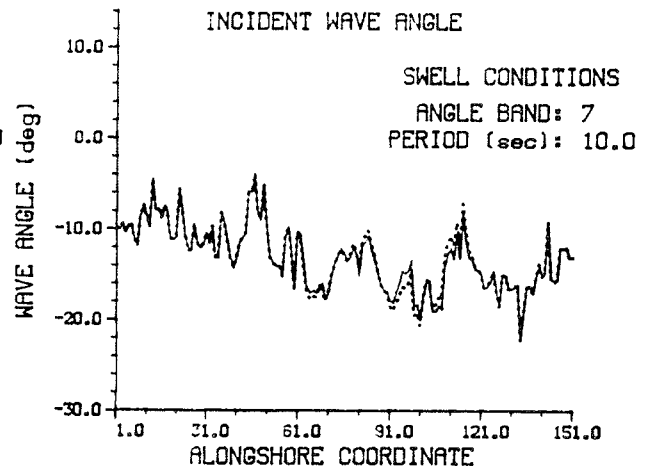
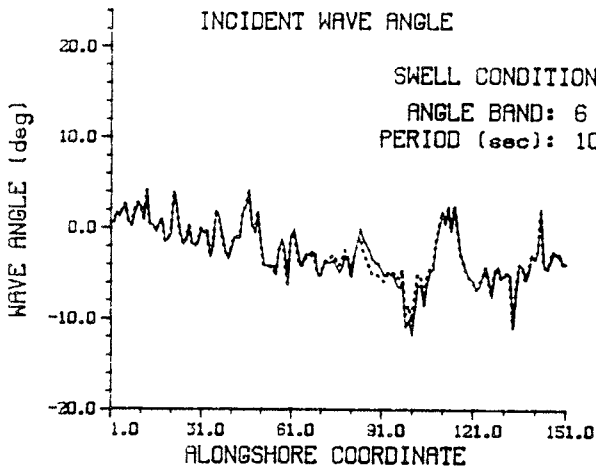
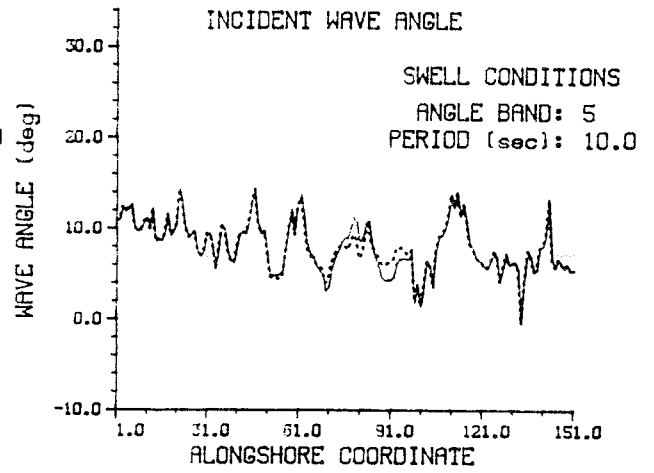
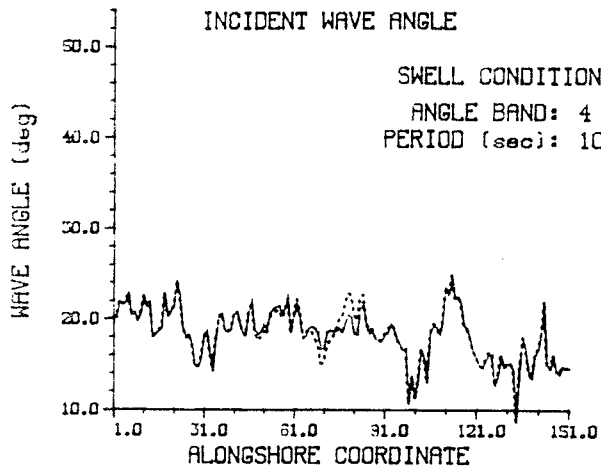


Figure C22. Swell conditions; wave angles, $T = 10.0$ sec

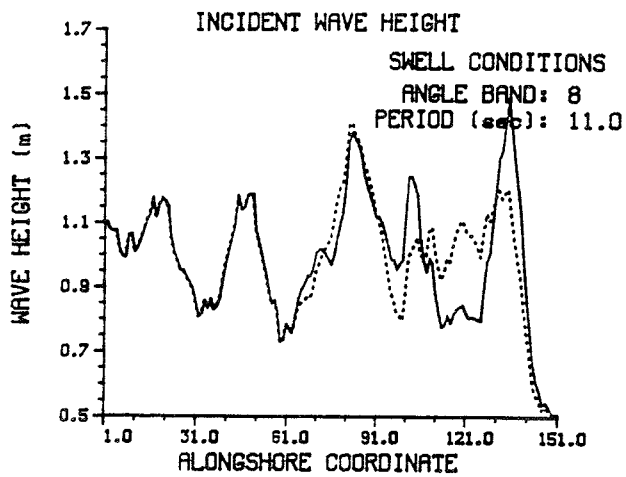
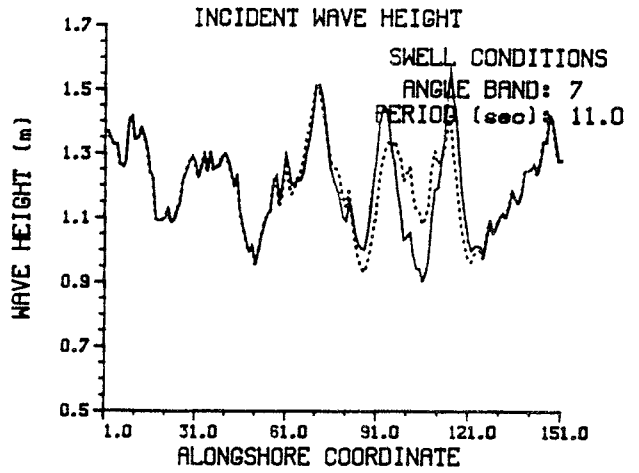
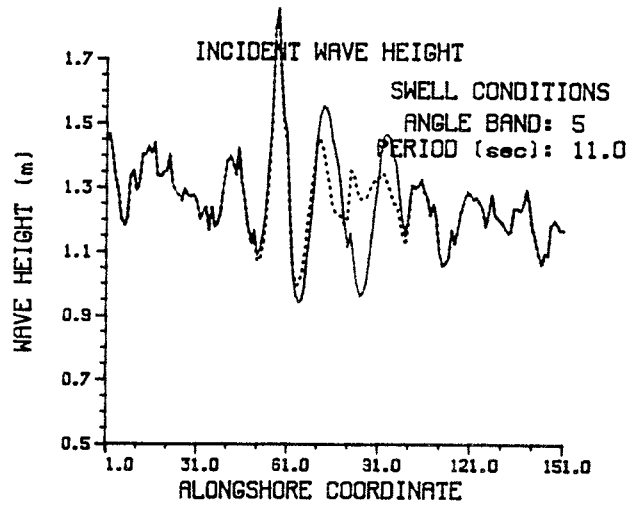


Figure C23. Swell conditions; wave height, $T = 11.0$ sec

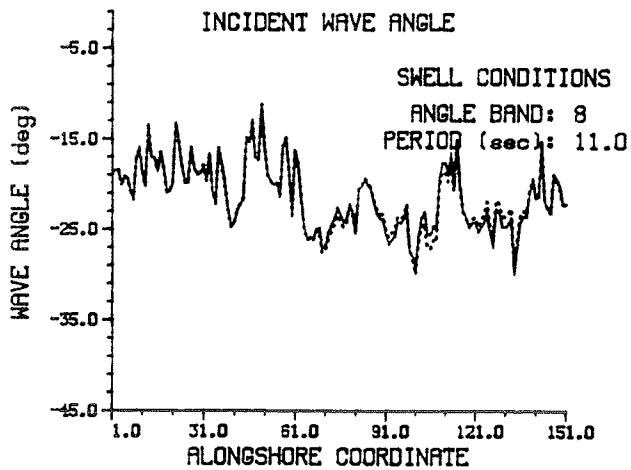
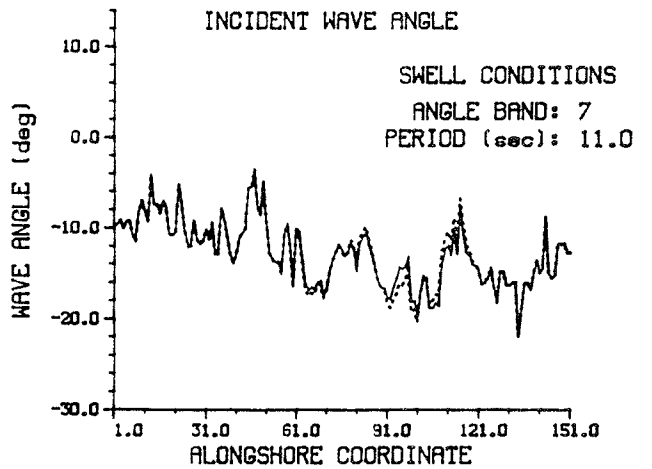
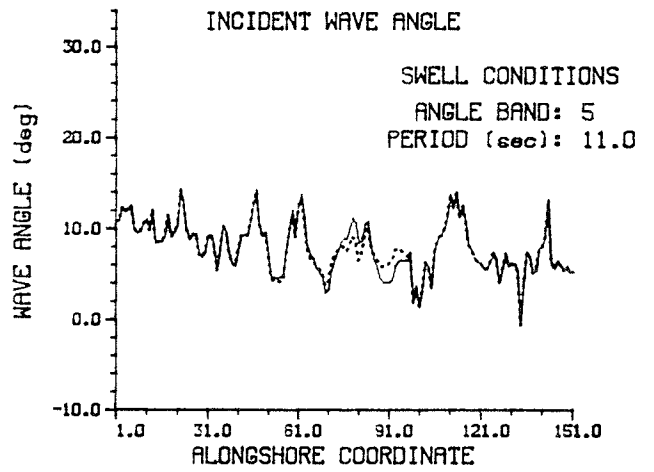


Figure C24. Swell conditions; wave angles, $T = 11.0$ sec

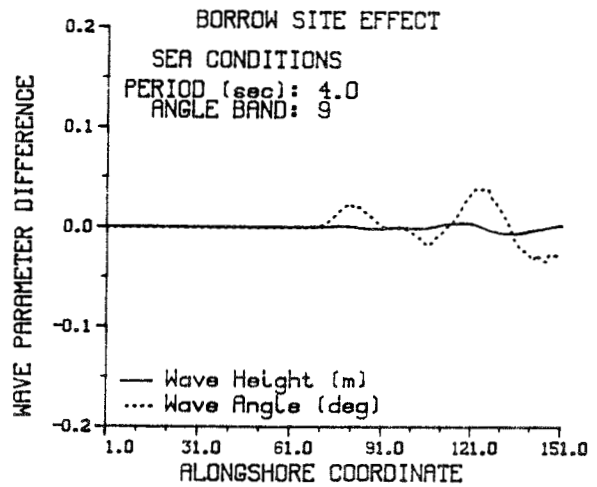
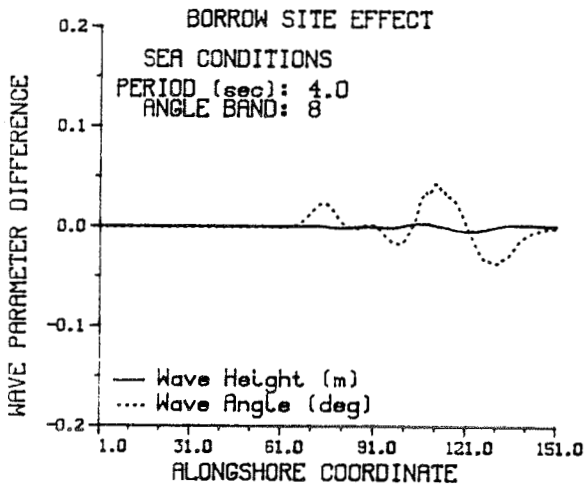
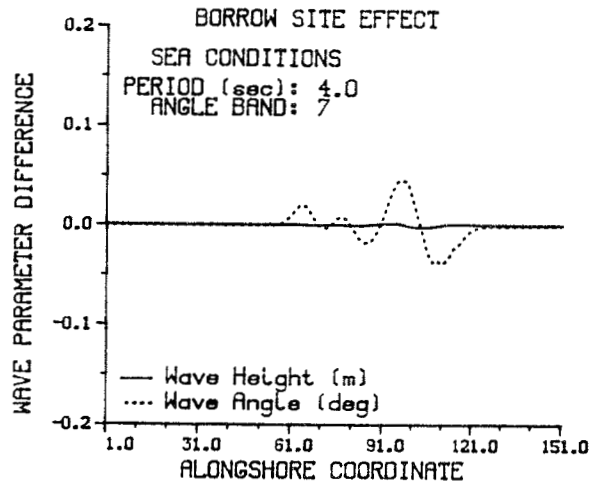
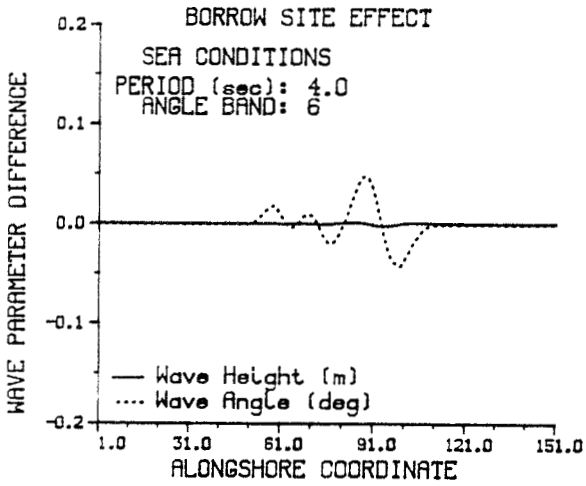
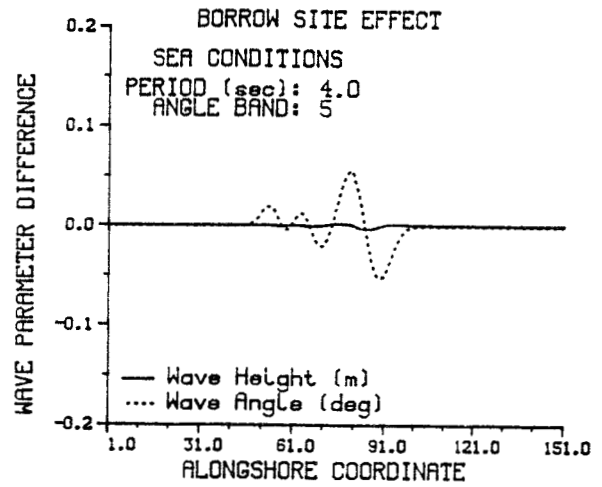
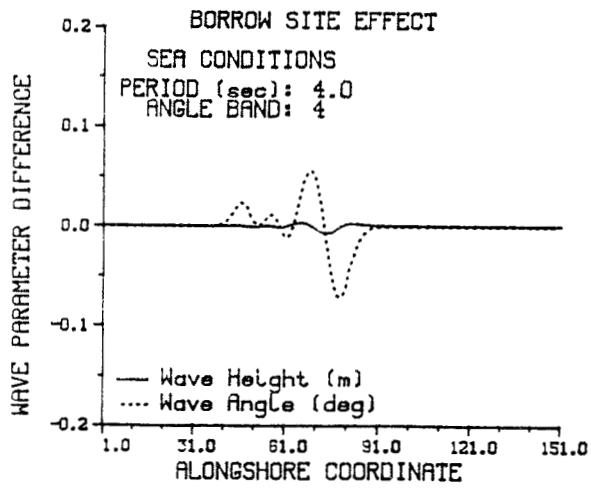


Figure C25. Sea conditions; borrow site effect, T= 4.0 sec

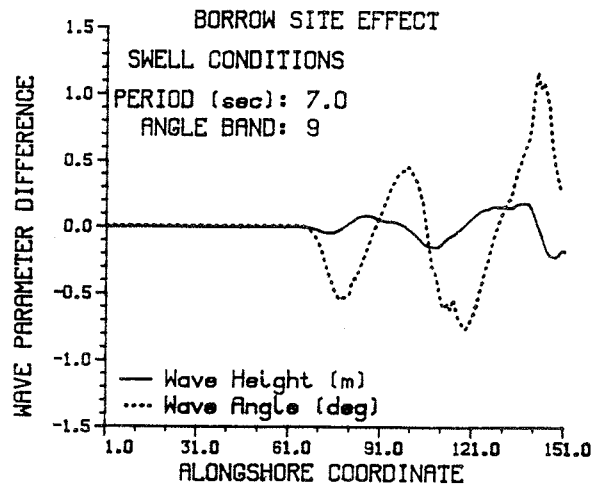
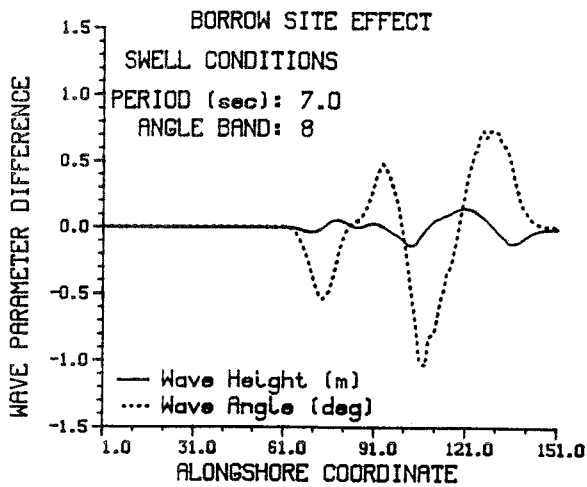
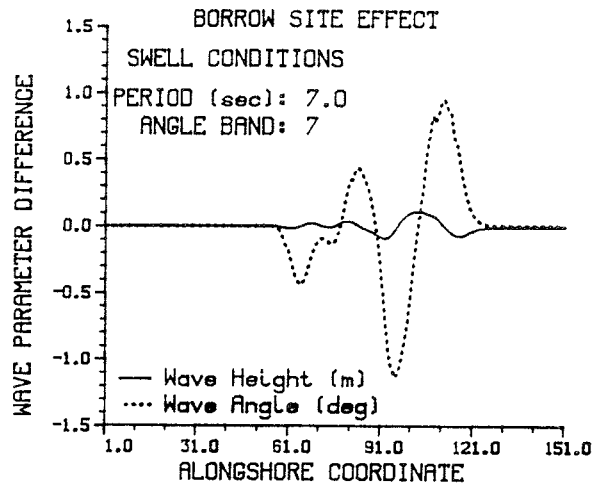
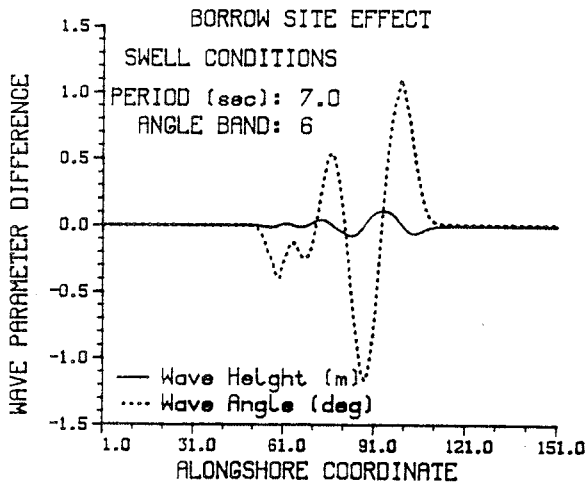
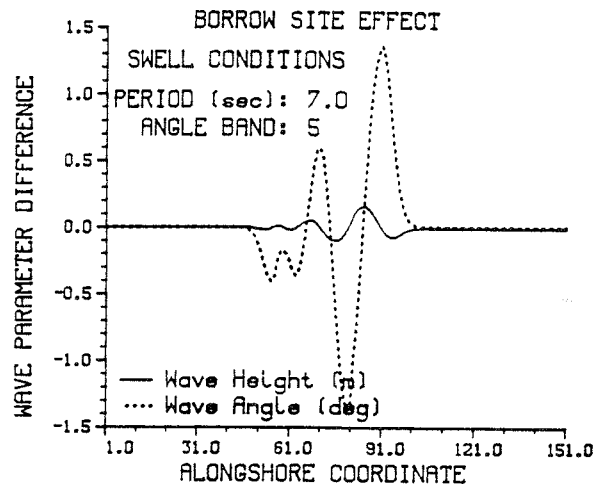
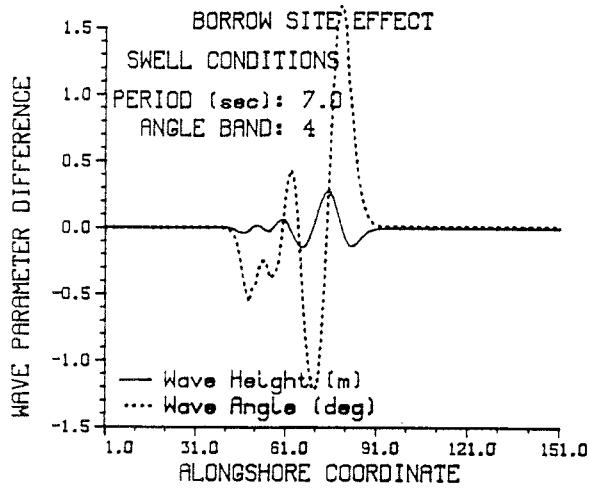
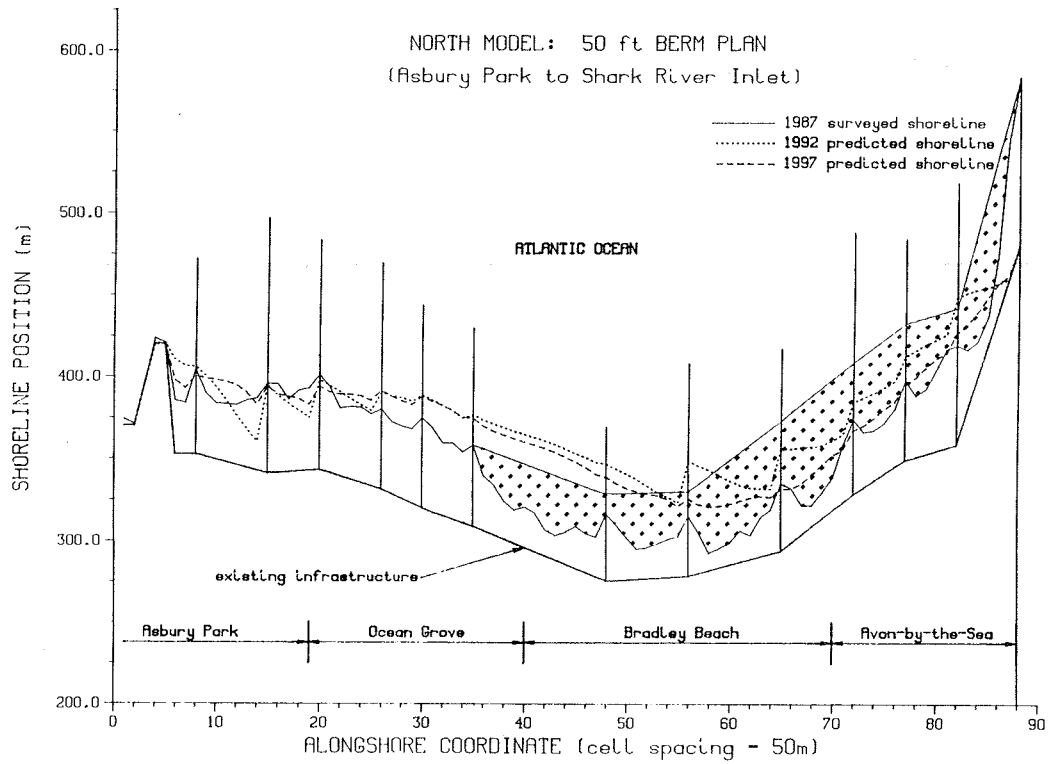


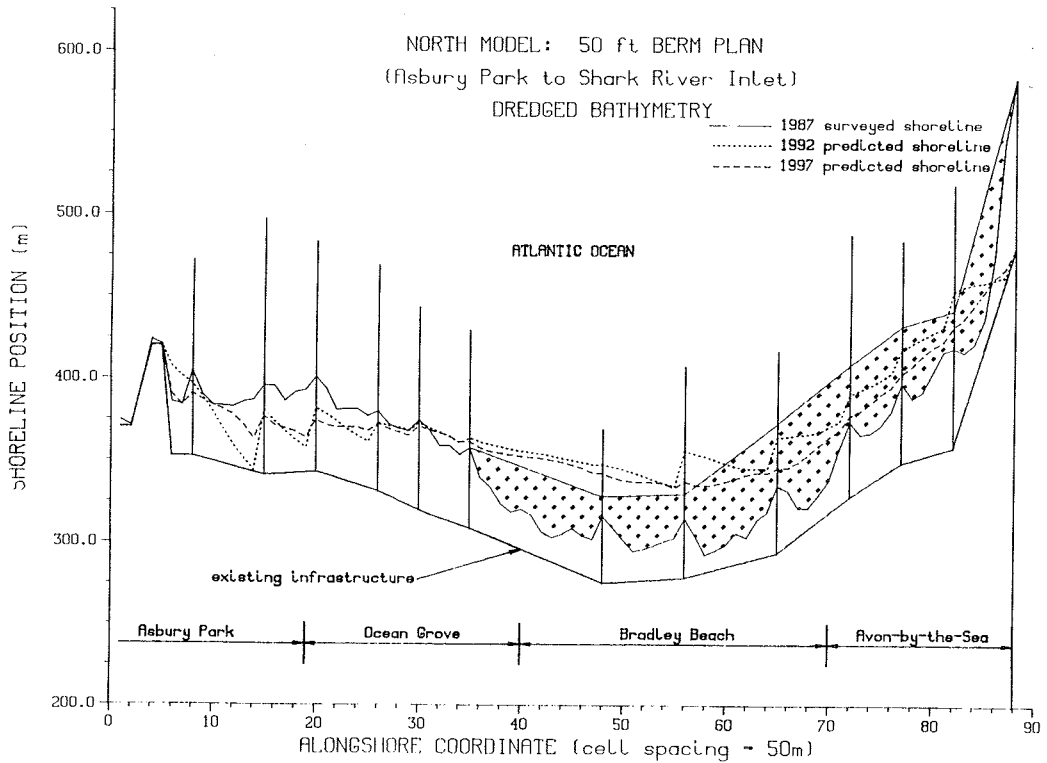
Figure C26. Swell conditions; borrow site effect, $T = 7.0$ sec

APPENDIX D: PRELIMINARY DESIGN ALTERNATIVES (MODEL RESULTS)

1. This appendix presents the results of the 24 model simulations made for the purpose of evaluating the long-term performance of the 6 preliminary shore protection design alternatives. Each design alternative was simulated twice with a simulation period of 10-years. Input wave conditions refracted over the existing bathymetry were used in the first simulation, and in the second simulation, input wave conditions refracted over a hypothetical dredged bathymetry were used. In the following figures the line and shading designation is as follows; the solid line is the 1987 surveyed shoreline position, the dotted line is the 5-year or 1992 predicted shoreline position, the dashed line is the 10-year or 1997 predicted shoreline position, and finally the diamond shaded area represents the shore protection plan as implemented on the 1987 surveyed shoreline position. The figures are organized as follows; for a given design alternative the results for the North Model reach (Asbury Park to Shark River Inlet) using the existing bathymetry waves is presented at the top of the page then at the bottom of the page the same design alternative except that the dredged bathymetry waves used; then on the next page, the results the design alternative simulation for the South Model reach (Shark River Inlet to Manasquan Inlet) are presented.

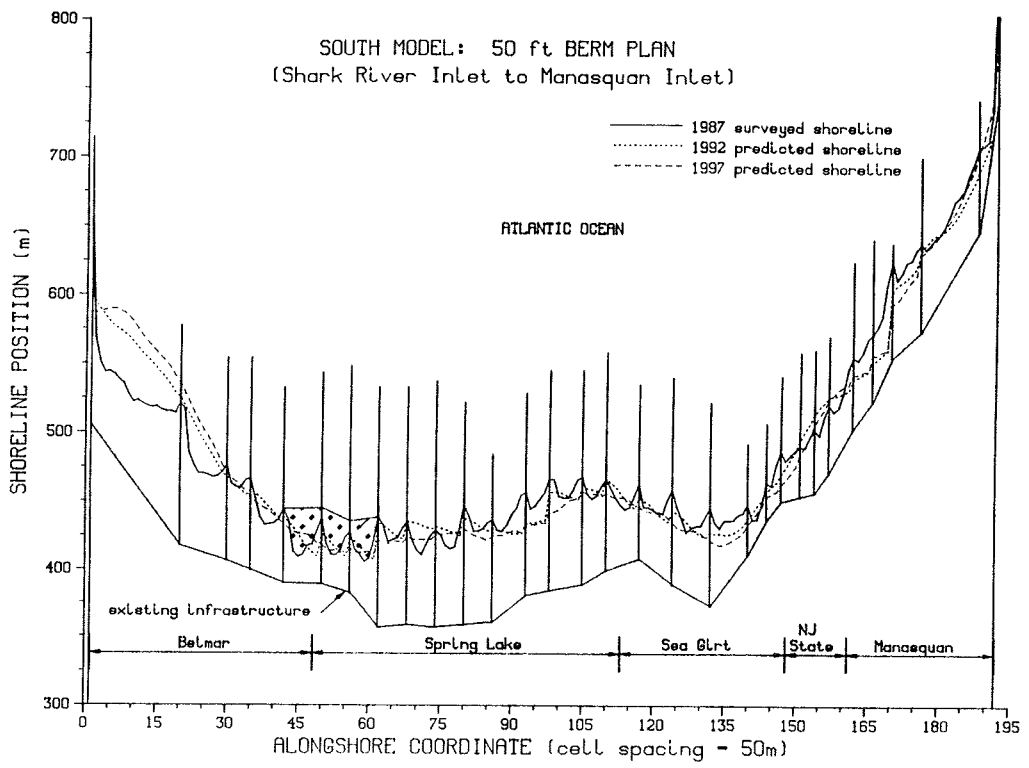


(a) existing bathymetry

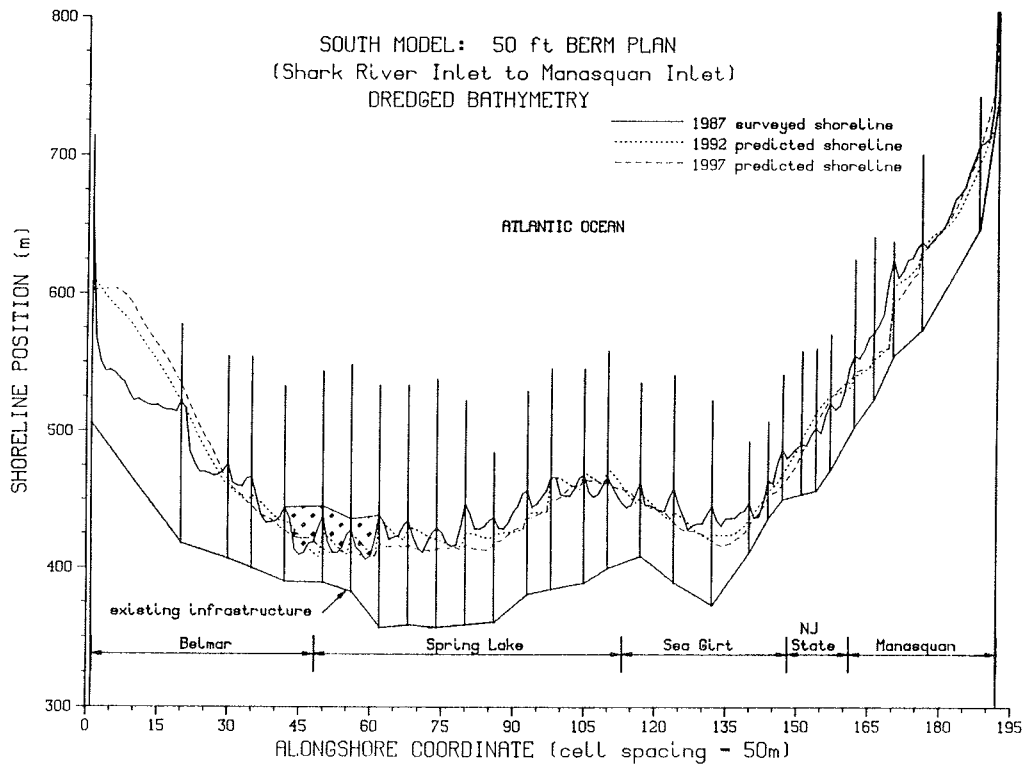


(b) dredged bathymetry

Figure D1 North Model, 50-ft beach fill plan simulation

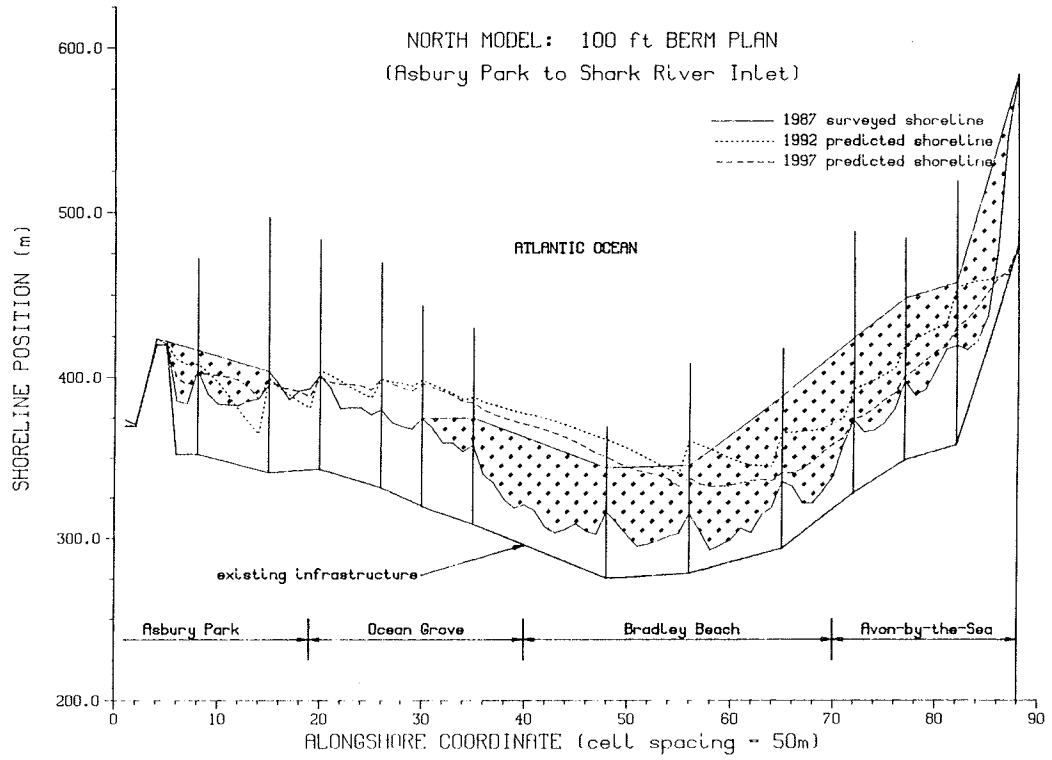


(a) existing bathymetry

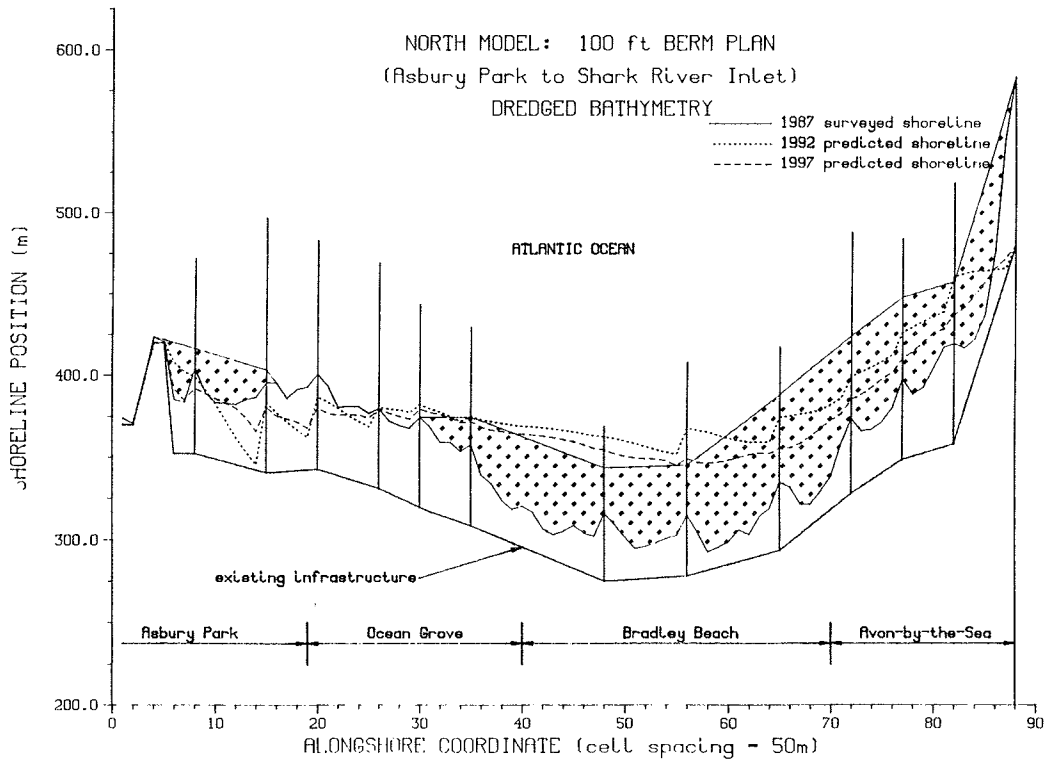


(b) dredged bathymetry

Figure D2 South Model, 50-ft beach fill plan simulation

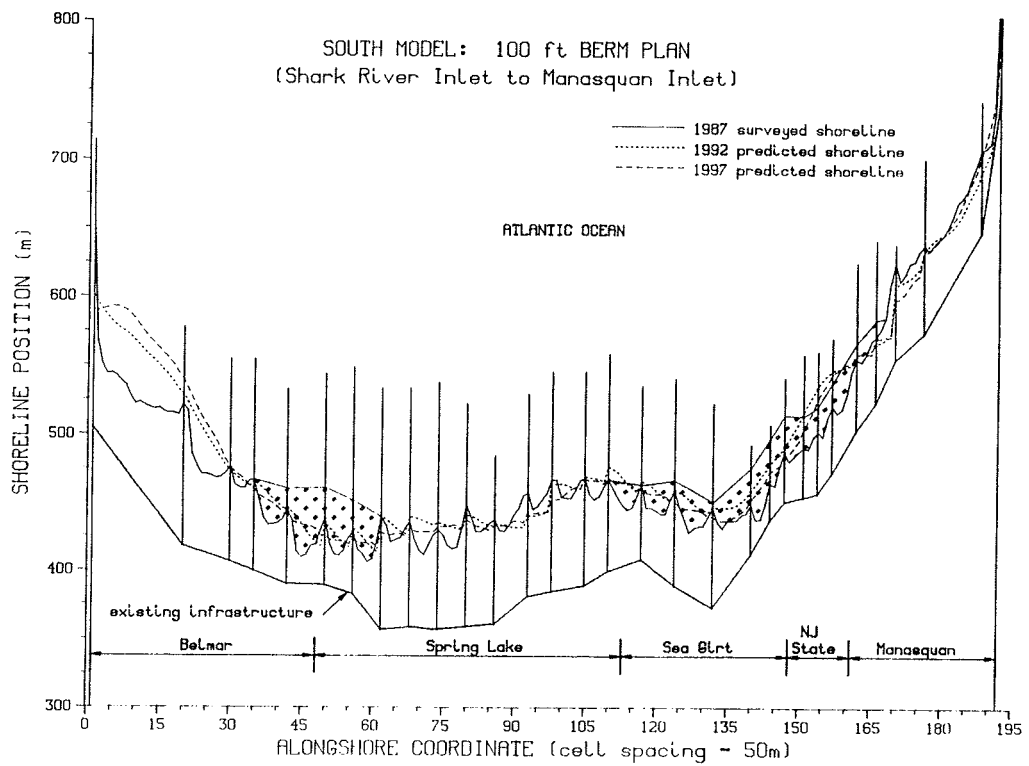


(a) existing bathymetry

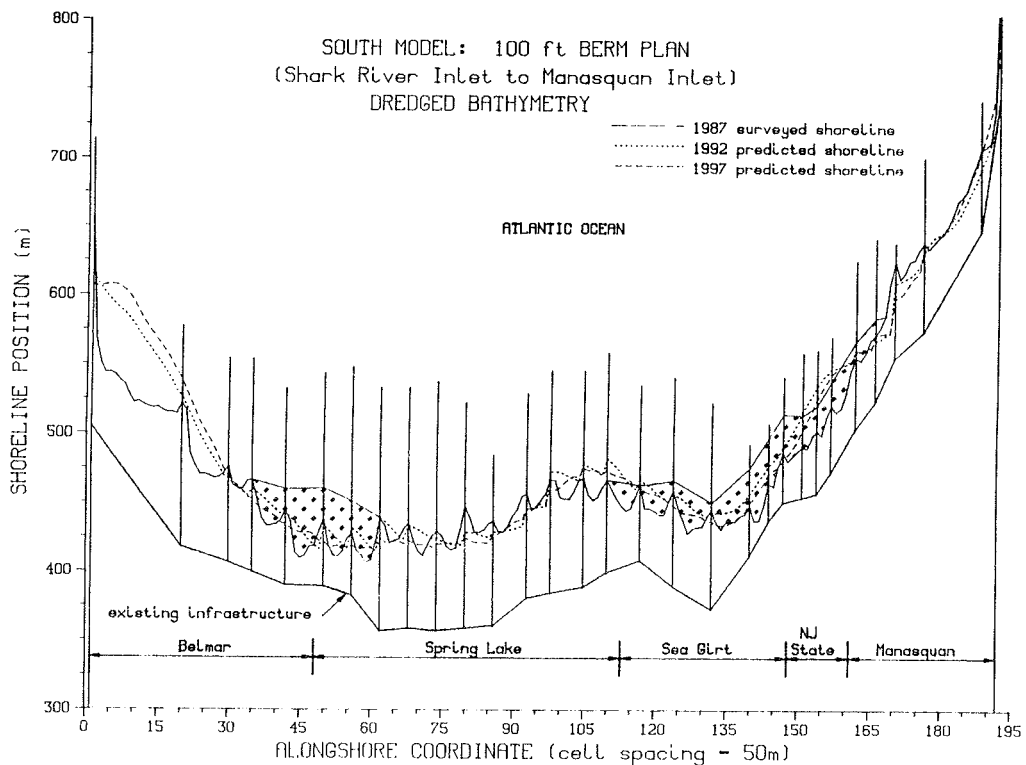


(b) dredged bathymetry

Figure D3 North Model, 100-ft beach fill plan simulation

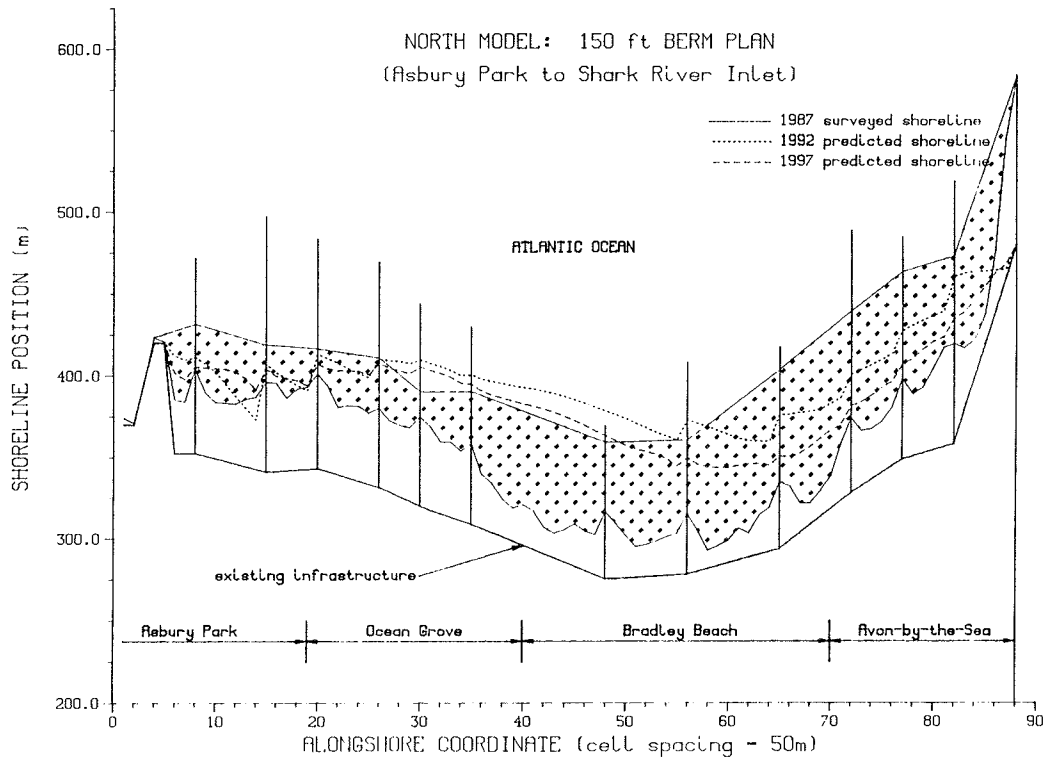


(a) existing bathymetry

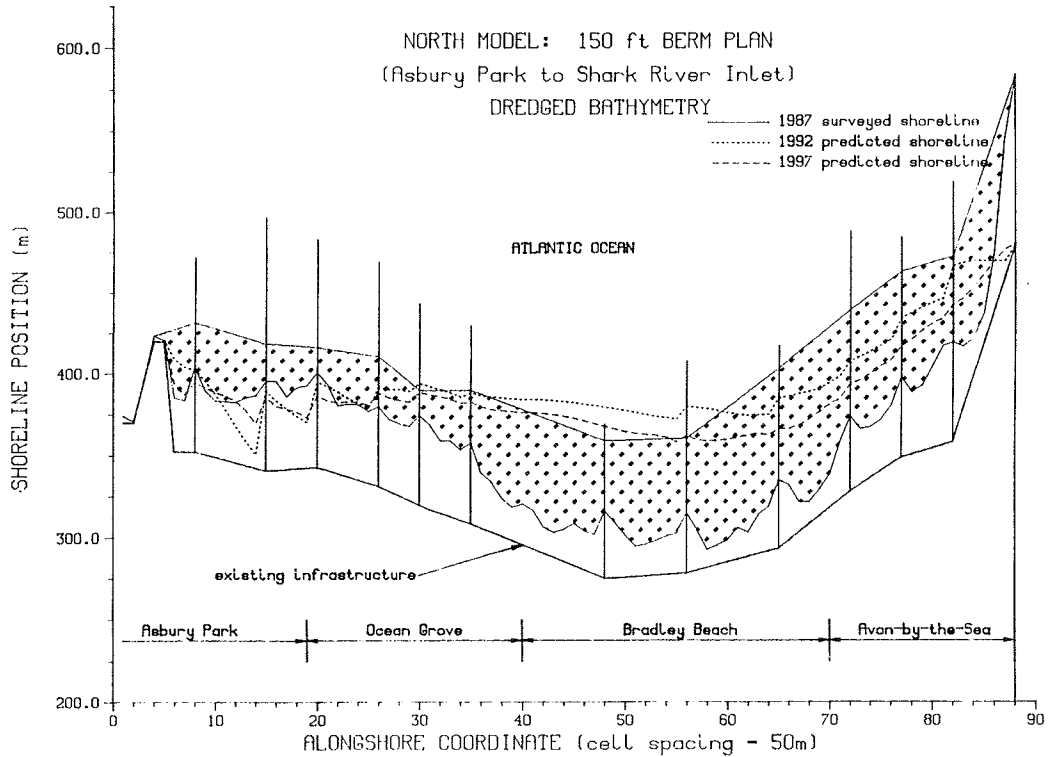


(b) dredged bathymetry

Figure D4 South Model, 100-ft beach fill plan simulation

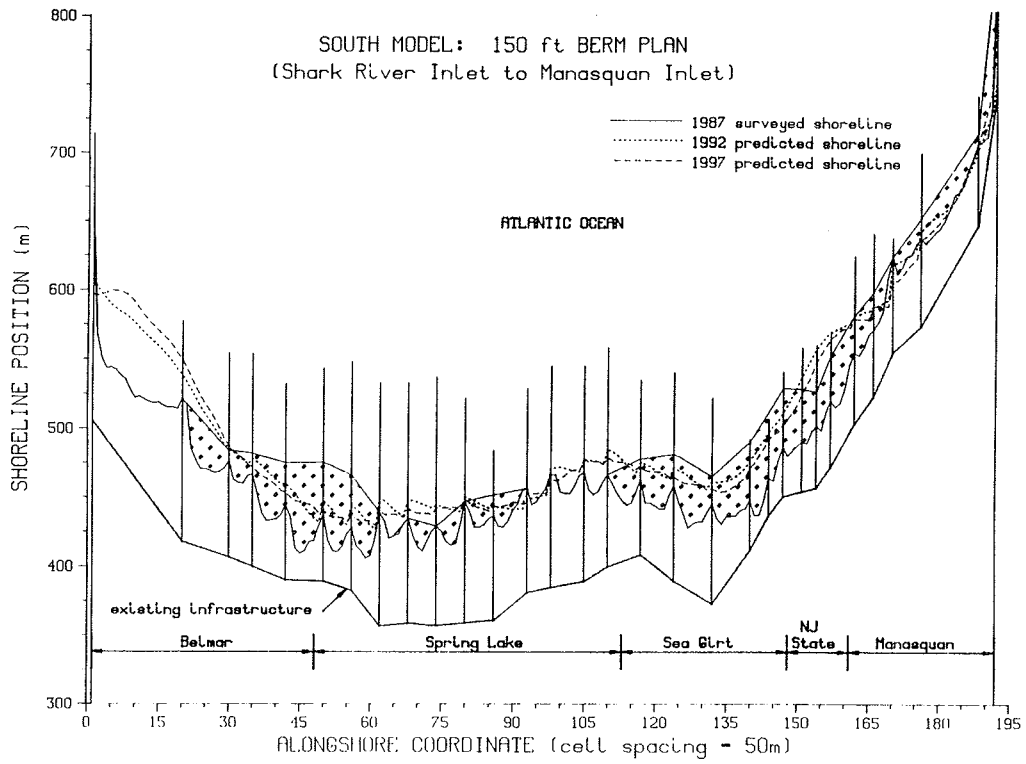


(a) existing bathymetry

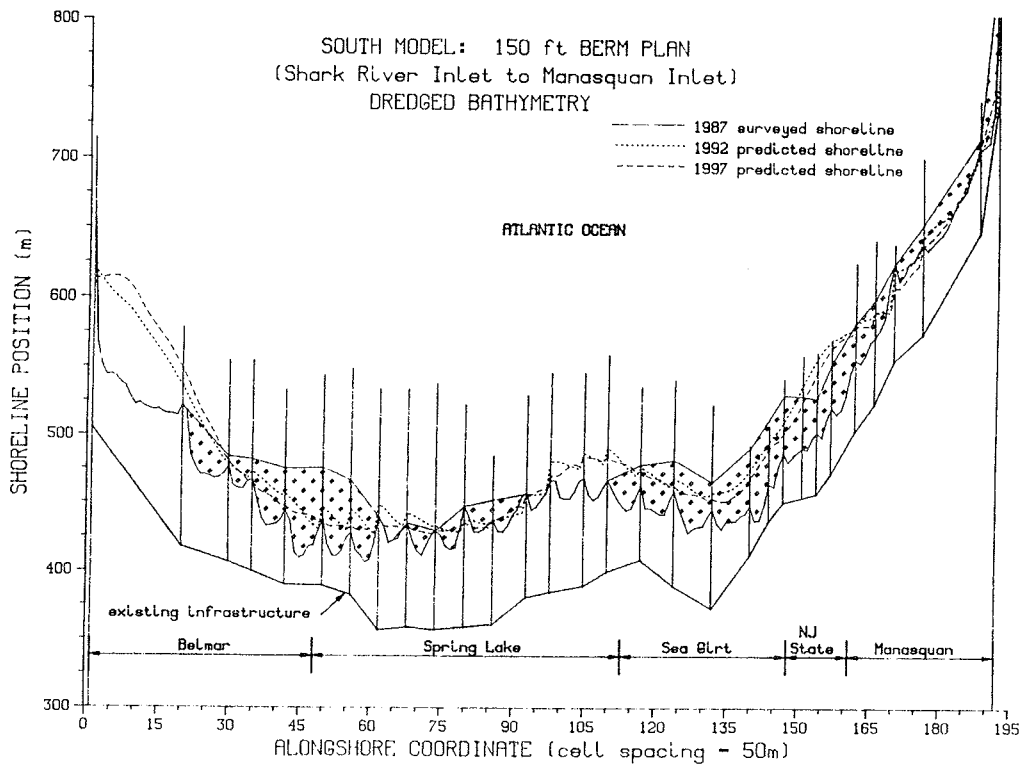


(b) dredged bathymetry

Figure D5 North Model, 150-ft beach fill plan simulation

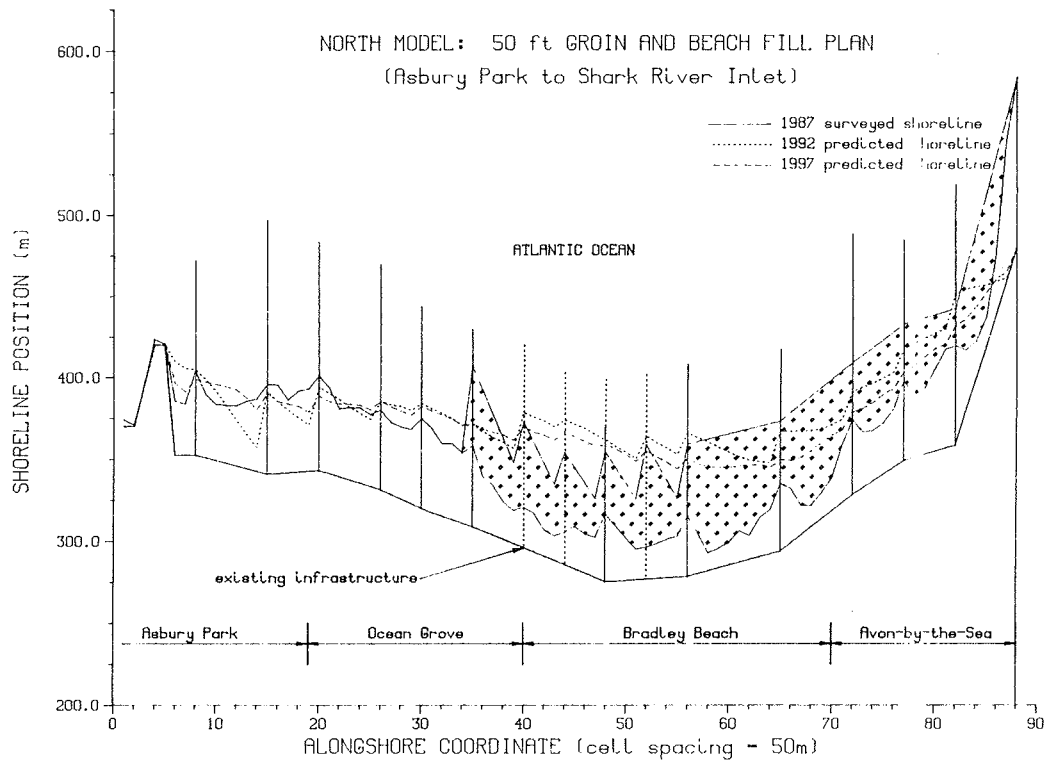


(a) existing bathymetry

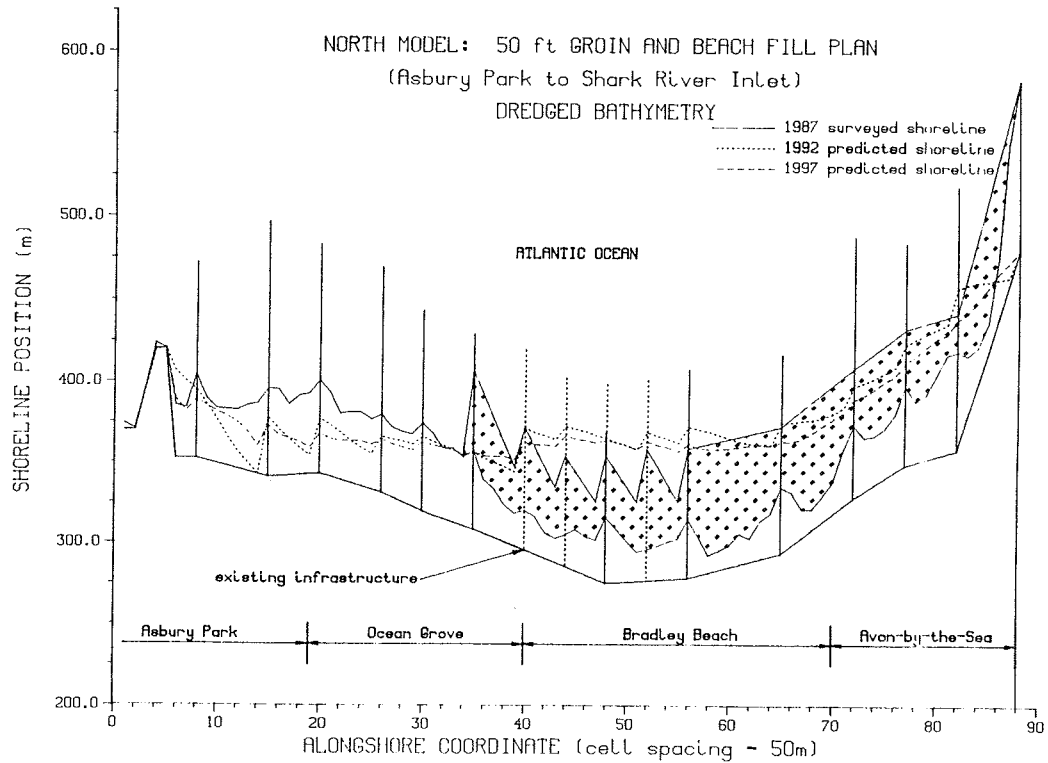


(b) dredged bathymetry

Figure D6 South Model, 150-ft beach fill plan simulation

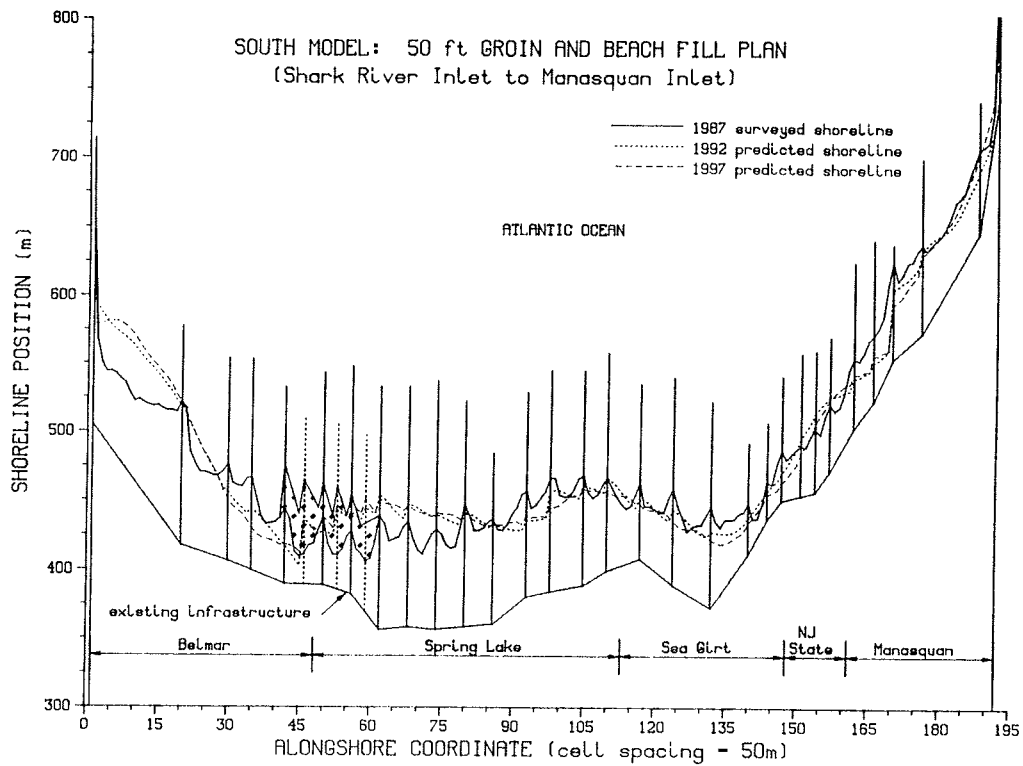


(a) existing bathymetry

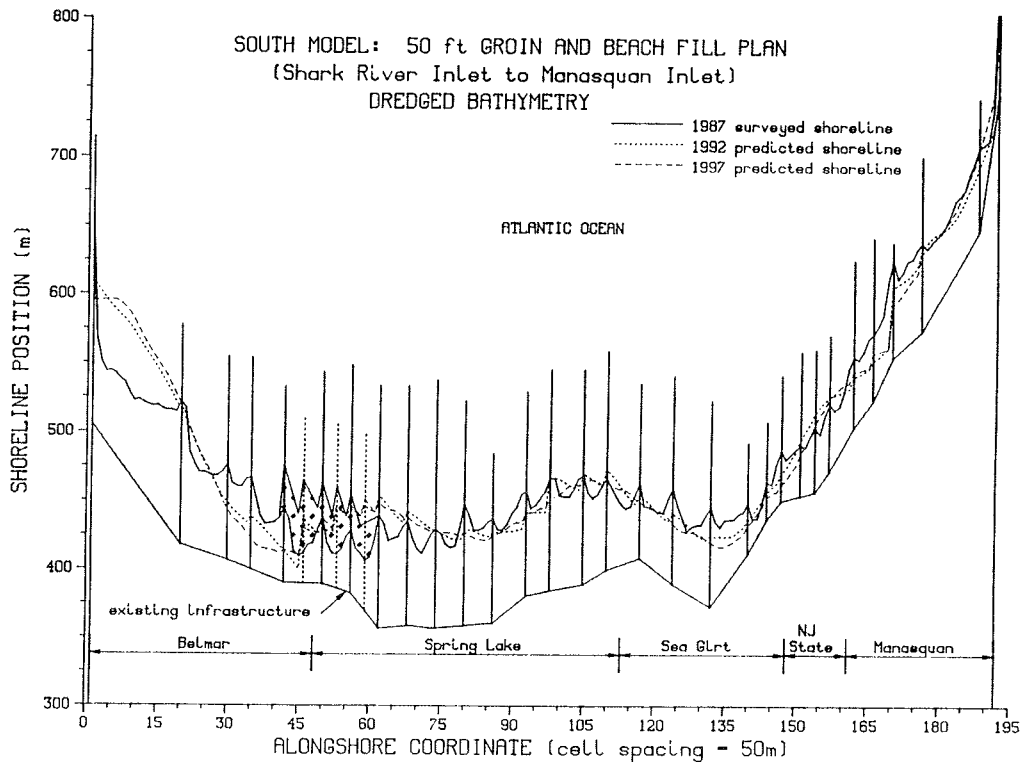


(b) dredged bathymetry

Figure D7 North Model, 50-ft groin and beach fill plan simulation

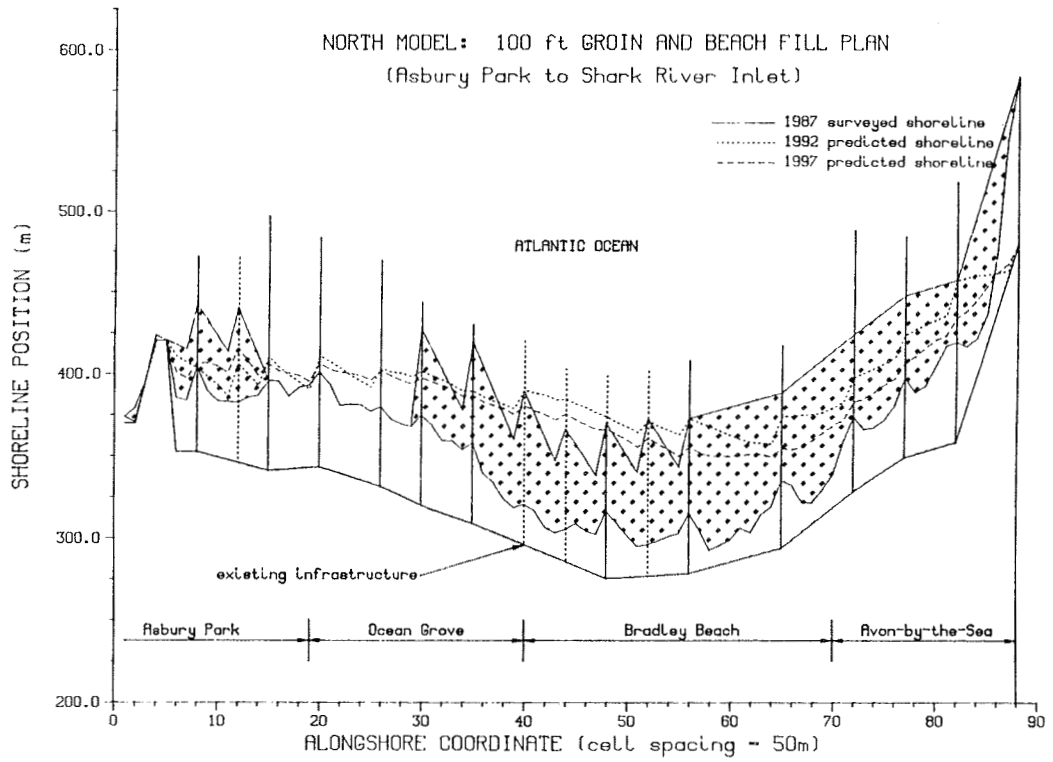


(a) existing bathymetry

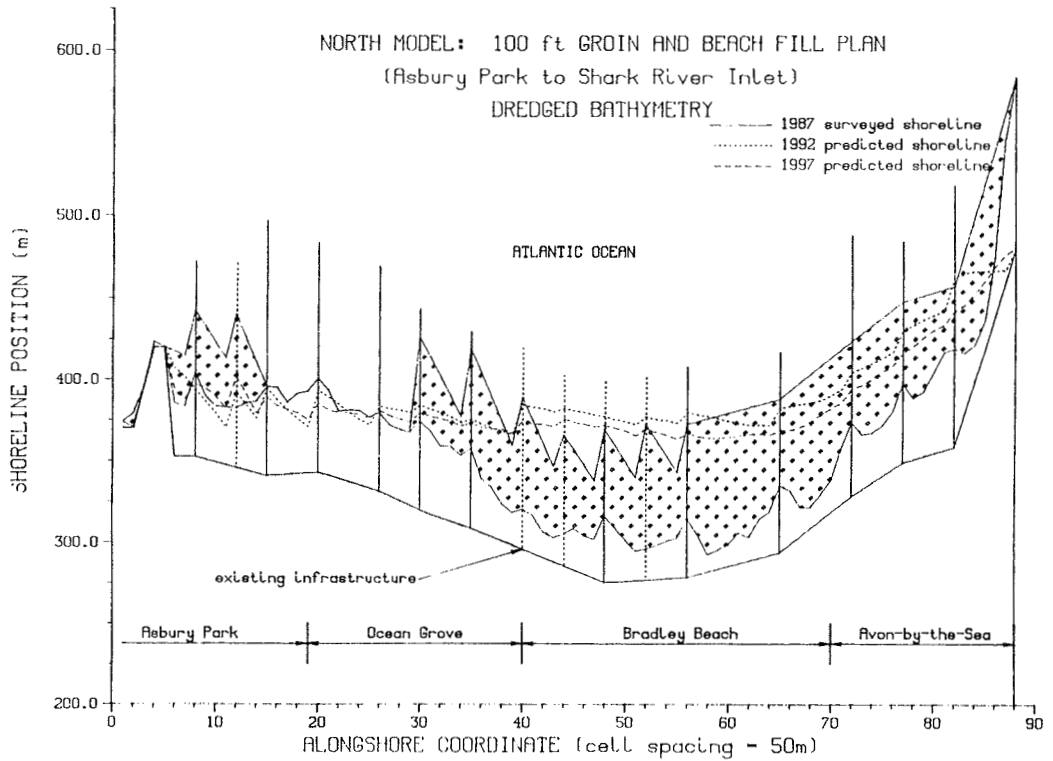


(b) dredged bathymetry

Figure D8 South Model, 50-ft groin and beach fill plan simulation

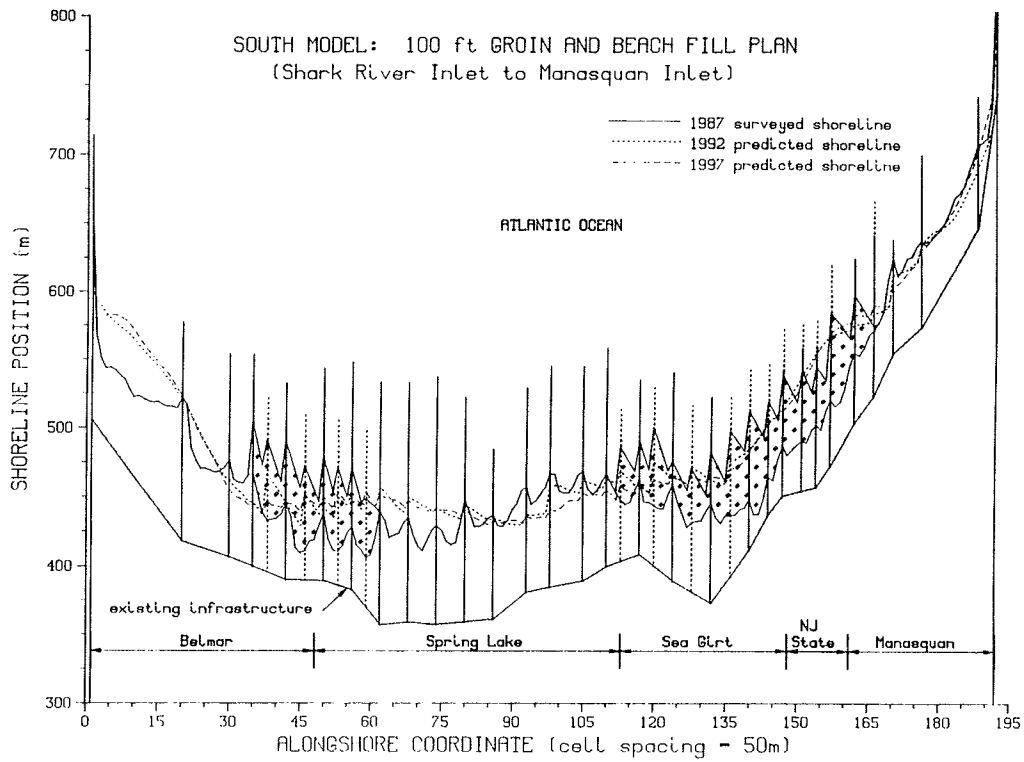


(a) existing bathymetry

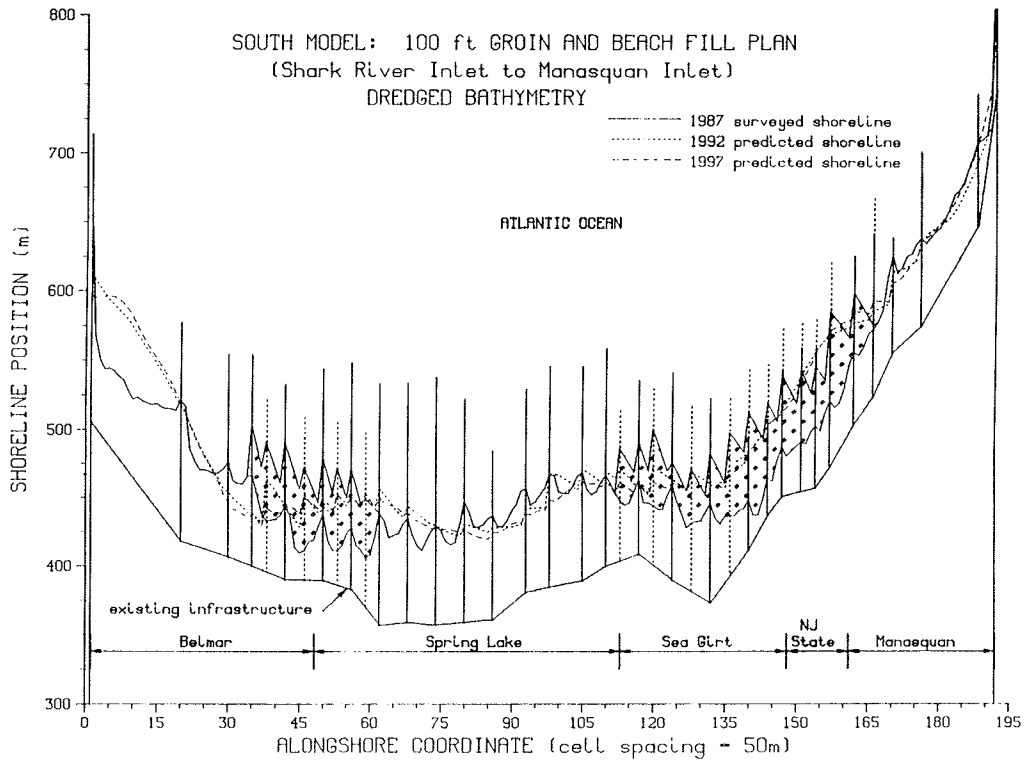


(b) dredged bathymetry

Figure D9 North Model, 100-ft groin and beach fill plan simulation



(a) existing bathymetry



(b) dredged bathymetry

Figure D10 South Model, 100-ft groin and beach fill plan simulation

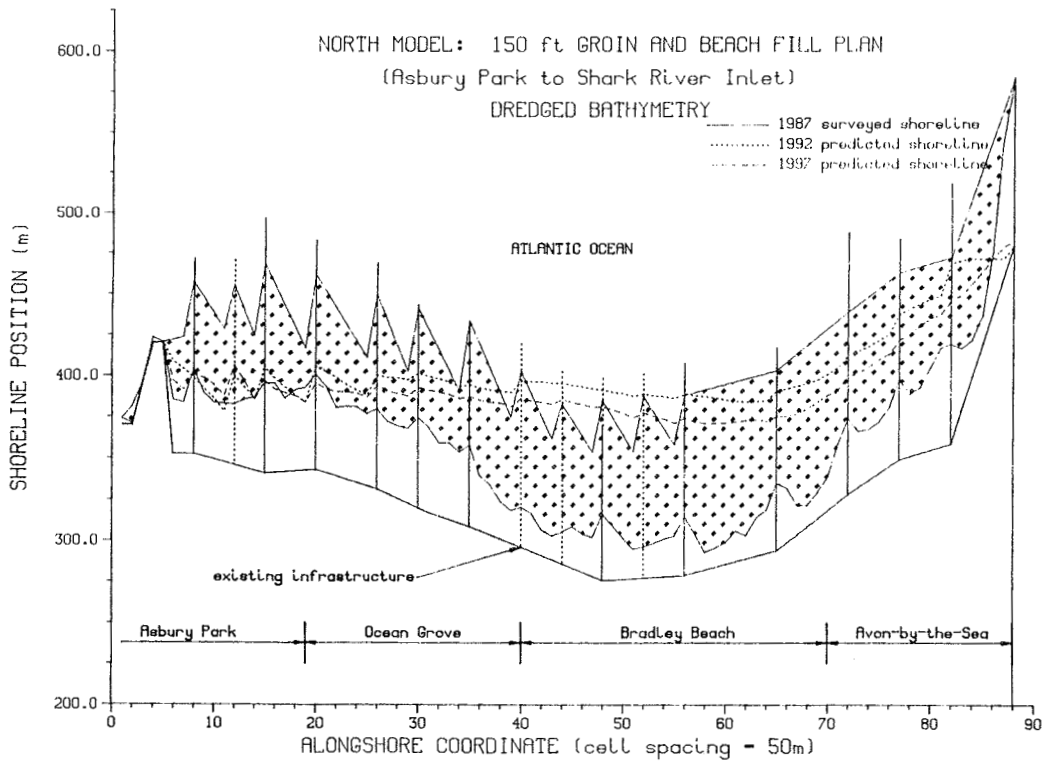
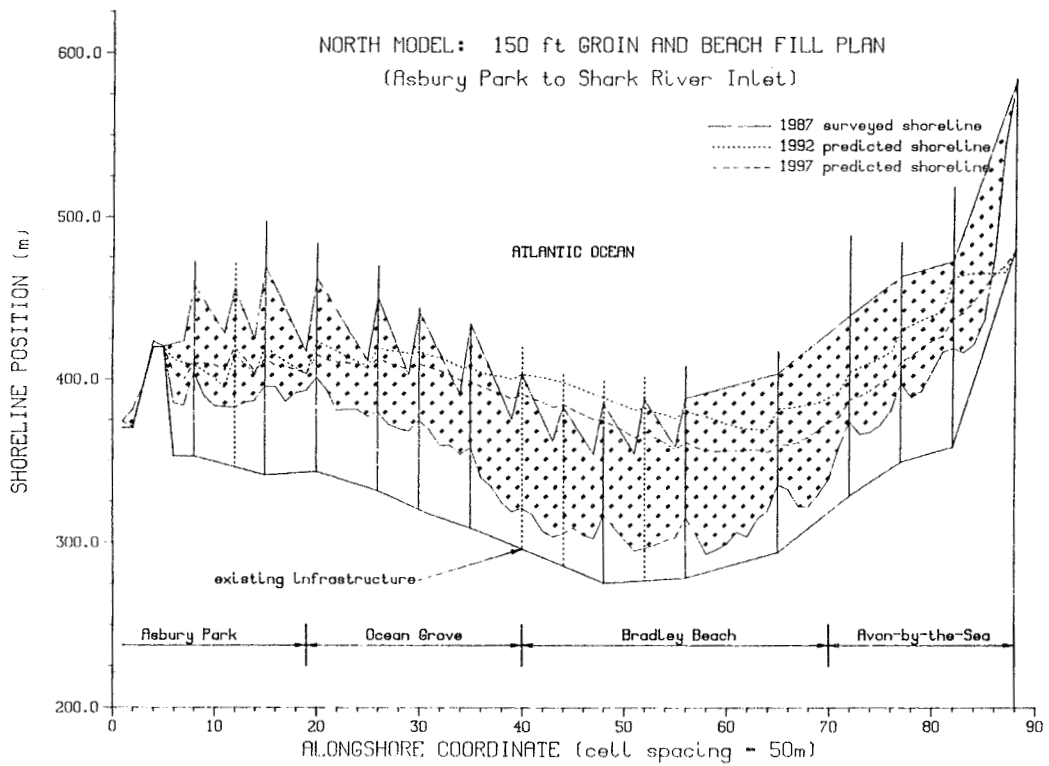
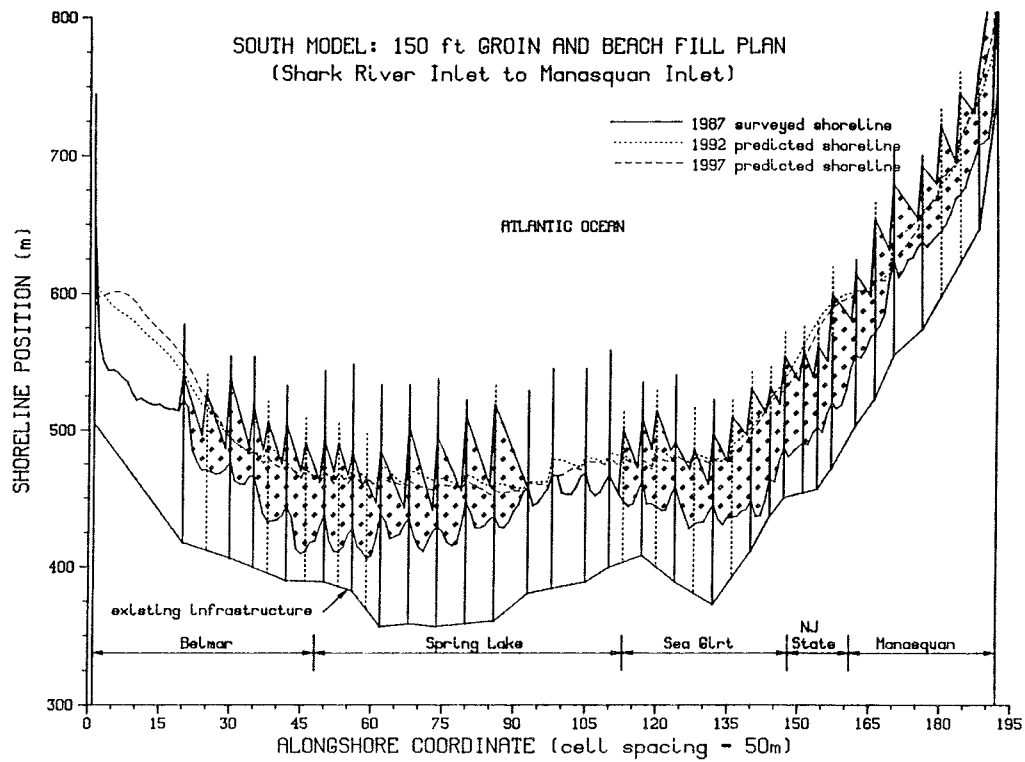
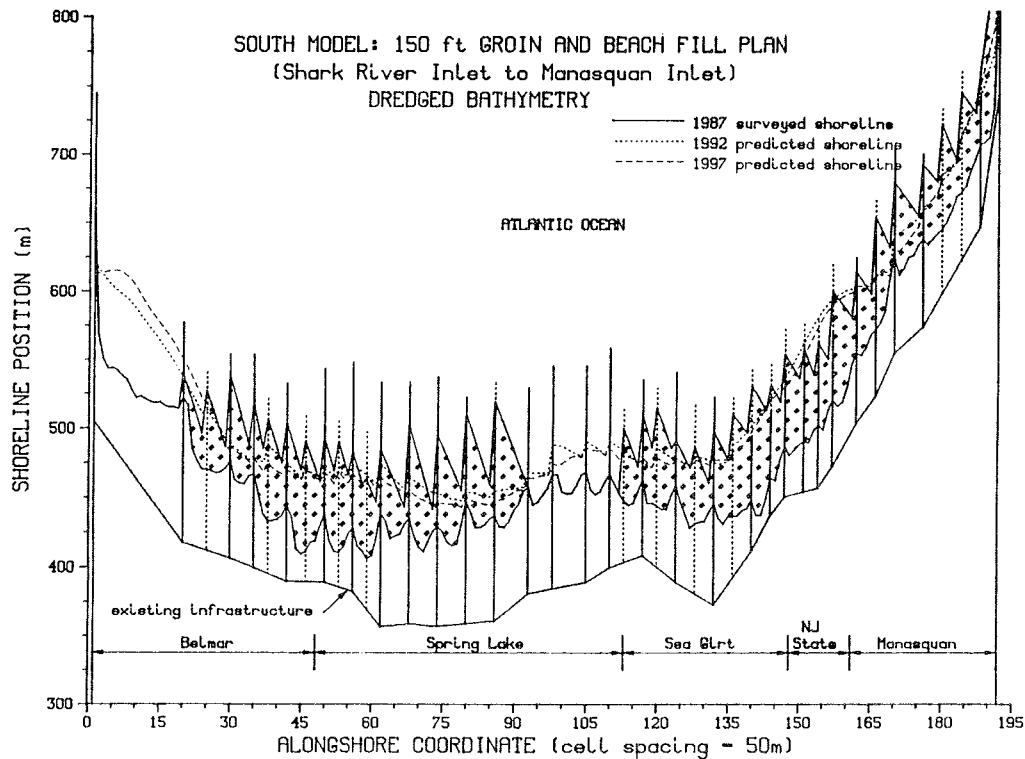


Figure D11 North Model, 150-ft groin and beach fill plan simulation



(a) existing bathymetry



(b) dredged bathymetry

Figure D12 South Model, 150-ft groin and beach fill plan simulation